Politecnico di Torino

ScuDo
Scuola di Dottorato ~ Doctoral School
WHAT YOU ARE, TAKES YOU FAR

Doctoral Dissertation
Doctoral Program in Energy Engineering (36^{th}cycle)

Modelling for the optimization of power plants and energy systems for combined production of energy vectors

By

Umberto Tesio

******

Supervisor(s):
Prof. Vittorio Verda, Supervisor
Prof. Elisa Guelpa, Co-Supervisor

Doctoral Examination Committee:
Prof. Ricardo Chacartegui, Referee, Universidad de Sevilla
Prof. Gianluca Carraro, Referee, Università degli Studi di Padova
Prof. Claudio Del Pero, Politecnico di Milano
Prof. Marta Gandiglio, Politecnico di Torino
Prof. Andrea Lanzini, Politecnico di Torino

Politecnico di Torino
2024

Declaration

I hereby declare that, the contents and organization of this dissertation constitute my own original work and does not compromise in any way the rights of third parties, including those relating to the security of personal data.

Umberto Tesio
2024

* This dissertation is presented in partial fulfillment of the requirements for **Ph.D. degree** in the Graduate School of Politecnico di Torino (ScuDo).

Abstract

The global increase in population and improved quality of life occurred in the last decades have led to a significant rise in the global energy demand, a trend expected to continue, particularly in developing countries. In the past, this demand has been met primarily through fossil fuels, resulting in widespread access to affordable energy. Concerns about the finite nature of fossil fuels and the global warming for which they are responsible have underscored the need for changing the approach used for the energy generation and achieve sustainable solutions. Four main strategies for achieving sustainability in the energy sector were identified: demand reduction, efficiency improvements, development of new technologies, and the transition to renewable energy sources.
A consistent implementation of these strategies is almost impossible without using optimization tools. In particular, the development of optimization models is very important for creating or improving energy technologies, since it allows to achieve the most convenient designs and operating conditions for a power plant or application. An extension of the operation problem of an energy plant is constituted by the operation of multiple power plants, energy networks and storage, which constitute Multi Energy Systems. The size and nature of these problems are significant and for these reasons their optimisation is a challenging task, but the benefits that can be achieved include reduced costs, energy savings and environmental impact.
The main aim of the works presented in this thesis is to provide a contribute to these topics by developing models for simulating and optimizing energy technologies and systems, addressing the integration challenges of renewable sources, and performing evaluations from energy and economic perspectives.

The global context and the energy optimization framework are discussed in order to provide an overview of the motivations that guided the works presented in the thesis and the perimeter of the research (Introduction, Chapter 1).

Successively, the methodology developed for optimizing an energy technology is presented and a model designed to optimize a novel CSP plant with thermochemical storage based on Calcium-Looping is introduced (Chapter 2). This complex case study allows the model to address key features relevant to such optimization problems. Additionally, various integration alternatives for the CSP-CaL technology are explored and their results are discussed and compared.

The optimization of Multi Energy Systems is faced by starting with a detailed literature review to provide an overview of the current state of research, focusing on the development of practical optimization models and their impact on problem nature and mathematical formulation (Chapter 3). Literature gaps are identified, as well as future research directions.

Successively, two optimization models for the joint operation optimization of Multi Energy Systems and thermal networks are presented. The first one takes advantage of a simplifying assumption to include a small thermal network (considered as internal to the MES) in the operation optimization (Chapter 4).

A more realistic case study is considered in the second one, where a small District Heating Network is considered for the heat transportation (Chapter 5). The methodologies are developed on two different detail levels, consistently with the case studies under consideration and the measures adopted to increase the flexibility. The addressing of the mathematical formulation is carefully discussed, as well as the convergence to the solution and the obtained results.

The last part of the thesis summarises the research carried out and a comment on the most significant results obtained is provided (Chapter 6). Finally, the concluding interpretations and considerations are given, together with a suggestion for possible future developments in relation to this research topic.

Dissemination

Most of the research carried out has been published in international journals and presented at international conferences. The scientific publications are here reported along with the papers published before the PhD start, since they constitute the initial part of a work developed during the PhD.

Journal Publications included in this thesis

[J1] Umberto Tesio, Elisa Guelpa, Vittorio Verda. Integration of thermochemical energy storage in concentrated solar power. Part 1: Energy and economic analysis/optimization. Energy Conversion and Management: X, 6, 100039, 2020.

[J2] Umberto Tesio, Elisa Guelpa, Vittorio Verda. Integration of thermochemical energy storage in concentrated solar power. Part 2: Comprehensive optimization of supercritical CO2 power block. Energy Conversion and Management: X, 6, 100038, 2020.

[J3] Umberto Tesio, Elisa Guelpa, Vittorio Verda. Multi-objective optimization of helium power cycle for thermo-chemical energy storage in concentrated solar power. Energy Conversion and Management: X, 12, 100116, 2021.

[J4] Umberto Tesio, Elisa Guelpa, Vittorio Verda. Comparison of sCO2 and He Brayton cycles integration in a Calcium-Looping for Concentrated Solar Power. Energy, 247, 123467, 2022.

[J5] Umberto Tesio, Elisa Guelpa, Vittorio Verda. Including thermal network operation in the optimization of a Multi Energy System. Energy Conversion and Management, 277, 116682, 2023.

[J6] Giulia Mancò, Umberto Tesio, Elisa Guelpa, Vittorio Verda. A review on multi energy systems modelling and optimization. Applied Thermal Engineering, 236, 121871, 2024.

Conference Proceedings included in this thesis

[C1] Umberto Tesio, Elisa Guelpa, Vittorio Verda. Optimal Indirect Integration of Steam Rankine Cycles in Concentrated Solar Power Coupled with Thermochemical Storage. E3S Web of Conferences, Rome, Italy, 2020.

[C2] Umberto Tesio, Elisa Guelpa, Vittorio Verda. Multi-objective optimization of helium power cycles for thermo-chemical energy storage in concentrated solar power. Proceedings of the 33rd International Conference on Efficiency, Cost, Optimization, Simulation and Environmental Impact of Energy Systems, Copenhagen, Denmark, 2020.

[C3] Umberto Tesio, Elisa Guelpa, Vittorio Verda. Implementation of thermal network simulation in operation optimization of an energy system. Proceedings of the 35th International Conference on Efficiency, Cost, Optimization, Simulation and Environmental Impact of Energy Systems, Copenhagen, Denmark, 2022.

Journal Publications not included in this thesis

[J7] Umberto Tesio, Elisa Guelpa, Carlos Ortiz, Ricardo Chacartegui, Vittorio Verda. Optimized synthesis/design of the carbonator side for direct integration of thermochemical energy storage in small size concentrated solar power. Energy Conversion and Management: X, 4, 100025, 2019.

Conference Proceedings not included in this thesis

[C4] Elisa Guelpa, Martina Capone, Umberto Tesio, Carlos Ortiz, Ricardo Chacartegui, and Vittorio Verda. High efficiency concentrated solar plant by increasing of power cycle temperature. Proceedings of the 32nd ECOS International Conference on Efficiency, Cost, Optimization, Simulation and Environmental Impact of Energy Systems, Wroclaw, Poland, 2019.

[C5] Elisa Guelpa, Martina Capone, Umberto Tesio, and Vittorio Verda. Exergoeconomic analysis for the optimal exploitation of heat in thermochemical storage units integrated with concentrated solar power. Proceedings of the 32nd ECOS International Conference on Efficiency, Cost, Optimization, Simulation and Environmental Impact of Energy Systems, Wroclaw, Poland, 2019.

[C6] Elisa Guelpa, Umberto Tesio, Martina Capone, and Vittorio Verda. Design Optimization of Thermochemical Storage System for 100% Renewable Power Production. Proceedings of the 22nd Conference on Process Integration, Modelling and

Optimisation for Energy Saving and Pollution Reduction, Agios Nikolaos, Crete, Greece, 2019.

[C7] Elisa Guelpa, Martina Capone, Umberto Tesio, and Vittorio Verda. Optimal Configurations for the Integration of Power Cycles in Concentrated Solar Plants with Thermochemical Energy Storage. Proceedings of the 22nd Conference on Process Integration, Modelling and Optimisation for Energy Saving and Pollution Reduction, Agios Nikolaos, Crete, Greece, 2019.

Conference abstracts

[C8] Umberto Tesio, Elisa Guelpa, and Vittorio Verda. Comparison between optimized power block integrations for Thermochemical Energy Storage based on Calcium-Looping in Concentrated Solar Power. 6th International Conference on Sustainable and Renewable Energy Engineering – ICSREE, Strasbourg, France. 2021.

Contents

List of Figures

List of Tables

Chapter 1

Introduction

The aim of this chapter is to present the research fields of the topics investigated in this thesis and to discuss the reasons behind the choice of these problems. Therefore, the research objectives are explained and the structure of the thesis is presented in order to provide an overview of the analysis developed.

1.1 Context

The constant increase of the global population and the improvements in the people's quality of life that the world experienced during the last century are the main reasons for the steep growth of the global energy demand. These trends are forecasted to continue for the next decades, mainly driven by second and third world countries [1]. In the past (and partially also in the present), the world's energy demand has been mainly covered by energy sources of fossil origin. The historical evolution of the infrastructures for the energy production and transportation allowed to reach relatively low prices for electricity, heating and cooling, as well as a high share of population with access to electricity (91% of the global population in 2021 [2]). These remarkable results have been achieved mainly thanks to the advanced stage of development reached by fossil fuels related technologies and their commercial availability.
However, many concerns regarding this context arose in the last two decades. In fact, despite the discovery of new hydrocarbon deposits and the development of technologies able to exploits oil fields previously considered as useless, the fossil

fuels are a finite resource on the earth. Their availability is estimated to last only few decades before they run out (54 years if the consumption rate is kept equal to the level of 2019 [3]) and their price increases with the complexity encountered for their extraction. In addition, the emissions of global warming gases due to the consumption of fossil fuels increased the consequences of the greenhouse effect, resulting in a worrying raise of the world's average temperature and serious damages on the environment's equilibrium [4]. The need for a sustainable energy production not based on fossil fuels is therefore out of the question.
The main strategies (with their corresponding benefits and challenges) identified to achieve the sustainability in the power sector are:

1. Demand reduction.
   It is very important to reduce the energy demand to the truly essential amount. This can be done by adopting a more rational approach to the use of resources, avoiding waste and introducing the concept of a circular economy in the energy sector [5].

   - Potentialities: in many cases, demand reduction can be achieved simply by changing habits and raising awareness among users. This means that physical changes to energy facilities/infrastructure may not be necessary.
   - Challenges: strategies based on demand reduction may be of difficult implementation since the coordinated operation of multiple subjects can be requested.

2. Efficiency increase.
   Noticeable efforts are put in the attempt to increase the performances of processes involving energy transformations [6]. Plants (and buildings) renovation with Best Available Technologies (BAT) or by modifying the current processes are among the alternatives to achieve this goal.

   - Potentialities: increasing the efficiency has as immediate consequence the reduction of the energy consumption.
   - Challenges: technical constraints, cost increases, complex designs and the need for advanced materials are some of the issues that could arise to improve the performances of an energy technology.

3. Develop new technologies.
   The development of new technologies is a key element for attaining high

efficiency in energy-related processes [7] and for exploiting as much as possible the available RESs and waste heat. In fact, old technologies can share techno-economical limits that cannot be overcome and the only alternative is to develop new devices or processes.

- Potentialities: new technologies can exploit resources that have not been utilized.
- Challenges: the development of novel technologies requires noticeable efforts, both in terms of money and time.

4. Energy transition.
   The previous considerations can provide an important help to face the issues arising in the energy sector, but the fundamental role is played by the substitution of fossil fuels with renewable sources [8]. This would allow not only to reduce, but to avoid the emissions of gases that have an impact on the green house effect.

   - Potentialities: renewable sources are available freely and in very high amounts. Their geographical distribution is more uniform compared to the fossil fuels [3], which can help to reduce the energy dependence of several countries.
   - Challenges: most of the renewable sources are available intermittently and their energy density on the territory is relatively low.

The economic plans involving unprecedented amounts of funds can be taken as demonstration of the commitment of many countries (especially the wealthiest ones) to the implementation of the energy transition. To provide an order of magnitude, the International Energy Agency (IEA) calculated that, just in the period from 2020 to June 2023, 1.34 trillion of USD has been allocated on global scale for clean energy investment support [9].

The power sector is a wide and complex field that can be imagined as structured on three main levels, as visually represented in Figure 1.1. The main actors playing in the energy sector are: a) the energy producers; b) the energy consumers; c) the transportation infrastructures; and d) the energy storage. Together, these components form an energy system, an example of which is shown at the top of the figure.
The following level constituting the power sector concerns the single units of the

system. The producers are the most important elements since they generate the electricity required by the consumers and each of them can carry out this task relying on different technologies. Focusing the attention on a single power plant, the energy production is performed by a series of devices which carry out different processes (energy conversions, thermodynamic transformations, etc.). The example of a thermal cycle is proposed in the center of the figure.
The last level is represented by the single energy devices, which are made by multiple parts and pieces. At this level the components physically execute the energy processes that allow the operation of the device and, as a consequence, of the system in which they operate. An example of energy device is shown at the bottom of the figure.

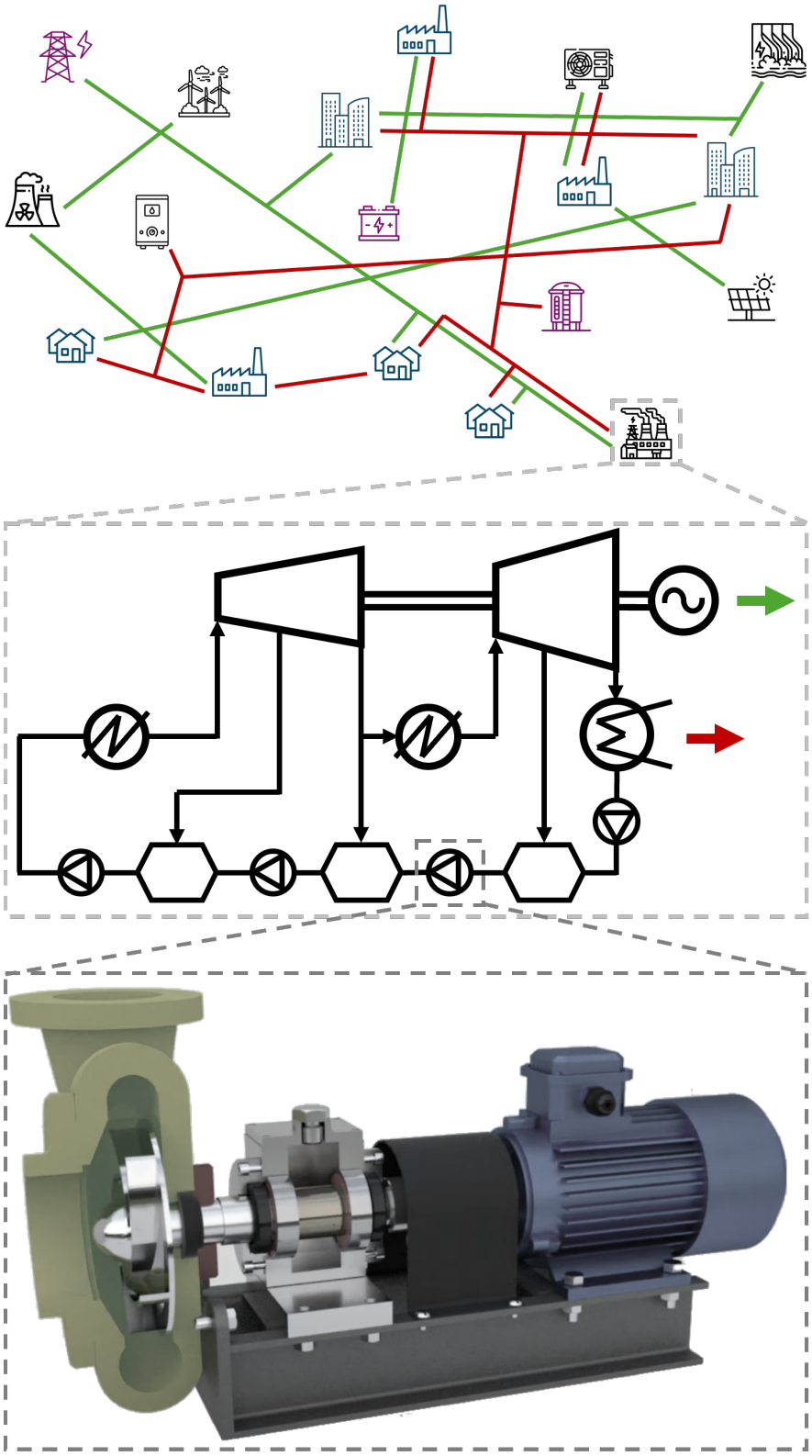

Fig. 1.1 The most important levels in the field of energy engineering

The existence of a mutual dependence among these levels is therefore obvious and, being nested within each other, their relation follows a hierarchy. A high number of decisions must be taken to design and operate the elements constituting each of the three layers, which means that these layers represents a problem to be addressed and solved. The scale characterizing the layers is very different (in terms of both space and time) and, as a consequence, the size of the corresponding problems will be different as well. In addition, the nature of the problems themselves will be differently, since the physical phenomena ruling the layers are not the same.

The research presented in this thesis is focused on the first two layers of the energy sector. This choice was made because, as will be discussed more in detail in the following sections, these are the fields that most require the development of optimisation models.

1.2 Thesis goals

International and intergovernmental institutions such as the International Energy Agency, Intergovernmental Panel on Climate Change (IPCC), and United Nations (UN), as well as the scientific community, have been conducting researches in the last decades to find out the possible directions that the modern society should follow to achieve the environmental sustainability. The objectives of the energy transition are clear but the concrete way to achieve them is still unknown, since it requires to solve new issues that have never been addressed before. There are still many steps to be taken, and among the most important ones there are:

1. Adopting models for the simulation and optimization of energy technologies. The development of advanced devices is almost impossible without the previous development of mathematical models able to simulate the expected operation. At the same time, it is important to assess that the novel technology is optimally created in terms of synthesis, design and operation. For this reason it can be advantageous to build an optimization model in addition to the simulation model.

2. Developing models for the optimization of Multi Energy Systems (MESs). A MES is composed by a set of technologies cooperating to produce multiple energy vectors to cover the demand of the users. For each technology it is

possible to install multiple units of different size. As a consequence, the technologies to use in the energy production, the number and size of the units, and their operation schedules are choices that must be taken with the aim of obtaining an optimal configuration.

3. Dealing with the intermittency of renewable sources.
   The availability of most of the renewable sources is intrinsically fluctuating in time and cannot be decided a priori. This aspect is a crucial issue for their integration in the production side, since it becomes more difficult for energy infrastructures and energy systems to guarantee the satisfaction of the demand and the stability of the operation. Accurate forecast models, energy storages and operation optimization models are therefore needed to properly address the inclusion of renewables and address the energy transition.

4. Ensuring adequate energy, economic and CO_2 payback times.
   The renovation of the production system must be conducted in a coherent way. To ensure the usefulness of the energy transition it is important to guarantee that the payback time of the operations performed is sufficiently short. In this case, the most important perspectives to evaluate the payback time are the energy, economic cost and CO_2 emissions.

5. Developing new policies.
   The motivations underlying the energy transition are clear and compelling, but they are not entirely sufficient to determine a spontaneous decision by the various actors in the energy sector to implement the necessary measures. Further actions are required at governmental level, especially in terms of policies. Laying down obligations, allocating incentives and modifying taxation are some of the actions that can be taken to enhance the economical advantage in the implementation of the energy transition.

Among these key aspects, it was chosen to focus the attention on the first three, which can be considered as the most fundamental ones from an engineering point of view.

In general terms, the aim of the present thesis is to provide a contribute in the research for optimization models in the framework of the development of new energy technologies and the operation of Multi Energy Systems. As can be easily imagined, simulating and optimizing an energy application is a very different task if the case

study under consideration is a single energy plant (or technology) rather than an entire energy system. For this reason, it was decided to develop two separate approaches for the two research objectives.
With the aim of following the path identified for achieving the energy transition, the integration of renewable sources is addressed in both the frameworks investigated.
An important scope of this thesis was to conduct researches and develop models with an approach aimed to reach a comprehensive treatment. This effort was intended to be done since the inclusion of as many aspects as possible increases the quality and realism of the analysis carried out.
With a similar purpose, the optimization models were developed with the aim of obtaining approaches that cover a wide range of energy system components and processes and can be adopted regardless of the specific case studies they refer to.
A final scope of this research was to develop models that allow to optimize the systems under consideration from different perspectives (e.g. energy efficiency, economic costs, etc.), which can be considered as an extension of the aim of performing a comprehensive treatment.

1.3 Novelties

The research conducted and discussed in this thesis presents some interesting novelties. The model developed for the optimization of single energy technologies is applied to a very innovative Concentrated Solar Power (CSP) plant with a thermochemical energy storage. Regarding the investigation on Multi Energy Systems, the comprehensive literature review conducted to identify the state of art of the research is presented from a new perspective, which is the one of the mathematical formulation of the models. Finally, the most important novelty of the optimization processes developed in the MES field is represented by the inclusion of the thermal network and other flexibility sources in the model, which allow to achieve a more realistic simulation and more reliable results.
A more detailed discussion of these elements of novelty can be found at the beginning of the corresponding sections.

1.4 Structure of the thesis

The outline of the thesis is discussed below and for each of its sections an explanation of the related contents is reported.

In Chapter 2 the methodology for optimizing a power plant or a single energy technology is presented. A model was developed to perform a comprehensive optimization of an innovative CSP plant with a thermochemical storage based on Calcium-Looping. This case study was selected because of its complexity, which allowed to address in the model all the most important features that can be found in this kind of problems. In addition, being an interesting and novel technology, different alternatives for the CSP-CaL integration were investigated and the results are discussed and compared.

In Chapter 3 a detailed literature review of the optimization of Multi Energy Systems is reported with the aim of obtaining an overview on the state of art in this wide research field. Particular attention was paid to the aspects related to the development of the optimization models form a practical perspective, analyzing the impact of the characteristics addressed to increase the realism of the MES's simulation on the problem's nature and its mathematical formulation. In addition, the literature gaps were identified, providing useful hints for possible future developments in this field.

Successively, a first attempt to integrate the simulation of a thermal network in the operation optimization of a MES is presented in Chapter 4. Coherently with the case study taken under consideration, the network is simulated with some simplifications and both the mass flowrates and the temperatures are included in the optimization. This approach was based on an iterative process on the decomposed problem and allows to find high-quality near-optimal solutions in relatively short times.

In Chapter 5 another methodology was developed in order to reach a more realistic treatment, considering the coupled operation of a MES and a District Heating Network. The quality of the simulation of the system was improved by removing the simplification hypotheses adopted in the previous analysis, and some measures to increase its flexibility were adopted. The optimization structure developed relies on two nested processes, where both deterministic and heuristic solvers are exploited in order to deal with the high complexity characterizing the operation problem.

In Chapter 6 the conclusions of the thesis are presented, summing up the research conducted, the main results obtained and the final considerations. In addition, some hints for possible future developments of this research are provided.

A visual representation of the structure of the thesis is provided in Figure 1.2 in order to clarify the organization of the dissertation. Here, the structure of the discussion is in accordance with the topics addressed and the related chapters of the thesis.

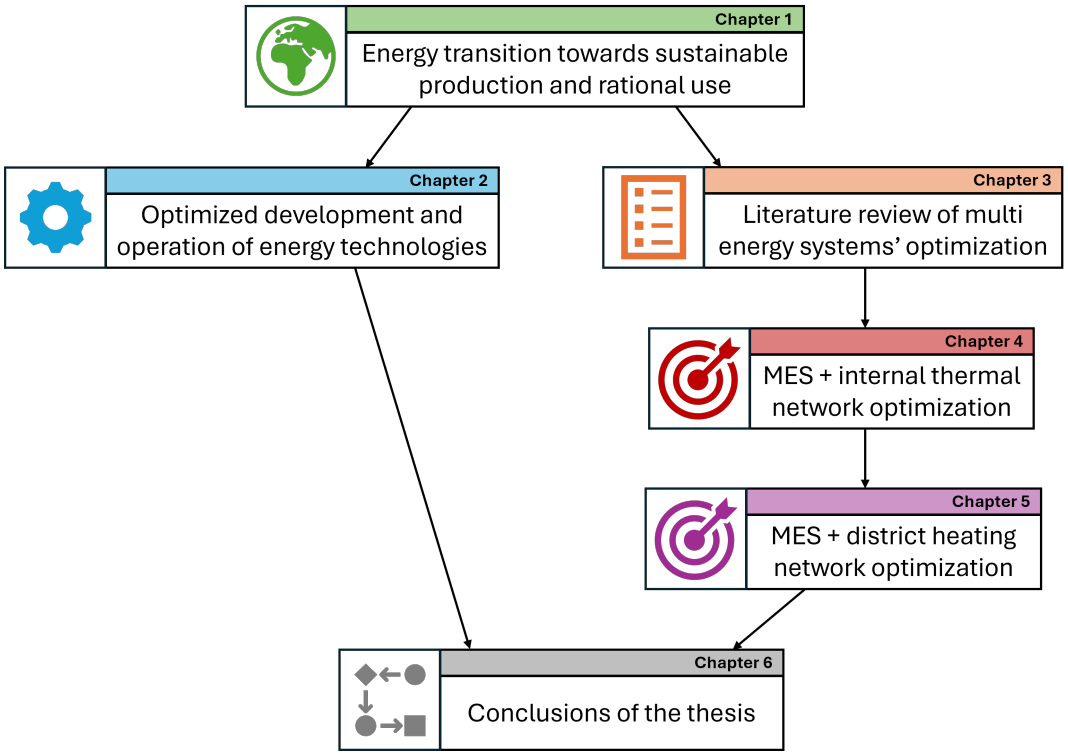

Fig. 1.2 Structure of the thesis

Chapter 2

Optimization of energy technologies

This chapter is devoted to the research conducted in the field of the optimization of energy plants or technologies. For first, the framework is introduced and discussed in section 2.1, then, the case study adopted is presented in section 2.2, while the methodology developed for its optimization is reported in section 2.3. The optimization model is adapted and executed for some applications presented in sections 2.4-2.7 and the final comparisons and conclusions are reported in section 2.8.
The structure of this chapter is visually represented in Figure 2.1 to provide a clear and immediate idea of the discussion addressed in the following sections.

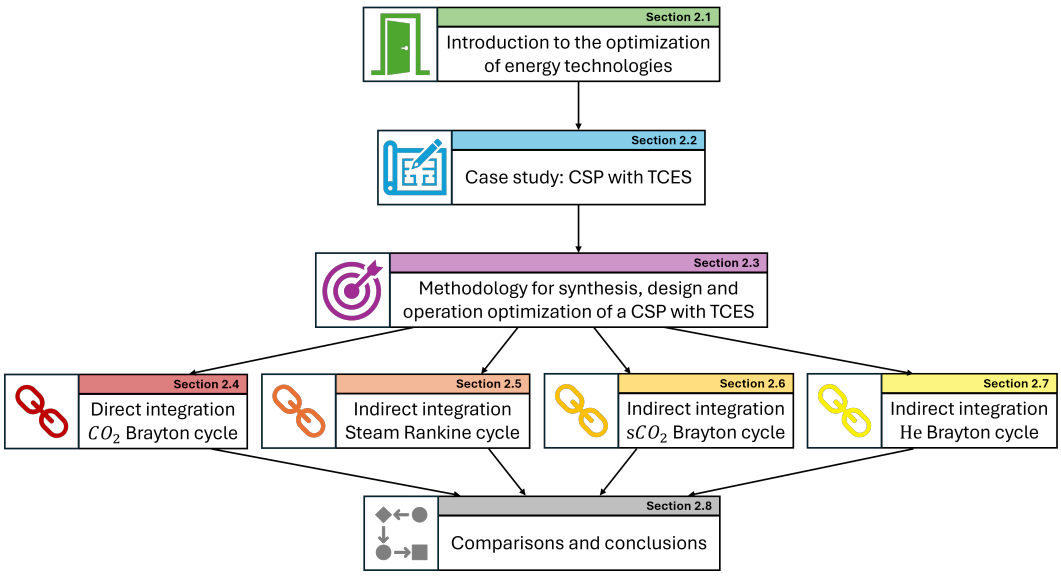

Fig. 2.1 Structure of the discussion conducted in Chapter 2

Part of the research presented in the present Chapter was published in Energy Conversion and Management [J1-J3], Energy [J4], and E3S Web of Conferences [C1].

2.1 Introduction

This chapter has the aim of presenting the research conducted in the framework of the synthesis, design and operation optimization of an energy plant. The general context is introduced in subsection 2.1.1, the main features, advantages and issues of this framework are highlighted in subsection 2.1.2. Successively, an overview of the most commonly used strategies for the optimization is provided in subsection 2.1.3 and the aims of the study are presented in subsection 2.1.4.

2.1.1 General framework and motivations

Increasing the efficiency of energy processes or developing new energy technologies is, in several cases, a complex task. Some of the most relevant examples in the energy engineering field are: operation of power plants; smart grids management; topology of energy networks/infrastructures; location of power plants. One of the main reasons behind their complexity relies in the necessity to deal with a large number of degrees of freedom. In other words, it is required to make numerous decisions, which deeply influence the resulting process in terms of efficiency, economic costs, environmental impact, reliability, etc.
Another source of complexity can arise from the necessity to create a model for the simulation of the device (or process) under consideration. This step is mandatory if an optimization must be carried out and it can create considerable issues if the process that must be simulated has a complex nature (e.g. a model that require Computational Fluid Dynamics simulations or other computationally expensive processes).

Sensitivity analysis is the simplest approach that can be followed in this kind of decision-making processes. It consists in studying how the variation of some parameters (or input data) influences the application considered. Therefore, it is simply performed by running multiple simulations executed with the same inputs except for the parameter whose impact on the outputs is under study. Sensitivity

analysis is not considered an optimization method because it only allows to explore a limited (and predefined) number of cases.

When a coherent optimization is intended to be performed, it is necessary to develop (or exploit) a suitable algorithm. The development (or adoption) of an optimization algorithm must be made according to the features characterizing the problem that is intended to be solved. The main aspects that must be taken into account in this case are discussed in the following subsection.

2.1.2 Features and objectives

One of the first aspects that must be defined in the development of the optimization method is the extent of the optimization itself. This means that it must be clarified if the goal of the optimization concerns synthesis, design [10] or operation [11]. In particular:

- the synthesis problem consists in the choice of the devices/technologies that will be used in the process;
- the design problem requires the definition of the locations, connections and sizes of the devices;
- the operation problem defines how the selected components are operated.

Synthesis, design and operation can be considered as different layers composing the structure of the problem, strictly linked between them, and the order in which they are mentioned corresponds with their hierarchy. Developing a method that addresses simultaneously these three aims allows to achieve a comprehensive optimization, since the energy technology is created or improved in the most proper way under different perspectives.

Once that the extent of the problem is set, the objective function can be addressed. As already mentioned, there are no limits on the nature of the optimization criterion, nor on its number. Single and multi objective optimizations can be carried out and the most common purposes are efficiency maximization, economic costs minimization, and CO_2 emissions minimization.

The last step of the problem formulation consists in identifying the independent variables [12]. As will be discussed shortly, this is an important phase since their

choice has a strong impact on the mathematical formulation of the problem.
On a practical point of view, the input data and the optimization variables are sufficient to build the simulation model of the process that is intended to optimize. The process is usually simulated by computing dependent variables and other outputs, in addition to the addressing of constraints.

When dealing with energy technologies, thermodynamic transformations of fluids and electrical conversions are usually involved. According to the processes executed in the operation and the characteristics of the energy plant, several issues can arise in the development of the optimization model. Among the main ones, there are:

1. the impossibility to explicit the mathematical formulation. The most common case in which this happens is when non-ideal fluids are involved in the thermodynamic transformations, since the thermophysical properties cannot be analytically expressed and suitable databases must be employed for their computation. As a result, a reduced number of solvers can be used to carry out the optimization since they must be able to handle implicit formulations adopting a black box approach;

2. the presence of nonlinear and non-convex terms, which increases the complexity of the problem and (usually) does not allow to ensure the achievement of the global optimality. Also in this case, specific solvers must be used for the optimization of these problems.

2.1.3 Existing strategies

Before introducing the case study analysed in the present thesis and the corresponding methodology, a short but useful overview of the most common strategies found in the scientific literature is provided. Most of the optimization models for technologies based on thermodynamic cycles are structured with a black-box approach [13]. This choice is justified by the complex non-convexity forms that are usually present in these problems and by the impossibility to formulate the complete problem in an explicit form, since the thermophysical properties of non-ideal fluids must be computed with devoted libraries. As a consequence, metaheuristic methods are by far the preferred ones. Genetic Algorithm (GA) [14] and Particle Swarm Optimization (PSO) algorithm [15] are the most commonly employed, but there are many other options,

such as Artificial Neural Network (ANN) method [16], Simulated Annealing (SA) [17], Artificial Bee Colony (ABC) algorithm [18], etc. The same solvers are used for optimizing technologies operating with renewable sources, as well as for energy technologies that do not involve thermodynamic processes, for example PhotoVoltaic (PV) power stations [19], wind farms [20], hydroelectric plants [21], and Electric Vehicles (EV) [22]. Metaheuristic solvers cannot ensure global optimality and are only able to deal with problems with relatively small dimensions (order of $10^0 \div 10^1$ variables), but they show good capabilities in exploring the domain and escape local optima.

Optimisation processes are usually developed according to the nature of the application formulation, but in some cases the formulation can be rearranged to allow the use of a methodology that is considered as more appropriate. A typical example consists in applying simplifying assumptions with the scope of removing some of the non-linear and/or non-convex terms, at the price of an impact on the simulation accuracy and the optimization extent. The advantage of this approach is that it allows to use deterministic methods for the optimization (e.g. [19] and [23]), which are, compared to the metaheuristic ones, faster, more accurate and capable to deal with higher number of variables. The choice of the deterministic algorithm is based on the nature of the problem: the Simplex algorithm is typically used to solve linear problems, while nonlinear convex problems can be addressed with gradient methods and interior point methods (which are used as well for non-convex methods but with proper arrangements).

The choice between deterministic and metaheuristic methods is also influenced by the extent of the optimization itself. Usually, the synthesis and design problems do not entail the addressing of a considerable amount of variables, since they are proportional to the number of components involved in the process. On the other hand, optimising the operation problem can be much more computationally expensive. In fact, the time period considered in the analysis is discretized in a series of timesteps and for each of them a complete set of operation variables must be defined. Therefore, the choice of the optimization extent has an important impact on the problem size and, consequently, on the decision for the method to use for the optimization execution.

Finally, tailored optimization methods can be developed for specific branches of the energy framework. The most representative example is the pinch analysis [24], which is a technique to minimize the thermal demand of industrial processes and

to design optimal Heat Exchanger Networks (HENs). Therefore, the objective is predefined and the method is not suitable for other kinds of applications since the algorithm was developed for this specific goal.

2.1.4 Aims of the present study

The aim of the present study is to identify a methodology to optimize the synthesis, design and operation of an energy plant. The main aspects characterizing these systems must be included in the analysis, such as technical constraints, heat transfer processes, and layout connections. In order to be as versatile as possible, the resulting methodology should be applicable to case studies different from the one considered for its development, giving at the same time the possibility to choose between single-objective and multi-objective optimization, according to the desired level of analysis that is intended to be reached. The application fields of the methodology developed will be discussed in the final sections of this study.

2.2 Concentrated Solar Power plant with Thermo-Chemical Energy Storage

The purpose of this part of the research is to investigate, develop or adapt a method to perform an optimization as comprehensive as possible of an energy technology. The innovative ThermoChemical Energy Storage (TCES) based on Calcium-Looping (CaL) for a Concentrated Solar Power (CSP) plant results to be a very suitable case study, since it presents all the aspects whose inclusion would be interesting to be evaluated. Among these there are: nonlinear and non-convex terms; implicit formulation of the problem; the addressing of the synthesis, design and optimization problems; the simultaneous presence of thermodynamic transformations, heat transfer processes and power generation. Succeeding in addressing its optimization would allow to obtain a method that can be used for almost any other energy technology, since the case study considered is characterized by all of the complex aspects that usually characterize these systems.
The case study analysed in the present thesis is presented in subsection 2.2.1, while a review of the scientific literature is provided in subsection 2.2.2.

2.2.1 Technology description

CSP is a technology that collects and concentrates the solar radiation with a heliostat field and converts it into heat to produce electricity with a thermodynamic cycle [25]. One of its most interesting potentialities is represented by the possibility to reach high temperatures, which can allow to exploit performing power cycles [26]. On the other hand, the fluctuations characterizing the availability of the solar radiation constitutes an issue for achieving a dispatchable power production [27]. Energy storage is the most suitable solution to this problem and a wide range of alternatives for its implementation are available [28].

Chemical looping is a process based on a reversible chemical reaction of oxidation and reduction. This process generates or absorbs energy depending on whether the exothermic or endothermic reaction is performed. This characteristic allows to exploit the chemical looping to store energy in chemical form: providing thermal energy to perform the endothermic reaction, it is possible to obtain and store the products until the exothermic reaction is carried out, getting back the energy previously supplied. Thanks to its characteristics, Calcium-Looping (CaL) is among one of the most interesting alternatives. In this case, the endothermic reaction is called calcination, while the exothermic reaction is named carbonation. Consequently, calciner and carbonator are the two chemical reactors where the two reactions take place.

$$Calcination \quad CaCO_{3(s)} + HEAT \rightarrow CaO_{(s)} + CO_{2(g)} \quad \Delta H_r^0 = 178\ kJ/mol \quad (2.1)$$

$$Carbonation \quad CaO_{(s)} + CO_{2(g)} \rightarrow CaCO_{3(s)} + HEAT \quad \Delta H_r^0 = -178\ kJ/mol \quad (2.2)$$

As reported in Equations 2.1 and 2.2, the compounds participating in the process are: calcium oxide (CaO) at solid state; calcium carbonate ($CaCO_3$) at solid state; and carbon dioxide (CO_2) at gaseous phase. The molar enthalpy of reaction is reported as ΔH_r^0. To ensure an adequate rate of reaction it is important to maximize the reactants' contact surface, which is done by reducing the solid phases into powders. The relation between the pressure and temperature at the equilibrium conditions is described by Equation 2.3 [29], where $P_{CO_2,eq}$ is the partial pressure of the CO_2 (in

bar) and T_{eq} is the temperature (in K).

$$P_{CO_2,eq} = 4.137 \cdot 10^7 \exp\left(-\frac{20474}{T_{eq}}\right) \tag{2.3}$$

The same thermophysical relation is presented in graphical form in Figure 2.2, where the chart axes (temperature and CO_2 partial pressure) are in logarithmic scale and the line represents the equilibrium conditions between the two reactions. The carbonation reaction takes place spontaneously in the region above the curve and the opposite happens for the calcination, with a reaction kinetics that increases with the distance from the equilibrium conditions. In correspondence to partial pressures that are commonly achieved in industrial chemical processes the equilibrium temperatures are in the range between 600°C and 1000°C. As a consequence, the CaL results to be an interesting option for TCES because of the capacity to provide heat at high temperatures during the discharging phase, that allows to achieve high power production applications.

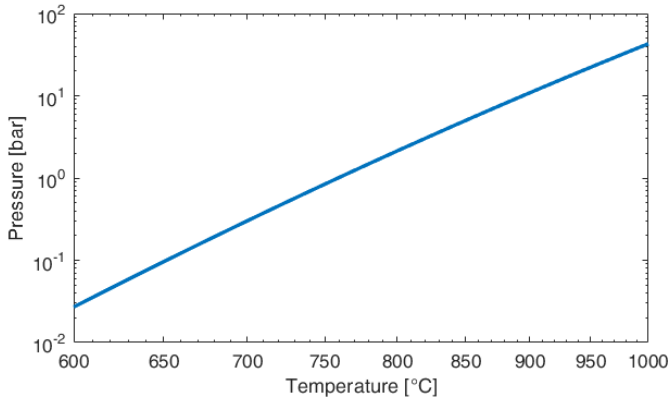

Fig. 2.2 Pressure-temperature equilibrium conditions for calcination-carbonation reactions

Until the last few years, the Calcium-Looping technology was mainly investigated in the field of Carbon Capture and Storage (CCS) [30], where it encountered some barriers due to the disadvantageous operating conditions occurring in the CCS application. However, considering the high operating temperatures and the possibility to operate as TCES, is currently analyzed combined with Concentrated Solar Power plants. The concept at the base of its integration in the CSP plant is showed in a simplified form in Figure 2.3. The solar radiation that is reflected and concentrated by the heliostat field on the solar receiver (located at the top of the central tower)

provides the energy required to carry out the $CaCO_3$ calcination, which constitutes the charging process of the TCES. The two products of the calcination (CaO and CO_2) are stored at ambient temperature until they are used to perform the carbonation, where the heat released by the exothermic reaction is exploited in a thermal cycle to generate electricity. As will be discussed further on, according to the type of CSP-CaL integration, the power generation can be entrusted to a separate power block or can be jointly performed with the carbonation process. For both the calcination and carbonation, the reactants and products are respectively preheated and cooled to obtain a heat recovery and increase the performance of the process. In addition, it is necessary to compress/expand the CO_2 before/after storing it, in order to reduce the volume of the storage itself. For simplification purposes, the compression and expansion stages are not reported in Figure 2.3. To facilitate the discussion and refer more immediately to the different plant sections, the system has been conceptually divided into some parts, as can be seen in the figure. These are: solar side, calciner side, storage side, carbonator side, and, if present, the power block side.

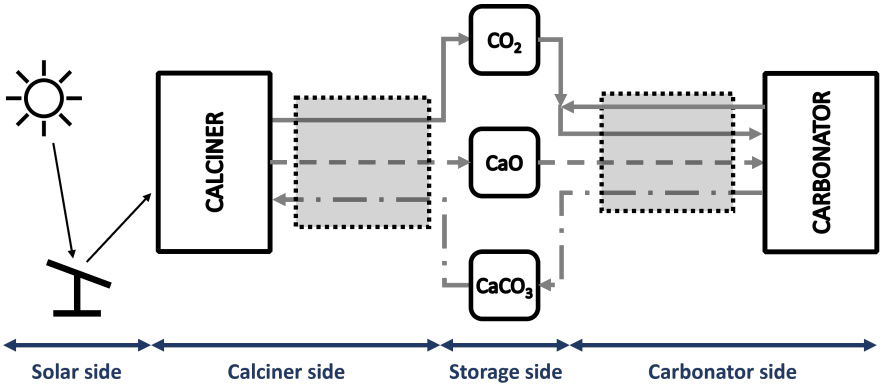

Fig. 2.3 Basic conceptual scheme of CaL-CSP integration

The reason why it is interesting to investigate the CSP-CaL integration is that it has some noticeable advantages. Among these there are:

- $CaCO_3$ can be obtained from limestone, which is an abundant, non-toxic and cheap material [31]. In addition, eventual waste of $CaCO_3$ or CaO can be profitably discarded by creating synergies with the cement industry. These aspects are important in the perspective of developing a sustainable technology, both in environmental and economic terms;

- the chemical compounds participating in the chemical looping can be stored at ambient temperature, avoiding thermal losses [32]. To do that, it is necessary to perform a heat recovery on the products of the reactions, with the additional advantage of increasing the performance of the process;
- the possibility to reach high efficiencies by attaining high temperatures in the charging and discharging phases, as well as exploiting performing power cycles [33];
- the energy density can reach very high values [34], allowing to keep relatively small dimensions of the storage vessels.

On the other side, there are some issues affecting the CaL that must be faced in order to successfully apply this technology in the industry of the energy storage. Despite being known from some decades [35], the CaL have not found an application field in which it has been widely exploited. Some components used in other industrial processes (e.g. fluidized bed reactors, solid-solid heat exchangers) can be also used in the CaL process but their effectiveness in operating in this context has yet to be verified. Another important issue is due to the CaO deactivation. This is a complex phenomenon [36–38] that can be briefly explained as the degradation in the capacity of the CaO to completely react with the CO_2 in a fixed time period of the carbonation reaction. The reasons for this are the pores clogging and the sintering of the CaO grains, both due to the effects of high temperatures. CaO deactivation has therefore an impact on the CaL process and can be quantified by a parameter called CaO reactivity, also referred as X. The ratio represented by the CaO reactivity is reported in Equation 2.4. A high value of X must be preferred since it reduces the amount of inert CaO that participates to the carbonation, increasing the process efficiency. Studies on the CaO reactivity reduction during the calcination-carbonation cycles show that values between 0.2 and 0.5 can be assumed for the CSP-CaL integration, according to the CaO precursor selected [39].

$$X = \frac{moles\ of\ reacted\ CaO}{stoichiometric\ moles\ of\ CaO} \tag{2.4}$$

2.2.2 Integration alternatives and literature review

The Thermo-Chemical Energy Storage (TCES) based on Calcium-Looping can be both directly or indirectly integrated in a central tower CSP plant. It is worth to notice that the differences between these alternatives are only related to the plant section where the carbonation is carried out, since the storage vessels of CaO, CO_2 and $CaCO_3$ decouple the charging and discharging processes. In other words, the storage side makes the operation of the calciner side and carbonator side independent between them.
Before presenting the integration alternatives, a short description of the calciner side is provided. The solid stream made of both $CaCO_3$ and unreacted CaO is extracted from its storage and, after a preheating process, enters the calciner reactor. Under pure CO_2 atmosphere at ambient pressure, calcination temperature has to be around 930–950°C to ensure complete calcination in short residence times [40]. Lower calcination temperatures are needed by performing the calcination under He or steam [41–43], although in this case the energy penalty could be higher due the energy consumption of the separation process. After calcination, CO_2 and CaO are cooled down and sent to their storage vessels. To reduce the storage tanks size, CO_2 is compressed up to its design pressure of 75 bar [44, 45] and, in order to minimize the compression work required, one or more inter-cooling steps can be included. In addition, the carbon dioxide is re-expanded and part of the energy previously consumed in the compression process is recovered, reducing considerably the energetic penalty brought by the compression itself [46].
Concerning the CaL-CSP integration, the two alternatives are presented below with their respective literature review. Their treatment is more focused on the carbonator side (and eventually on the power block side) since, as already discussed, it is the only part that presents differences among the integration alternatives.

- Direct integration
  The operating principle at the base of the direct integration relies on the fact that the power fluid enters the carbonator and directly absorbs the heat released by the exothermic reaction. Successively, the power fluid is expanded in a turbine to convert this thermal energy into electricity. The thermodynamic cycles adopted in this case are two: closed CO_2 and open air/CO_2 Brayton cycles. Figure 2.4 shows the conceptual layout (without the heat exchanger networks) of the closed CO_2 direct integration, which is the most interesting

alternative. In the CaL discharge process, CO_2 is extracted from the storage tank, heated and expanded in the Storage Turbine (ST) up to the carbonator operating pressure. In order to maximize the expansion work, one or more reheating steps can be added. The other reactant, the CaO, is preheated and sent to the reactor to produce calcium carbonate according the exothermic reaction. After carbonation, solids are separated from the gaseous stream and the CO_2 is expanded in the Main Turbine (MT); then, sensible heat is recovered from both CO_2 and solids streams. Finally, the carbon dioxide stream enters the Main Compressor (MC) and it is recirculated inside the process, while the $CaCO_3$ and the unreacted CaO are sent to their storage vessel.

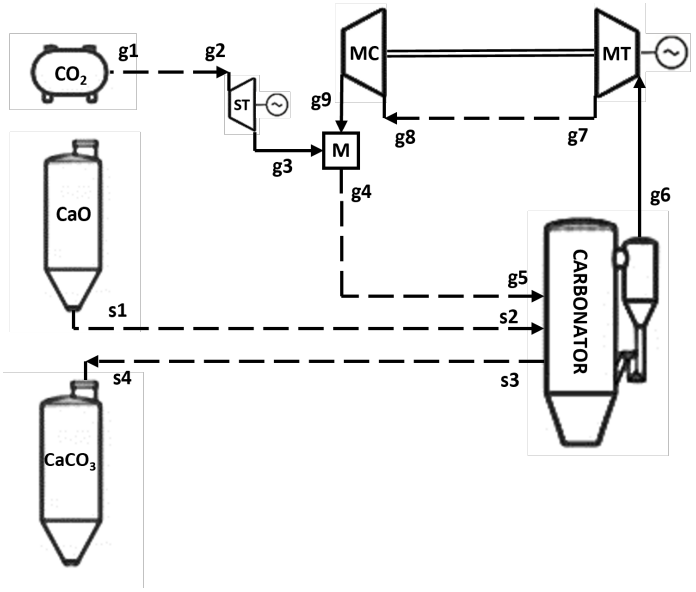

Fig. 2.4 Base layout of direct integration without heat exchanger network

Optimal operating conditions for the closed CO_2 direct integration with energy storage at ambient temperature are investigated in [46, 47, 44] through both pinch analysis and sensitivity analysis. The addition of a Rankine cycle fed by the calciner CO_2 outflow and high temperature solids storage is studied in [48], where high efficiencies are obtained despite the necessity to assume a low CaO activity value (0.15). Furthermore, a study for the adoption of a CaL direct integration for the storage of the electricity surplus produced by photovoltaic fields is performed in [49], demonstrating a significantly lower plant investment cost when compared to batteries. Concerning the open air/CO_2 Brayton cycle, it was proposed and investigated in [50] and, although

its good performance, the drawback of carbon dioxide emission in the ambient affects the plant operation because of the carbonation carried out under a non-pure CO_2 reactor atmosphere, representing an intrinsic drawback for this alternative.

- Indirect integration
  The indirect integration includes a separate power block. The heating power is provided to a thermal cycle through a heat exchanger and this allows to have a higher degree of freedom in the choice of the power fluid and in the layout of the thermal cycle. In addition, the operating pressures are not constrained by the pressure attained in the carbonator. Figure 2.5 shows the basic layout of the carbonator section for the indirect integration, without reporting the HEN and the power block. The discharging process starts by preheating the CO_2 and the CaO extracted from their respective storage. Once that the CO_2 is expanded in the Storage Turbine (ST) to reach the carbonator operating pressure, the two reactants enter the carbonator. At the exit section, both the carbonator outflows are cooled down and the $CaCO_3$ (together with the unreacted CaO) is sent to its vessel while the CO_2 in excess pass through a Blower (B) and is recirculated in the process. In order to perform an analysis as comprehensive as possible, two alternatives are taken into account to supply heat to the power block. In the first case, a Heat Recovery is performed on the Carbonation Products (HRCP configuration, A in the figure), while in the second case a Heat Transfer is executed on the Carbonator Wall (HTCW configuration, B in the figure).

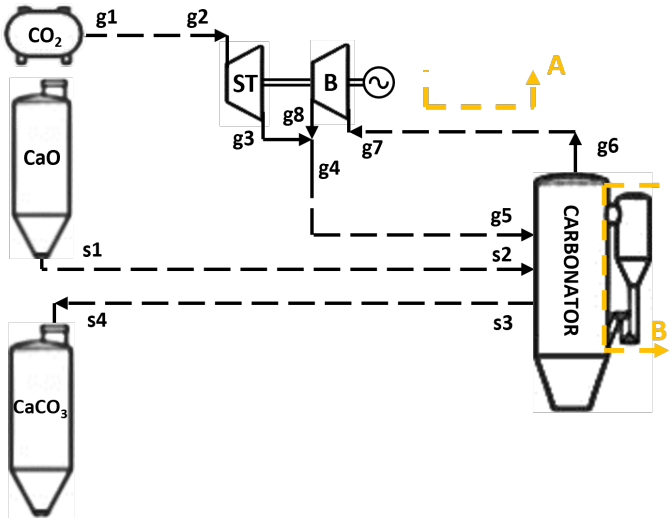

Fig. 2.5 Base layout of indirect integration without heat exchanger network

The Steam Rankine cycle (SRC), the supercritical CO_2 (sCO_2) Brayton cycle and the combined cycle are analyzed in [44] as possible candidates for this kind of integration. Despite the sCO_2 power block reaches the highest efficiency, it results to be the least performing option when integrated in the CaL process. This happens because the total integration efficiency depends on the performances of both the power cycle and the thermal transfer process conducted in the carbonator side. However, in this case it is assumed that the thermal cycle is fed only by the gaseous carbonator outflow. An alternative CaL layout is investigated in [48], where the energy storage occurs at high temperature to simplify the process integration scheme. Similar to this last configuration, but with a more complex design, in [51] is analyzed the choice of a direct (closed CO_2 loop) or indirect (steam Rankine cycle) integration in series with an Organic Rankine Cycle (ORC) for the low-temperature heat recovery. It resulted that the advantage between the two alternatives depends on the operating conditions. A comparison of the works found in literature about this topic is provided in [31] with the addition of interesting comments.

2.3 Methodology

The methodology developed for the synthesis, design and operation optimization is reported and discussed in this third section. For first, the approach used to simulate

the processes and the components involved in the system is presented (2.3.1), then, the independent variables and the objective function to be optimized are discussed (2.3.2 and 2.3.3). Finally, the development of the optimization model is exposed in subsection 2.3.4.

2.3.1 Simulation model and assumptions

Before performing the optimization of a plant, it is necessary to be able to simulate its operation. For the sake of simplicity, the simulation of the plant sections shared by the different integration alternatives is exposed below, while the details related to the power blocks and their integration are reported in the corresponding paragraphs of the next section. Since the analysis is intended to be conducted both in energy and economic terms, the cost functions assumed to compute the price of the components are reported together with the equations for the simulation of their operation.

Carbonator side

The chemical reactor is modelled with the same energy balance set in [46], which simply accounts the sensible heat of the compounds involved in the reaction and the heat of reaction made available by the carbonation. This balance is reported in Equation 2.5, where F is the molar flowrate, Φ_{disp} is the dispersed flux, and $\Delta H_R(T_{crb})$ is the molar heat of reaction as a function of the carbonation temperature (T_{crb} in $[K]$). This last term is computed as reported in Equation 2.6. The reaction kinetics is not investigated because this aspect is not among the purposes of the present work. The chemical composition of the outlet substances is assumed as known, meaning that the degree of reaction is imposed. The analysis of the carbonator side (as for the power block) is conducted assuming a stationary operation.

$$F_{CaO_{in}}\overline{c_p}_{CaO}(T_{crb}-T_{CaO_{in}})+F_{CO_{2,in}}\overline{c_p}_{CO_2}(T_{crb}-T_{CO_{2,in}}) + F_{CaCO_{3,out}}\Delta H_R(T_{crb})=-|\Phi_{disp}| \quad (2.5)$$

$$\Delta H_R(T_{crb})=\Delta H_R^0+(\overline{c_p}_{CaCO_3}-\overline{c_p}_{CO_2}-\overline{c_p}_{CaO})(T_{crb}-298) \quad (2.6)$$

The compressions/expansions that take place in the compressors/turbines are simulated by imposing an isentropic efficiency for the turbomachinery, as synthetically reported in Equation 2.7. The corresponding electric powers are then computed with

Equations 2.8 and 2.9. Despite the main connections and processes of the carbonator side are defined, the mass flowrates of the reactants and products are required to exchange heat in order to enter in the main components at the correct temperature.

$$h_{out} = h_{out}(P_{out}, \eta_{is}) \tag{2.7}$$

$$|P_{el}^{turb}| = G(h_{in} - h_{out})\eta_{el} \tag{2.8}$$

$$|P_{el}^{comp}| = \frac{G(h_{out} - h_{in})}{\eta_{el}} \tag{2.9}$$

The layout and the size of the Heat Exchanger Network that tackles this task is not predefined and is part of the design problem. By arbitrary choice, the HEN is required to avoid the consumption of any external source of heat, in order to exploit only the renewable solar energy instead of additional fossil fuels. This task is addressed by the pinch analysis, which ensures the existence of a HEN with external heating and cooling demands that are obtained as a result of the pinch analysis itself. As will be later discussed, these external requirements can be changed such that the assumption of null heating demand is fulfilled.
Thermo-physical properties of the involved substances are taken from [52] for CO_2, [53] for CaO and [54] for $CaCO_3$. Any other data assumed for the simulation of the carbonator side operation is taken from [43, 48, 44] and reported in Table 2.1.

Table 2.1 Carbonator side data assumptions

Parameter	Component/stream	Value
Operation time	Carbonator side	24 h
CaO activity	CaO	0.5
Thermal losses	Carbonator	$1\% \cdot$ reaction heat
Isentropic efficiency	Storage turbine	0.8
	Blower	0.8
Electrical efficiency	Electric motor	0.98
Pressure losses	Mixed CO_2	6%
	Recirculated CO_2	4%
	Storage CO_2	1%
Storage temperature	Storage vessels	20 $°C$
CO_2 storage pressure	CO_2 Storage vessel	75 bar
Solid conveying electrical consumption	CaO, $CaCO_3$	$10\ kJ/(kg \cdot 100m)$
Storages-carbonator distance	CaO, $CaCO_3$	100 m
Heat rejection electrical consumption	Coolers	$0.8\% \cdot$ rejected heat
Minimum ΔT	Gas-gas HEXs HTF-solid HEXs	15 $°C$

Regarding the economic aspect, the cost functions (and eventual procedures) used for the estimation of the prices of the components involved in the operation of the plant section corresponding to the carbonator side are reported below. All the prices are discounted to 2018 with CEPCI index and expressed in U.S. Dollars (USD). In case the cost functions found in literature are not referred in USD, a ratio of 1.18 €/$ is assumed, corresponding to the 2018 average value [55].

- CO_2 turbomachinery
  Investment Cost (IC) associated to CO_2 turbomachinery operating at subcritical conditions (Storage Compressor and Storage Turbine) is estimated with the methodology proposed in [56] and reported in Equations 2.10 and 2.11. The idea behind this method is to define an equivalent configuration with air as working fluid. Operating temperatures, pressures and mass flow are computed

for this equivalent case and they are referred with the subscript *eq*.

$$IC_{turb,CO_2} = G_{eq,turb}\frac{492.2}{1-\eta_{is,turb}}\frac{TIP}{TOP_{eq}}\cdot \cdot \ln\left(\frac{TIP}{TOP_{eq}}\right)(1+\exp(0.036\cdot TIT-65.66)) \quad (2.10)$$

$$IC_{comp,CO_2} = G_{eq,turb}\frac{59.1}{1-\eta_{is,comp}}\frac{COP_{eq}}{CIP}\ln\left(\frac{COP_{eq}}{CIP}\right) \quad (2.11)$$

$$G_{eq,turb/comp} = G_{turb/comp}\frac{\rho_{eq,in}}{\rho_{in}} \quad (2.12)$$

$$\rho_{eq,out} = \frac{G_{eq,turb/comp}}{G_{turb/comp}}\rho_{eq} \quad (2.13)$$

Here, G_{eq} is the equivalent mass flowrate $[kg/s]$, η_{is} is the isentropic efficiency, TIP is the Turbine Inlet Pressure $[bar]$, TOP_{eq} is the equivalent Turbine Outlet Pressure $[bar]$, TIT is the Turbine Inlet Temperature $[K]$, CIP is the Compressor Inlet Pressure $[bar]$, and COP_{eq} is the equivalent Compressor Outlet Pressure $[bar]$. The equivalent mass flowrate is computed with Equation 2.12, while the equivalent outlet pressure is obtained through the CoolProp data library for air, imposing the equivalent density ($\rho_{eq,out}$ from Equation 2.13) and the temperature at the machinery outlet.

- CO_2 blower
  The cost of the CO_2 blower in the carbonator side is calculated with Equation 2.14, as proposed in [56]. Notice that the blower shaft power ($\dot{W}_{blower}$) is in $[kW]$.

$$IC_{blower} = 129520\left(\frac{\dot{W}_{blower}}{445}\right)^{0.67} \quad (2.14)$$

- Adiabatic carbonator
  In case that the heat of reaction is intended to be completely provided to the products of the carbonation, an adiabatic reactor must be chosen. In this case, the component price is proportional to its volume, which depends on the volume flowrate of the inlet streams. The cost function reported in Equation 2.15 and proposed in [57] for entrained flow (EF) reactors is assumed, where

$\dot{V}_{in}$ is the volume flowrate of the streams entering in the carbonator (in $[m^3/s]$).

$$IC_{EF,crb} = 106200 \ \left(\dot{V}_{in}\right)^{0.5} \tag{2.15}$$

- Electric generator
  The Electric Generator (EG) price is obtained with Equation 2.16, where the electrical power output ($\dot{W}_{el,EG}$ in $[kW]$) is taken as scaling parameter [58].

$$IC_{EG} = 106 \left(\dot{W}_{el,EG}\right)^{0.95} \tag{2.16}$$

- Heat exchangers
  The heat transfer between the CaL streams is performed trying to satisfy, whenever possible, two good practices [28]: first, avoid thermal transfer between solid streams and second, avoid splitting solid streams. Both of them are aimed to reduce the technical complexity of the plant operation and in case the first practice cannot be fulfilled, the heat transfer between the solids is performed with an auxiliary fluid circulated between two solid-fluid HEXs. For this reason, the thermal transfer between two solid streams will have a minimum temperature difference equal to the double of the value set in case of solid-fluid heat exchange.
  For the purposes of this analysis, only two types of heat exchanger are considered: fluid–fluid HEXs and fluid–solid indirect HEXs. Equation 2.17 provides the investment estimation related to the former category [56], while, according to authors knowledge, cost functions suitable for the cases analyzed in the present work referred to the second type are not found in scientific literature. A proper function (Equation 2.18) is therefore extrapolated from the study of a gas–solid exchanger [58] that fulfills the cost target set in the DOE SunShot project [59]. For this purpose, a function with the same mathematical form is used. However, since the prediction of the global heat transfer coefficient in case of thermal transfer between fluids and solids is more difficult, the product UA (in W/K) is set as one of the scaling parameters instead of only the heat transfer surface (A, in m^2). In this way, besides the operating pressure (P, in bar), its investment cost is proportional to the thermal power exchanged and

the logarithmic mean temperature difference (LMTD).

$$IC_{fl-fl,HEX} = 3197A^{0.67}P^{0.28} \tag{2.17}$$

$$IC_{fl-sol,HEX} = 18.48(UA)^{0.67}P^{0.28} \tag{2.18}$$

Heat transfer surfaces for fluid–fluid HEXs are computed assuming global heat transfer coefficients found in [60, 61, 56] and reported in Table 2.2. For the cooler/condenser sizing, the ambient air is assumed as heat sink with infinite thermal capacity.

Table 2.2 Global heat transfer coefficients for fluid–fluid HEXs

HEX/fluids	U $\left[\frac{W}{m^2K}\right]$
SRC economizer	250
SRC evaporator	200
SRC superheater	125
SRC condenser	150
$CO_2 - CO_2$	300
$CO_2 - sCO_2$	300
$He - He$	700
$CO_2 - He$	300
He – air	300
CO_2 – air	300

Storage side

As already mentioned, the three compounds participating in the Calcium-Looping are stored at ambient temperature. The volumes of the storage are obtained by computing the mass balance on vessels in the design day and assuming as design volume the value corresponding to the moment in which the mass stored reaches the highest level. The CaO and $CaCO_3$ storage investment costs are assumed as negligible because of their small size (due to high solids density), the absence of thermal insulation (reactants at ambient temperature) and the gauge pressure equal to zero. Consequently, in the present analysis the cost of the storage side is only related to the pressurized CO_2 vessel. It is worth to mention that, despite the solid compounds are stored at ambient temperature, it is possible to send them to their

relative vessels at a temperature close but not equal to the nominal value [46]. Since the storage vessels are not insulated, the residual sensible heat goes dispersed to the environment, avoiding the addition of a dedicated air cooler.

- CO_2 vessel.
  The price of the CO_2 vessel (Equation 2.19) for the storage at 75 bar is obtained with the procedure suggested in [62] for cylindrical pressure vessels. c_{ss} is the unit cost of Stainless Steel ([$\$/kg$] taken from [63] for 304L alloy), ρ_{ss} is the metal density ([kg/m^3]) and V_{ss} is the steel volume ([m^3]). The entire procedure is not reported here but further details concerning the calculation of V_{ss} can be found in [62].

$$IC_{CO_2,stor} = c_{ss}\rho_{ss}V_{ss} \tag{2.19}$$

Calciner side

The assumptions used for the simulation of this plant section are taken from [48, 51, 64, 65] and summed up in Table 2.3. The model developed in [46] is used to simulate the chemical reaction carried out in the solar calciner, while the electric consumption due to the solid lift in the central tower can be estimated as indicated in [65].

Table 2.3 Calciner side data assumptions

Parameter	Component/stream	Value
Operating temperature	Calciner	950 $°C$
Cut-in power	Calciner	$0.2 \cdot \Phi_{clc,des}$
Thermal efficiency	CPC	0.97
	Calciner	0.75
Isentropic efficiency	Compressors	0.8
Electrical efficiency	Electric motor	0.98
Compression intercooling stages	CO_2 compressor	5
Pressure losses	CO_2 coolers	1%
Solid conveying electrical consumption	CaO, $CaCO_3$	$10\ kJ/(kg \cdot 100m)$
Storages-calciner distance	CaO, $CaCO_3$	100 m
Heat rejection electrical consumption	Coolers	0.8%·rejected heat
Minimum ΔT	Gas-gas HEXs HTF-solid HEXs	15 $°C$

The calciner side simulation is performed with a fundamental simplifying hypothesis: the operating temperatures and pressures of the components involved in the charging process are stationary during the operation period. This is assumed by imaging that the flowrates are adjusted by a control logic that has the aim of keeping the operation temperatures of the calciner side equal to their setpoint value. Therefore, only the mass flow rates change proportionally to the solar radiation absorbed by the solar receiver. The heat exchangers are dimensioned for the rated power of the calciner side (i.e. the nominal thermal flux to the receiver). As a result, in case of lower heat inputs (and consequently lower flow rates), the HEN results to be oversized, leading to a more performing thermal transfer. The hypothesis of constant operating conditions for the Heat Exchanger Network is therefore precautionary and does not bring efficiency over-estimations.
In order to minimize the considerable compression power (CO_2 must be brought from 1 bar to 75 bar), the addition of inter-cooling stages is recommended [46]. Significant advantages are not encountered in the recovery of the heat generated by the compression, because of the low temperature at which it is available, its

relatively small amount and the complexity introduced in the layout structure. It is therefore assumed to release this heat to the ambient. According to [66, 67], the compressors' pressure ratio is imposed to be equal for all the stages, while the number of inter-cooling steps is subjected to the optimization process, as explained in the following section.

The thermal transfer between the reactants and products of the calcination is simulated through the pinch analysis. Due to the low number of fluids involved in the thermal transfer process, the fixed ratio between their mass flowrates and the assumptions made on the calciner side configuration, the HEN layout does not change with the operating conditions of the chemical reactor. As a consequence, for this plant portion it is possible to obtain the HEN layout before performing the optimization process. The resulting configuration of the calciner side is shown in Figure 2.6, where the inter-cooled compression is synthetically represented with a single compressor and cooler. As will be explained in the following chapter, the $CaCO_3$ split ratio has no impact in energy terms on the process, but it influences the HEN cost because of the change of LMTD occurring in the interested heat exchangers and it is therefore necessary to properly consider this phenomenon.

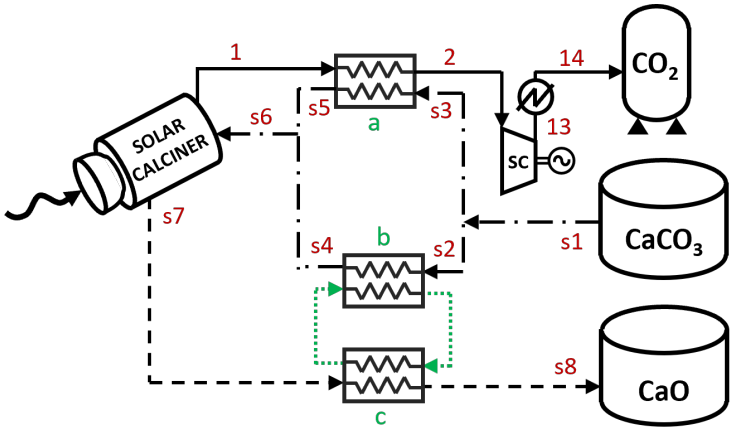

Fig. 2.6 Calciner side layout

Avoiding the thermal transfer between solids in the calciner side HEN is impossible, since there is only one cold stream to be preheated ($CaCO_3$ and unreacted CaO). As already mentioned for the carbonator side, heat transfer between solids poses technical problems, and the simplest way to carry it out is to use two fluid-solid HEXs that operate with a heat transfer fluid (shown in green in the figure) that is

circulated between the two units. Taking into account the temperatures reached, the fluid must be a gas, and the same LMTD can be imposed on the HEXs to obtain two equally sized units. The cost functions used for the HEXs and the Storage Compressors are the same reported in the paragraph devoted to the carbonator side, while the ones corresponding to the components which have not yet been mentioned are reported below.

- Solar calciner.
  Falling particle receivers, centrifugal particle receivers, fluidized bed receivers and rotary kilns are possible candidates as solar calciner [47, 31, 68]. Considering the required operating conditions (calcination carried out under pure CO_2), the technology state of development and the data available on the literature, a rotary kiln reactor with a Compound Parabolic Concentrator (CPC) is assumed as solar calciner [69, 70]. As suggested in [64], the calciner's investment cost is computed with Equation 2.20, while Equations 2.21 and 2.22 are used to estimate the price of the CPC.

$$IC_{clc} = 533394 \left(\frac{\Phi_{clc}}{293} \right)^{0.48} \tag{2.20}$$

$$\Phi_{CPC} = \frac{\Phi_{clc}}{\eta_{CPC}} \tag{2.21}$$

$$IC_{CPC} = 37.56\,\Phi_{CPC} + 57303 \tag{2.22}$$

Both the calciner gross power (Φ_{clc}) and the thermal flux on the CPC are expressed in kW, while η_{CPC} is the CPC efficiency. In addition, it is important to specify that, due to technical and operation constraints, the size of a single reactor cannot overcome the value of 55 MW [64]. The use of multiple solar calciners (of identical dimensions) must be therefore taken into account.

Solar side

The solar side is simulated through a simplified approach. The winter solstice is set as the nominal day to dimension this plant portion in order to guarantee a certain power production of the power block in the most unfavorable day of the year. The plant location, the Direct Normal Irradiation (DNI) calculation and the hourly efficiency of the heliostat field (including atmospheric attenuation, mirrors reflection, shadowing and blocking, spillage and cosine losses) for a north-field are taken from [71] (DA-

HAN power plant). The solar side is modelled as follow: from the carbonator side simulation the daily amount of $CaCO_3$ to be reconverted into CaO and CO_2 (with the relative CaO unreacted) is obtained. Given the calciner reactants inlet temperatures, it is possible to compute the net thermal energy requested at the chemical reactor ($E_{clc,net}$) as the sum of chemical and sensible energy requirement (Equation 2.23).

$$E_{clc,net} = n_{CaCO_3}\Delta h_r + M_{CaCO_3}\overline{c_p}_{CaCO_3}(T_{clc} - T_{in_{CaCO_3}}) + \\ + M_{CaO_{un}}\overline{c_p}_{CaO_{un}}(T_{clc} - T_{in_{CaO_{un}}}) \quad (2.23)$$

Where n_{CaCO_3} is the moles number of calcium carbonate, $M_{CaCO_3/CaO_{un}}$ is the $CaCO_3$/unreacted CaO mass quantity provided to the reactor, $\overline{c_p}_{CaCO_3/CaO_{un}}$ is the corresponding average specific heat capacity, $T_{in_{CaCO_3/CaO_{un}}}$ is the calciner inlet temperature of the two substances and T_{clc} is the calciner design temperature.
The net thermal power $\Phi_{clc,net}$ employed to carry out the endothermic reaction is obtained with Equation 2.24, where $\eta_{clc/CPC/helio}$ stands for the calciner/CPC/heliostat field efficiency and A_{helio} is the total heliostats area.

$$\Phi_{clc,net}(t) = \eta_{clc}\eta_{CPC}\eta_{helio}(t)A_{helio}DNI(t) \quad (2.24)$$

According to [64], the minimum calciner net thermal power $\Phi_{min,clc,net}$ is imposed as a fraction of the design calciner net heat flux $\Phi_{des,clc,net}$. These values are the lower and upper bounds of the reactor operation (Equation 2.25).

$$\Phi_{min,clc,net} = 0.2 \cdot \Phi_{des,clc,net} \quad (2.25)$$

The endothermic reaction starts at t_{on}, when the solar radiation overcomes the calciner minimum operating power and ends at t_{off}, when the thermal flux goes below the same limit. The reactor maximum achievable power is set equal to the design value; any power surplus provided by the heliostats is lost. As a consequence, the $E_{clc,net}$ can be written as shown in Equation 2.26.

$$E_{clc,net} = \int_{t_{on}}^{t_{off}} min(\Phi_{clc,net}(t); \Phi_{des,clc,net})\, dt \quad (2.26)$$

The heliostat field area and calciner design power are two degrees of freedom to compute the $E_{clc,net}$. This means that different pairs of values able to satisfy the

energy requirement of the calciner can be found. In fact, for a fixed amount of $CaCO_3$ that is needed to be calcined, the solar calciner size and the heliostats area are inversely proportional: when the receiver nominal power decreases, the solar field area increases in order to extend the useful operating time and compensate the lower power that the reactor is capable to absorb (and vice versa). Considering this behavior, when the calciner side cost decreases, the solar side investment increases. For a fixed production of CaO and CO_2, the most performing configuration (in energy terms) is the one with the minimum heliostat field area because it exploits a lower amount of solar energy. However, it is not possible to establish a priori that this configuration is also optimal under an economic perspective. A suitable optimization (discussed in the following section) is implemented in order to take into account this phenomenon. The costs functions used to estimate the investment costs of the two main components constituting the solar side are reported below.

- Central tower
  For the evaluation of the central tower investment cost, Equations 2.27 and 2.28 are extrapolated from charts in [72].

  $$H_{tow} = 15.67\ {\Phi_{CPC}}^{0.485} \tag{2.27}$$

  Equation 2.27 is referred to the case of north field arrangement, where H_{tow} is the tower height (in [m]) and Φ_{CPC} is expressed in [MW].

  $$IC_{tow} = \begin{cases} 379\ {H_{tow}}^2 - 16370\ H_{tow} + 1633200 & H_{tow} \leq 122m \\ 287\ {H_{tow}}^2 - 43661\ H_{tow} + 6338000 & H_{tow} > 122m \end{cases} \tag{2.28}$$

  The tower price is computed with a piecewise function to take into account the change of its construction material (from steel to concrete) necessary to sustain the high stresses occurring in high towers.

- Heliostat field
  The investment cost of the heliostat field is obtained through data fit of specific cost values presented in [73]. The resulting cost functions are reported in Equations 2.29 and 2.30.

  $$IC_{helio} = c_{helio} \cdot A_{helio} \tag{2.29}$$

$$c_{helio} = 3853 \cdot {A_{helio}}^{-0.2976} \tag{2.30}$$

Here, c_{helio} is the specific cost of the heliostat field (in $[\$/m^2]$), while A_{helio} (in $[m^2]$) is the area of the mirrors constituting the heliostat field.

2.3.2 Independent variables

The parameters assumed as independent variables are reported in Table 2.4 in correspondence of the plant section to which they refer. Here, *OC* stands for optimization criterion, *#IC* is the number of inter-cooling steps for the CO_2 compression, T_{carb} is the temperature at which the carbonation is carried out, $T^{in}_{CO_2/CaCO_3}$ is the $CO_2/CaCO_3$ temperature at the carbonator temperature, $STIT$ is the Storage Turbine Inlet Temperature, BIT is the Blower Inlet Temperature, G_{CaO} is the mass flowrate of CaO extracted from the storage, and $PBTF$ stands for Power Block Thermal Feeding. The variables related to the power block are not displayed in the table since they are dependent on the CSP-CaL integration investigated, and will be mentioned in the corresponding subsections, while the HEN layout is optimized through the pinch analysis and does not count as an independent variable.

Table 2.4 Independent variables of the system (HEN and power block excluded)

Plant section	Variable's name						
Solar side	A_{helio} $[m^2]$	H_{tow} $[m]$	*OC*				
Calciner side	${\Phi_{clc}}^{des}$ $[kW]$	*#IC* $[-]$	$[-]$				
Carbonator side	T_{carb} $[^\circ C]$	$T^{in}_{CO_2}$ $[^\circ C]$	$T^{in}_{CaCO_3}$ $[^\circ C]$	$STIT$ $[^\circ C]$	BIT $[^\circ C]$	G_{CaO} $[kg/s]$	$PBTF$ $[-]$

To better visualise the points or sections of the system to which the variables refer, Figure 2.7 is shown. Also in this case, the HENs optimization and the parameters related to the power block are not reported.

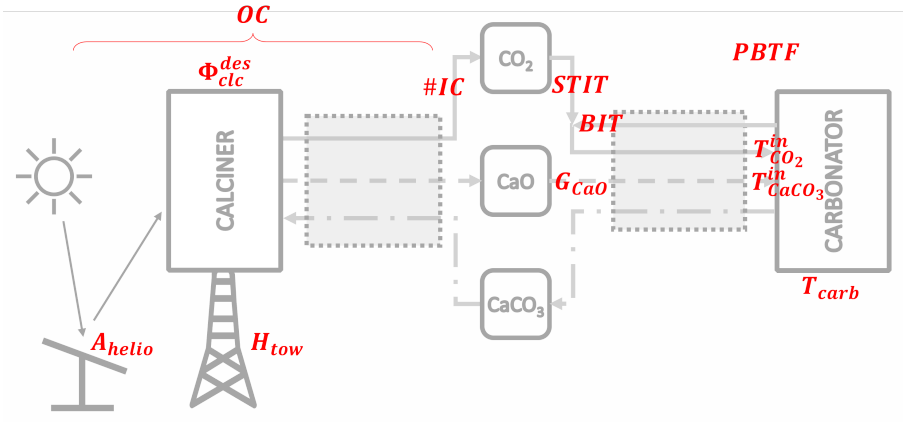

Fig. 2.7 Location of the independent variables in the system

2.3.3 Objective functions

The multi-objective optimization is performed in order to evaluate the compromises between plant efficiency and investment costs, as well as to investigate the influence of the parameters assumed as independent variables on two fundamental aspects characterizing the system: the energy performance and the investment cost. The total plant efficiency (η_{tot}) is computed with Equation 2.31, where $E_{el,tot}$ is the net total electricity production referred to the design day, Q_{sol} is the energy made available by the sun during the design day, and $\dot{W}_{el,CrbS/ClcS}$ is the net electric power produced/consumed by the carbonator/calciner side.

$$\eta_{tot} = \frac{E_{el,tot}}{Q_{sol}} = \frac{\int_{day}(\dot{W}_{el,CrbS}(t) + \dot{W}_{el,ClcS}(t))dt}{\int_{day} A_{helio} DNI(t)dt} \tag{2.31}$$

Regarding the economic aspect, the specific plant cost (ic_{tot}), defined as the plant investment cost divided by the daily energy production, is taken as objective function. The reason for the normalization of the total investment cost is that, despite all the integration alternatives are designed such that the discharging section of the plant has a 2 MW_e production, there can be (small) differences in the daily amount of electricity produced. This difference is due to the configuration assumed by the CaL, which influences the electric production mainly through the compression and expansion of the CO_2 streams. Consequently, this aspect must be taken into account in order to make a coherent treatment.

$$ic_{tot} = \frac{\sum_i [IC_i]}{E_{tot,el}} \tag{2.32}$$

2.3.4 Optimization model

The development of the optimization model is usually conditioned by the nature of the mathematical formulation assumed by the simulation model. For this reason, the procedure for the system's simulation is summarized in Figure 2.8, where the plant sections are highlighted in blue, and the most important constraints are in red. Starting from the power block, the thermal cycle can be simulated by imposing the electrical power and by setting the design and operation variables. Successively, the carbonator side is simulated by fixing the related variables and iteratively adjusting the streams participating in the carbonation in order to obtain a configuration that does not need an external thermal contribution. This is done exploiting a bisection method and the pinch analysis. The section of the plant performing the charging process is simulated by fixing the size of the solar calcined and obtaining the size of the heliostat field or vice versa. Finally, the storage vessels can be dimensioned with a direct calculation.

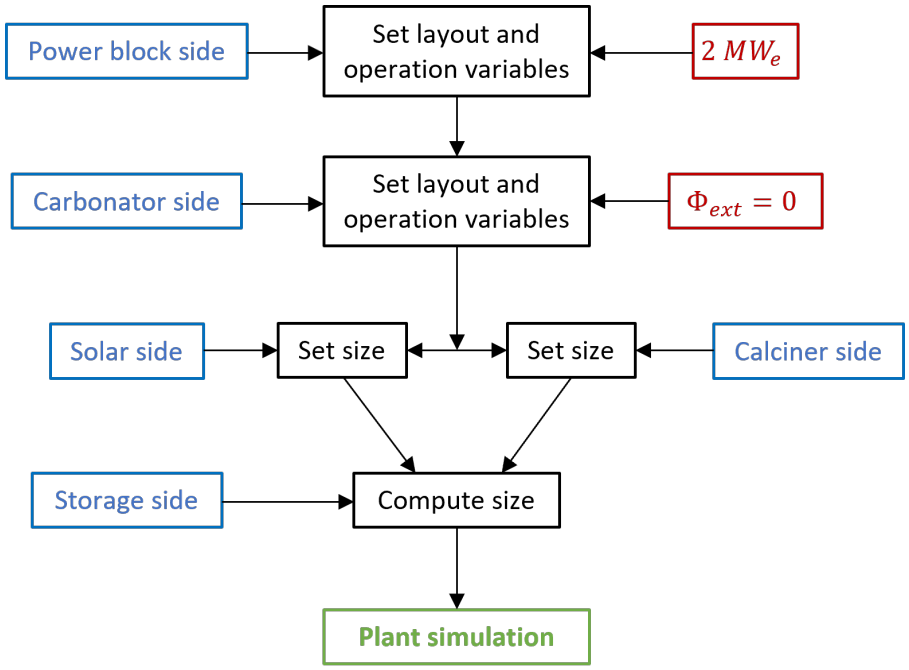

Fig. 2.8 Conceptual flow chart of the simulation process

As already mentioned, it is intended to optimize the CSP plant in a comprehensive way, addressing at the same time the synthesis, design and operation problems. The model for the simulation of the plant operation is characterized by many sources of complexity. The strategies that are usually used to deal with non-linear and non-convex terms cannot be exploited in the case under consideration since the mathematical formulation is not completely explicit and other optimization techniques (e.g. pinch analysis) are nested inside of the simulation model. Taking into account the input data available, the assumptions adopted and the mathematical formulation used to simulate the plant, a heuristic approach results to be the most suitable strategy to optimize the CSP-CaL integration. More in detail, it is worth to notice that the aspects that must be dealt with particular attention are:

- including the simulation of the heat transfer processes (made through the pinch analysis) in the optimization;
- addressing all the technical and conceptual constraints (e.g. avoiding heat transfer between solid streams and the use of external energy sources);
- the potential high number of independent variables to be optimized;
- the computation time required to solve the problem;
- the possibility to optimize the problem under different and concurrent perspectives.

In light of all these aspects, a multi-objective optimization model is developed, whose structure is showed in form of flow chart in Figure 2.9. Steps highlighted in orange indicate optimizations of operating conditions of processes involving active components (e.g. turbines, compressors), while blocks in blue are referred to optimizations of thermal transfer processes.

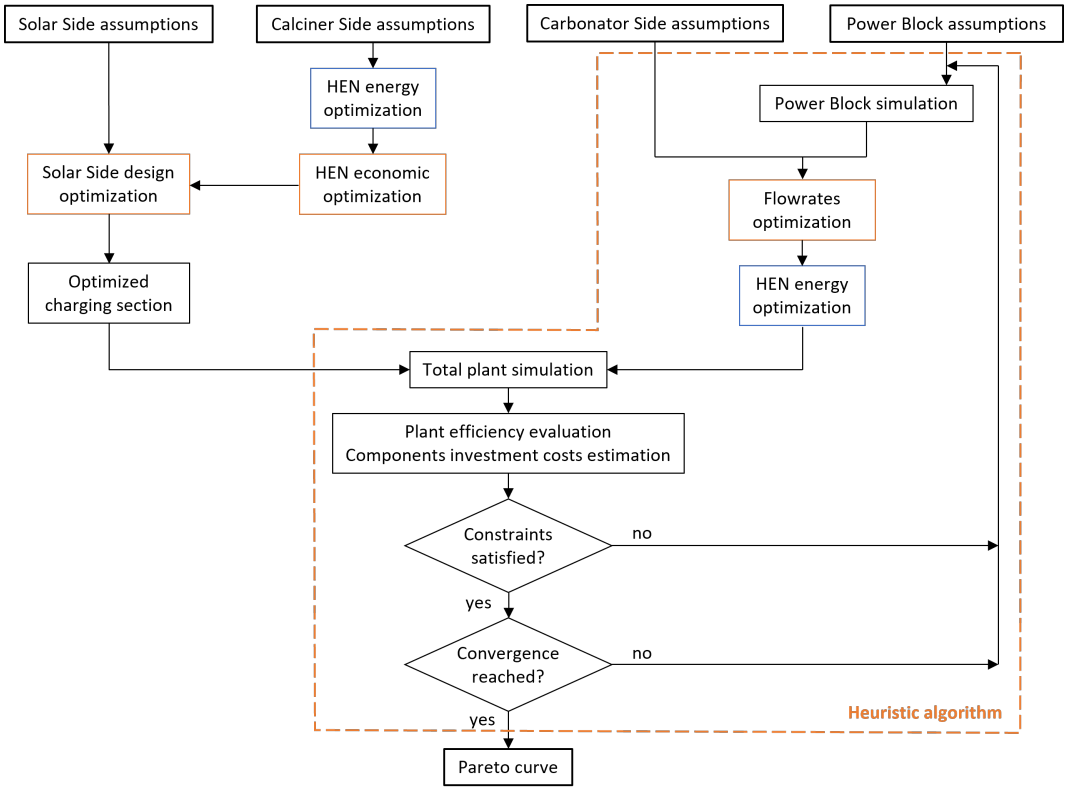

Fig. 2.9 Conceptual structure of the optimization process

In order to minimize the computational time, the execution of multiple and smaller optimizations is usually preferred with respect to a single optimization with higher dimension. For this reason, separate optimizations are performed whenever a sub-problem is recognized to be independent from the others. In particular, thanks to the operating decoupling effect introduced by the storage, the optimization of the plant sections devoted to the charging and discharging processes can be executed in a partially independent way. For first, a general description of the approach adopted is provided in order to give an overview of the optimization's structure, then, the single steps constituting the process are described more in detail.
Regarding the charging section, two series of energy and economic optimizations are executed to obtain the optimal sizes of the components of the solar side. At the same time, the thermal transfer processes are simulated with the pinch analysis, the HEN design is obtained and a simple sensitivity analysis is carried out to optimize in an economic perspective the heat exchangers constituting the network. By merging these steps it is possible to obtain the optimal configuration of the charging section as a function of the daily amount of $CaCO_3$ that must be converted.

The discharging section is managed by a genetic algorithm that optimizes most of the independent variables belonging to this section. As first step, the power block is simulated (if present). Then, nested into the GA, a bisection method is used to optimize the flows circulating during the discharging process and, nested into the bisection algorithm, the heat transfer processes occurring in the carbonator side are simulated and optimized with the pinch analysis.
In this way, the entire plant is dimensioned, its operation is simulated and the parameters quantifying the energy performance and the economic investment can be computed. The constraints satisfaction and the convergence status are checked by the GA and, if the two requirements are compelled, the process ends. According to the integration alternative considered (and therefore the number of variables in the problem) the computational time required by the process to end is between 20 minutes and 2 hours.

Solar side

Single-objective optimizations are executed for different amounts of $CaCO_3$ that must be converted daily. More in detail, for each value, two optimizations are performed, one with an energy objective function and the other with an economic objective function. The optimizations are performed with the MATLAB function *fminsearch* (tolerance set to 10^{-8}) and their execution is very fast thanks to the fact that a single independent variable is addressed (in each optimization). At this point it is possible to extrapolate (through data fitting) a function that links the daily consumption of $CaCO_3$ (or production of CaO and CO_2) with the optimal size of the solar calciner and the components constituting the solar side. This function is then used in the optimization of the discharging section (identified with the orange dotted line in Figure 2.9), allowing in practice to optimize the entire plant.

Calciner side

The aspects/parameters to be optimized in the calciner side are: the heat exchanger network; the stages in the CO_2 compression; the solar calciner size. From the optimization step for the solar side, this last parameter is expressed as a function of the daily consumption of $CaCO_3$ and therefore it does not need to be considered in other ways. The effects determined by changing the number of stages in the CO_2 compression do not influence the optimization of the rest of the charging section of the plant and for this reason the recompression steps are optimized together with the discharging section. The thermal transfer processes are instead simulated and optimized with the pinch analysis. As already mentioned, the operating temperatures

are not supposed to change and the mass flowrates will vary keeping constant their ratio. The HEN can be therefore designed, since the eventual changes introduced by varying the independent variables will not affect the HEXs layout but only their size. By designing the HEN, it results as necessary to split the $CaCO_3$ stream extracted from the storage (Figure 2.6). The value of the splitting ratio is not unique, since multiple values can allow a thermal transfer that does not violates the thermodynamic principles. On the other hand, the value assumed by this parameter influences the HEN cost and for this reason it is chosen by performing a sensitivity analysis, as reported in Figure 2.10 (computed for a mass flowrate of solids equal to $11.88 kg/s$).

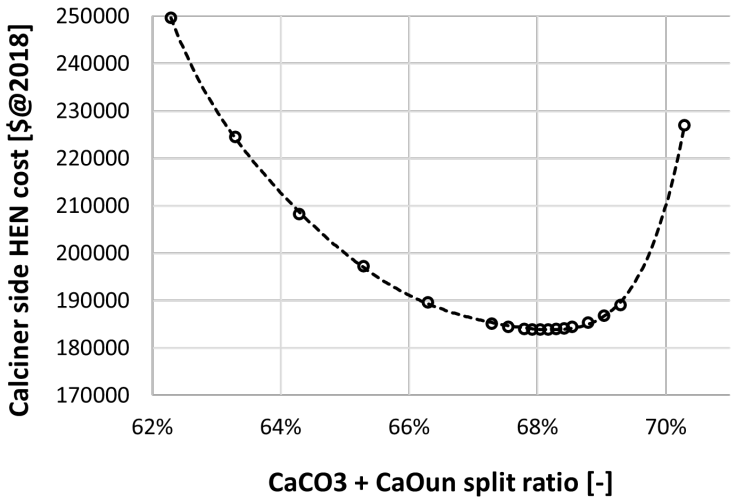

Fig. 2.10 Sensitivity analysis for the solid stream splitting

Carbonator side

Most of the independent variables related to the discharging process (as well as the number of recompression stages in the charging section) are optimized with a Genetic Algorithm for multi-objective optimization. In particular, the MATLAB function *gamultiobj* (based on the NSGA-II algorithm) is used keeping the default tolerance (set to 10^{-4}). Starting from the input data and the trial values of the independent variables, the operation of the power block (if present) is simulated. Consequently, the operating temperatures and pressures of the carbonator side are computed and the joint execution of a bisection method (convergence tolerance set to 10^{-5}) with the pinch analysis is exploited to obtain the mass flowrates circulating in the discharging process such that the consumption of an external heat source is avoided.

It is important to notice that, differently from the case of the calciner side, the HEN

layout will be different for each individual of the generation in the metaheuristic algorithm. A suitable (optimization) algorithm should be used to design the HEN, consequently allowing to compute the HEN cost, which is needed for the economic objective function. Implementing this further step only to obtain a precise estimation of the HEN cost does not justify the collateral increase of the complexity and computational time. In fact, as demonstrated in the results, the investment due to the HEN in the carbonator side is much smaller compared to the ones required by the other components. To take advantage of this aspect and avoid the implementation of an additional nested algorithm, a strategy was developed to link the composite curves of the pinch analysis with the corresponding HEN price through a new parameter. In this way, a simple and fast estimation of this cost can be performed during the optimization process. The equivalent product between the global heat transfer coefficient and the heat transfer area (UA_{eq}) is introduced, computed with a summation on all the segments composing the hot and cold composite curves (Equation 2.33).

$$UA_{eq} = \sum_i \left[\frac{\Phi_i}{\Delta T_{lm,i}} \right] \tag{2.33}$$

Some interesting cases are simulated in a preliminary run. For those, the Heat Exchanger Network is synthetized (with the software *ASPENenergyanalyzer*) and the corresponding investment costs and UA_{eq} are computed. A cost function for the carbonator side HEN is therefore easily derived performing a data fit on the results obtained and implemented in the optimization algorithm. The term used as scaling parameter is the UA_{eq}, which can be easily estimated from the pinch analysis. Two different functions must be developed if the thermal feeding of the power block can be executed either on the carbonator wall or with a heat recovery on the reaction products, and this because the consistent differences occurring in the resulting HEN layouts prevent to use the same correlation for both the cases.

At this point, the two parts of the plant are merged and the complete plant is simulated. The parameters used as objective functions are calculated, the satisfaction of all the technical constraints is verified and the progress on the convergence is checked. The process is repeated until the two last conditions are fully satisfied.

Power block side

As already mentioned, the power block is optimized by the GA, with the rest of

the plant section executing the discharging process. Its design and operation can be simulated combining the input data and the trial values assumed by the independent variables during the iterations. In particular, the mass flowrates are computed to guarantee a net electricity production equal to $2MW$. In this way, the comparison among the different CSP-CaL integrations investigated is made for plants having a common size.

The structure of the optimization process is reported in Figure 2.11, with more detail than before. Also in this case, steps highlighted in orange indicate optimizations of operating conditions of processes involving active components, while blocks in blue are referred to optimizations of thermal transfer processes.

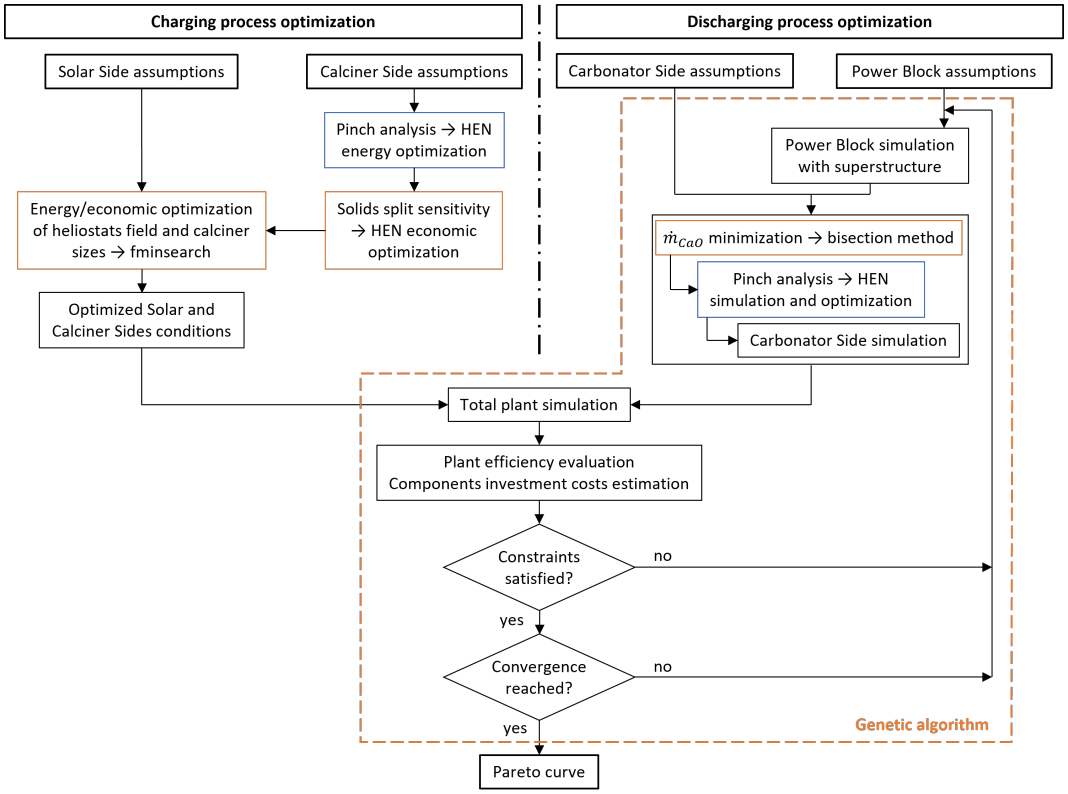

Fig. 2.11 Optimization structure in form of flow chart

The optimization approach used in the present study is conceptually similar to the HEATSEP method, presented by Lazzaretto in [74] and successfully applied in [75–77] for the optimization of various power cycles. In particular the similarities can be found on the main structure, since HEATSEP is based on a heuristic algorithm in which is nested the pinch analysis. However, because of the characteristics of

the CSP-CaL case study, the present optimization process shares some important differences, such as the combined use with external optimizations (for the charging section), the strategy used to compute the mass flowrates in the discharging phase, and other arrangements devised to address the technical constraints and promote the convergence.

Finally, before presenting the CSP-CaL integrations that were optimized and the results obtained, it is important to comment the applicability of the methodology developed. As already mentioned, the model is able to optimize almost any kind of energy process thanks to its characteristics. However, although the use of a metaheuristic algorithm for optimisation offers many advantages, it is important to note that it also presents an unavoidable limitation. In fact, the number of variables and constraints that these kind of solvers are able to manage is much smaller compared to the case of deterministic algorithms. As a consequence, the limit on the application of this methodology does not rely on the nature of the mathematical formulation used to model the system/plant, but it is related to the size of the problem, which should be in the order of some tents of variables.

2.4 Direct integration - Brayton cycle

In this section the direct integration is described and the results of its optimization are presented and discussed. For the sake of honesty, it must be pointed out that the energy optimization of this integration was developed before the beginning of the PhD period. However, in order to provide a complete discussion of the CSP-CaL optimization, it was chosen to include the direct integration in the thesis. The same logic was applied for the indirect integration of the sCO_2 Brayton cycle.

2.4.1 Integration description

The configuration of the discharging plant section in case of direct integration is showed in Figure 2.4 without the HEN design. A CO_2 Brayton cycle is exploited to produce energy and it is fully integrated in the discharging process. This alternative can be seen as the simplest and the most complex one at the same time. In fact, the absence of an external power cycle and the adiabaticity of the carbonator contribute to keep the layout relatively essential, but the fact that the CO_2 is both a reactant

and the power fluid makes necessary to pay more attention during the integration process and the operation. The concept at the base of this integration is that the thermal energy provided by the exothermic reaction carried out in the carbonator is absorbed by an amount of CO_2 provided in excess to the reactor. Since it is necessary to expand this gaseous stream to produce electricity, the chemical reactor must be pressurized, which is another aspect to pay attention to. In alternative, the carbonation could be executed at ambient pressure and vacuum conditions could be attained at the end of the expansion. However, air infiltrations could take place in this case and to prevent this possibility the CO_2 pressure in the entire operation of the Calcium-Looping process is constrained to be above $1bar$.
Regarding the modelling aspects, the simulation of the discharging process is obtained by simulating the carbonator side, where the energy balance used to simulate the carbonation is the main step to compute the discharging operation. In particular, knowing the carbonation temperature and the inlet temperatures of the reactants, the ratio between the mass flowrates is calculated, and the bisection method is used to compute the values that ensure a null requirement of external heat and, at the same time, allows to carry out an adiabatic reaction.
The input data specific to this integration are reported in Table 2.5.

Table 2.5 Direct integration data assumptions

Parameter	Component/stream	Value
Isentropic efficiency	Main Turbine	0.9
	Main Compressor	0.87
Mechanical efficiency	Main Turbine + Main Compressor	0.97
Electrical efficiency	Main Turbine + Main Compressor	0.97
Minimum CO_2 pressure	Carbonator side	$1bar$

The independent variables addressed for the direct integration optimization (in addition to the ones previously presented for the rest of the plant) are reported in Table 2.6 with their variation range. Here, P_{crb} is the carbonator pressure, β_{MT} is the pressure ratio of the Main Turbine, and $MCIT$ is the Main Compressor Inlet Temperature.

Table 2.6 Independent variables specific to direct integration

Variable's name	Lower bound	Upper bound
P_{crb}	$1.5bar$	$15bar$
β_{MT}	1.2	14
$MCIT$	$35°C$	$300°C$

Regarding the economic optimization, Equations from 2.10 to 2.13 (discussed in Section 2.3) are used to estimate the costs of the Main Turbine and Compressor, while the cost functions specifically referred to this kind of integration are presented below.

- Carbonator side's HEN
  The cost function used to estimate the price of the HEN in the carbonator side was obtained through data fitting and it is reported in Equation 2.34 (where UA is in $[W/K]$ and the result in [\$]).

$$IC_{HEN,CrbS} = 99.72 \cdot UA^{0.67} \tag{2.34}$$

2.4.2 Results and comments

The Pareto curve obtained from the multi-objective optimization is showed in 2.12. As well known, the points on the upper right and lower left correspond to the configurations that would be obtained from an energy and economic optimization, respectively. The highest plant efficiency attained with this integration is 19.37%, decreasing down to 18.74% (-4% in relative terms) to reach the configuration that requires the lowest specific investment cost, which is 128 $[\$/MJ]$ (0.8% less than the amount corresponding to the most performing case). Despite the objective functions are in contrast between them, the differences between the results constituting the Pareto curve are not extreme, especially for the investment cost. The reason behind this phenomenon is that the synthesis and design problems affect in a negligible way this kind of integration, and the independent variables addressed are mostly referred to the operation problem. Since the type and number of component is fixed (except for the number of compressors in the calciner side), the variation of the specific plant cost is due to the small changes of the components' size occurring when different

operating conditions are set as the nominal ones.
More in detail, the variables that always converge to their highest bound are the carbonation temperature and the number of compressors in the calciner side, while the opposite happens for the inlet temperature of the main compressor. These behaviours have the clear effect of improving the plant performance and their influence is strong enough to determine, at the same time, a reduction of the investment cost. The other variables assume intermediate values. In particular, moving from the least to the most performing configuration, the carbonation pressure and the pressure ratio of the main turbine tend to decrease slightly. At the same time, the CaO and the $CaCO_3$ temperatures at the carbonator inlet increase in order to perform a more efficient heat recovery of the carbonation products, which determines an increase of the HEN investment cost.

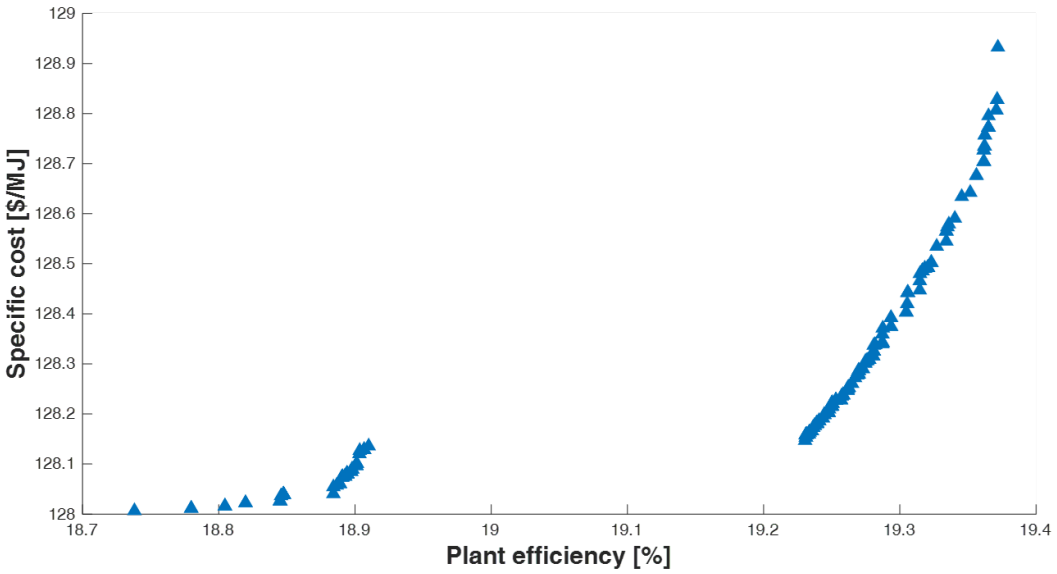

Fig. 2.12 Pareto curve for the multi-objective optimization of the direct integration

The following results are related to the energy-optimized configuration, since it can be considered as the most interesting option thanks to the high performance, which does not determine a considerable increase of the investment costs.
The heat transfer process conducted in the carbonator side is one of the most important steps on the plant operation and it is worth to mention some meaningful results which concern this part. Figure 2.13 shows the hot and cold composite curves obtained from the pinch analysis. As can be noticed, the demand of external

heating is avoided and the two curves are relatively close for most of the process, demonstrating the efficiency of this step.

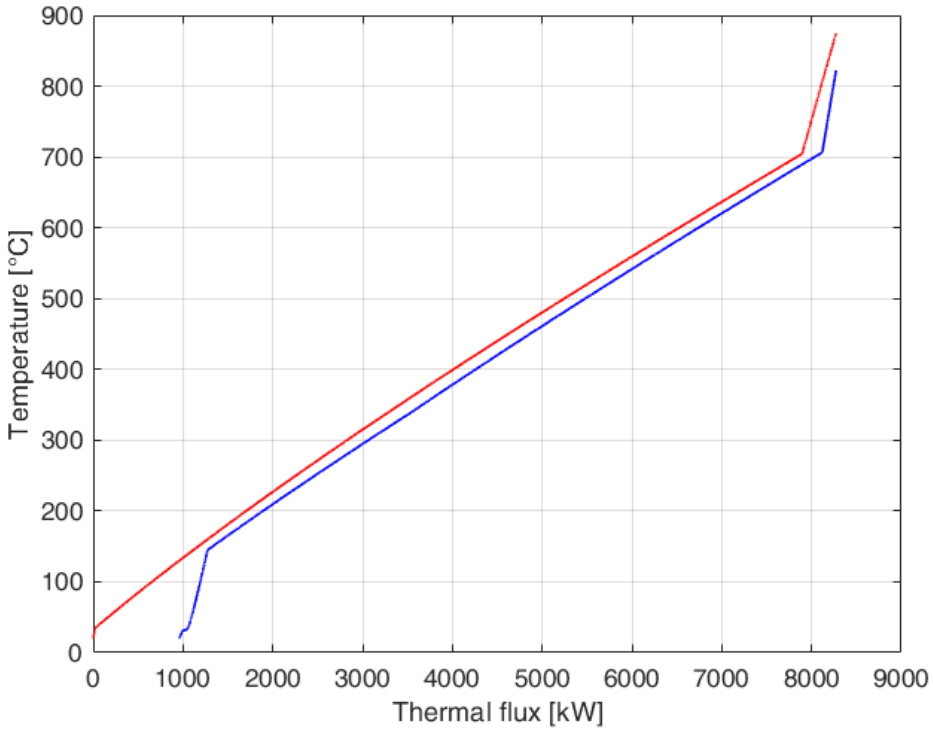

Fig. 2.13 Hot and cold composite curves from pinch analysis for the direct integration

From the grand composite curve (Figure 2.14) can be observed that the pinch point is reached two times, confirming the quality of the heat exchange performed. However, since each point of minimum temperature difference separates the thermal transfer process in two independent parts, the HEN can be expected to have a complex layout, and its design mus be carefully developed.

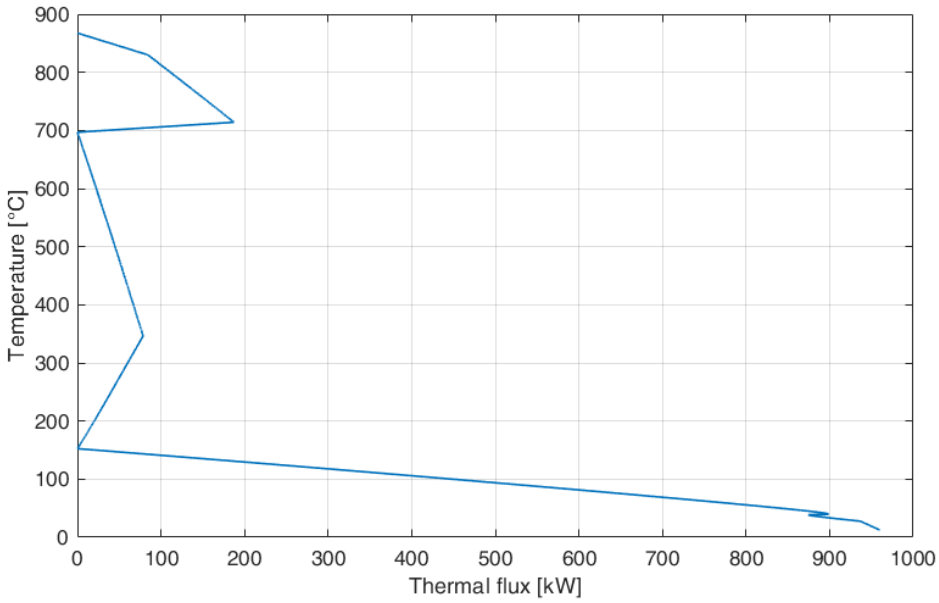

Fig. 2.14 Grand composite curve from pinch analysis for the direct integration

The final layout for the carbonator side is reported in Figure 2.15. The number of HEX units is seven (plus one air cooler) and the heat transfer between solid streams was successfully avoided, as well as the splitting of solid flows. The mass flowrate of CO_2 provided in excess to the carbonation reaction is around 5 times the solid stream exiting the reactor and for this reason it is the fluid most exploited to heat up the reactants taken from the storage at ambient temperature.

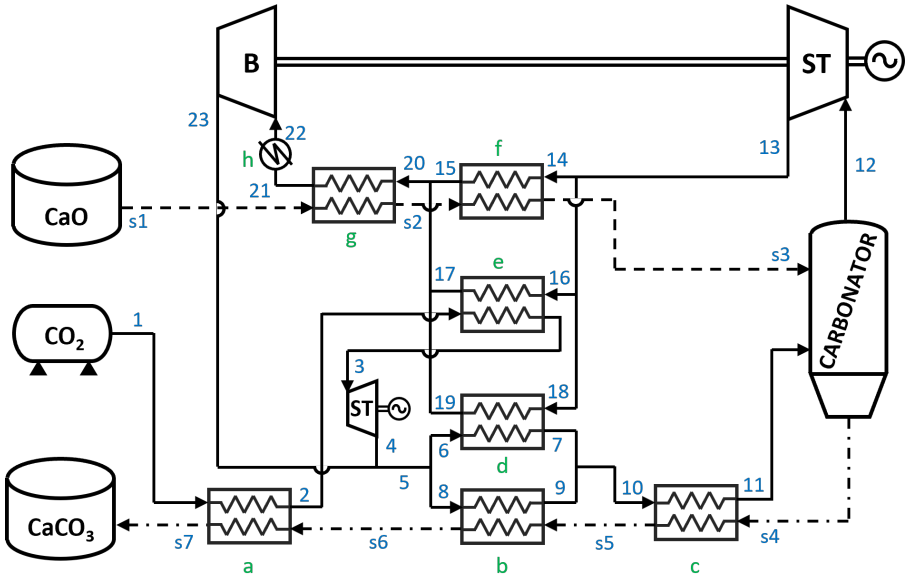

Fig. 2.15 A feasible layout of the carbonator side for the direct integration

2.5 Indirect integration - Steam Rankine cycle

In this section the indirect integration of a Steam Rankine cycle is described and the results of its optimization are presented and discussed.

2.5.1 Integration description

The Steam Rankine cycle is known by almost 150 years [78] and it is by far the most commercially developed power cycle between the alternatives investigated. The size of $2MW_e$ assumed in the present study is considered among the small scale plants for this kind of technology, but it is still an interesting option to evaluate thanks to the matching operating conditions. The configuration of the carbonator side for the SRC indirect integration is the one showed in Figure 2.5. In this case, the GA is free to choose between a thermal feeding of the power block performed on the carbonator wall or with a heat recovery on the carbonation products.
The superstructure of the power block is reported in Figure 2.16, where the components that can be included or removed from the cycle are colored in light blue, while the fixed ones are in white. The most complex layout includes one reheating step and two turbine bleedings. No other arrangements for enhancing the efficiency

are considered since the layout complexity would become excessive considering the power block size.

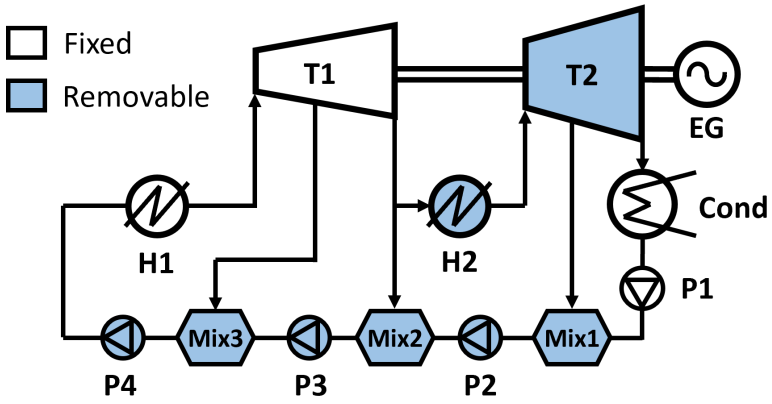

Fig. 2.16 Superstructure of the power block based on a Steam Rankine cycle

Regarding the simulation process, the power block is the first element of the discharging section to be simulated. The water flowrates circulating in the power block are computed by imposing the condition of saturated liquid at the exit of the mixers (Mix1, Mix2 and Mix3) and a net electric power production of $2MW$. The operation of the carbonator side is computed starting by the turbomachinery, then, the energy balance on the carbonator is used to find the ratio between the mass flowrates circulating during the discharging process and the pinch analysis nested into the bisection method is used to find the values of the flowrates. As can be noticed, the simulation of the carbonator side is conducted as already exposed for the direct integration, with the difference that the contribution due to the heat transfer on the reactor wall must be included in case the power block is thermally fed by the carbonator itself.
The input data specific to this integration are reported in Table 2.7.

Table 2.7 Data assumptions for SRC indirect integration

Parameter	Component/stream	Value
Isentropic efficiency	Steam turbines	0.85
	Pumps	0.75
Mechanical efficiency	Steam turbines	0.97
Electrical efficiency	Steam turbines	0.97
Pressure loss	H_2O in HEXs	2%
Condensing pressure	H_2O	$0.1 bar$
Minimum vapor fraction	H_2O	0.88

The independent variables addressed for the SRC indirect integration optimization (in addition to the ones previously presented for the rest of the plant) are reported in Table 2.8 with their variation range. Here, $T1IP$ is the inlet pressure of turbine T1, TIT is the inlet temperature of the two turbines, $RehEx$ indicates the existence of the reheating step, P_{int} is the intermediate pressure at which the reheating step is performed, b_{T1} indicates the existence of a steam bleeding in T1, $P_{b,T1}$ is the bleeding pressure in T1, b_{int} indicates the existence of an intermediate bleeding, b_{T2} indicates the existence of a steam bleeding in T2, $P_{b,T2}$ is the bleeding pressure in T2, and $eco/eva/sup/reh_{cw}$ indicate the possibility to provide the thermal flux required by the economizer/evaporator/superheater/reheater on the carbonator wall.

Table 2.8 Independent variables specific to SRC indirect integration

Variable's name	Lower bound	Upper bound
$T1IP$	$80bar$	$140bar$
TIT	$400°C$	$540°C$
$ReHEX$	*Binary variable*	
P_{int}	$5bar$	$135bar$
b_{T1}	*Binary variable*	
$P_{b,T1}$	$6bar$	$136bar$
b_{int}	*Binary variable*	
b_{T2}	*Binary variable*	
$P_{b,T2}$	$0.2bar$	$60bar$
eco_cw	*Binary variable*	
eva_cw	*Binary variable*	
sup_cw	*Binary variable*	
reh_cw	*Binary variable*	

Regarding the economic optimization, some cost functions are added to estimate the investment costs of the components that are specific to this integration.

- Steam turbine

  The investment cost of the steam turbine is computed with Equation 2.35, taken from [60]. Here, $\dot{W}_t$ is the turbine shaft power (in $[kW]$), $\eta_{is,t}$ is the turbine isentropic efficiency, and TIT is the turbine inlet temperature (in $[K]$).

$$IC_{t,SRC} = 4125\ \dot{W}_t^{0.7} \left[1 + \left(\frac{0.05}{1-\eta_{is,t}}\right)^3\right] \left[1 + \exp\left(\frac{TIT - 866}{10.42}\right)\right] \tag{2.35}$$

- Water pump

  The investment cost of the water pump is computed with Equation 2.36, taken from [60]. Here, $\dot{W}_p$ is the pump shaft power (in $[kW]$), and $\eta_{is,p}$ is the pump isentropic efficiency.

$$IC_{p,SRC} = 750\ \dot{W}_p^{0.71} \left[1 + \frac{0.2}{1-\eta_{is,p}}\right] \tag{2.36}$$

- Fluid bed carbonator
  In case transferring heat to the power block through the carbonator wall is requested, a fluidized bed (FB) reactor is considered [56]. Equation 2.37 is suggested for a case study where sCO_2 is the power fluid, where Φ_{crb} (in $[kW]$) is the reactor thermal power released by the carbonation.

$$IC_{FB,crb}^{sCO_2} = 19594 \ (\Phi_{crb})^{0.5} \tag{2.37}$$

  A simple strategy (Equations 2.38 and 2.39) is developed to adapt this cost function to the case under consideration, where the power fluid is water. According to [79], the cost of a cooled carbonator is assumed to be determined for the 85% by the heat exchangers on the wall (this parameter is referred as α). The heat transfer surface (A) is taken as scaling parameter and the reference cost for the reactor (case with sCO_2) is calculated for the same carbonator power. The cost of a carbonator operating with water/steam is therefore computed from this reference price.

$$IC_{FB,crb}^{H_2O} = IC_{FB,crb}^{sCO_2} \left(\alpha \ \frac{A_{H_2O}}{A_{sCO_2}} + (1-\alpha) \right) \tag{2.38}$$

$$\frac{A_{H_2O}}{A_{sCO_2}} = \frac{\sum_i \left[\frac{\Phi_{H_2O,i}}{U_{H_2O,i} \cdot \Delta T_{lm,H_2O,i}} \right]}{\frac{\Phi_{sCO_2}}{U_{sCO_2} \cdot \Delta T_{lm,sCO_2}}} \tag{2.39}$$

  The logarithmic mean temperature difference is computed with inlet/outlet temperatures of each stage constituting the water heating and the reactor operating temperature. For the overall heat transfer coefficient (U), an internal flow in a pipe is assumed. Consequently, it can be approximated with Equation 2.40, where h_{int} and h_{ext} are the convective heat transfer coefficients of the water/steam flow and the external flow, respectively. For the power fluid, h_{int} is computed with different correlations, according to the heating step considered: the Dittus-Boelter correlation is used for the economizer and the heater/reheater, assuming a fully developed turbulent flow, while the Guerrieri-Talti correlation is taken for the evaporator [80, 81]. The h_{ext} value is found in [82]. The sCO2 and the water velocities are imposed according to [83] and [81], both referred to turbulent flows.

$$U \simeq \left[\frac{1}{h_{int}} + \frac{1}{h_{ext}}\right]^{-1} \tag{2.40}$$

- Carbonator side's HEN
  The cost function used to estimate the price of the HEN in the carbonator side was obtained through data fitting. Equation 2.41 is used in case the power block is fed with a heat transfer performed on the carbonation products, while Equation 2.42 is considered when the heat transfer takes place on the carbonator's wall (where UA is in $[W/K]$ and the result in [\$]).

$$IC_{HEN,CrbS} = 137 \cdot UA^{0.67} \tag{2.41}$$

$$IC_{HEN,CrbS} = 2.392 \cdot UA + 38495 \tag{2.42}$$

2.5.2 Results and comments

The Pareto curve obtained from the multi-objective optimization is shown in Figure 2.17. The cheapest configuration presents a specific investment cost of $152.4\$/MJ$ and a plant efficiency equal to 15.1%, while a performance of 16.3% (+8% in relative terms) is reached with the energy optimization and determines a specific cost of $159.8\$/MJ$ (+5% in relative terms). The plant efficiency increases as much as the thermal feeding of the power block is moved from the carbonator side HEN to the carbonator wall. A non-adiabatic reactor is much more expensive than an adiabatic one, and this cost difference determines the increase of the specific investment cost. Starting from the less performing configuration, a first improvement is encountered executing the steam reheating on the carbonator wall ($CWHT\ REH$), and further improvements are observed when also the economizer ($CWHT\ ECO$) is added. As expected, the absence of an isothermal heat transfer ($CWHT\ EVA$) in the thermal recovery process brings a considerable advantage, but the best option is obviously represented by the complete heating performed on the reactor wall. The fact that other possible setups do not appear in the Pareto front means that they are not convenient both in energy and economic terms with respect to the configurations found. It is interesting to notice that passing from a charging section dimensioned according to an economic criteria to another one optimized in energy terms brings appreciable changes in the system efficiency maintaining a nearly equal specific plant cost.

The Pareto front is not only discontinuous, but also defined by a limited number of regions. The reason of this phenomenon is due to the nature of the problem and, in particular, to the nature of the independent variables. The synthesis and design problem of the power block is mostly addressed with binary variables. The change from one state to the opposite one occurring in these parameters introduce discontinuities in the values assumed by the objective functions, as well as in the Pareto curve. In addition, despite the operation variables are continuous, they show the tendency to converge almost to the same values in all the configurations constituting the Pareto front. In particular, it is worth to mention that the layout and operation of the Rankine cycle results to be the same in all the cases, reaching the configuration that maximizes the power block efficiency even in case of pure economic optimization. This can be reasonably explained considering that the cost difference of a more complex (and performing) power block with respect to a simpler one is justified by the smaller size (and price) of the charging plant section, which represents the most significant contribution to the total capital investment.
Despite the layout of the thermal cycle does not change, the carbonator side configuration changes completely along the Pareto front. When the power block is thermally fed on the carbonator wall (energy optimization), the layout of the carbonator side becomes simpler (six HEXs units) thanks to the fact that the power fluid is not anymore heated up in the heat recovery process. At the same time, it is observed that the CO_2 mass flowrate entering the carbonator is equal to the stoichiometric amount, therefore a single solid stream can be found at the reactor outlet.

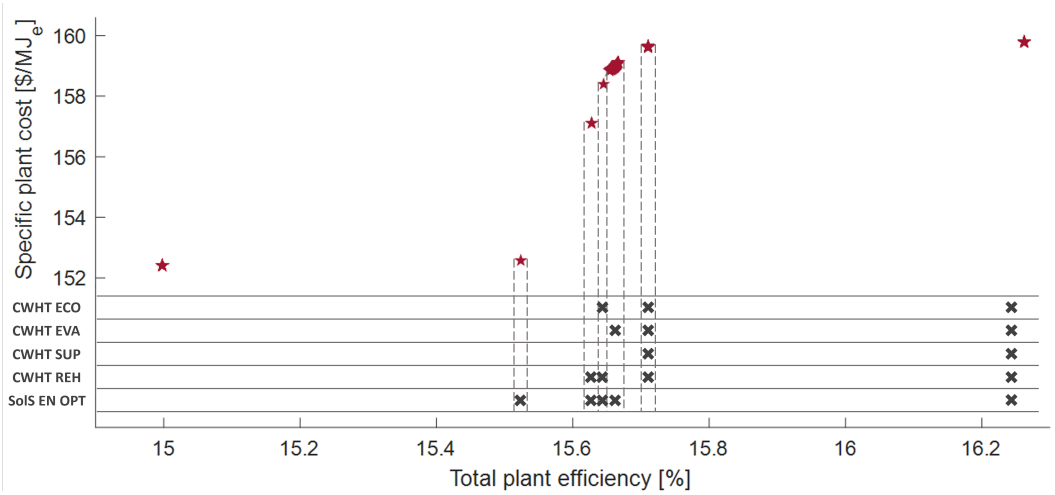

Fig. 2.17 Pareto curve for the multi-objective optimization of the direct integration

The configuration that is considered as the most interesting to analyze is the one corresponding to the economic optimization. In fact, as will be later explained, this configuration has the lowest specific investment cost among the integrations investigated. The following images are therefore referred to this specific case.
The hot and cold composite curves for the heat recovery performed in the carbonator side are reported in Figure 2.18. Performing a thermal feeding of the power block based on the heat recovery of the carbonation products brings to a configuration with a relatively poor heat transfer efficiency, as can be deduced from the distance between the two curves. The isothermal stage determined by the evaporation is the main cause of this.

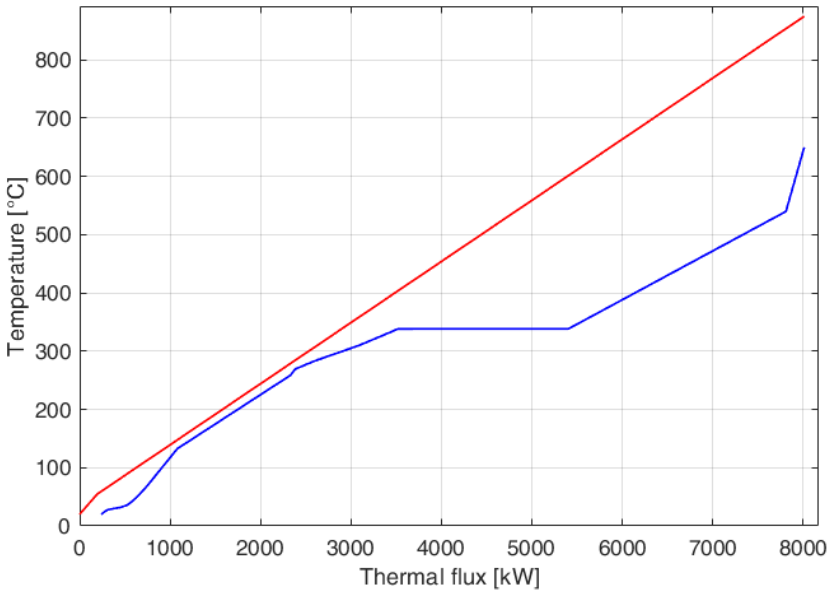

Fig. 2.18 Hot and cold composite curves from pinch analysis for the steam Rankine indirect integration

The grand composite curve obtained from the pinch analysis is showed in 2.19. The heat transfer presents two pinch points, at low/medium temperatures: one at 140°C and the other at 277°C. They take place where the mixed CO_2 and the water of the Rankine cycle start to participate to the heat recovery process.

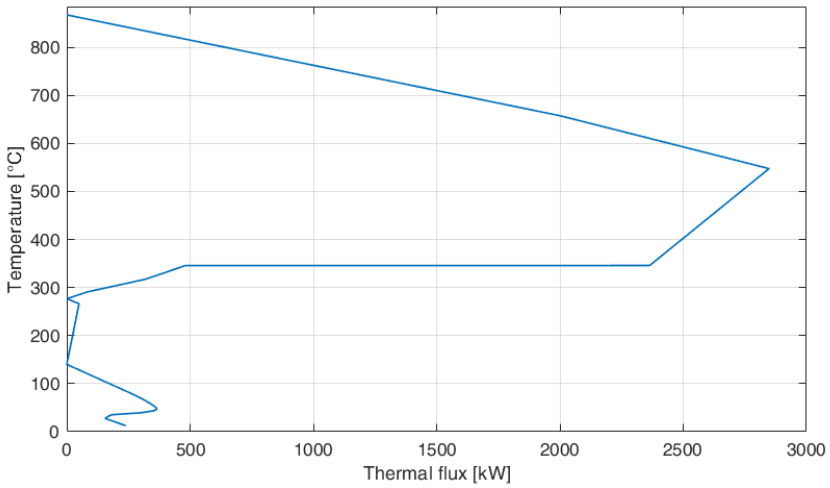

Fig. 2.19 Grand composite curve from pinch analysis for the steam Rankine indirect integration

Figure 2.20 shows the resulting layout of the power block and the carbonator side for the economic optimization. Since the carbonator is adiabatic, the CO_2 is provided in excess to the reactor, with a mass flowrate around 3.3 times the stoichiometric amount. The configuration is relatively complex and the HEN is composed by 9 HEXs units. The first water heating is very demanding in terms of thermal power requested and, in order to accomplish it, splitting the water stream results to be necessary to exploits both the carbonation products exiting the reactor. In addition, due to the complex heat recovery process, it is not possible to avoid the splitting of the $CaCO_3$ (and unreacted CaO) stream.

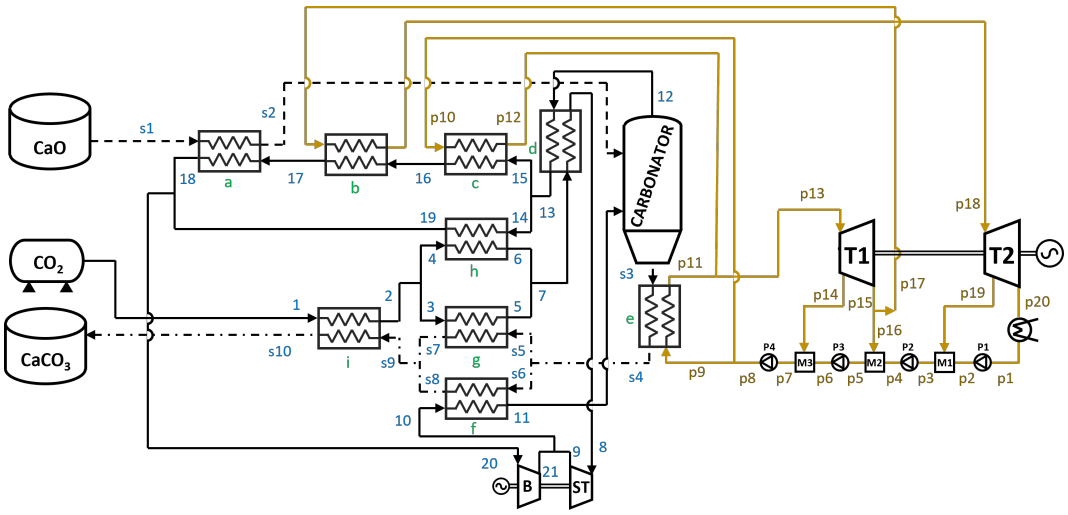

Fig. 2.20 A feasible layout of the carbonator side for the steam Rankine indirect integration

2.6 Indirect integration - sCO_2 Brayton cycle

In this section the indirect integration of a sCO_2 Brayton cycle is described and the results of its optimization are presented and discussed. As already mentioned, this kind of integration, together with the direct integration, was mostly investigated before the PhD years. However, it is included in the present discussion to provide a broader perspective on the alternatives for the CSP-CaL integration.

2.6.1 Integration description

The interest for supercritical carbon dioxide cycles in CSP increased significantly during the last years and several layouts are proposed in literature [84–86] showing encouraging performances. The alternatives investigated in the present work start from the simplest configuration (single compressor, turbine, regenerator, heater and cooler) up to the most complex case, which includes reheating, inter-cooling, recompression and pre-compression stages. The superstructure approach is exploited also in this case for the power block layout. A complete configuration, obtained as the sum of the different layouts, is provided to the optimization process and when the algorithm spontaneously tends to impose a null flowrate/pressure drop/temperature difference on a specific component, this is automatically bypassed by the power fluid

and therefore eliminated from the layout. The superstructure layout is shown in Figure 2.21 (LTR/HTR stand for Low/High Temperature Regenerator); the components filled in yellow can be removed during the optimization process, while the ones in white are fixed. The dashed lines at the split for the recompression branch indicate that the connection can assume only one between the two alternative positions (0 or 1, as if it was a switch), which determines if the layout is in a precompression configuration rather than in pure recompression. The choice between the layouts considered is made taking into account both cycle performance and topology complexity [87, 88].
Regarding the optimization process, the same steps described for the SRC indirect integration are followed for this case study.

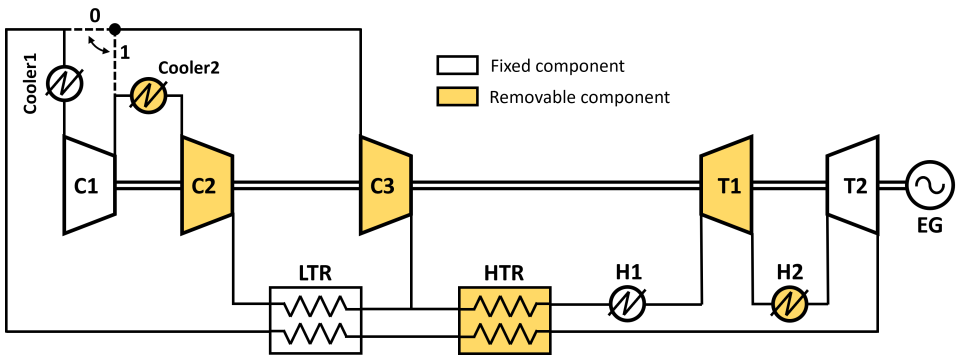

Fig. 2.21 Superstructure of the power block based on a sCO_2 Brayton cycle

The assumptions made for the thermodynamic cycle are taken in accordance to the data found in [84, 88–90] and are reported in Table 2.9. As in the other case studies, dry cooling with ambient air is assumed for the heat rejection in the power block. Two specific constraints are addressed for this integration:

- the minimum temperature difference is imposed between the LTR cold inlet and hot outlet in order to guarantee the maximum heat recovery on the flow exiting the turbine;
- the inlet temperatures of the two turbines are set to be equal.

Table 2.9 Data assumptions for sCO_2 Brayton cycle indirect integration

Parameter	Component/stream	Value
Isentropic efficiency	Turbines	0.92
	Compressors	0.88
Mechanical efficiency	Steam turbines	0.97
Electrical efficiency	Steam turbines	0.97
Pressure loss	Regenerator hot side	1.5%
	Regenerator cold side	1%
	Heater	1.5%
	Cooler	2%
Minimum ΔT	Heater	$20°C$
	Cooler	$15°C$

The independent variables of the optimization related to the power block are reported in Table 2.10 with their variation ranges, whose bounds are fixed according to [88, 91]. These are: recompression split position (RSP), first Compressor Inlet Pressure ($C1IP$), first Turbine Inlet Pressure ($T1IP$), Recompression Flow Fraction (RFF), Turbines Inlet Temperature (TIT), Cold Side LTR Outlet Temperature ($CSLTROT$), first compressor pressure ratio (β_{C1}), first turbine pressure ratio (β_{T1}) and minimum temperature difference achievable in the regenerators ($\Delta T_{min,R}$). Is worth to notice that it is possible to exclude CSLTRT from the independent variables in case of isothermal mixing between the two regenerators. In the present case, this parameter is assumed as variable to evaluate the possible convenience in mixing the streams at different temperatures, expanding the optimization extent.

Table 2.10 Independent variables specific to sCO_2 Brayton indirect integration

Variable's name	Lower bound	Upper bound
RSP	*Binary variable*	
$C1IP$	$75bar$	$95bar$
$T1IP$	$180bar$	$250bar$
RFF	0.4	0.1
TIT	$500°C$	$700°C$
$CSLTROT$	$100°C$	$450°C$
β_{C1}	1	4
β_{T1}	1	4
$\Delta T_{min,R}$	$5°C$	$20°C$

Regarding the economic aspect, the cost functions that are added to the ones already presented in the previous sections are the ones for the estimation of the investment costs of the components constituting the power block.

- sCO_2 turbine
  The cost function for the sCO_2 turbine [92] is reported in Equations 2.43, where $\dot{W}_t$ is the turbine shaft power.

$$IC_{t,sCO_2} = 8279\ (\dot{W}_t)^{0.6842} \tag{2.43}$$

- sCO_2 compressor
  The cost function for the sCO_2 compressor [92] is reported in Equations 2.44, where $\dot{W}_c$ is the compressor shaft power.

$$IC_{c,sCO_2} = 7331\ (\dot{W}_c)^{0.7865} \tag{2.44}$$

- sCO_2 heat exchangers
  The cost of the regenerators and the air coolers is estimated with the strategy proposed in [92], which allows to obtain the normalized cost value (c in $\left[\frac{\$}{W/K}\right]$) through a linear interpolation of the corresponding UA values. The simple relation reported in Equation 2.45 is used for the purpose.

$$IC_{HEX,sCO_2} = c_{HEX} \cdot UA_{HEX} \tag{2.45}$$

The data used for the interpolation is reported in Table 2.11.

Table 2.11 Normalized cost values for data interpolation

		$UA[W/K]$				
		$5 \cdot 10^3$	$3 \cdot 10^4$	$1 \cdot 10^5$	$3 \cdot 10^5$	$1 \cdot 10^6$
$c\left[\frac{\$}{W/K}\right]$	Regenerator	5.89	1.31	1.22	1.03	0.94
	Air cooler	9.66	3.05	1.65	1.40	1.27

- Carbonator side's HEN
  The cost function used to estimate the price of the HEN in the carbonator side was obtained through data fitting. Equation 2.46 is used in case the power block is fed with a heat transfer performed on the carbonation products, while Equation 2.47 is considered when the heat transfer takes place on the carbonator's wall (where UA is in $[W/K]$ and the result in $[\$]$).

$$IC_{HEN,CrbS} = 3.402 \cdot UA \tag{2.46}$$

$$IC_{HEN,CrbS} = 2.3923 \cdot UA + 38495 \tag{2.47}$$

2.6.2 Results and comments

The Pareto curve obtained from the multi-objective optimization of the sCO_2 Brayton cycle indirect integration is presented in Figure 2.22. The reasons for the discontinuities are the same already discussed for the integration of the steam Rankine cycle. A total plant efficiency of 21% is attained with the most performing configuration, which has a specific investment of $179.5\$/MJ$. On the other hand, a cost of $161.6\$/MJ$ (-10% in relative terms) and a performance of 16.3% (-22.4% in relative terms) are achieved in case of economic optimization. The considerable variation between the two opposite cases is due to the great variety of configurations that can be achieved both on the design and on the operation level. Also in this case, providing the heat required by the power block with a direct heat transfer on the carbonator wall increases the total plant efficiency and the specific cost. Concerning the thermal cycle, the sCO_2 compression is always performed with an inter-cooling step, demonstrating the importance of reducing the power absorption

for the compression of the supercritical fluid. The Genetic Algorithm always includes the recompression branch (and therefore the third compressor), except for the configuration representing the economic optimization, where the absence of this element allows to slightly reduce the investment but determines a noticeable decrease of the total performance. In addition, when the recompression is executed, the "pure recompression" configuration is selected, which consists in providing the fluid stream to the recompression without having performed a pre-compression (configuration 0 in Figure 2.21). Finally, the reheating stage is always considered when the power block is fed on the carbonator wall, while both the configurations of single and double turbine are selected in case of heat recovery on the carbonation products.
The number of inter-coolings occurring in the calciner side compression, the inlet temperature and pressure of the power block turbine always closely approach their maximum. On the other hand, the inlet pressure of the first compressor and the $\Delta T_{min,R}$ always converge in a nearby of their minimum. The Storage Turbine Inlet Temperature reaches higher values for a less performing power cycle, in order to extract more power from the pressurized stoichiometric CO_2, whose flowrate tends to increase. Three aspects occurring in case of HTCW are worth to be mentioned: first, the carbonator side operating parameters remain nearly constant and only the power block variables are observed to change. This behavior is actually reasonable: in fact, the power cycle integration into the carbonator side has a smaller impact since the thermal flux released to the power block is directly provided by the chemical reaction and not by a thermal recovery performed on the carbonation products. For second, the sensible heat contained in the reactor outflows is exclusively exploited for the inlet streams preheating, and the STIT can maintain its maximum value since heat at high temperature is not employed for feeding the thermodynamic cycle. The last aspect to mention is that the carbonation temperature does not reach its maximum achievable value and it can be explained considering that this allows to bring the two curves closer, enhancing the heat transfer efficiency.

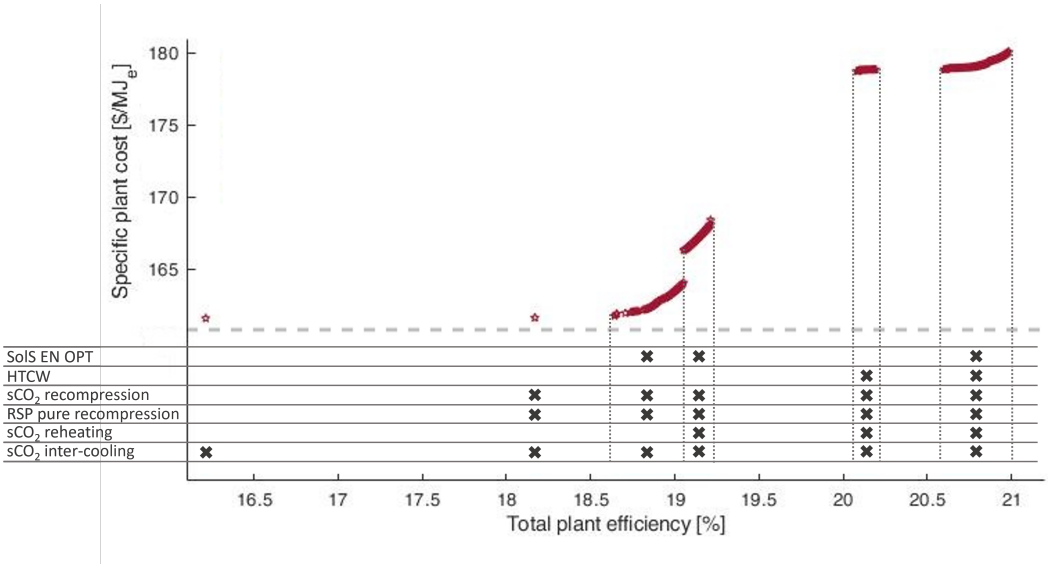

Fig. 2.22 Pareto curve for the multi-objective optimization of the direct integration

The configuration presented in the following images is chosen because of its low specific investment cost, which is similar to the one obtained with the economic optimization but, at the same time, shows a higher efficiency. It corresponds to the case in which the GA selects the pure recompression with an inter-cooling step, the heat required by the power block is provided with a heat recovery and the solar side is optimized in energy terms.

The two composite curves for the thermal transfer process of the carbonator side are showed in Figure 2.23. The curves are relatively close each other, especially in the range between 150°C and 500°C (approximately), which is the region where the sCO_2 stream of the power block is not present.

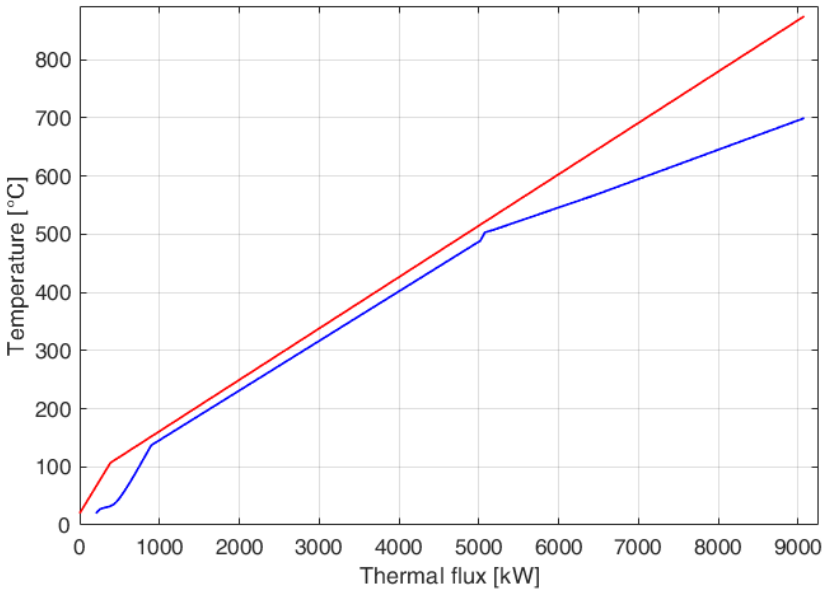

Fig. 2.23 Hot and cold composite curves from pinch analysis for the sCO_2 Brayton indirect integration

As can be observed in Figure 2.24, which shows the grand composite curve computed with the pinch analysis, the GA finds an operation where the heat transfer process reaches the pinch point for two times. These points are the extreme temperatures of the range already mentioned and play an important role in the heat recovery process.

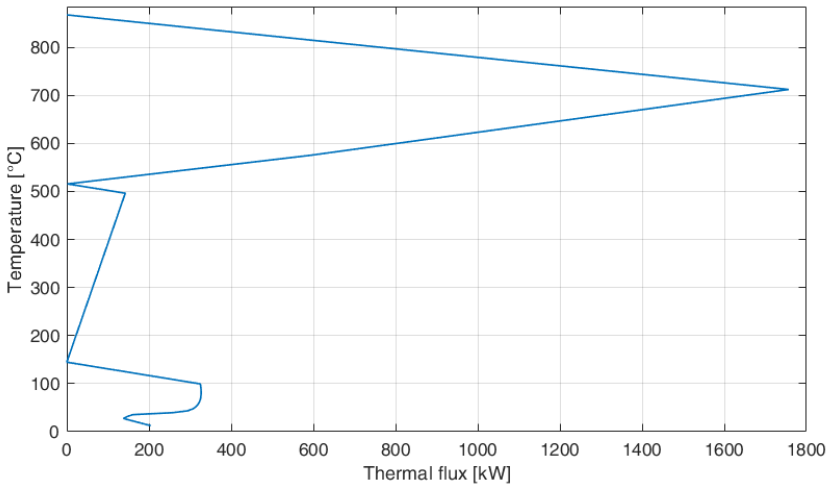

Fig. 2.24 Grand composite curve from pinch analysis for the sCO_2 Brayton indirect integration

The layout of the carbonator side and the power block is showed in Figure 2.25. The heat exchanger network is relatively complex and it is composed by 8 HEXs units (except for the two sCO_2 regenerators). Due to variations in the thermophysical properties of the CO_2 in the supercritical state, the gaseous flowrate extracted from the storage requires three units to be heated up to the inlet temperature of the storage turbine. However, both the splitting of solid flows and the thermal transfer between solids are avoided.

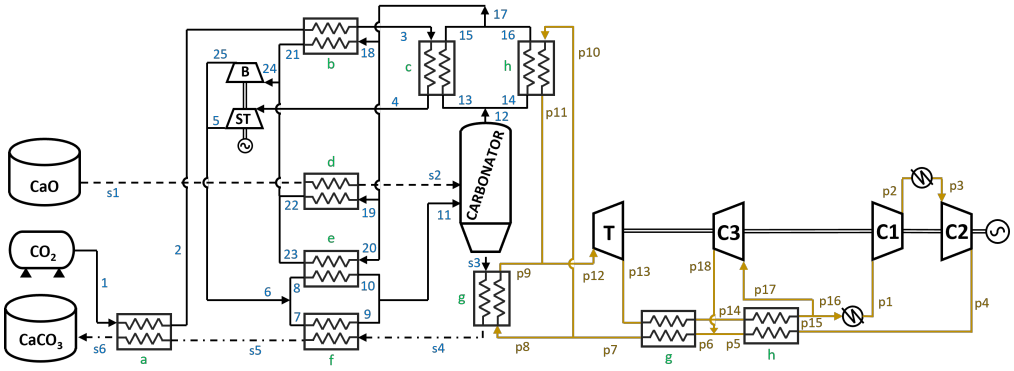

Fig. 2.25 A feasible layout of the carbonator side for the direct integration

2.7 Indirect integration - He Brayton cycle

In this section the indirect integration of a He Brayton cycle is described and the results of its optimization are presented and discussed.

2.7.1 Integration description

Closed Brayton thermal cycles with helium as power fluid are an interesting alternative between the available options because of the expected high efficiencies [93] attainable tanks to the high operating temperatures and the thermophysical properties. The great majority of the studies that can be found in scientific literature on helium Brayton cycles are conducted in the field of nuclear power plants [94, 95] but, in more recent works, these thermal cycles are also investigated for CSP [96, 97]. Advantages and drawbacks characterizing He power blocks are highlighted in [98]: low (but non-negligible) pressure losses, good heat transfer coefficients, no Mach number restriction, high number of turbomachinery stages, leakages and early stage of development. In addition, a comparison between helium and supercritical carbon dioxide cycles is performed in [99].
Some of the (already cited) aspects that characterize this technology must be carefully treated, since they have important effects either on the efficiency or on the investment costs. In particular: 1) high number of stages for turbomachinery (especially for compressors); 2) non-negligible impact of pressure drops in heat exchangers on cycle performance; 3) intercoolings/reheatings effects on efficiency. Concerning this last point, the number of intercoolings and reheatings are included between the independent variables of the problem through a superstructure. Up to four turbines and eight compressors are considered in the investigation executed in [100] but, in order to avoid an excessive layout complexity, three turbines and four compressors are set as maximum achievable number of turbomachinery in the present work. The total layout assumed for the optimization process is shown in Figure 2.26, where the fixed components are filled in white, while the yellow ones can be added/removed.
Regarding the optimization process, the same steps described for the two previous indirect integrations are also followed for this case study.

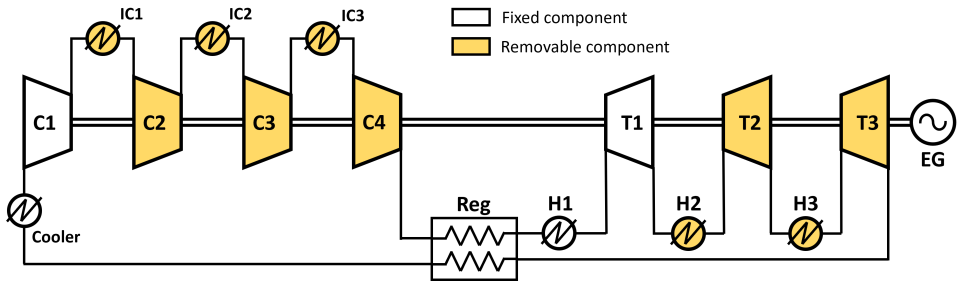

Fig. 2.26 Superstructure of the power block based on a *He* Brayton cycle

The assumptions for the power block modelling are summed up in Table 2.12 and are taken according to [97, 101]. Helium is considered as an ideal gas and dry cooling with ambient air is adopted for the heat rejection. Pressure losses occurring in the regenerator are set as a function of the LMTD in order to take into account the fluidynamic drawbacks related to a more efficient regeneration. In addition, two constraints are addressed to optimize this indirect integration: the maximum turbine inlet pressure is set to 75 bar, and the inlet temperature of the turbines is imposed to be equal.

Table 2.12 Data assumptions for *He* Brayton cycle indirect integration

Parameter	Component/stream	Value
Polytropic efficiency	*He* Turbines	$0.932 - 0.0117 \ln(\beta_t)$
	He Compressors	$0.916 - 0.0175 \ln \beta_c$
Electrical efficiency	Steam turbines	0.97
Pressure loss	Regenerator hot side	$19.2/\Delta T_{ml}$ %
	Regenerator cold side	$3.12/\Delta T_{ml}$ %
	Heater	2%
	Cooler	1.6%

The independent variables to be optimized are listed in Table 2.13 with their corresponding variation ranges (taken according to [97, 102]). Here, $C1IP$ is the inlet pressure of compressor C1, $\#C$ is the number of compressors, $\beta_{C_{1/2/3/4}}$ is the pressure ratio of the compressors, $\Delta T_{min,reg}$ is the regenerator minimum temperature difference, TIT is the turbines inlet temperature, $\#T$ is the number of turbines, and $\beta_{T_{2/3}}$ is the pressure ratio of turbines T2 and T3.

Table 2.13 Independent variables specific to He Brayton indirect integration

Variable's name	Lower bound	Upper bound
$C1IP$	$1.2bar$	$26bar$
$\#C$	1	4
$\beta_{C_{1/2/3/4}}$	1.16	5
$\Delta T_{min,reg}$	$5°C$	$25°C$
TIT	$600°C$	$850°C$
$\#T$	1	3
$\beta_{T_{2/3}}$	1.16	5

Regarding the economic aspect, the investment cost of the He turbomachinery is estimated by adapting the coefficients of the cost functions already used for the sCO_2 turbines and compressors (Equations 2.43 and 2.44) with the costs found in [103]. In addition, the same approach used for the SRC indirect integration is adopted in case a heat transfer on the carbonator wall is required (Equations form 2.37 to 2.40). Also in this case it is necessary to verify that the hypothesis of turbolent flow of the He stream in the HEX pipes is satisfied. The other cost functions used for this kind of integration are reported below.

- Carbonator side's HEN
  The cost function used to estimate the price of the HEN in the carbonator side was obtained through data fitting. Equation 2.48 is used in case the power block is fed with a heat transfer performed on the carbonation products, while Equation 2.49 is considered when the heat transfer takes place on the carbonator's wall (where UA is in $[W/K]$ and the result in [\$]).

$$IC_{HEN,CrbS} = 3108.4 \cdot UA^{0.462} \tag{2.48}$$

$$IC_{HEN,CrbS} = 2.3923 \cdot UA + 38495 \tag{2.49}$$

2.7.2 Results and comments

Figure 2.27 shows the Pareto curve obtained with the multi-objective optimization of the indirect integration of the He Brayton cycle. The solar side is nearly always

optimized in energy terms, except for the point corresponding to the economic optimization. For the power block, the Genetic Algorithm finds that the optimal number of compressors is three for the entire length of the curve. Two turbines are selected in case of thermal feeding executed with a Heat Recovery on the Carbonation Products, while three are chosen when a Heat Transfer on Carbonator Wall is performed. The former configuration allows to reach the best results in economic terms and the latter layout makes possible to obtain the highest performances. A significant variation is observed for the configuration with HTCW. The reason for this phenomenon is the strong influence of the inlet temperature of the helium turbines on the two objective functions. Keeping a high carbonation temperature and reducing the helium maximum temperature allows to decrease the reactor investment cost (the higher temperature difference lowers the heat transfer surface required) at the price of an efficiency penalty. For this reason, helium TIT changes from its maximum achievable ($850°C$ with efficiency equal to 21.85%) to $789°C$ (with total efficiency 20.8%). The minimum temperature difference reached by the regenerator is another parameter that influences the system performance (although not so significantly as the one previously cited). Lower values allow a better heat recovery but, according to the methodology adopted, determine higher pressure losses. Considering these two conflicting aspects, the solution found by the algorithm shows a minimum temperature difference equal to $8.2°C$ (in case of maximum performance) that progressively rises up to $13.8°C$ (for the economic optimization).

Finally, it is worth to discuss how the choice for the compromise between plant efficiency and costs is carried out by the algorithm. The cost of the charging plant section is always the most significant contribution to the total capital investment, therefore it could be expected that less performing power blocks require charging processes with higher sizes, introducing penalties in both energy and economic terms. However, results demonstrate the existence of configurations in which the costs increase related to the charging section is overcome by the price decrease occurring in the discharging process.

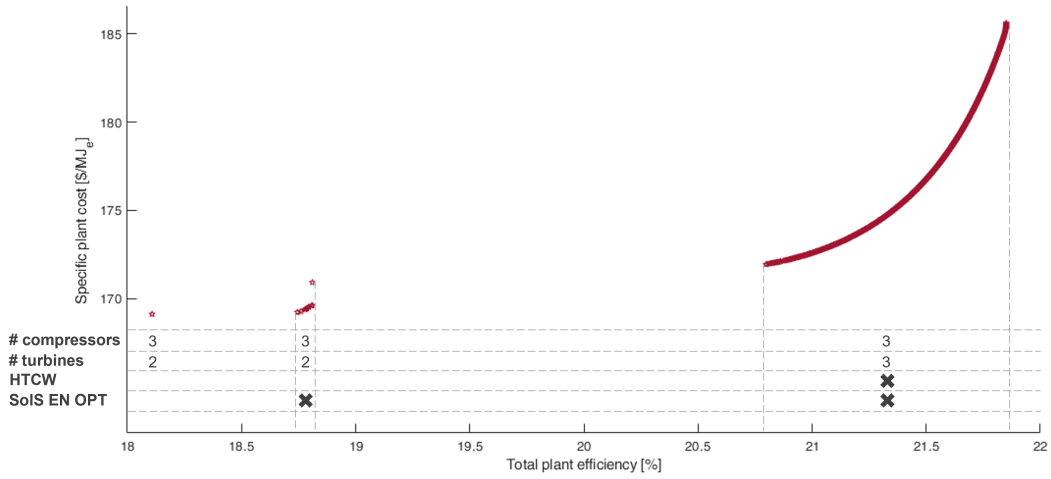

Fig. 2.27 Pareto curve for the multi-objective optimization of the direct integration

The configuration selected and analyzed more in detail is the one corresponding to the energy optimization. The main reason for this choice is the interesting plant efficiency attained and the layout setup of the carbonator side.
Hot and cold composite curves obtained with the pinch analysis are shown in Figure 2.28. The fact that $CaCO_3$ and unreacted CaO are the only carbonator outflows (at high temperature) makes it impossible to avoid solid–solid thermal transfer in the heat recovery process. The presence of this phenomenon is coherently taken into account during the pinch analysis execution by properly modifying the minimum temperature difference achievable by this specific stream. Despite the two curves have similar slopes, they are not very close to each others. However, this aspect does not represent an important disadvantage since the thermal power exchanged is not considerably high compared to the other energy fluxes involved in the process.

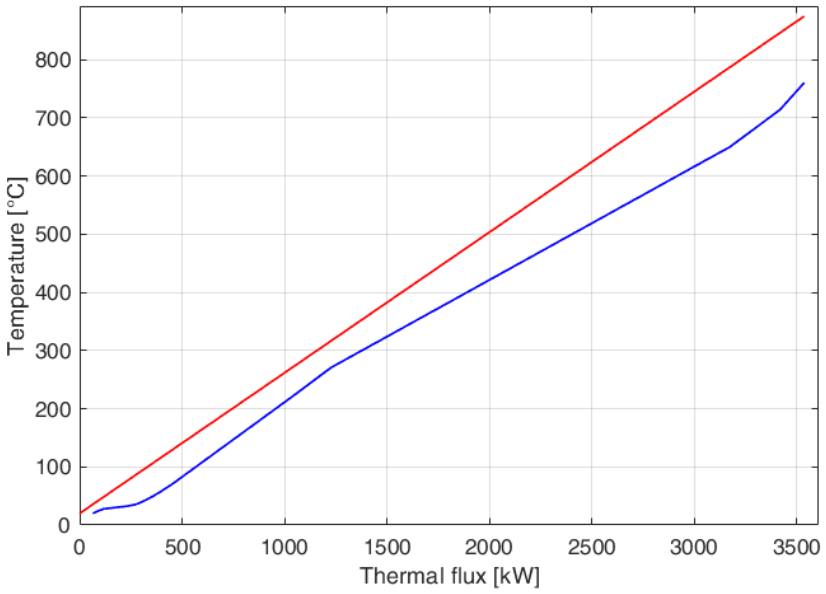

Fig. 2.28 Hot and cold composite curves from pinch analysis for the *He* Brayton indirect integration

In Figure 2.29 the grand composite curve is presented. In this case, the pinch point is reached only one time, in correspondence of the heating of the CO_2 extracted from the storage.

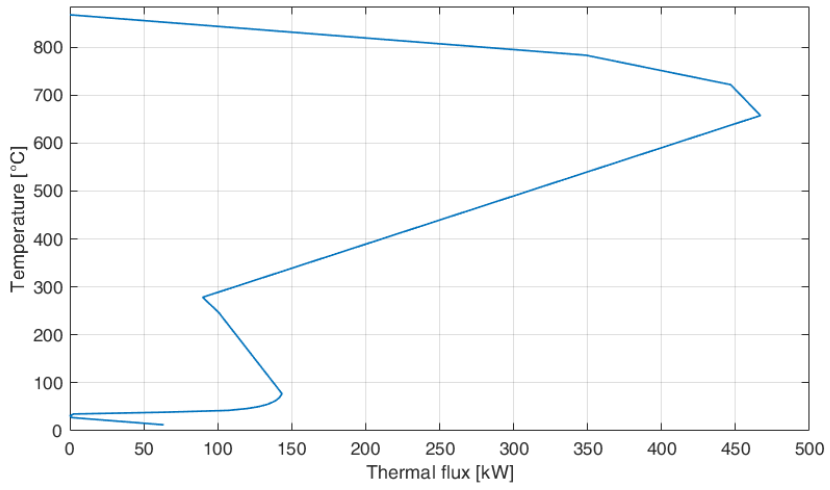

Fig. 2.29 Grand composite curve from pinch analysis for the *He* Brayton indirect integration

The layout of the discharging section of the plant is presented in Figure 2.30. In this configuration the maximum number of He turbines is reached, but the same does not happen for the He compressors. The reason is that the reheating and inter-cooling stages influence the system efficiency in different (and non-trivial) ways. In fact, a higher number of compressors and turbines allows to execute an efficient compression and expansion, but, at the same time, the pressure losses determined by intercoolers and reheaters introduce non-negligible penalties to the power block performance. As a result, three compressors and three turbines are found by the algorithm to be the optimal setting in order to achieve the maximum energy performance. The Helium temperature at the turbines inlet is $850°C$, while the first compressor and first turbine inlet pressures are $11.5bar$ and $33.7bar$ respectively. The compressors show nearly identical values of pressure ratio (equal to 1.46) and the same is observed for the turbines (equal to 1.4). Concerning the carbonator side, it is important to notice that the algorithm converges to a configuration in which the amount of CO_2 provided to the carbonation reaction is equal to the stoichiometric value. Since there is not a recirculating stream of CO_2 at the outlet of the reactor, it cannot be avoided to preheat the CaO with the $CaCO3$ and the presence of a heat transfer fluid (between the two solids) must be taken into account. At the end of the preheating process, CO_2 and CaO enter the carbonator at $714°C$ and $761°C$ respectively. Both carbonation temperature and storage turbine inlet temperature reach their maximum value. The heat recovery at the carbonator wall has two main consequences. First, the carbonator operation becomes more complex and its investment cost increase sensitively because of the presence of heat exchangers. Second, the carbonator side Heat Exchanger Network layout becomes simpler and the heat exchanger sizes are smaller, since it is only devoted to the reactants preheating.

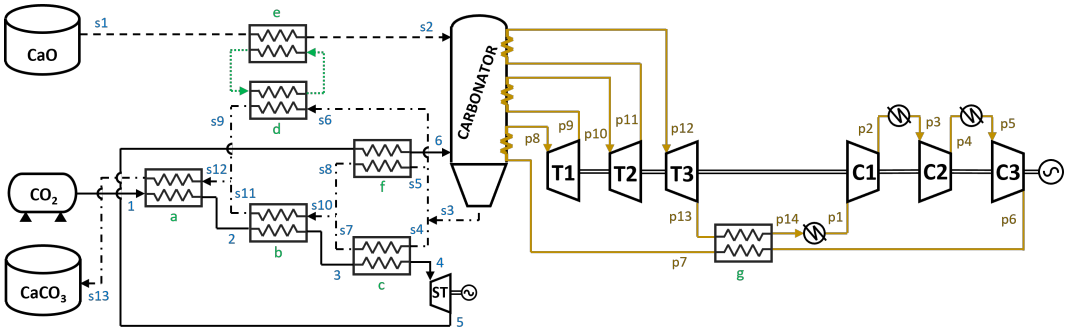

Fig. 2.30 A feasible layout of the carbonator side for the direct integration

2.8 Comparison of the integration alternatives

The aim of this section is to compare the integrations investigated in the present work in order to highlight the differences among them. The amount of results obtained from the multi-objective optimizations is huge and a detailed comparison would be excessive taking into account that the primary scope of the study is to develop a comprehensive methodology for the optimization of power plants, independently from the case study and the input data assumed. For this reason, the comparison reported below can be considered as the essential version of the analysis that could be conducted.

For first, it can be interesting to observe the differences occurring in case of single-objective optimization, such as for the economic optimization. Figure 2.31 shows the values attained by the two main parameters when the specific plant cost is minimized. The cheapest alternative is represented by the direct integration, with a specific investment of $128\$/MJ$. The other options determine an increase in the cost up to $+32\%$. The competition between the two objective functions was confirmed from the observation of the previous Pareto curves, but this trend is not completely respected when the different integrations are compared. In fact, despite the direct integration shows the lowest investment cost, it does not have the lowest energy performance, which is reached by the indirect integration of the steam Rankine cycle. The reasons for the economical advantage shared by the direct integration is mainly due to its relatively simple plant layout, the non-demanding operating conditions, and the absence of a thermal transfer step between the power block and the carbonator side.
In all the configurations obtained from the economic optimization, the GA converges to a solution in which the carbonation reaction is executed into an adiabatic reactor and the power block is fed with a heat recovery on the products. Therefore, avoiding the configuration in which the heat is provided to the power block with a heat transfer on the reactor wall results to be fundamental to achieve the lowest investment costs for all the integrations investigated.

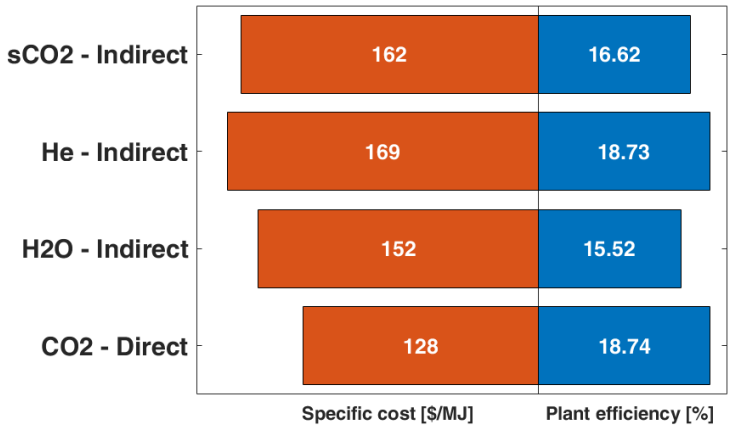

Fig. 2.31 Comparison of the objective functions for the economic optimization

On the other hand, Figure 2.32 shows the same comparison in case the plant efficiency is maximized. The indirect integration of the *He* Brayton cycle results to be the most performing integration with a plant efficiency of 21.85%, but, at the same time, it is the most expensive one. The second alternative is represented by the indirect integration of the other Brayton cycle based on supercritical CO_2, which is, in relative terms, 4% cheaper and less efficient. Among the results of the energy optimization, the direct integration shares the lowest investment cost despite not being the least performing alternative, which is represented by the indirect integration of the steam Rankine cycle.

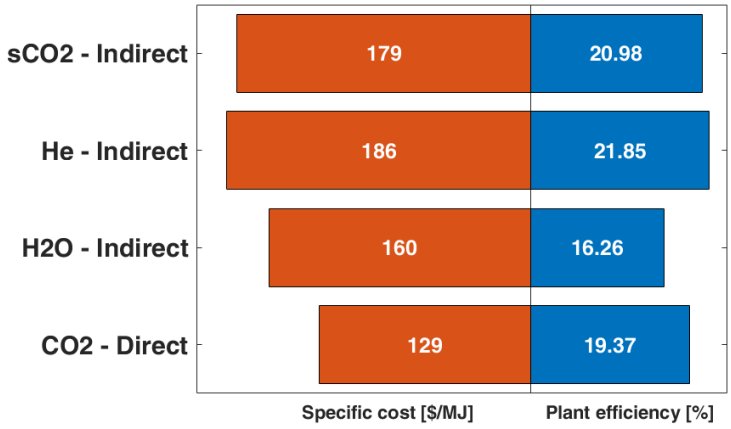

Fig. 2.32 Comparison of the objective functions for the energy optimization

All the Pareto curves obtained from the separate multi-objective optimizations are reported in Figure 2.33. As can be noticed, the indirect integrations are located in a relatively consequential order. In particular, the cases with the steam Rankine cycle and the sCO_s Brayton cycle are almost consecutive, while the integrations of the two Brayton cycles overlap each others. The direct integration has an intermediate performance range compared to the other options, but the entire Pareto front reaches lower investment costs. As a result, it is located relatively distant from the other curves and it mainly overlaps the Pareto front of the sCO_s Brayton cycle.

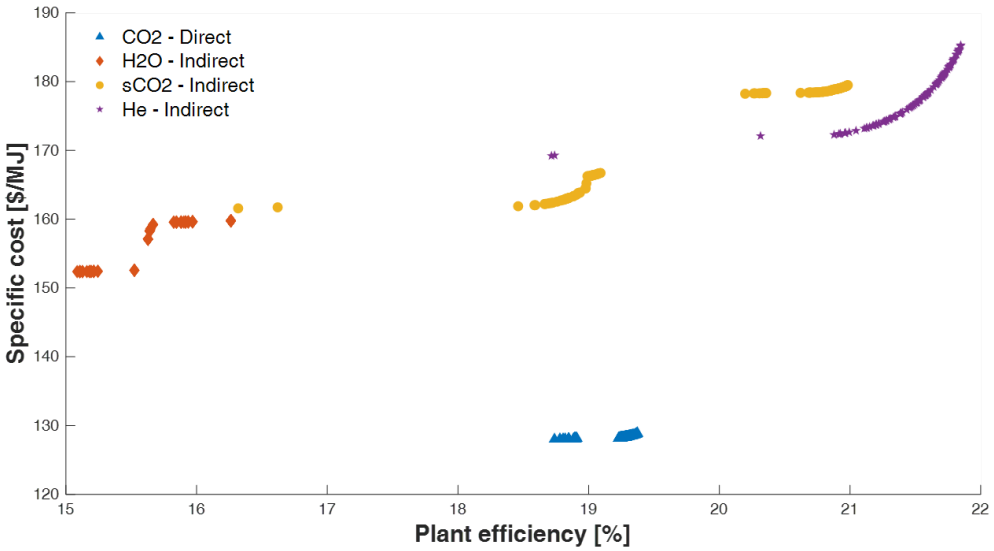

Fig. 2.33 Pareto curves of the CSP-CaL integrations investigated

Finally, it is worth to observe the composite Pareto curve, obtained by plotting in the same graph all the frontier curves and removing the dominated segments, as showed in Figure 2.34. This composite Pareto curve includes the two extreme alternatives. On one side, the indirect integration of the *He* Brayton cycle, which exploits a very performing power block, composed by many reheating and inter-cooling steps and it is exclusively fed on the carbonator wall. On the other side, the direct integration, based on a closed CO_2 Brayton cycle with compression and expansion stages performed in single steps and the carbonation process executed in an adiabatic reactor. Both the segments grow horizontally, indicating that the efficiency variation is greater compared to the difference of the investment cost, while the considerable space separating the two sections highlights the intrinsic difference between these integrations.

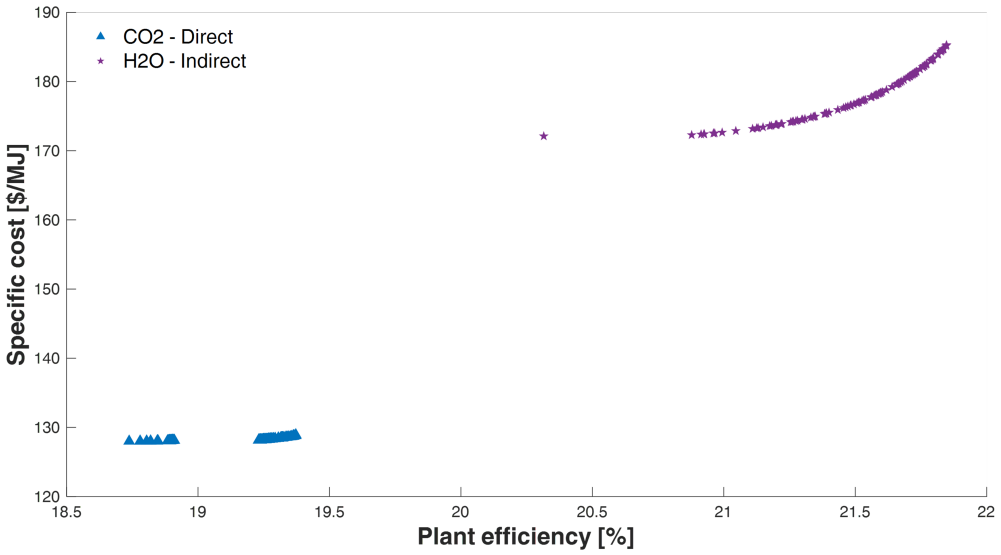

Fig. 2.34 Cumulative Pareto curve of the CSP-CaL integrations investigated

The choice of a CSP-CaL integration among the alternatives investigated is a task that depends on a multitude of aspects and for this reason it is not possible to state that a specific integration is always better than the other ones.
In the present analysis, two criteria were assumed to synthetically evaluate the CSP-CaL configurations: the total efficiency and the specific cost. However, other aspects were observed as well, such as the layout complexity and the operating conditions. The chemical reactors (calciner and carbonator) are the most important components for the thermochemical storage process and despite their typology is already existing and used in other fields, their applicability in the CaL process must be demonstrated and the necessity to realize tailored arrangements can be reasonably expected. For these reasons, the following considerations can be drawn according to the type of carbonator that, in a real case study, will be able to execute the exothermic reaction as successfully as possible.

- In case an adiabatic reactor is installed, the most interesting alternative is represented by the direct integration. Being characterized by low investment costs, a simple layout, non-demanding operating conditions and good performances, it can be considered as the option with the best overall features and a good compromise between the energy and economic aspects.

- In case a non-adiabatic carbonator is chosen, it can be worth to consider the indirect integration of an He Brayton cycle. Despite the numerous steps for the He compression and expansion, the layout of the discharging plant section results to be relatively simple thanks to the heat transfer on the carbonator wall. The specific investment cost is the highest achieved among the options investigated, but it is justified by the efficiency attained, which is the highest as well.

In addition to the comparison between the configurations studied, it would be interesting to compare the CSP-CaL integration with the other types of central tower CSP plants. However, the variety of conditions for which the plants are designed is such that a coherent comparison cannot be carried out by simply looking at the results obtained in research works from the scientific literature. The total efficiency computed in the present thesis is referred to the design day, while the results found in literature are expressed for an entire year or in peak conditions. Some values of peak performances are reported just to give a rough idea of the range of efficiency characterizing the other CSP technologies: a) the PS10 plant attains 21.7% with a steam Rankine cycle [104]; b) the sCO_2 power block in [84] allows to reach 23.4%; and c) a maximum efficiency of 24.3% is predicted for an unspecified thermal cycle in [105]. As reported in the results presented in the present subsection, the performance range obtained from the optimization of all the CSP-CaL integration is $18.5\% - 22\%$ and it's referred to the design day. It is reasonable to expect that the peak performances will be few percentage points higher than the daily average, which brings the efficiency of the CSP-CaL system in line with the ones presented in literature. The fundamental advantage shared by the plant analysed relies on the fact that it exploits a thermochemical energy storage, which can store energy in the medium-long term without thermal losses.

Chapter 3

Optimization of Multi Energy Systems: a literature review

This chapter is devoted to the research conducted in the field of Multi Energy Systems and their optimization. Section 3.1 introduces the topic, while a comprehensive review of the studies presented in the scientific literature is provided in 3.2.

Part of the research presented in the present Chapter was published in Applied Thermal Engineering [J6].

3.1 Introduction

The framework (subsection 3.1.1) and the general aspects characterizing the Multi Energy Systems (subsections 3.1.2 and 3.1.3) are presented and discussed in this section, with the aim of introducing this wide topic and explain the aims of the present study about this research field. Finally, the goals of this study are exposed in subsection 3.1.4.

3.1.1 Framework

The term Multi Energy System is used to indicate a system composed by multiple devices/plants which employ different technologies which cooperate to transform energy sources or energy vectors into other energy vectors. They can be considered

as the last step in the evolution of the systems for the energy production, which started with the concept of separate production (i.e. a single technology producing a single energy vector), it passed through the combined production (i.e. a single technology simultaneously producing multiple energy vectors), and arrived at the idea of MESs.
As will be discussed more in detail in the following subsections, there are numerous reasons that make MESs a very interesting research field, such as the efficiency that could be attained in the energy production processes, the reduction of the costs associated to the energy vectors, and the decrease of the impact on the environment. To attain these goals, the MES must be properly optimized. As a consequence, several challenges related to its modelling must be addressed, and, because of the relative novelty of this field, a solution to these issues has not yet been found.

3.1.2 General features

A conceptual representation of a Multi Energy System is provided in Figure 3.1, where the connections among the categories of units can be observed. MESs can be constituted by any kind of technology for the production, consumption, storage and transportation of energy. Electric Generators (EG), Heat Only Boilers (HOB), Combined Heat and Power units (CHP), Combined Power and Cooling units (CPC), Electric Heat Pumps (EHP), Gas Heat Pumps (GHP), Fuel Cells (FC), Absorption Chillers (AC), PhotoVoltaic panels (PV), Solar Thermal panels (ST), Wind Turbines (WT), energy storages, Electric Networks (EN), and District Heating Networks (DHN) are the most common technologies included as part of the MES investigated in the literature, but any other option can be considered as well.

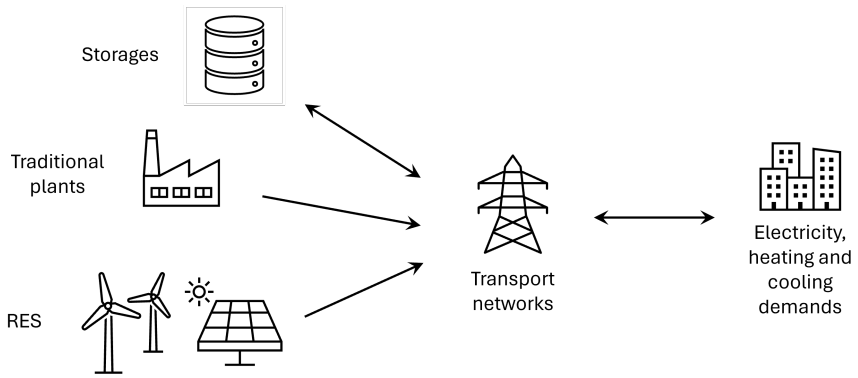

Fig. 3.1 Conceptual scheme of a Multi Energy System

3.1.3 Potentialities and challenges

Multi energy systems are inherently complex and structured systems. The intermittency of renewable sources, the technical constraints of the components, the dynamic variation of energy prices and energy loads are only some of the elements that make their management a difficult task. As a consequence, optimization tools for the evaluation of these systems are indispensable. Among the most important benefits gained with the MES optimization, the followings are worth to be mentioned:

- lower consumptions of primary energy, and, consequently, operating costs and emissions. Based on the case studies proposed in the literature, the cost reduction in economic terms typically ranges from 5% to 25%. Significant advantages can be achieved as well when the optimization criterion is the primary energy reduction or the decrease of the CO2 emissions (up to one half [106–113]). Combined heat and power production is only an example of the benefits that can be achieved compared to separate generation [114, 115];

- a better planning of component operation and the compliance of technical constraints respect the common practice operation set. In fact, in real applications, load following techniques (e.g. Following Electric Load, Following Thermal Load, etc.) are usually employed, which manage the components operation according to a predefined hierarchy. Differently from an operation strategy, an optimization process allows to solve the unit commitment problem with a higher degree of freedom, since a hierarchy between the components operation is not defined. This typically results in smaller operation costs (from 5% up to 25% [107, 113]);

- distributed generation can significantly reduce peaks and congestions in energy networks. This advantage is increased if its operation is the result of an optimization process. This is due to the lower amount of energy vectors requested to the grids thanks to the proximity of generators and users, which can be matched without resort to external networks. In addition, the capability to include network constraints in the optimization contributes significantly in avoiding operation criticalities (e.g. network congestion, [116, 117];

- a rational management of storage units. These components are commonly operated based on predefined strategies (e.g. discharge performed during peak

periods and charge executed when demand is low). However, the operation set with these strategies is usually far from the optimal one and does not allow to fully exploit the advantages brought by the presence of an energy storage, such as energy/economic benefits and flexibility increase.

Therefore, from a theoretical point of view, the advantages of MES optimization have been widely demonstrated. Nevertheless, for optimal strategies to be put into practice in real scenarios, the optimization model must be able to realistically describe the energy system. Indeed, despite the undeniable benefits, modelling multi energy systems in a realistic way still presents several challenges that have to be met. The most important ones are:

- the intrinsic dependence of the solution to the initial assumptions, which can significantly affect the meaningfulness of the results. As a consequence, this can determine a non-complete applicability of the solution obtained in case the real conditions are excessively different from the simplified ones. To guarantee a reliable solution, the assumptions adopted should be adequate for any operation configuration in which the system could operate;
- the limited amount of real phenomena and practical aspects that can be implemented in the optimization model (e.g. components performance, decision variables, etc.). In fact, some features characterizing MESs are difficult to be considered because they require a complex modelling. Therefore, simplifications result necessary;
- high computational times and convergence issues that arise when the problem reaches high dimensions. This can be caused by the need to consider long time periods in the analysis (e.g. as in the case of synthesis, design and operation optimization) or to include the uncertainties affecting the problem. In those cases, the model must be able to find a solution as close as possible to the global optimum in a reasonable amount of time.

3.1.4 Aims of the study

The scope of this part of the work is to investigate the optimization of Multi Energy Systems and to contribute, where possible, to part of its development. As can be

imagined, this research field is very wide, both for the aspects that constitute it and for the amount of scientific papers written in the two last decades.
As a consequence, one of the aims of this study was to realise a detailed literature review before undertaking any kind of research activity. This review was developed in collaboration with my research group at the Energy Department of Politecnico di Torino. For first, it was necessary to investigate the practical strategies created to model and optimize the MESs, making some distinctions according to the differences shared by the case studies. By presenting this overview it was possible to find out the scientific gaps in the research and, according to them, the development of a new analysis on the integration of thermal networks in MES optimizations.

3.2 Literature review

A literature review is presented in order to observe the state of the art and to discuss the strategies already existing for the solution of the MESs problems. The discussion is divided in subsections: for first, the most important elements characterizing the MES modelling and optimization are presented (from now on, they will be called discriminating elements, subsection 3.2.1). The MES modelling is discussed for both a simplified approach (3.2.2) and a more realistic one (3.2.3). The different aims of the optimization are investigated in subsection 3.2.4, while the inclusion of uncertainties and flexibility sources is presented in subsections 3.2.5 and 3.2.6. Finally, the development and execution of the optimization model is discussed in practical terms in subsection 3.2.7 and the conclusions are presented in subsection 3.2.8.

Given the enormous popularity of applying optimization tools to these types of systems, several works can be found in the scientific literature that provide comprehensive reviews on MES. The first review papers, written from 2006 to 2009 [118–120], discuss the concept of multi energy system and present the technologies that can be used for the combined generation. A holistic overview on MES, with a critical discussion on main characteristics, modelling approaches, aggregation concepts, and analysis tools for their operation and planning is presented in [121]. Concerning the synthesis and design problems for smart energy systems, a comprehensive analysis of optimization strategies can be found in [122, 123], with references on decision-making processes. Some distinctions based on the size of

the systems are made in [124–126], where the most common control strategies and optimization processes for MESs operation are discussed. Regarding large shares of renewable sources, [127, 128] provide a comprehensive and detailed investigation of some important aspects, such as renewable energy availability analysis, load profile analysis, geographical domain and the choice of both time period and time step. In addition, relevant references are given for the different approaches typically used in the literature. Important aspects related to renewable sources are the uncertainty and flexibility of energy systems; these aspects are reviewed in [129, 130], considering both modelling and optimization purposes. Finally, the modelling alternatives, the problem formulation, and some exploitable solvers are presented in [131, 132], highlighting pros and cons of the approaches found in the literature. The evaluation of the system performance based on available data, thermodynamic simulation or dynamic modelling are discussed in [133], with a deepening on thermodynamic techniques for cooling and thermal system arrangements (trigeneration, multigeneration, etc.).

3.2.1 Discriminating elements

The discriminating elements are key characteristics of multi energy systems that strongly influence both the problem formulation and the optimization solution. In other words, they can change the nature of the problem and, therefore, the way it can be solved. The most important discriminating elements identified by the authors are:

- **Optimization purpose**
  The optimization process can include up to three different tasks: synthesis, design, and operation.

- **Single-objective/multi-objective**
  The optimization can be done with a single objective function (e.g. cost, primary energy consumption, emissions) or a multi-objective function. This choice does not affect the problem formulation, but it could influence the choice of the solver. Longer computational times must be accounted for the multi-objective optimization, since multiple feasible solutions must be found, and their position in the Pareto curve must converge.

- **Non-linearities**
  The problem to be solved can become non-linear for different reasons:

1. nonlinear performance of system components. The performance of a component varies at partial load operation, in off-design conditions. Efficiencies usually have nonlinear trends, sometimes even non-convex. Therefore, non-linearities are introduced in order to properly describe the performances of the components.
2. nonlinear investment costs. The investment costs vary non-linearly with the size of the component, due to scaling phenomena and other economic aspects. The presence of non-linearities strongly influences the formulation of the problem, the choice of the solver, the computational time and the reliability of the solution.

- **Technical constraints of system components**
  All components operating in energy systems are characterised by technical constraints. To represent the behaviours of the technologies, the problem formulation and the solver must be appropriate.

- **Time interval and time step**
  The length of the time interval that is taken in analysis (e.g. hours, days, years, etc.) can be very important. Considering longer periods means including a higher number of time steps and therefore a higher number of independent variables. By contrast, concerning the time step ($15min$, $30min$, $1h$, $2h$ etc.), larger values help reducing the problem size, but they bring a loss of precision in the operation simulation.

- **Uncertainties**
  Many inputs by the optimization process and referred to the future time periods can be difficult to be estimated (i.e. energy/fuels prices, energy demands, and availability of renewable sources). If the solution must include the effects of the uncertainties, suitable techniques must be adopted during the problem formulation. This increases the problem complexity and the computational cost.

- **Presence of energy storages**
  Energy storages allow decoupling the energy demand and generation, providing a higher degree of freedom to the system operation. However, their presence introduces a correlation between time steps, which can no longer be considered independent. Consequently, the optimization process moves

from a series of small problems (several optimizations, each per time step) to a single problem (one optimization over all time steps). Therefore, the problem becomes larger in size. This makes the solution process more complex to solve due to the exponential relation that links computation time and problem size.

- **Flexibility measures**
  Beside energy storages, other solutions exist to increase the system flexibility. Among them are the adoption of demand response strategies and the exploitation of the infrastructure transients (e.g. district heating network used as thermal storage). The inclusion of these aspects can be very complex, especially for the dynamic simulation of the network, where the presence of bilinear terms and high sizes of the problem must be addressed.

In addition, there are few other aspects that contribute shaping the formulation of the problem. These are not listed between the discriminating elements because they have a weaker influence on the problem formulation. As a consequence, the changes required to take them into account are minor. These are: the typology of energy vector/product; the objective function; the presence of renewable sources in the energy system.
The importance of identifying the discriminating elements is driven by the fact that, influencing the mathematical formulation of the problem, they pose limitations on the selection of the optimization solver. As can be found in the scientific literature, high dimensional problems for MESs optimization are usually simplified and reformulated in order to be executed with deterministic solvers, which can reach better solutions compared to heuristic methods. The optimization problems should not include sources of non-convexity and, possibly, sources of nonlinearity. The classes of this kind of optimization are: Linear Programming (LP), Nonlinear Programming (NLP), Mixed Integer Linear Programming (MILP), and Mixed Integer Nonlinear Programming (MINLP). The differences of these categories are related to the problem formulation, computational times and solution quality; these are discussed further on.

3.2.2 Simplified operation

The optimal scheduling of a multi energy system constituted by generation, conversion, and storage technologies is investigated in the present sub-section. The

operation of the components is simulated in a simplified form, addressing the following features: a) presence of energy storages; b) energy components have neither minimum operating load nor partial load operation; c) no uncertainty inclusion; d) the absence of other flexibility measures in the system. For a similar case, the most suitable time horizon is the short-term, which is usually addressed considering a daily operation discretized with an hourly resolution [134]. Thanks to the assumptions considered in this simplified version of the problem, the use of integer variables is not necessary and nonlinear equations are not addressed. The reference model for this type of problems is a Linear Programming model, which is written in the standard form as reported in Equation 3.1 and can be solved using LP solvers, which are among the fastest and more efficient algorithms able to reach the global optimum [135].

$$\begin{aligned} &\min_{o} f(o) \\ &s.t. \begin{cases} g_i(o) \leq 0 & \forall i \in \{1,..,m\} \\ h_j(o) = 0 & \forall j \in \{1,..,p\} \end{cases} \\ &o \in \mathbb{R} \end{aligned} \tag{3.1}$$

where o is the vector containing the decision variables referred to the system operation, $f(o)$ represents the linear objective function, $g(o)$ and $h(o)$ are the linear inequality and equality constraints, m and n are the total number of inequality and equality constraints, respectively. The definition of the decision variables, the objective function, and the constraints of the problem are discussed in the following list.

- **Component's simulation**
  The operating power of each technology is usually described by a single decision variable. However, there can be some units that need to be described by two variables. This situation arises, for example, when interactions with external networks (power grid, district heating, etc.) are modelled. In these cases, it is possible to employ two distinct variables: one for purchases from the network, and another one for sales to it. Notice that a single variable can be utilized as well, assuming positive and negative values with different meanings

(e.g. positive values for purchases and negative values for sales), but some limitations would arise. The same applies to energy storages with regard to their charging and discharging phases.
Each alternative has its pros and cons. The choice of using only one real variable implies a reduction of the number of variables and therefore a reduction in the computational effort. In addition, this choice allows the problem to be kept simple from a practical point of view. In fact, with the two-variables modelling, additional constraints to prevent simultaneous charging/discharging of the storage or simultaneous buying/selling from/to the grid must be included in the formulation. On the other hand, using a single variable to simulate the operation of the energy networks can create criticalities when an economic optimization is performed. In this case, two variables are needed since the purchase price and the selling price of the same energy carrier are different. Furthermore, if the selling cost is lower than the buying cost (as usually happens), no constraint needs to be added because the simultaneous buying and selling is intrinsically always disadvantageous.

- **Optimization criterion**
  One of the most widely used objective functions is the economic one, here proposed as an example. As far as the operation optimization is concerned, the objective function includes only the operating costs, consisting of the costs of fuels imported into the energy system and the costs/revenues due to exchanges with energy networks. Consequently, a general form of the economic objective function can be written as Equation 3.2.

$$C^{OP} = \sum_{k=1}^{t^{end}} \left[\sum_{j \in U} \left(\sum_{f \in F} c_{f,j,k} I_{f,j,k} \right) + \sum_{i \in V} \left(c_{i,k}^{BUY} P_{i,k}^{BUY} - c_{i,k}^{SELL} P_{i,k}^{SELL} \right) \right] \Delta T \tag{3.2}$$

  Where F is the set of the fuels purchased (such as natural gas, hydrogen etc.), while V is the set of energy vectors managed within the system (heat, cold, electricity, etc.) and U is the set of generation and conversion technologies. Furthermore, $I_{f,j,k}$ is the amount of fuel f imported in the time step k by component j, and c is the related unit cost. In the same way, P_i^{BUY} and P_i^{SELL} represent the bought/sold power for each energy vector i, while c_i^{BUY} and c_i^{SELL} are the related unit costs.

In addition, practical optimization problems often require minimizing or maximizing several conflicting objectives simultaneously, leading to the multi-objective optimization field. Two main approaches can be identified for achieving this: Pareto-based approaches and aggregation approaches. Pareto-based approaches (e.g., Nondominated Sorting [136–141], Strength Pareto Evolutionary Approach [139, 142, 143] etc.) look for the Pareto front without making any choices among the selected solutions. In this case, multiple objectives are optimized simultaneously. Once the Pareto optimal set is found, decision-makers need to choose the "best compromise solution", based on the specific optimization problem or personal preferences. On the other hand, aggregation approaches (such as the weighted sum method [144–148], or constrained approach [149–152, 144]) combine different objectives into a single objective function. These methods are widely used due to their ease of implementation. In this case, preferences are expressed before the optimization, which is why they are also referred to as "a priori methods".

- **Constraints**
  The fundamental constraints for this type of optimization problem are: energy balances; constraints for storage modelling; constraints related to the layout of the system.

  An equality constraint must be included in the mathematical formulation of the problem for each energy vector. The general form is reported in Equation 3.3.

$$\sum_{j \in U} \left(P_{i,j,k}^{OUT} - P_{i,j,k}^{IN} \right) + P_{i,k}^{BUY} - P_{i,k}^{SELL} + P_{i,k}^{ST} - P_{i,k}^{LOAD} = 0 \qquad \forall i \in V, \ \ \forall k \in \{1, .., t^{end}\} \quad (3.3)$$

  These sets of constraints state that, for each energy carrier i and at any time step k, the sum of imported (P^{BUY}) and generated powers (P^{OUT}) must equal the sum of exported (P^{SELL}) and consumed powers (P^{IN}). In addition, power related to the charging and discharging phases of the storage (P^{ST}) should be included in the balance equation.

  The main factors that need to be taken into account when modelling energy storage are the limitation on charging/discharging powers; the storage capacity

as maximum limit for the stored energy or, alternatively, the upper and lower limitations of the state of charge (typically used for electrical storage); the energy balance of the storage. A relatively good simulation of the energy storage operation can be obtained by addressing these phenomena (or technical constraints), but in case a more realistic modelling is required, some other aspects should be included, such as: charging/discharging efficiency of the energy storage; self-discharge due to energy losses; impact of ambient temperature (for thermal storage).
The storage units can be described through linear equations. The modelling approach based on two independent variables is presented in Equations 3.4 - 3.8. More in detail, Equations 3.4 and 3.5 sets the upper and lower limits for charging/discharging power, while Equation 3.6 ensures that physical storage limits, due to its finite capacity (*CAP*), are not violated. As an alternative to the previous equation, it is possible to impose that the state of charge (i.e. the available capacity expressed as a percentage of its rated capacity) is within the permissible range in each time step. Finally, Equation 3.7 ensures that the discharged energy was previously stored. The binary variable y^{ST} is required to prevent simultaneous charging and discharging of the storage. Energy losses are included in the storage simulation and they are modelled by the loss coefficient l, which represents a percentage of energy that is lost in each time step and it takes into account that energy storage is not free over time. This phenomenon is particularly important for thermal storage and a method to estimate this parameter based on the ambient temperature and the storage capacity is described in [153]. However, if short term storage is under consideration, thermal losses are expected to have an impact that can be considered as almost negligible. The periodicity constraint can be included in order to impose the same storage level at the beginning and at the end of the considered time interval, as reported in Equation 3.8. Finally, concerning the electrical storage, charging and discharging efficiencies are the most used parameters, with typical values between 0.75 and 0.90 [37].

$$0 \leq P_{i,k}^{CH} \leq y_{i,k}^{ST} \cdot P_{i,k}^{CH,max} \qquad \forall i \in V, \forall k \in \{1,..,t^{end}\} \tag{3.4}$$

$$0 \leq P_{i,k}^{DIS} \leq (1 - y_{i,k}^{ST}) \cdot P_{i,k}^{DIS,max} \qquad \forall i \in V, \forall k \in \{1,..,t^{end}\} \tag{3.5}$$

$$0 \leq (1-l_i)^t CAP_i^{START} + \sum_{k=1}^{t} (1-l_i)^{t-k} (P_{i,k}^{CH} - P_{i,k}^{DIS}) \Delta t \leq CAP_i$$
$$\forall i \in V, \forall t \in \{t^{start}, .., t^{end}\} \quad (3.6)$$

$$-(1-l_i)^t CAP_i^{START} - \sum_{k=1}^{t} (1-l_i)^{t-k} (P_{i,k}^{CH} - P_{i,k}^{DIS}) \Delta t \leq 0$$
$$\forall i \in V, \forall t \in \{t^{start}, .., t^{end}\} \quad (3.7)$$

$$-(1-l_i)^{t^{end}} CAP_i^{START} - \sum_{k=1} (1-l_i)^{t^{end}-k} (P_{i,k}^{CH} - P_{i,k}^{DIS}) \Delta t = CAP_i^{START}$$
$$\forall i \in V \quad (3.8)$$

Some examples of articles where single-variable modelling is selected in the analysis are [154–159], while the two-variable modelling is selected in [160–167].

Layout constraints are often overlooked, under the simplifying assumption that all components can be connected indiscriminately. However, parallel and series connections between different devices can be found in most of real applications. A representative example concerns heat generation technologies that operate at different temperature levels. In this case, the different circuits typically communicate via heat exchangers. On a practical level, in order to include the actual connections of the components in the mathematical formulation, the energy balances must be modified. For each energy vector, two types of constraints must be inserted. The first one (Equation 3.9) states that the output power of each generation/conversion technology must be less than the sum of the powers consumed by the interconnected technologies. On the other hand, the second constraint (Equation 3.10) expresses that the input power of each technology must be less than the sum of the powers produced by the interconnected generators. In Equations 3.9 and 3.10, i represents the energy vector, jp and jc are subscripts to distinguish producer from consumer technologies and a indicates the state of the connection between the considered technologies (1 if connected and 0 otherwise). It should be noted that the set Up includes not only producer technologies, but also purchase from the networks and discharging phase of storage. Similarly, the set Uc denotes

both consumer technologies but also selling to networks and charging phase of storage. If it is necessary to distinguish the producers of each energy vector from its consumers, layout constraints must be included in the problem formulation. In this case, the only formulation that can be used is the one based on two variables.

$$P_{i,jp}^{OUT} \leq \sum_{jc \in U_c} P_{i,jc}^{IN} a_{jp,jc} \qquad \forall i \in V \tag{3.9}$$

$$P_{i,jc}^{IN} \leq \sum_{jp \in U_p} P_{i,jp}^{OUT} a_{jp,jc} \qquad \forall i \in V \tag{3.10}$$

- **LP models of MESs in literature**
  The simplified model proposed has a very simple mathematical formulation and can be solved very quickly even if characterized by a high number of variables. However, the simplifying hypotheses adopted could bring to a inaccurate representation. As a result, there are few articles in the literature that perform the operational optimization using exclusively an LP formulation [168–173]. Among them, Georgiou et al. [174] propose a LP optimization scheme for the minimization of the net grid energy usage of a nearly Zero Energy Building (nZEB). However, the study proposes to include a further step at the end of the optimization: the import of the optimal dispatching in the software System Advisor Model (SAM), in order to address a more realistic modelling of storage and take into account the power conversion losses. More frequently, however, the use of the linear approach is embedded in a more complex optimization framework. In this case, the simplified linear approach allows the characteristics of the system to be broadly taken into account, allowing to analyse more complex aspects [175]. For example, Lauinger et al. [176] developed a decision-support tool in the form of a linear program in order to apply a stochastic programming approach, able to account for the uncertainty of the weather parameters. This choice is justified by the fact that stochastic programming increases the computational complexity in proportion to the number of considered weather scenarios, requiring the formulation of simple and fast operation problem. Another article that presents a similar methodological approach is [177]. Furthermore, a two-level nested optimization is presented by Capone et al. [178] in order to model the multi energy system taking into account the thermal dynamics of the

district heating network. The upper-level uses the genetic algorithm to optimize the demand-side management, while the lower-level optimization uses a linear programming algorithm to find the best operation of the production plant. Finally, the short computational times characterizing LP problems can be particularly advantageous when the optimization process has to be repeated, for example for finding the Pareto curve in a multi-objective optimization [170].

3.2.3 Realistic operation

The model presented in the previous subsection provides an ideal formulation of the MES operation. Simplifying assumptions are sometimes used even at the cost of significant impacts on model accuracy. In general, the choice of whether to include technical constraints within the optimization can strongly influence the results of the optimal operation and load characteristics of individual technologies. In the present work, the more detailed description of the components operation obtained by including their technical features will be referred as "realistic performance". This subsection has the aim of reporting the strategies mostly used in the scientific literature for building optimization models that consider realistic performances for the components. These elements are discussed in the following list.

- **Minimum operating power**
  Most of the technical devices cannot operate in arbitrary low part load. Constraints on the minimum powers of the components can be included in the model by acting on the upper and lower boundary of the variables. In particular, the formulation is given in Equation 3.11.

$$P_{j,k}^{IN,MIN} \cdot y_{j,k} \leq P_{j,k}^{IN,MIN} \leq P_{j,k}^{IN,MAX} \cdot y_{j,k} \qquad \forall j \in U, \forall i \in \{1,..,t^{end}\} \quad (3.11)$$

  Where y is the binary decision variable representing the on/off state of the technology and $P^{IN,MIN}$ and $P^{IN,MAX}$ are the extreme values of its working range. If the binary variable is set to zero, the only value that the P^{IN} variable can assume is 0 (and therefore the technology is off). If, instead, y is equal to 1, the technology is switched on at a level between its real minimum and maximum operating power.

It is worth to notice that the addition of this constraint is trivial for components whose performances have been piecewise linearized (see the following points), since the binary variables are already present, and therefore, considering the minimum operating powers does not increase the dimensions of the problem.

- **Minimum up and down time constraints**
  For some types of devices, the associated on/off schedule cannot assume arbitrary values. More in detail, each unit shall remain switched on for at least a predefined number of time periods after start-up. This constraint is called minimum up time constraint. Similarly, each unit must respect minimum down time constraints, remaining switched off for at least a predefined number of periods after shutting down. For example, this is typical of cogeneration units due to their slow dynamics. This technical constraint is important also because each unit, in addition to operation and maintenance costs, can have a start-up cost, incurred each time the unit is switched on. This cost is usually due to the inertia of the component (i.e. it consumes primary energy without producing any useful effect [179]). Consequently, neglecting these constraints may lead to erroneous estimates that may impact the feasibility of a technology in the energy system. In the literature, three approaches can be found to manage this issue.
  One possible way to set the minimum times for a technology to be switched on or off is to include the following constraints in the problem formulation (Equation 3.12-3.14).

$$z_{j,k} = y_{j,k} - y_{j,k-1} \qquad \forall k \in \{2,..,k^{end}\} \tag{3.12}$$

$$\sum_{t=k}^{k+N^{ON,MIN}} \left[y_{j,t}\right] \geq N^{ON} - (z_{j,k} - 1)M \qquad \forall k \in \{2,..,k^{end} - N^{ON}\} \tag{3.13}$$

$$\sum_{t=k}^{k+N^{OFF,MIN}} \left[y_{j,t}\right] \leq (1 + z_{j,k})M \qquad \forall k \in \{2,..,k^{end} - N^{OFF}\} \tag{3.14}$$

Where y is a binary variable equal to 1 if the device is on and 0 otherwise; z is a dummy variable to recognise the start-ups and shut-downs; $N^{ON,MIN}$ and $N^{OFF,MIN}$ are the minimum number of time steps in which the component must stay on and off, respectively; and M is an arbitrary big and constant

number, usually called Big-M. These constraints allow the on/off vector to be scanned, relating the current instant to previous and subsequent ones, in such a way that the minimum time constraints are respected. It is worth to notice that, in order to compute the first z of the series, it must be provided a binary value for y as the initial state of the component (when $k = 0$). Obviously, these constraints require a single optimization over several time steps, as in case of storages (since the various time steps are linked by Equations 3.13 and 3.14). This type of modelling is used in [152, 163, 180–182].

Minimum up and down time constraints can also be modelled in a less rigid way. This can be done by adopting some limitations or penalties to prevent the operation of components characterized by frequent starts and stops. In most cases, these effects are monetised by introducing in the objective function specific costs (known as "start-up and shut-down costs") for each component start and/or stop [183, 184].

A less frequently used method is limiting starts and stops per day a priori [185–187]. The aforementioned methods for start/stop restrictions can also be applied simultaneously [188, 189].

- **Ramp rate constraints**
  Another technical constraint that accounts for transitional behaviour of the devices is the ramp up/down constraint. In particular, it aims to limit the output power variation between each time step in order to represent a physical limit due to the real operation of the components and to improve the lifetime of the device. This type of constraint also handles information related to subsequent time steps, so it is not possible to adopt it within a series of separate optimizations. It can be written in the form reported in Equation 3.15.

$$\Delta P_j^{RD} - (1 + z_{j,k})M \leq P_{j,k} - P_{j,k-1} \leq \Delta P_j^{RU} + (1 - z_{j,k})M \qquad \forall k \in \{2, .., k^{end}\}, \forall j \in U \quad (3.15)$$

Where ΔP^{RD} and ΔP^{RU} are the ramp-down and ramp-up powers, respectively. Notice that the constraints are not applied when startups or shutdowns take place. Concerning the scientific literature, [152, 185, 190, 163, 191] are some of the works that employ this kind of constraint in the analysis of the multi energy system operation.

- **Maintenance costs**
  The inclusion of maintenance costs within the optimization model is mainly done in two different ways.

  In the first case, maintenance costs are usually single-step costs unlike operating costs which scale with input power. As a consequence, they should only be added to the objective function only if the technology operates in the considered time step. This type of information can be managed only through the use of binary variables. The calculation of these costs is reported in Equation 3.16.

$$C^M = \sum_{j \in U} \left[\sum_{k=1}^{k^{end}} \left[c_j^M \cdot y_{j,k} \right] \right] \tag{3.16}$$

  Where c_j^M is the specific maintenance cost of the $j-th$ technology, while y is the binary variable that represents the on/off state of the component (equal to 1 if on, 0 otherwise).

  In the second alternative, maintenance costs can be assumed to be proportional with the produced power and, consequently, with the operating cost [184, 189]. In other cases, they are given as a fraction of the capital cost [160, 192, 193]. It should be noted that, despite this last option shares the advantage of not using binary variables, maintenance costs are considered in a more approximate way.

- **Part load performance**
  Although most models assume that the component efficiency is constant even when the system component is operating under off-design conditions, a critical aspect is the decrease of the nominal efficiency at part load. Unlike constant efficiency devices, nonlinear devices create a natural incentive to operate close to optimum efficiency, discouraging part-load operation. In addition, the inclusion of non-linear performance in the optimisation model not only allows fuel consumption to be minimized, but also allows the increase in emissions at part loads to be taken into account in the analysis. As a result, production planning and exchanges with storage and energy networks could change considerably. In particular, modelling of off-design conditions is crucial when load profiles are highly variable. For example, the challenge for increasingly popular small-scale technologies (i.e. CHP units for residential applications) is to decrease the minimum load level and increase part-load

efficiency to meet variable energy demands. Moreover, also on a large scale, it is important to model this aspect since the operating regimes of central power plants are changing from pure base load to variable renewable energy balancing. The constant efficiency approximation may be close to the reality for some technologies and operating conditions, but a very rough simplification for others. For example, among different prime movers used in cogeneration and trigeneration plants, the simple cycle gas turbine is characterized by the most pronounced degradation of efficiency (about 63% of the nominal value at half load). Simple cycle gas turbines are followed by micro gas turbines and internal combustion engines (that have similar decreasing percentage, 88% and 84% respectively) [194].

- **Investment costs**
  The specific cost of many types of equipment typically decreases as the size increases. In most cases this relation is nonlinear (e.g., wind turbine, internal combustion engine, gas turbine, absorption chiller, etc.)[194]. This non-linearity is typically neglected in order to simplify the mathematical formulation, and constant investment costs per unit of capacity are used [76,100]. However, the error made by assuming a linear relation between the two quantities can be non-negligible when dealing with small-scale technologies. For example, with regard to the above-mentioned prime movers used in cogeneration and trigeneration plants, moving from a size of $10kW$ to a size of $200kW$, a reduction in the unitary plant cost of 28% for simple cycle gas turbines, 37% for internal combustion engines, and up to 47% for gas micro-turbines can be observed [194].

- **Non-linearities and linearization of NLP problems**
  Nonlinear optimization problems are intrinsically more difficult to solve and nonlinear programming procedures cannot guarantee that the solution is a global optimum, unless the optimization problem is convex. A possible alternative to always guarantee the global optimum and, at the same time, to exploit the advanced stage of development of MILP solvers, is the linearization of the nonlinear terms. This technique consists in replacing the original objective function and/or constraints with linear approximations. More in detail, any equation curve of second (or higher) order is divided into multiple regions in which the curve is approximated to a straight line. In this regard, a key

factor is the choice of the number of regions. On one hand, if the efficiency curve is not divided into an adequate number of regions, the model does not adequately account for non-linearities in the system. On the other hand, if the number of regions becomes significant, the variables of the problem increase considerably and, consequently, the calculation time. Advanced discussions about linearization techniques can be found in [195, 196]. Figure 3.2 shows graphically the piecewise linearization method.

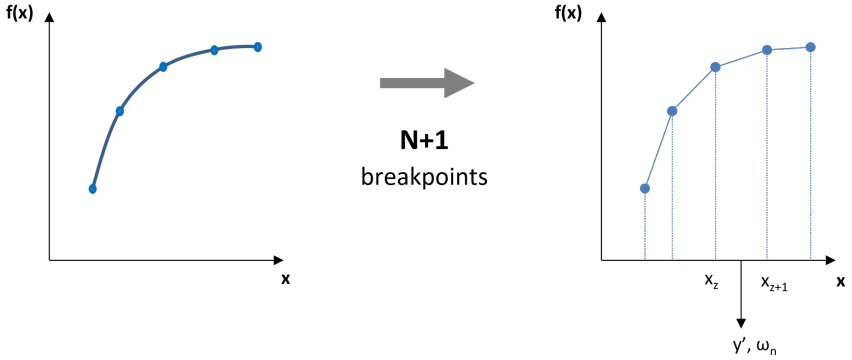

Fig. 3.2 Example of piecewise linearization technique

A basic algebraic formulation of a piecewise-linear approximation of a function $f(x)$ is given hereafter.

$$x_z \cdot y'_n \geq \omega_n \geq x_{z+1} \cdot y'_n \tag{3.17}$$

$$\sum_{n=1}^{N} [y'_n] \leq 1 \tag{3.18}$$

$$x = \sum_{n=1}^{N} [\omega_n] \tag{3.19}$$

$$f(x) = \sum_{n=1}^{N} [f_n(\omega_n)] \tag{3.20}$$

First of all, known N as the number of intervals for the linearization, denote x_z $(z = 1, .., N+1)$ as the breakpoints of $f(x)$. Then, it is necessary to include in the formulation N continuous variables ω and N binary variables y'. The field

of existence of the variables ω is defined in Equation 3.17, while the limit for choosing no more than one interval at a time is addressed with Equation 3.18. Finally, the original parameters (x and $f(x)$) can be computed with Equation 3.19-3.20, where fn is the linear approximation of the curve in the n-interval.

- **MILP models of multi energy systems in literature**
  Among the alternatives that address the scheduling optimization problem by taking into account the technical constraints that characterize these systems, the most commonly adopted formulation in literature for solving short-term operation is the Mixed-Integer Linear Programming ([188, 197–205]).
  Brahman et al. [206] obtained a MILP model of a residential energy hub, focusing on advantages related to load shifting, load curtailing and flexible load modelling considering a maximum heating and cooling temperature deviation from desired set points. Several binary variables were used to represent the on/off states of the cogeneration unit and equipment identified as shiftable loads, along with the charge and discharge states of the storage units.
  Morais et al. [207] presented an optimal operation of a renewable micro-grid and the effectiveness of the presented methodology is demonstrated through its application to a real case study. The dispatching is formulated as a MILP problem since two variables are required for modelling the storage batteries.
  Daraei et al. [208] adopted the MILP method to evaluate the interaction between local renewable resources and CHP plants and its influence on the CHP production planning and energy demand.
  Finally, in this context, one of the most significant research works is presented by Wirtz et al. [209]. The authors of the paper investigated 24 MILP models with different levels of details for the design of MES and pointed out that, for the analysed case, part load efficiency inclusion leads to lowest system costs but highest computational time. The large number of variables required for the linearization makes this model the one with the most impact on the optimization. In contrast, the adoption of minimum part load and start-up costs have a small impact on optimization.

- **NLP models in literature**
  As for linear models, there are not many research articles in the literature on nonlinear modelling approaches for MES management.
  Zhao et al. in [210] present the optimal scheduling of the energy systems under

day-ahead electricity pricing. The authors point out that their proposed predictive control model based on an NLP algorithm is unable to take into account certain performance limits such as minimum load ratios of the technologies or the minimum water flow for the thermal storage. The NLP formulation is most used in decomposed problems for analysis with a wider extension. In fact, in problems where the number of variables to be optimized becomes considerable, one technique is certainly the decomposition of the integral problem into sub-problems.

For example, an attempt of reducing the computational complexity of a problem can be found in [185], where the authors propose the optimal scheduling of a gas-electricity integrated distribution system and a multi-CCHP system. In this work, due to the detailed modelling of the networks and their integration within the energy system, a two-stage optimization is proposed. In particular, each phase is a NLP problem: the first presents all continuous variables, while in the second an on/off component model is obtained from the results of the previous phase.

- **MINLP models in the literature**

  Even though the MINLP approach requires an additional computational effort as it combines linear programming, nonlinear programming and integer programming algorithms, several papers use this methodology to model energy systems [211–215].

  Moghaddam et at. [216] present a MINLP model for the 24-hour scheduling of a residential energy hub. One of the innovations of the paper is that the presented model takes into account part-load efficiency and is able to limit the start-up/ shut-down of equipment.

  Deng et al. [217] proposed a MINLP scheduling model based on the input of real load and operation parameters of equipment. Both nonlinear input–output characteristics and discrete working ranges of energy equipment are considered. A comparative analysis with the existing scheduling strategy was conducted and it pointed out that the MINLP model proposed truly reflected the real operating condition of equipment.

  On the other hand, a consistent number of studies using MILP approach presented in literature are not only able to handle the technical constraints of technologies but also nonlinearities (via linearization technique). Bischi et al. [187] include in the model the nonlinearity of the performance curves of

the components through a piecewise linear approximation (thus transforming a MINLP into a MILP), also considering the impact of temperature. They solved the MILP optimization model with different levels of accuracy (5,10,20 intervals) of the piecewise linear approximation of the nonlinear performance curves. The results of the presented case study suggest that 10 intervals are a trade-off between accurate estimates of the optimal objective function and computational time.

Almassalkhi et al. [218] developed a mixed integer piecewise linear programming formulation of an energy hub system considering nonlinear energy conversion processes, energy storage, and hub emission limits. Results highlight a reduction in effects inherent to constant efficiency assumption in supporting operational and planning decisions. For example, the traditional hub models can significantly undersize energy storage as compared to the piecewise linear energy hub formulation. Finally, the choice of whether to include operational constraints and nonlinearities within the optimization can be of fundamental importance when performing combined synthesis, design, and operation optimization.

Arcuri et al. [219] formulated a model for selecting the optimal typology, size, and operative strategy of a trigeneration system for the civil user, analysing different cogeneration plants. The mathematical model proposed is nonlinear since the analysis takes into account three nonlinear constraints: the variation in nominal efficiency and unit cost of the cogeneration plant in relation to its size and the decrease in nominal efficiency in part-load configuration.

Marocco et al. [193] proposed the optimal design of a stand-alone renewable multi energy system, focusing on the feasibility of H2-based devices in remote areas. To this end, affine approximations to the electrolyser and fuel cell efficiency curves were included in the analysis to obtain a more detailed and accurate techno-economic estimate.

- **Comparison between optimization approaches**

  As stated in the previous sections, several articles in the literature address the scheduling optimization problem by taking into account realistic modelling of system components, proposing MILP, MINLP and NLP optimization. In some cases, different optimization methods are applied to the same case study, resulting in comparable results from the different approaches.

  Ommen et al. [220] examined the three most frequently used operation opti-

mization methods (LP, MILP, and NLP) in order to investigate their impact on operation management of energy system technologies. Due to the added constraints in the MILP model (minimum powers, ramp rate and shut-up/shut-down constraints) and the NLP model (nonlinear performance curves) that limit the operation of the technologies under investigation, the number of operation hours of alternative units increases (+23% for MILP, +39% for NLP compared to the linear case). The changes are especially visible in case of using the NLP optimization, where efficiencies are reduced in conditions of part load. The results indicate that the MILP optimization is most appropriate from a viewpoint of accuracy and runtime.

Lu et al. [221] proposed a MINLP model including in the analysis the nonlinear input–output characteristics of energy system components, discrete work intervals and limitations of their minimum operating period and the results are compared with an NLP optimization approach. Also in this case, the authors point out that, although the difference in terms of objective function between the two approaches is small, integer programming truly reflects the system actual operation.

Although with a focus on more electrical issues, Nemati et al. [221] perform the optimal day-ahead unit commitment and economic dispatch in a microgrid by proposing two different algorithms (a genetic algorithm and a MILP algorithm). Both algorithms were adapted to the application under consideration; in particular, the MILP was combined with an external tool to correctly handle non-linearities thus avoiding the complex resolution of a complete MINLP problem.

Moradi et al. [189] employed an advanced dynamic programming method for a microgrid energy-scheduling. By applying the quadratic programming method to the system formulation, the model is divided into linear and quadratic terms. Appropriate technical constraints, such as generation capacity constraints and the number of starts and stops, were included in the analysis.

In addition, Zhou et al. [201] compared a MILP and a MINLP model to analyse the impacts of equipment off-design characteristics on the design and optimal operation of trigeneration systems. The results show that the assumption of constant efficiency has a rather small impact on the optimization results. This occurs provided several other devices are present in the system including thermal storage and grid connection. In this case it can be guaranteed that the

efficiency of the power generation technology does not deviate significantly from its nominal efficiency.

In light of the works analysed, it is possible to draw a final consideration: the LP formulation allows to solve very quickly the operation problem at the price of a reduction in the precision of the simulation of the components. This can significantly decrease the precision of the solution since it does not adequately represent the energy system. The MINLP formulation provides the simulation of the system with the best quality, but finding the global optimum can be non-trivial, especially for non-convex or high dimensional problems, exposing to the risk of convergence to local optima.
Finally, the MILP formulation results to be a good compromise between these two alternatives, since it guarantees to find the global optimum of the problem and it ensures a satisfying accuracy of the components operation, provided that the linearization process is performed with an adequate precision.

3.2.4 Synthesis, design and operation

The levels at which the MES optimization can be performed are: synthesis (i.e. choosing the types of components); design (i.e. choosing the components' size); and operation (i.e. choosing the schedule of the components' functioning).
The operation optimization is the most investigated problem in the MES field. However, when a wider treatment is intended to be performed, it is necessary to add the synthesis and design problems together with the operation optimization. Solving the complete optimization is particularly meaningful from a practical point of view, since it represents the real problem that is required to be solved in order to properly build an energy system from scratch.
One of the first literature reviews that collected the main strategies developed for this purpose is [222], where the synthesis and design problems are posed at the centre of the discussion. The alternatives identified in this work are mentioned, discussed and referenced in the following sub-paragraphs, according to the aspect that is intended to be commented. Another review [223] showed that, if only the synthesis and design problems are required to be solved, both deterministic and heuristic methods are adopted in the scientific literature, but when the operation must be assessed as well, the second ones may be not very efficient if used alone.

- **Time period selection**
  To correctly deal with the synthesis and design problems it is necessary to make an evaluation on a long-term period, theoretically (but not mandatorily) equal to the lifetime of the system. Obviously, considering the complete time period with an adequate discretization is not feasible in the practice, therefore, some representative days of the year are assumed with the aim of reducing quantitatively but not qualitatively the time steps. The period considered to perform a long term analysis can range from 5 years [224] up to 15 years [225], neglecting the differences between the single years. The yearly time period has been accounted with a number of representative days between 4 and 24 [224, 226–231], typically with an hourly discretization. Some indications for correctly considering the transfer of information between the representative periods simulated (e.g. energy storage) are contained in [163].

- **Problem definition**
  The most basic approach to deal with this problem consists in expanding the formulation developed for the operation optimization, including the synthesis and design variables, and the capital cost of the components for all the time steps considered. The synthesis variables are binaries that indicate the presence of a certain technology, while the design variables can be continuous or discrete and are referred to the size of the selected component. Capital costs and components' performances are typically nonlinear but can be piecewise linearized with the technique discussed in the previous paragraph.

- **Optimization techniques**
  As a result, the problem can be formulated as a single MINLP [232, 233] or MILP [186, 194, 224, 234–245] respectively. In these cases, the synthesis and design problems are addressed with the help of a superstructure, a theoretical layout that includes all the components that are described by the optimization variables.

- **Problem dimensions and computational cost reduction**
  If the synthesis and design problems are considered in addition to the operation problem, the dimensions of the problem increases significantly (up to $10^4 - 10^5$ variables in total [186, 234, 239, 246]). In fact, additional variables are required to represent the synthesis and design parameters, as well as to account the higher number of time steps needed to represent the system lifetime.

As an attempt to reduce the computational costs, different decomposition strategies have been developed and implemented. The most common one has been applied for the first time in order to optimize single CHP plants [247] and consists in dividing the single optimization in two nested levels (Master and Slave Problem, MP and SP respectively): in the outer stage (MP), synthesis and design are optimized with a heuristic solver, while in the inner stage (SP) the operation problem is solved with a deterministic solver. Therefore, the SP is optimized for any evaluation MP performs one iteration, but thanks to the SP small dimensions it is possible to take advantage from the exponential correlation between computational times and problem sizes.
For the master problem, several heuristic algorithms are adopted and compared in [226]: the Tabu Search is faster in finding the optimum, but the Ant Colony Optimization reaches for first the convergence criterion.
Genetic Algorithm is adopted also in [228, 160, 248, 249], while Particle Swarm Optimization is employed in [250]. The choice of the heuristic solver must be evaluated according to the features that characterize the problem itself, in order to find the optimization method that better fits the case study under consideration. The problem decomposition is particularly advantageous when the time steps that constitute the representative days are not correlated between them (i.e. absence of energy storages or flexibility measures, etc.); in this case, the single optimizations become particularly fast (fractions of second) and can be executed in parallel.

In addition, there are other decomposition strategies that are less commonly applied but that are worth to be mentioned. A comparison between heuristic and semi-deterministic master problems is performed in [251], adopting respectively the evolutionarily stable strategy and the NLP derivative-free algorithm Particle Generating Set-Complex, resulting in a faster convergence of the latter one. The decomposition strategy is demonstrated to be advantageous, showing computational times equal up to the 5.4% of those required by the full MILP formulation [226].

Another interesting development of the decomposition consists in avoiding the definition of a fixed superstructure for the addressing of the master problem [252–254]. The formulation is still similar to the case with the superstructure, but a higher degree of freedom can be reached.

- **Operation with following electric/thermal load**
  If the operation is managed with load following techniques (Following Electric Load, Following Thermal Load, etc.), and therefore the system operation is not optimized, the synthesis and design problems can be solved in a single stage with MINLP solvers [212, 225], Genetic Algorithm [255–268], Owl Search Algorithm [269], Crow Search Algorithm [270] or Particle Swarm Optimization [117, 271, 272]. Typically, these problems have limited dimensions, therefore heuristic algorithms are the preferred choice thanks to their simple implementation, and their capability in dealing with nonlinear and non-convex objective functions or constraints.

- **Benefits of combined optimization**
  On the overall, solving the complete problem for the synthesis, design and optimization of the energy system allows to make a comprehensive analysis of the combined generation and a consistent comparison with the separate generation. The advantages of the combined generation are confirmed even on the long-term, with reductions of annual costs in the order of $12-17\%$ [234, 273], a decrease of the emissions up to $56-66\%$ [234, 273], or a lowering of the primary energy consumption of $10-34\%$ [230, 243, 273], according to the optimization criteria that is chosen.

- **Mathematical formulation**
  In light of all the elements collected from the scientific literature, the formulation proposed in the present work for the implementation of the synthesis, design and operation problem is in the decomposed form. A synthetic mathematical formulation is provided in Equation 3.21.

$$
\begin{aligned}
&\min_{s,d} f(s,d,o) \\
&s.t. \begin{cases} min_o\, f(s,d,o) \\ s.t. \begin{cases} g_k^{SP}(o) \geq 0 & \forall k \in \{1,..,n\} \\ h_\omega^{SP}(o) = 0 & \forall \omega \in \{1,..,q\} \end{cases} \\ g_i^{MP}(s,d) \leq 0 \quad \forall i \in \{1,..,m\} \\ h_j^{MP}(s,d) = 0 \quad \forall j \in \{1,..,p\} \end{cases} \\
&s,d,o \in \mathbb{R} \vee \mathbb{Z}
\end{aligned}
\tag{3.21}
$$

Where s and D are the variables of the synthesis and design problem, respectively, while g^{SP}, h^{SP}, g^{MP} and h^{MP} are the inequalities and equalities of the Master Problem and Slave Problem. Regarding the master problem, the synthesis variables are binaries indicating the selection of a specific technology (ω), while the design variables are discrete or continuous and represent the rated power (RP) of the selected component. The boundary of the rated powers is defined with Equation 3.22, where the multiplication between the binary variable and the upper and lower values (RP_i^{max} and RP_i^{min}) forces the rated power to zero in case the technology is not selected.

$$
\omega_i \cdot RP_i^{min} \leq RP_i \leq \omega_i \cdot RP_i^{max} \qquad \forall i \in U \tag{3.22}
$$

In case multiple components are available for each kind of technology, convergence problems often arise. This happens because the same MES configuration can be reached through different combinations of the MP variables [182]. This can be avoided by imposing hierarchy constraints [201] between the sizes of the components belonging to the same technology (Equation 3.23), which means that the components are not randomly selected, but their choice is made with order.

$$
RP_{i,r} \leq RP_{i,r-1} \qquad \forall i \in U, \forall r \in \{2,..,r^{max}\} \tag{3.23}
$$

In Equation 3.23 r^{max} is the maximum number of devices that can be installed for a single technology. In this case, the rated powers of the units belonging to

the same technology are imposed to follow an ascending order.
Concerning the operation optimization of the SP, its formulation can be made in the same way described in the two previous paragraphs, considering the synthesis and design variables as known inputs of the problem.

3.2.5 Uncertainties

A considerable amount of input data is required to simulate and optimize the Multi Energy Systems. Despite these data are usually considered as fixed and known, most of them are actually affected by uncertainties. The most representative example are the weather conditions, but even the performances and costs of the components can be uncertain according to the type of analysis that is conducted. The correct management of the uncertainties is one of the most important aspects in the field of energy systems for both short and long-term planning. Neglecting the uncertainties in the short-term optimization (e.g. day ahead analysis) can lead to a sub-optimal planning of the power production and even to critical or congested conditions, while the effect on the long-term optimization can be the undersizing/oversizing of the employed technologies [274].
The implementation of uncertainties is often discussed in reviews on energy systems [275, 276] and some works are completely focused on this topic. The parameters subject to uncertainty are recognized and discussed in [274]. A detailed overview on probabilistic, possibilistic, and combined methods, beside information gap decision theory is provided in [277], where both strengths and weaknesses are highlighted for each strategy. Deterministic and inexact optimization models are compared in [278], and precise considerations are provided regarding their limitations. Finally, a clear explanation of the criteria to follow to choose the most suitable method according to the data availability is provided in [279]. The gaps in the application of some techniques for addressing uncertainties in MESs are discussed, as well as the challenges represented by computational costs and mathematical formulation of more recent techniques for uncertainty management.
The most common sources of uncertainty on the input of the problem are: a) the prices of the energy vectors and their related environmental parameters such as emission factors; b) the energy demands; c) investment costs; d) the production from renewable sources; e) the ambient conditions [279]; f) the devices' performance [280, 281]; and g) the operating reserve of power plants [282]. Furthermore, it

is important to note that, although most research articles on the subject treat each uncertain parameter as independent from each other, actually there may be potential correlation between them (e.g. between energy load and electricity price [180] or between different energy demands [255]). The interdependence between inputs can be defined by the covariance, which describes the correlation between two random variables.
The main aspects concerning the uncertainties in MESs optimization are discussed in the following sub-paragraphs.

- **Approaches to include uncertainty**
  Suitable forecasting models must be adopted to properly estimate the parameters affected by uncertainty [276]. This task is usually addressed in a separate analysis. Since the focus of the present work is devoted to the optimization problem, the strategies employed to develop a model able to generate input data according to the probabilistic phenomena are not further discussed. A comprehensive discussions is provided in [283–287].

  When the research objective is to deal with data uncertainty in multi energy system optimization, two different approaches can be employed: uncertainty/sensitivity analysis, and optimization under uncertainty. The first one aims at understanding the impact of uncertainty on model output, while the second method aims at identifying the optimal decision that should be taken "here-and-now" based on the uncertain parameters. Many research articles perform sensitivity analysis to identify which inputs have a major impact on optimization results [198, 192, 288, 289]. This type of approach does not take into account the dynamic nature of decision-making under uncertainty and its information flow. The two main representatives for the inclusion of the uncertainties in the optimization are: a) stochastic programming; and b) the robust optimization. They differ on the basis of the information on the random events: in stochastic programming the probability distribution of uncertain data has to be known or estimated, while in robust optimization the uncertain data are assumed to be varying in a given uncertainty set.

  However, there are many other methods in addition to stochastic programming and robust optimization. According to the degree of simplification, the complexity of the optimization model can significantly vary. A considerable number of tailored alternatives can be found in the scientific literature. Among

these, scenario-based stochastic programming is one of the most employed strategies; this consists in defining some scenarios (i.e. sets of input data) and then, taking into account their respective probability of occurrence, finding the solutions that provide optimal strategy in facing each scenario ([290, 291]). In other words, the goal is to find a solution that is feasible for all (or almost all) the possible parameter realizations and optimizes the expectation of some function of the decisions and the random variables. A relatively common strategy to coherently determine the different scenarios is to generate a high number of cases (order of 10^3 [282, 292]) with the Monte Carlo method, and then reducing them to a small number (5 in [282], 9 in [293], 10 in [292, 294], from 5 to 20 in [295]) with a clustering algorithm [296] or other techniques [297, 298]. Due to the dimensions of this problem, deterministic solvers (MILP and MINLP) are preferred by far to obtain low computational costs.

- **Security, reliability and availability**
  Other aspects related to the uncertainties that are often studied are the security, reliability, and availability of the energy system; many different models developed to include them in the optimization process can be found in the scientific literature. The N-1 principle consists in guaranteeing the security of the system even when one of the elements of the energy hub fails. This approach is applied in [299, 293] with multistep optimizations. Robust Optimization (RO) [300, 280, 293, 301, 302] has the aim of finding a result that satisfies the worst case that could occur and is often used for reliability and availability.

  Moreover, the two-stage formulation is widely used in stochastic programming. In this type of problem, the decision maker has to make some strategic decisions ("first-stage decisions") that are not easy to change on a short time scale and that can be made without full information on random events. After random events occur, corrective actions ("second-stage decisions"), that can be adapted on a short notice, are taken in response to each random outcome. The objective function of the optimization problem is composed of two parts: the cost of the first-stage decision and the expected cost of the second-stage decision taking into account the probability that each scenario has to effectively happen. If the number of scenarios is finite, the stochastic problem can be represented by its equivalent deterministic problem.

- **Mathematical formulation**

  Taking into account the advantages and complexities characterizing the inclusion of uncertainties in the optimization of multi energy systems, the scenario-based stochastic programming represents a good alternative for the implementation of uncertainties. Differently to other approaches, it has no peculiar constraints related to guaranteeing technical concepts such as security, reliability, or availability. Thanks to this degree of freedom, it can be found relatively often in the scientific literature.

  For this reason, its mathematical formulation is proposed in the present work. In particular, the two-stage formulation is reported in Equation 3.24 and is referred only to the operation problem.

$$
\begin{aligned}
&min \bar{f}(o', o", \xi) \\
&s.t. \begin{cases} min_o f(s,d,o) \\ s.t. \begin{cases} g_k^{SP}(o) \geq 0 & \forall k \in \{1,..,n\} \\ h_\omega^{SP}(o) = 0 & \forall \omega \in \{1,..,q\} \end{cases} \\ g_i^{MP}(s,d) \leq 0 \quad \forall i \in \{1,..,m\} \\ h_j^{MP}(s,d) = 0 \quad \forall j \in \{1,..,p\} \end{cases} \\
&s,d,o \in \mathbb{R} \vee \mathbb{Z}
\end{aligned}
\tag{3.24}
$$

$$
\bar{f}(o) = f(o') + \sum_{\sigma=1}^{r} [\pi_\sigma f(o", \xi_\sigma)] \tag{3.25}
$$

  where ξ is the random vector of the uncertain data, σ is the index of the scenarios, r is the number of scenarios, π is the related probability, o' and $o"$ are the first-stage and the second-stage decision variables, respectively. The objective function of every scenario is computed with 3.25).

  Not only optimal operation, but also optimal design can be addressed adopting a two-stage stochastic programming. In this case, first-stage decision variables are the sizes of components, while second-stage decision variables are related to the demand pattern change (energy system scheduling) [295, 303–305].

3.2.6 Flexibility measures

The degree of flexibility is the capability to guarantee the power balance of consumers and producers through efficient changes of operation. Some sources of flexibility are identified in [306], where an overview of the papers from the scientific literature treating this topic is given.
Energy storage are by far the most important flexibility source to the system since their influence on both the operation and the modelling of the optimization process is noticeable. The other measures that can increase the system flexibility are: i) energy substitution; ii) inertia of thermal networks and buildings; iii) Demand Response Programs (DRP); and iv) ancillary services.

- **Energy substitution**
  Energy substitution means to achieve the same energy product (e.g. cold) by adopting a different energy vector (e.g. absorption chiller fed by heat instead of electric chiller) [307]. In this way it is possible to exploit another source to satisfy the same loads if an energy vector is no longer available.

- **Inertia of thermal networks and buildings**
  The inertia of hydraulic circuits for heat transfer (which include District Heating/Cooling networks) is a physical phenomenon determined by the hydraulic and thermal laws that rule the transport systems. This phenomenon can be appreciated because of the high masses that usually characterize DH networks. Different control strategies are exposed in [306], referred to the energy system configuration (centralized or distributed). Conservation laws have to be set out in order to simulate the physics of the network and three strategies can be found in scientific literature to address the DH inclusion in the MES optimization problem.

  In some works the design problem of the TN is included in the optimization, but in a simplified form [112, 236, 308–310]. The TN is simulated with only the connection parameters (i.e. incidence/connectivity matrix) and the thermal powers flowing into the branches. Heat losses are addressed as a percentage (proportional to the distance between the nodes [245]) of the flowing energy and the sizing of the pipes is performed according to the maximum power reported in the time period analysed [242, 311].

A more detailed optimization is obtained by simulating the operation of the thermal network with temperatures and flow rates. However, when both are considered as variables, the energy balance of the pipes becomes nonlinear. To overcome this issue and preserve the linearity of the model, the network can be assumed to operate under partially known conditions, such as Constant Flow Variable Temperature (CFVT) or Constant Temperature Variable Flow (CTVF). In the first case, the flow rates are considered as known and the temperatures have to be optimized, vice versa for the second case. CFVT is considered as the most applied in real operation and is assumed in [312–316], while CTVF is much less investigated [246].
The Variable Flow Variable Temperature (VFVT) configuration can be assumed, but complex models must be developed. The Newton-Raphson method is used in [317] for solving the nonlinear problem, while strong efforts for the linearization process are made in [293].

Despite the previously cited works include the DH in the optimization, none of them is formulated to consider the inertia of the network. However, in case of thermal networks of high dimensions, the effects of transients can be noticeable and cannot be neglected [318, 319]. To fulfil this purpose, the concept of time delay must be introduced for each branch of the network, often requiring the addition of integer variables. In this case, for CTVF or CFVT configurations, an heuristic solver (Particles Swarm Optimization) is used in [320], while deterministic algorithms are employed in [321–324] (eventually including the building inertia [325]). An intermediate strategy is adopted in [289, 291], where an heuristic Master Problem solves a Demand Response problem and, nested into the MP, the DH network is simulated with the node method and a simplified unit commitment problem is executed with Linear Programming. Obviously, the highest complexity of the problem is reached when both VFVT configuration and network inertia are considered. Finite volumes are used in [326] and finite differences are employed in [327] to simulate and optimize the DH with iterative processes. However, employing these methods with deterministic solvers is a very complex task because of the incompatibility between the strategies used for the solution of the matrix calculation and the algorithm of the solver itself [306]. Decomposition strategies are often proposed to optimize part of the problem with MILP/MINLP solvers. In [328], a quadratic solver is used to solve the DH problem in a Slave Problem coupled

with an iterative Master Problem. A more complex model is developed in [237], where Benders decomposition, relaxed formulation and an iterative process are employed jointly with the simulation of the network based on a water mass method, which simulates the network with the node method and accounts the thermal inertia by averaging the temperature at the outlet of the branches.

- **Demand Response Programs**
  Demand Response is a strategy aimed at modifying the user energy demand [329, 330]). Demand Response increases the flexibility of an energy system and its effect can be enhanced by other flexibility measures, as pointed out in [331]. Compensation of renewable generation fluctuations, reduction of grid congestions, reduction of power import/export and cost reduction are the main benefits (identified in [332]) that can be attained with DRP. In more quantitative terms, a cost reduction between 1.7% and 3.6% is obtained in [307, 333, 334] and savings over 5% are said to be expected for case studies with more suitable characteristics. However, lack of appropriate market mechanisms and market requirements of ahead planning are important challenges to deal with.

  Concerning the DRP implementation in the optimization model, new variables for the time shifting of loads and, eventually, the percentage of participation have to be introduced, but without introducing other sources of non-linearities [282, 290, 291, 294, 295, 302, 307, 335–338]). As already mentioned, DRP are useful to reduce the effects of power fluctuations and deviations from the predicted loads; for this reason, most of the cited works include DRP in optimization with uncertainties. In addition, residential customer dissatisfaction can be defined in order to quantify the impact of the load modification [339].

- **Ancillary services**
  Ancillary services are operation techniques focused on the producers and are mostly referred to electricity networks. They consist in guaranteeing a flexible generation capacity and the balance of the deviations of the loads from their predicted levels. The most common ones are power curtailment [340–343], operating reserve and Flexible Ramping Products (FRP, or ramping reserve). Power curtailment is performed for technical and economic reasons, but strong efforts are made in order to prevent this condition [344–346] because of its intrinsic inefficiency. Operating reserve is a production capacity that can be

made available in a short period (from seconds to tens of minutes) in order to compensate an unbalance on the grid. Frequency response, spinning reserve and supplemental reserve are the main kinds of operating reserves [347]. A Flexible Ramping Product is a ramping capability commodity that can be dispatched in a 5-minute timeframe to meet demand changes on the network. Operating and ramping reserves are often included with simple constraints [292, 321, 323, 348–352], which have the aim of ensuring a spinning/ramping reserve in the solution found by the optimization process. A more complex treatment must be developed if they are intended to be treated contemporary to the uncertainty [282, 353, 354].

3.2.7 Optimization model development and execution

Figure 3.3 summarizes the structure of the entire approach proposed in this review. The operation optimization with ideal performances can be considered as starting point (on the right of the figure) but without the presence of energy storage, which represents the most simplified case and it is formulated as a LP (time steps are not linked between them). Then, according to the additional description of the energy system, the corresponding resulting formulation of the problem is reported with a Venn diagram. In order to address the real performances of the components (technical constraints, nonlinear performance curve, etc.) the problem turns into a MI(N)LP, where the nonlinearities can be piecewise linearized and, for this reason, the letter N is reported between brackets in the acronym. The same notation (i.e. reporting some letters of the acronym in brackets) is used in the figure when energy storages or other flexibility measures are added in the layout; in this case the formulation is turned into a (MI)LP, where integer variables can be avoided (at least in some circumstances), as discussed in the modelling of energy storage (subsection 3.2.2). In addition, the sets of the diagram are coloured according to the structure of the optimization process, i.e. if it is composed by a single optimization or a series of independent optimizations (one for each time step, which can be done when time periods are independent between them). The other part of the schematic represents the cases in which the synthesis and design problems are included in the operation optimization.

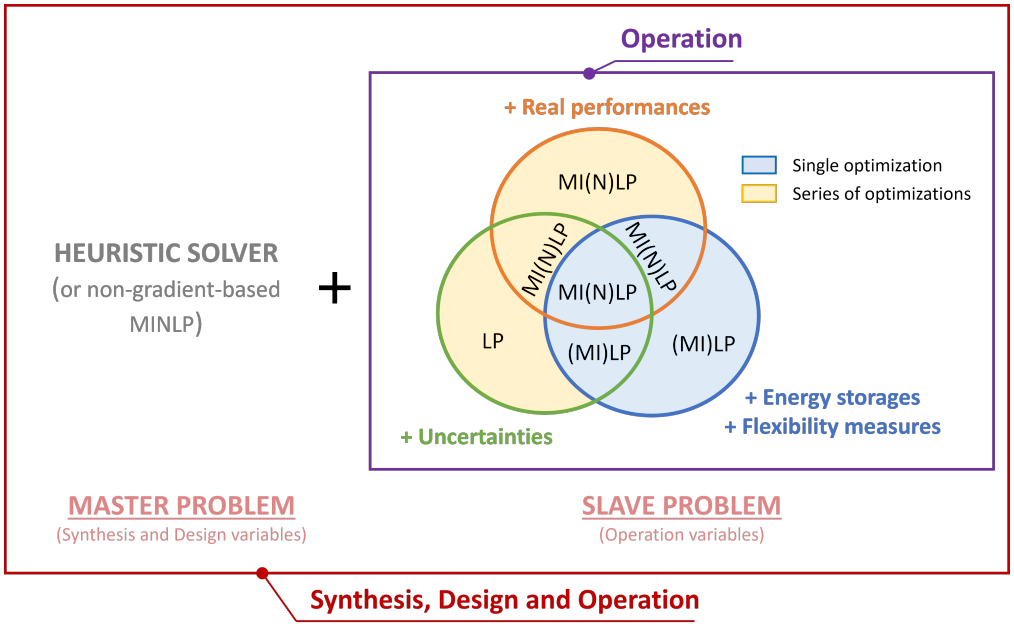

Fig. 3.3 Mathematical formulation of the MES optimization

The choice of the optimization solver is a crucial aspect since it can noticeably influence the computational times and the quality of the solution. A very high amount of solvers have been developed for each class of optimization problem. Table 6 represents a summary of the most employed solvers Table 3.1: these are grouped according to the optimization method and the problem formulation. Open-source software are written in green, while the ones in red require a commercial license. The names of the heuristic solvers are shortened with their acronyms: ACO (Ant Colony Optimization), ABC (Artificial Bee Colony), CS (Cuckoo Search), MA (Memetic Algorithm), BBO (Biogeography Based Optimization), SNO (Social Network Optimization). Knowing the maximum problem size (i.e. number of variables) that a solver is able to manage (without losing solution accuracy or requiring excessive computational times) can be very useful from a practical perspective. However, this is a complex information to achieve since it depends on many different and specific aspects. An attempt to answer this question is performed in the present study and an indication is provided in the table in terms of orders of magnitude (oom). These values have been taken according to the articles analysed for the review work, some benchmark studies found in literature [355–357] and other sources [358–360].

Table 3.1 Commercial solvers for MESs optimization

Method	Formulation	Solvers			Max. size (oom)
Deterministic	LP	CLP	CBC	GUROBI	10^7
	MILP		GLPK CPLEX	Intlinprog MOSEK	10^5
	NLP	Ipopt MATHNLP CONOPT MINOS	BONMIN JUNIPER SCIP COUENNE	BARON DICOPT KNITRO LINDO	$10^4 - 10^5$
	MINLP		ANTIGONE	XPRESS	$10^3 - 10^4$
Heuristic	NLP	PSO ABC ACO CS	GA MA		10^2
	MINLP		BBO SNO		

Finally, it can be noticed that NLP and MINLP solvers can be adopted also for LP and MILP problems, but this option is not considered since inefficient. In addition, some MILP solvers (e.g. CPLEX and GUROBI) are able to manage some kinds of nonlinearities, such as quadratic or conic terms. Nevertheless, since these are very specific and limited cases, they are not accounted as nonlinear solvers. Finally, in case of nonlinear formulation, it is fundamental to pay attention in recognizing if the problem is convex or not. Some solvers are not able to deal with non-convexity and the sizes of non-convex problem should be kept as low as possible to avoid convergence issues.

3.2.8 Comments and conclusions

In light of the articles examined in this literature review, some conclusions can be drawn regarding the state of art of the modelling and optimization of multi energy systems:

1. The level of detail reached by most of the models presented in literature allows a relatively realistic representation of the system operation; this is

obtained by addressing the real performance of the components, including descriptive constraints (layout connections, ramping constraints, minimum operating times, etc.), and adopting a suitable time step ($1h$).

2. Linearization techniques are often adopted in order to take advantage of the Mixed Integer Linear Programming (MILP) solvers, while decomposition strategies are commonly exploited when the synthesis and design optimization are addressed along with the operation problem.

3. Several strategies are proposed to include the effects of uncertainties and, despite there is not a best one, in general no drastic changes are required in the problem formulation.

4. Including the simulation of energy networks (in particular District Heating/Cooling) in the model has a high impact on the problem formulation. It allows to improve the optimization quality and it introduces another source of flexibility. Nevertheless, this leads to an increase of the number of variables and the addressing of nonlinear and non-convex equations.

In addition, the main research gaps identified are:

1. the lack of validation studies, even when the input data are taken from real case studies. The importance of this task is straightforward, since it would demonstrate on a practical way the advantages of MES optimization that are only theoretically proven. Therefore, validation is required both to assess the quality of the mathematical model developed to simulate the MES, as well as to prove that the resulting optimal operation can be applied in a real system;

2. the development of a suitable control system for the entire MES, its inclusion in the optimization model and the provision of results in a form that can be directly provided to the control system itself. This task would increase the description quality of the MES and allow the practical implementation of the optimization process. The complexity related to this task is due to the fact that it requires to operate the MES according to the schedule found with the optimization, but, at the same time, it must be possible to deal with any eventual deviation from the predefined operation;

3. a wider inclusion of flexibility sources in MES optimization processes. In fact, most of the models proposed in literature tend to apply considerable simplifications. On the other hand, when no assumptions are made, the resulting modelling becomes very complex and computationally intensive. The development of strategies able to ensure a good level of detail without being excessively time demanding would allow to achieve an advantageous implementation of more flexibility sources, which are a key element for MES operation. In this way, it would be possible to obtain reliable operating schedules with computational times that are compatible with the requirements of the real applications;

4. the integration of energy transport infrastructures in the MES simulation and optimization. In fact, the capability of transferring an energy vector from a producer to a consumer is usually taken for granted, despite it should be verified. The technical constraints and other physical phenomena that characterize the operation of energy transport infrastructures can pose important limitations to the purposes of the MES optimization. This is particularly true for MESs coupled with DHN, which have higher inertia and dispersion phenomena compared to electrical or gas networks.

The last two aspects are among the ones that were addressed in the research conducted during the PhD period. These analysis are presented in Chapter 4 and Chapter 5.

Chapter 4

Operation optimization of a MES with an internal thermal network

In the present chapter, the model developed in the framework of the MESs operation optimization is presented. The topic is briefly introduced in section 4.1, the case study analysed is presented in section 4.2, while the methodology developed is explained in 4.3. Finally, section 4.4 sums up the results and conclusions of this investigation.

Part of the research presented in the present Chapter was published in Energy Conversion and Management [J5].

4.1 Framework and motivation

As already discussed in the literature review, the integration of the energy transport networks in MESs optimizations is a research gap that is worth to be deepened. This aspect is very important since it allows to increase the quality of the MES simulation and, as a consequence, the reliability of the optimization itself. In addition, the optimization result can improve noticeably since the transport networks can increase the flexibility of the system, bringing positive effects on an energy and economic point of view.
The aim of this study is to investigate the inclusion of the thermal network simulation (operating with the VFVT strategy) in the operation optimization of a MES. This

analysis can be considered as a first step of a wider investigation and for this reason a basic case study is chosen, characterized by a thermal network of relatively small dimensions.

4.2 Case study

The structure of the MES considered in the present analysis is relatively simple, both because of the number of components and their connections. This choice was made because the optimisation methodology was newly developed and it was intended to test its effectiveness on a MES that did not present issues specifically related to the complexity of the case study under consideration. All the energy vectors and technologies involved in the MES operation are reported in Figure 4.1. The energy system has the task of satisfying the demand of two energy vectors: electricity (in light blue) and heating (in red). Concerning the fuels, methane (in yellow), hydrogen (in blue) and LPG (in purple) are considered in the present study. The production process of the hydrogen is not included in the analysis, therefore it is assumed as a fuel imported from the outside of the system. It is worth to mention that connections represented for the exchange of the thermal powers must be considered only as conceptual and not as topological (i.e. the real layout of the networks is different from the one represented in the figure).

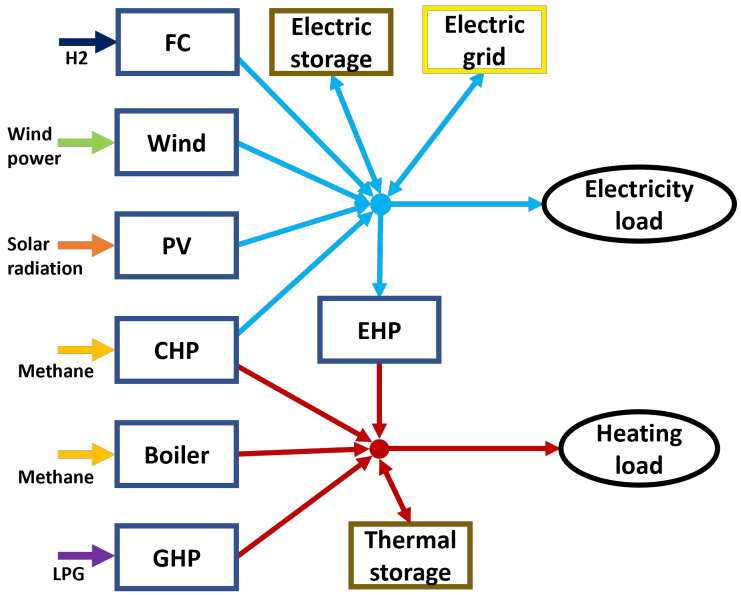

Fig. 4.1 Conceptual scheme of the MES taken as case study

In this case study, the technologies involved in the electricity/heating generation are: Combined Heat and Power (CHP), Heat only Boiler (HOB), Electric Heat Pump (EHP), Gas Heat Pump (GHP), Fuel Cell (FC), Photovoltaic panels (PV), wind turbine (Wind), electric storage, thermal storage and the connection with the electric grid. However, it is worth to notice that the methodology is not linked to any specific technology since the mathematical formulation used to model the components does not change with their typology.
As time period, a single day (24 h) discretized with a timestep of 15 min is considered.

Being out of the extents of this analysis, the electric grid is not simulated and only its connection with the MES is considered.
Before discussing the modelling of the heat transportation, it is necessary to point out the distinction between thermal networks inside the MESs and external District Heating Networks adopted in the present work. The latter ones are usually characterized by medium/large size, from the case of a small city up to an entire town. The DHNs topology can be either ring-shaped or tree-shaped, and it is constituted by two pipes (for the supply and the return of the hot water). Regarding the physical aspects, the noticeable spatial extension of DHNs determines non-negligible heat dispersions (due to convection heat losses) and time delays in the propagation of hot water across the pipes.

On the other side, thermal networks operating inside MESs are required to connect the technologies producing or consuming heat. In this kind of systems, these components are considered to be located at relatively short distance. This assumption was made considering two aspects: a) usually, the units for the thermal production cannot be located freely on a territory because of their size, emissions (noises and flue gases), and risks; b) the possibility to operate the units in series is included in the analysis. Installing the thermal units in the same area (and therefore on short distances) would allow to meet the space and safety requirements, as well as to connect the units in a more rational way. As a result, the effects determined by the thermal inertia of the network and the heat losses can be neglected, introducing a reasonable simplifying assumption, which is adopted in this analysis. In addition, the layout of MESs networks can presents many differences compared to DHNs. For example, the distinction between supply and return pipes may not be straightforward as in the case of DH, since more complex connections could link the technologies. Each thermal generator is equipped with a water pump and the mass flows circulating in the network can be adjusted more precisely with respect to DHNs, where, in case of meshes, it is not always possible to impose all the desired flowrates. In light of that, the present study is conducted assuming that all the directions of the mass flowrates are known, and any amount of flowrate can be set in each branch. In addition, from now on, the thermal infrastructure for the exchange of heating powers considered in this case study will be synthetically referred as TN (i.e. a thermal network inside the MES and not an external DHN) and the aim of the study is limited to this kind of network.

The layout of the thermal network taken as case study in the present work is shown in Figure 4.2. This setting is selected since it provides a high degree of freedom for the operation of the network itself. The thermal generators are coupled such that the EHP and the GHP are connected in parallel, and the same is done for the boiler and the CHP. Each of the two couples has a bypass branch that allows to skip the components whenever they are not operating, or it is needed to meet technical constraints on temperatures/flowrates across the network. Each component can operate independently from the other it is coupled to, and either the separate or simultaneous operation of the two couples is possible. In this last case, the two couples can be connected both in parallel and in series. In case of series connection, the couple composed by the two heat pumps is placed for first because the outlet

temperatures attained by these technologies are typically lower than the ones reached by HoBs and CHPs.

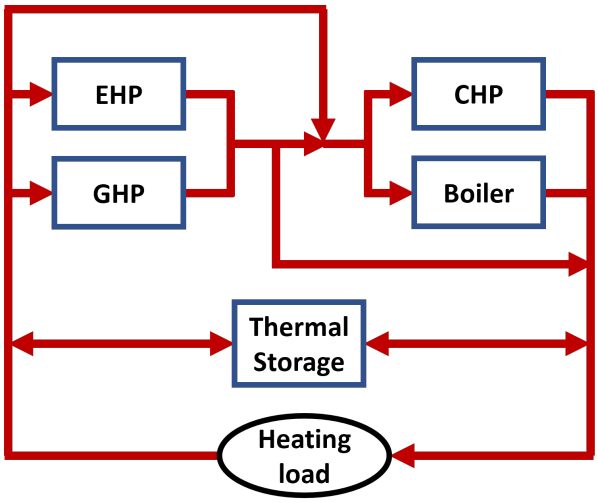

Fig. 4.2 Scheme of the internal thermal network

4.3 Methodology

As already mentioned, the aim of this analysis is to develop a model for optimizing the operation of a Multi Energy System, including the operation of the internal thermal network (i.e. the network that allows the heat transportation among the thermal generators and the thermal load inside of the MES). The VFVT regulation of the network makes possible to achieve the highest degree of freedom in the operation and it is reasonable to expect that the energy system will take advantage from that. For this reason, this is the regulation assumed for the thermal network.
The aim of the optimization is restricted to the operation and does not include the synthesis and design. This choice was made expecting that the complexity and size of the problem would become particularly challenging for the development of an optimization algorithm. In addition, the operation optimization was prioritized since it represents a task that must be continuously addressed during the system's life, while the synthesis and design problems are requested to be solved only once, during the planning of the MES.

4.3.1 Performances of components

The performances of the technologies constituting the MESs are widely recognised by the scientific literature to be nonlinear [361].The most common formulation to represent the operation of the components is a third-degree polynomial with a single variable. Typically, the independent variable is the input power (the power of the fuel/vector consumed), while the dependent variable is the output power (the power of the energy vector produced). In addition, a more detailed description can be achieved by using a polynomial with two independent variables, which may be preferred in case of components with a relatively complex operation, such as the CHP [187].
One of the aims of this study is to include the effects of the operating temperature of the thermal generators on their performance. With this purpose, a parameter that will be called "characteristic temperature" is defined for each heat generator. The characteristic temperature can be defined as the temperature that is able to represent the dependence of the efficiency on the operating temperatures. Depending on the technology, this parameter can be the temperature at the inlet, at the outlet, the average between these two, or any other form. As a consequence, two independent variables are addressed to describe the performance of the technologies adopted: the inlet power (P_{in}), and the characteristic temperature (T_{cmp}). This can be seen in the general formulation of the performance of the components, reported in Equation 4.1, where P_{out} is the outlet power, while a, b, c, d, and e are fixed numerical coefficients. As arbitrary choice, the T_{cmp} appears only at first-degree in the polynomial; however, thanks the approach adopted to implement the optimization, any other preferred degree can be chosen in the equation. Further details can be found in the Appendix.

$$P_{out} = a \cdot P_{in}^3 + b \cdot P_{in}^2 + c \cdot P_{in} + d \cdot T_{cmp} + e \tag{4.1}$$

Concerning the optimization process, developing a model with a linear formulation would guarantee the achievement of the global optimum and would allow to use commercial solvers with an advanced stage of development. For this reason, Equation 4.1 is linearized with the piecewise approach. The linearization techniques are discussed below, despite a description was already reported in the section related to the literature review. Notice that the mathematical formulation used in this case study is different from the one presented before and was selected because of its conceptual similarity when applied in the case of 1D or 2D linearization.

In case the component's performance depends on a single parameter, its operation at partial loads is mathematically described by a curve. This curve is discretized into different segments by fixing some nodes (values) of the independent variable x_i inside of its range of variation, and the corresponding values of the dependent variable y_i, where the subscript i goes from 1 to the number of linearization nodes N (this set is named I). Then, a continuous variable α_i (bounded between 0 and 1) is associated to each node, while a binary variable h_i is assigned to each segment of linearization. After having added some constraints on these linearization variables (details in [196]), it is possible to reformulate the original variables as shown in Equations 4.2 and 4.3.

$$P_{in} = sum_{i \in I} \left[x_i \cdot \alpha_i \right] \tag{4.2}$$

$$P_{out} = sum_{i \in I} \left[y_i \cdot \alpha_i \right] \tag{4.3}$$

In case the component's performance depends on two parameters, it is referred as 2D linearization, which is more complex with respect to the 1D case. The technique adopted in this study relies on the triangle method because of its higher accuracy in approximating a surface. Figure 4.3 presents a visual representation of this strategy, where a nonlinear performance surface is linearized with 4 nodes on each dimension (and therefore 3 intervals). This discretization identifies a mesh composed by 9 squared (or rectangular) elements. However, since the number of planes passing through 4 points is not unique, it is necessary to further divide the cells into triangles, obtaining 18 elements.

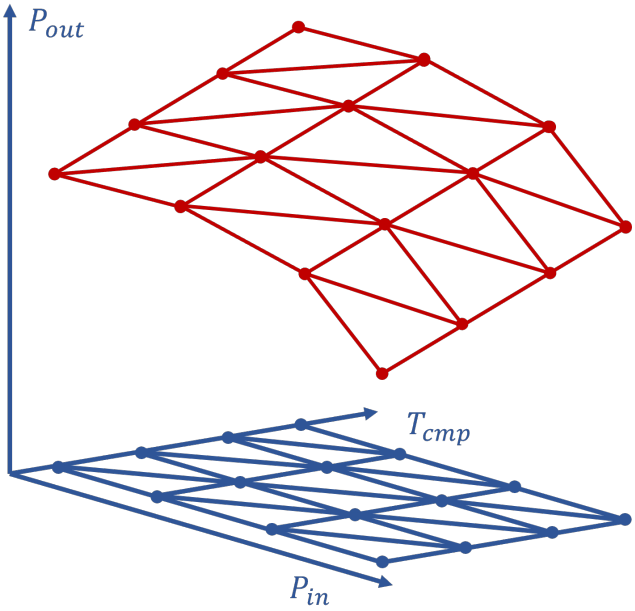

Fig. 4.3 Drawing of a surface linearized with the triangular technique

The performance surface is discretized with a mesh, fixing some values of the independent variables (x_i, y_j) inside of the domain, and the corresponding values of the dependent variable (z_{ij}). Then, a continuous variable (α_{ij} bounded between 0 and 1) is associated to each mesh node, while two binary variables (h^l_{ij} and h^u_{ij}) are assigned to each sector of the mesh. By addressing some auxiliary constraints (details in [196]) it is possible to reformulate the original variables as shown in Equations 4.4 - 4.6.

$$P_{in} = \sum_{i \in I} \left[x_i \sum_{j \in J} \left[\alpha_{ij} \right] \right] \tag{4.4}$$

$$T_{cmp} = \sum_{j \in J} \left[y_j \sum_{i \in I} \left[\alpha_{ij} \right] \right] \tag{4.5}$$

$$P_{out} = \sum_{i \in I, j \in J} \left[z_{ij} \cdot \alpha_{ij} \right] \tag{4.6}$$

Finally, the dependencies of the operation of the components and the discretization of their performances are reported in Table 4.1.

Table 4.1 Commercial solvers for MESs optimization

		CHP	Boiler	GHP	EHP	FC
Parameter	P_{in}	✔	✔	✔	✔	✔
	T_{cmp}	✔ (T_{in})	✔ (T_{in})	✔ (T_{out})	✔ (T_{out})	✘
Linearization nodes		4x4	4x4	4x4	4x4	4

Energy storage require a different modelling with respect to the other components of the MES. The electric and thermal storage are simulated with two continuous variables (P_{stor}^{ch} for the charging phase and P_{stor}^{dis} for the discharging phase) and one binary variable (β), which avoids a simultaneous charge and discharge of the storage. Refer to Equations 3.4 - 3.8 for the mathematical formulation.

4.3.2 Components constraints

In order to simulate the operation of the components constituting the MES, some constraints must be addressed.

The exchange of the energy vectors must be balanced. Since the thermal network will be simulated with separate constraints, the energy balance is imposed only on the electrical powers. Equation 3.3 is used for this purpose.

The minimum on/off operating times of the components are considered by addressing the inequalities presented in Equations 3.12-3.14. The ramping limitations are considered as well, but instead of addressing them on the operating powers of the components, they are implemented for the characteristic temperatures of the thermal units, with the aim of considering qualitatively the inertia effect of the components. These constraints are addressed with the formulation reported in Equation 3.15.

4.3.3 Thermal network model

In order to include the thermal network in the MES operation optimization, it is necessary to build a model that simulates the network operation according to the input data and assumptions adopted for the present analysis. It is not possible to model the network only with the heat fluxes flowing among the nodes, since the VFVT is

chosen as control strategy to manage the TN operation. Both the mass flowrates (G) and the temperatures (T) must be assumed as parameters describing the operation. With this purpose, the TN layout is designed with the graph approach, as shown in Figure 4.4. The flowrates are referred to the branches, while the temperatures are referred to the nodes. The thermal generators/consumers are associated to the branches, such that they are defined by one flowrate, one inlet temperature (inlet node), and one outlet temperature (outlet node). In the figure, they are labelled with their corresponding name/acronym, while the branches not tagged are simple connections between the nodes.

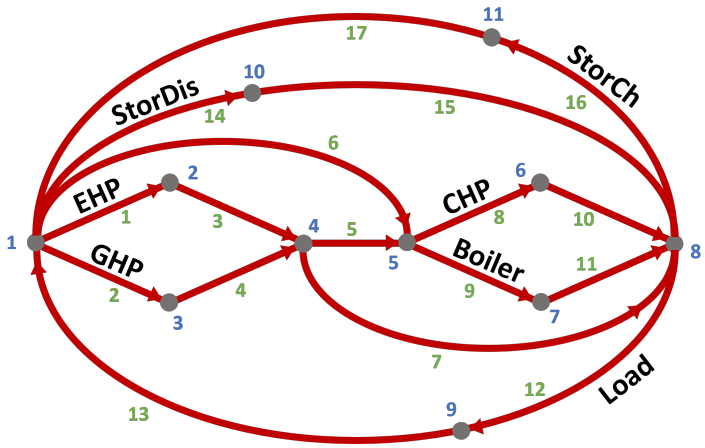

Fig. 4.4 Representation of the thermal network as a graph

On a theoretical level, with the graph approach, each component involved in the thermal generation/consumption could be modelled with a single branch and the corresponding heating flux provided/absorbed. However, according to the TN layout, with this approach it may happen that the water temperature at the outlet of a component and the temperature of the exit node of the branch are not the same. In particular, this would happen when the outlet flow of a thermal unit is mixed with another flowrate. For this reason, the thermal units are modelled with two branches in series, such that the identification of the outlet temperature of the components is immediate.

A different approach is developed to simulate the thermal storage, which is modelled with four branches: two for the discharging phases and other two for the charging phases. The reason for this choice relies in the fact that the directions of the flowrates circulating in the network must be fixed a priori. This cannot be done without addressing the simulation of the charging and discharging processes in different

branches, since the direction of their water flows is opposite.
The resulting graph of the thermal network is relatively small, since it is composed by 11 nodes and 17 branches. For this reason, it is considered a good starting point for the execution of the innovative method developed in this study. The model of the thermal network is synthesized according to the simplifying assumptions adopted. In fact, since thermal losses and inertia are neglected, each timestep can be assumed to operate in steady-state conditions. For the purpose of the optimization, once that the independent variables are defined, the TN is modelled by addressing the constraints.

The mass conservation is imposed implementing one balance equation at each node with the assumption of stationary conditions. Since the network does not present external injections/extractions of water, the sum of the flowrates circulating in the inlet branches must be equal to the sum of the flowrates circulating in the outlet branches. This concept is written in mathematical form in Equation 4.7, where N is the set of all the nodes of the network, while IN^k and OUT^k are the sets composed by the upstream and downstream branches of node k, respectively.

$$\sum_{i \in IN^k} \left[G_i^t\right] = \sum_{j \in OUT^k} \left[G_j^t\right] \qquad \forall k \in N, \forall t \in T \tag{4.7}$$

Energy balances are the constraints ensuring the satisfaction of the first thermodynamic principle. The variables involved are: i) the mass flowrates and the temperatures of the upstream flows mixing in a node; ii) the mass flowrates and the temperatures of the downstream flows of the same node; and iii) the heat fluxes exchanged by the upstream branches, representing a heat production/consumption. This constraint is addressed with Equation 4.8, where $c_{p,w}$ is the specific heat capacity of water and Φ_i is the thermal flux exchanged by the $i-th$ inlet branch.

$$\sum_{i \in IN^k} \left[c_{p,w} \cdot G_i^t \cdot T_i^t + \Phi_i^t\right] = \sum_{j \in OUT^k} \left[c_{p,w} \cdot G_j^t \cdot T_i^t\right] \qquad \forall k \in N, \forall t \in T \tag{4.8}$$

The different technologies involved in the operation of the thermal network are expected to have a range of temperatures at both their inlet and outlet. Since these constraints are needed to be respected only when the component is operating, the big-M technique is exploited to address them. Their mathematical formulation is reported in Equations 4.9 and 4.10, where: $T_c^{in/out}$ is the inlet/outlet temperature of

component c, C^{th} is the set of thermal components, and subscripts max/min indicate the maximum/minimum temperature achievable at the inlet/outlet of the component.

$$T^{in}_{c,min} - M \cdot (1 - s^t_c) \leq T^{in,t}_c \leq T^{in}_{c,max} + M \cdot (1 - s^t_c) \quad \forall c \in C^{th}, \forall t \in T \quad (4.9)$$

$$T^{out}_{c,min} - M \cdot (1 - s^t_c) \leq T^{out,t}_c \leq T^{out}_{c,max} + M \cdot (1 - s^t_c) \quad \forall c \in C^{th}, \forall t \in T \quad (4.10)$$

Beside the boundaries on the inlet/outlet temperature of the components, the operation of the technologies can be limited by constraints on the minimum or maximum temperature difference that the water can undergo by passing through the component itself. These constraints can be easily implemented with the same strategy presented before, as shown by Equation 4.11.

$$\Delta T_{c,min} - M \cdot (1 - s^t_c) \leq \Delta T^t_c \leq \Delta T_{c,max} + M \cdot (1 - s^t_c) \quad \forall c \in C^{th}, \forall t \in T \quad (4.11)$$

Beside the ramping constraints on the T_{cmp}, it is worth to consider the inclusion of other constraints on the ramp up/down of the mass flowrates crossing the heat generators and consumers. In fact, steep variations of the water flows could be impossible to be executed and, in general terms, it should be preferable to keep relatively continuous operating conditions. With this purpose, Equation 4.12 is implemented in the model, where ΔG_c is defined as the difference between G^t_c and G^{t-1}_c.

$$\Delta G_{c,min} - M \cdot (2 - s^t_c - s^{t-1}_c) \leq \Delta G_c \leq \Delta G_{c,max} + M \cdot (2 - s^t_c - s^{t-1}_c) \quad \forall c \in C^{th}, \forall t \in T \quad (4.12)$$

4.3.4 Thermal storage

According to the optimization steps under execution, the operation of the thermal storage is simulated with two different models. In one case, as already discussed,

Equations 3.4 - 3.8 are used, which simulate the operation through the storage heat flux, its state of charge and its capacity. As will be further explained, this strategy is adopted when the MES operation is optimized through the components' powers. In the other case, the water tank is simulated with a more physical approach, considering water flows, water masses and temperatures. Three simplifying assumptions are at the base of this model: i) the storage is divided into two water masses, one is hot and the other one is cold; ii) each of these two masses is perfectly mixed (i.e. the temperature is uniform); iii) the two water masses can exchange thermal powers with the external environment, but not between them. Both the hot and cold water masses have an inlet and an outlet stream, as can be seen in the simple schematic reported in Figure 4.5. The highlighted parameters are: the mass of the cold/hot water $M_{C/H}$, the temperature of the cold/hot water $T_{C/H}$, the inlet/outlet flowrates of cold/hot water $G_{C/H}^{in/out}$, the temperature of inlet/outlet flowrates of cold/hot water $T_{C/H}^{in/out}$.

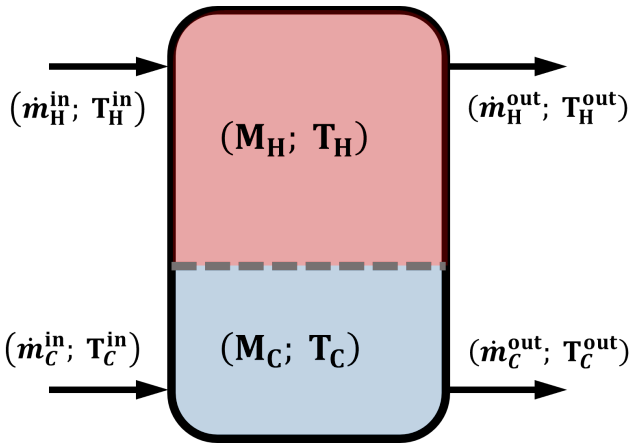

Fig. 4.5 Scheme of the thermal storage modelled with the simplified approach

Despite providing a simplified representation, the model proposed in Equations 4.13-4.19 is more realistic than the one based on the only thermal powers and can be integrated in the simulation of the heating network, since temperatures and mass flowrates are taken into account. More in detail, Equation 4.13 is defined for the mass conservation of the hot/cold water $M_{H/C}$; Equation 4.14 imposes that the hot/cold water mass is between zero and the total mass of the storage M_{stor}; Equation 4.15 is implemented for the energy conservation of the hot/cold water; thermal losses are defined in Equation 4.16; and finally, the temperature of the streams extracted from the storage is defined in Equation 4.17; and finally, Equation 4.18 imposes that

the energy contained in the storage $E^{stor,t}$, computed with Equation 4.19 is equal to the one found with the MES optimization $E^{stor,t}_{MES}$ (where was simulated with a 0D model).

$$M^{t+1}_{C/H} = M^{t}_{C/H} + (G^{in,t}_{C/H} - G^{out,t}_{C/H}) \cdot \Delta t \qquad \forall t \in T \tag{4.13}$$

$$0 \leq M^{t}_{C/H} \leq M_{stor} \qquad \forall t \in T \tag{4.14}$$

$$M^{t+1}_{C/H} \cdot T^{t+1}_{C/H} = M^{t}_{C/H} \cdot T^{t}_{C/H} + \left(G^{in,t}_{C/H} \cdot T^{in,t}_{C/H} - G^{out,t}_{C/H} \cdot T^{out,t}_{C/H} + \frac{\Phi^{loss,t}_{C/H}}{c_{p,w}} \right) \cdot \Delta t \qquad \forall t \in T \tag{4.15}$$

$$|\Phi^{loss,t}_{C/H}| = \frac{l^{stor} \cdot M^{t}_{C/H} \cdot c_{p,w} \cdot \left(T^{t}_{C/H} - T_{amb} \right)}{\Delta t} \qquad \forall t \in T \tag{4.16}$$

$$T^{out,t}_{C/H} = T^{t}_{C/H} + \frac{\Phi^{loss,t}_{C/H} \cdot \Delta t}{c_{p,w} \cdot M^{t}_{C/H}} = T^{t}_{C/H} - \left(T^{t}_{C/H} - T_{amb} \right) l^{stor} \qquad \forall t \in T \tag{4.17}$$

$$E^{stor,t} = E^{stor,t}_{MES} \qquad \forall t \in T \tag{4.18}$$

$$E^{stor,t} = c_{p,w} \left(M^{t}_{H} \cdot T^{t}_{H} + M^{t}_{C} \cdot T^{t}_{C} \right) \qquad \forall t \in T \tag{4.19}$$

As can be observed in Equation 4.13, the mass of the hot/cold water can be computed with a linear equation from the corresponding flowrates in the thermal network. On the other hand, the calculation for the temperature of these water masses is more complex, since it involves nonlinear equations with independent variables at the denominator of a fraction ($T^{t+1}_{C/H}$ made explicit from equation 4.15). This kind of nonlinearity is relatively difficult to be handled and most of the commercial solvers does not support its implementation. For this reason, the $T_{H/C}$ are introduced as independent variables to be optimized, such that the mathematical formulation of the energy balances for the thermal storage is quadratic.

4.3.5 Objective function

According to the criterion that is intended to pursuit, different objective functions can be chosen. For the present study, the economic objective function is selected. As a consequence, minimizing the expenditures to sustain during the system operation is the scope of the optimization. This function is defined as the summation of the operating costs determined by the purchase of fuels, the maintenance costs (which are collateral to the components operation), and the costs/earnings due to the purchase/sell of electricity from/to the grid. Regarding the mathematical notation, formulation reported in Equation 3.2 is used.

4.3.6 Decomposition approach for near-optimal solution

The complete model for the system simulation is composed by the union of the two sub-models previously described: the MES model and the model of the thermal network. The size of the problem is determined by the number of components, the level of detail chosen for the piecewise linearization, and the number of timesteps considered. The layout of the components does not have an impact on the number of variables but can increase the number of constraints, making the problem more difficult to be solved. The complete problem for the operation optimization of the system is therefore composed by 17,378 variables and 19,800 constraints. The distribution of the variables and constraint is provided in Table 4.2. Despite the MES selected has a simple structure, the resulting size of the problem is relatively high, especially considering the presence of a non-negligible number of binary variables and the quadratic constraints. The model has a MIQCP formulation, which has a nonlinear and nonconvex nature. The stage of development of commercial solvers of MIQCPs does not allow to solve this problem in a reasonable computational time and with an adequate accuracy. As a result, it is necessary to develop a strategy that is able to deal with the issues characterizing the problem, in order to find an alternative approach to perform the operation optimization.

Table 4.2 Number of variables and constraints

	MES	TN	Total
Binary variables	7392	0	7392
Continuous variables	7104	2882	9986
Linear equalities	770	1248	18456
Linear inequalities	10936	5502	0
Quadratic equalities	0	1344	1344

It is worth to notice that the two main sources of complexity (i.e the binary variables and the quadratic constraints) do not belong to both sub-models. In fact, the binary variables are addressed to simulate the MES, while the quadratic constraints are defined in the energy balances of the thermal network. If considered separately, the MES problem has a MILP formulation, while the model for the thermal network has a Quadratically Constrained Programming (QCP) formulation. Taking advantage of this aspect, it was possible to develop an optimization model based on an iterative approach.

In a conceptual perspective, the simulation of the thermal network is nested inside of the MES simulation. Decomposing the optimization defining the MES problem as the master problem and the thermal network problem as the slave problem could seem a natural choice. However, the presence of nonconvex constraints makes much more difficult to exploit the decomposition strategy. For this reason, the decomposition developed in the present study is based on a nonconventional approach, employing a recursive procedure where the operations of the MES and TN are optimized separately, despite the result of each is included in the input of the other. The structure of the entire optimization process is synthesized in the flowchart shown in Figure 4.6.

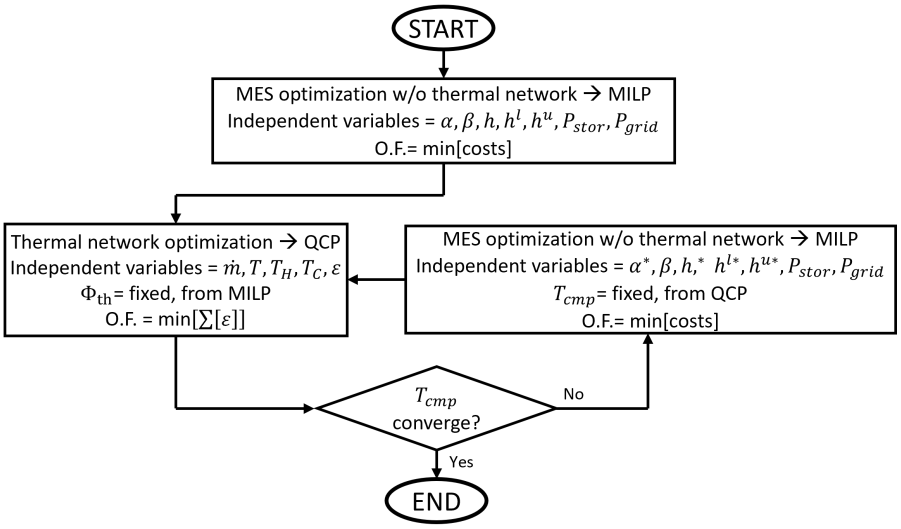

Fig. 4.6 Flow chart of the optimization process

The idea of the decomposed iterative approach is based on the following steps:

1. The first step of the process consists in optimizing the MES operation without considering any variable or constraint related to the thermal network. Since the heating power produced/consumed by the thermal generators/consumers are balanced by the constraints addressed for the energy conservation, the solution obtained from this particular version of the MES optimization keeps a physical meaning. The removal of the thermal network is done with a precise purpose: obtaining a simpler problem (with a MILP formulation) that can be considered as a relaxed version of the original one. As a consequence, the independent variables addressed in this first optimization are: α, h, h^l and h^u for the linearization of the performances of the generators; P_{grid} for the powers exchanged with the external grid; P_{stor} and β for the operation of the energy storage. Any other dependent variable, such as the powers of the fuels/energy vectors, the characteristic temperatures of the thermal generators and the operating status of the components, can be computed from these independent variables. Solving this problem allows to find, among the results, the values of the T_{cmp} that minimize the operating costs in the ideally favourable case where the thermal network does not impose any kind of constraints to the MES operation.

2. The following step is constituted by the optimization of the thermal network operation. Mass flowrates and temperatures are the parameters taken as independent variables. The thermal powers provided/consumed by the generators/users are imposed equal to the values obtained from the MES optimization. The resulting mathematical formulation is a nonconvex QCP. Despite the nonconvexity could be seen as a serious issue, the absence of integer variables and the relatively small dimensions of the problem are two crucial advantages. The aim of this step is to find the operating conditions of the network that allow to approach as much as possible the characteristic temperatures of the components found with the MES optimization. In other words, the objective is to find the mass flowrates and temperatures that allow to minimize the difference between the T_{cmp} obtained from the previous MES optimization and the T_{cmp} found optimizing the thermal network. The objective function that can be addressed is not unique since there are different ways to evaluate the error between two series of parameters. The option chosen in this study is the absolute value, as reported in Equation 4.20 (where k is the index of the iteration in which the T_{cmp} is computed). It is important to notice that the errors between the T_{cmp} computed by the MILP and the ones obtained with the QCP will have different impacts on the operation cost, according to the importance of the component. For this reason, the absolute values are multiplied by a weight w_c defined for each thermal generator, which are obtained with a sensitivity analysis. The problem becomes therefore a minimization of maximums. Auxiliary variables ε and the corresponding constraints are introduced in order to rewrite the absolute values in linear form (Equations 4.21 and 4.22).

$$OF = \sum_{c \in C^{th}} \left[w_c \cdot \sum_{t \in T} \left[\left| T^{t,k}_{cmp,c} - T^{t,k-1}_{cmp,c} \right| \right] \right] = \sum_{c \in C^{th}} \left[w_c \cdot \sum_{t \in T} \left[\varepsilon^t_c \right] \right] \qquad \forall t \in T \quad (4.20)$$

$$\varepsilon^t_c \geq T^{t,k}_{cmp,c} - T^{t,k-1}_{cmp,c} \qquad \forall t \in T \quad (4.21)$$

$$\varepsilon^t_c \geq T^{t,k-1}_{cmp,c} - T^{t,k}_{cmp,c} \qquad \forall t \in T \quad (4.22)$$

3. At this point, the convergence of the characteristic temperatures can be evaluated. With this purpose, two parameters are defined: the maximum error among all the T_{cmp} (Equation 4.23) and the maximum error among the average of the T_{cmp} for each component involved (Equation 4.24). If at least one of the two errors do not satisfy the tolerance imposed, the process performs a new loop by executing a new MES and TN optimization, until the convergence is reached.

$$\Psi^{max} = \max_{c \in C^{th},\, t \in T} (\varepsilon_c^t) \tag{4.23}$$

$$\Psi_{ave}^{max} = \max_{c \in C^{th}} \left(\underset{t \in T}{avg}(\varepsilon_c^t) \right) \tag{4.24}$$

4. The successive step occurs whenever the convergence criterion is not matched and it is very similar to the first one. The MES operation is again optimized without taking into account the thermal network. The only difference is that all the characteristic temperatures influencing the performance of some thermal components are fixed. Their value is set equal to the respective values obtained from the previous step of the process (i.e. the optimization of the thermal network. The task required to the MES optimization is therefore reduced to find only the operating powers of the technologies, whose performances are mathematically defined by curves and not anymore by surfaces (fixing the T_{cmp} reduces the performances dependencies from two to one).

The entire model is written in the Julia language, the MILP problem is executed by Gurobi, while Ipopt is used to perform for the QCP optimization.

Once that the complete structure of the model developed has been discussed, it is important to make a fundamental observation. The optimization approach presented, which is relatively similar to a fixed-point method, does not guarantee that the solution obtained at the end of the process is the global optimum. This is due to two main reasons: i) the MES and the thermal network are optimized in series and are not nested between them; ii) the result could change according to the objective function selected for the optimization of the thermal network.
However, it must be reminded that the global optimum cannot be demonstrated to be

reached for nonconvex problems. Making efforts in convexifying the problem could seem a good strategy for ensuring the global optimality, but the solution obtained in this case would be referred to an approximated version of the original problem, and therefore it would not delete all the issues.
On the other hand, the simple structure of the process, the absence of complex mathematical tools (e.g. relaxation strategies, reformulations, etc.) adopted to execute the optimization and the computational times required (as will be demonstrated) are important and promising aspects characterizing this model. For these reasons, in authors' opinion, near-optimal solutions found with the model developed in this study can be a very useful result to attain. To further enforce the reliability of the results obtained, the outcomes will be demonstrated to be high quality solutions, "satisfyingly close" to the global optimality.

4.4 Results and discussion

In this section the results obtained executing the optimization procedure are presented and discussed. The values of some meaningful parameters reached during the convergence of the iterative process are reported in Table 4.3.

Table 4.3 Number of variables and constraints

Iteration	OF MILP	OF QCP	Ψ^{max}	Ψ^{max}_{ave}	Computational times $[s]$	
	$[€/day]$	$[°C]$	$[°C]$	$[°C]$	MILP	QCP
1	102.89	255.5	16	3.7	96	59
2	103.69	9.5	2.8	173	128	50
3	103.74	0.02	0.03	0.002	33	70

The first iteration is actually the result of the first step of the process, the MES operation optimization without the thermal network, which is executed before the iterative cycle, and the following optimization of the thermal network. The two parameters defined to evaluate the convergence state of the procedure (Ψ^{max} and Ψ^{max}_{ave}) undergo a fast decay. In fact, the entire process took three iterations, with a computational time of 8 min on a laptop with an Intel i7-1065G7 CPU and 16 GB of RAM.

As previously mentioned, this first optimization of the MES operation represents a relaxed version of the complete problem. The thermal components are free to set their operation (i.e. powers and characteristic temperatures) without taking into account the limitations imposed by the presence of the thermal network. It is not guaranteed that this relaxed global optimum can constitute a feasible operating schedule for the real case study, however, its outcome (102.89€/*day*) can be taken as a useful theoretical reference. In fact, it represents a best boundary for any feasible solution of the optimization problem. This allows to make an interesting observation regarding the quality of the near-optimal solution obtained at the end of the process. The operation costs at the final iteration are equal to 103.74€/*day*, the 0.8% higher with respect to the relaxed global optimum. This means that, since the real global optimum must be between the relaxed global optimum and the (local) optimum obtained, the solution found with this model can have, in the worst case, operation costs the 0.8% higher with respect to the global solution. The optimization process developed, despite unable to guarantee the global optimality, demonstrates to achieve high quality results (or near-optimal solutions) of a complex problem in a reasonable amount of time.

In 2 out of 3 iterations, solving the MILP problem results to be more complex with respect to the QCP problem. However, the computational times requested by the two problems are comparable between them. The MES optimization has a linear formulation, but its higher size and the presence of binary variables make it more difficult to be solved. From the second iteration, the result of the previous MILP optimization is provided as initial guess to the solver; in addition, once that the characteristic temperatures are fixed, the size of the MILP is reduced and the performances previously addressed with surfaces are reduced to curves. Despite its smaller dimensions, the sources of nonconvexity and the non-trivial management of the thermal storage represent the main complexities affecting the QCP and contribute to determine its non-negligible computational time.

Regarding the other optimization outcomes, the electric and thermal powers related to all the technologies involved in the system operation are reported in Figure 4.7. The diagrams are stacked area graphs, where the powers produced by the generators are reported on the positive sector of the vertical axis (intended as entering, so positive energy fluxes) and vice versa for the ones absorbed by the consumers on the negative y-axis (intended as exiting, so negative energy fluxes). Electricity generation is mainly assigned to CHP and FC, with a small (and non-adjustable)

contribution from photovoltaic and wind powers. This electricity is employed to cover the load demand and supply the EHP; a remarkable excess is produced to be sold to the grid, especially when the selling price is higher. Buying the electricity from outside is an option that never takes place, while the electric storage operation is mostly devoted to the closure of the balance.

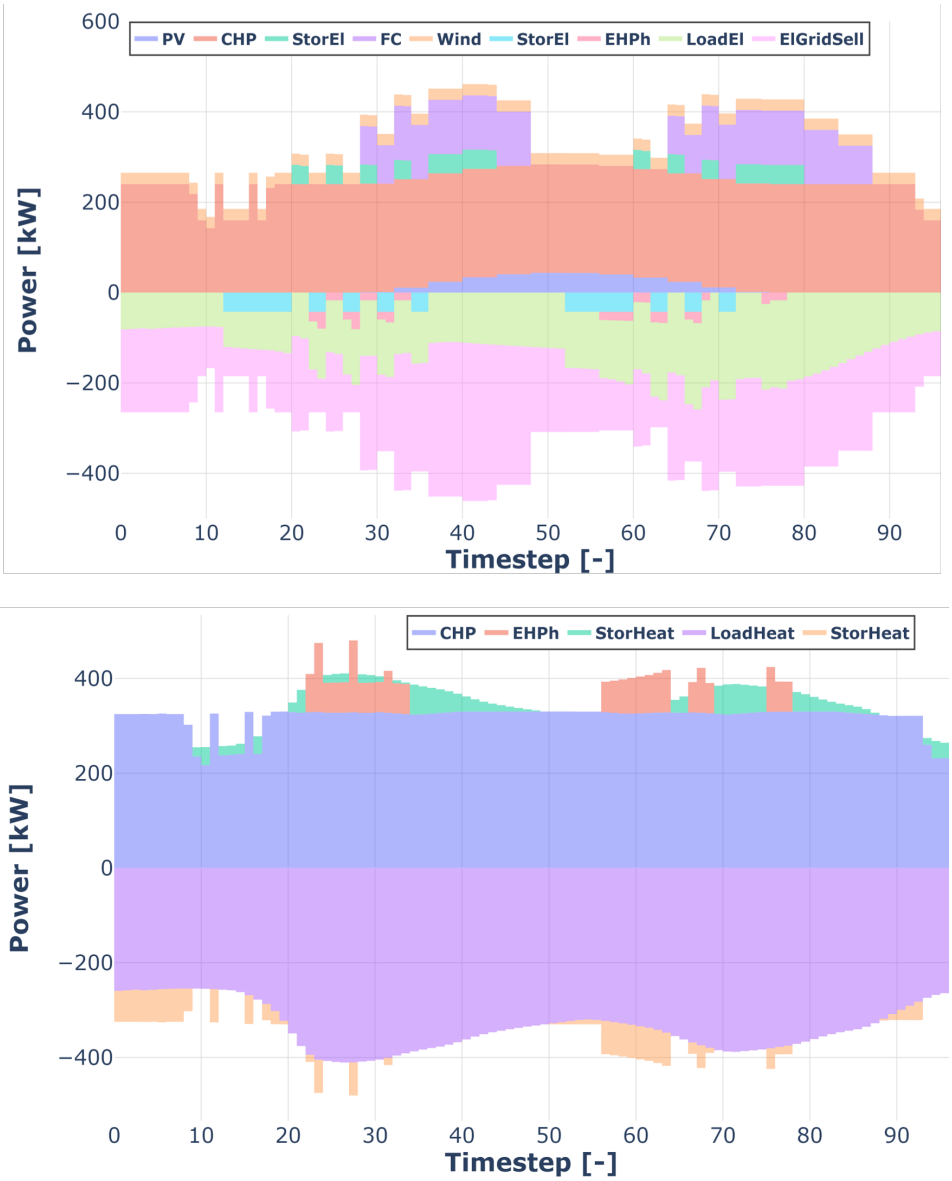

Fig. 4.7 Optimized operation for the MES, with electric powers on the top and heating powers on the bottom

The heating demand is satisfied with only the CHP and the EHP, since the boiler and the GHP are not the most efficient and cheap alternatives. The charging and discharging phases of the thermal storage are relatively frequent. Whenever possible, the CHP is used at its nominal load, which allows to reach the highest efficiency. The EHP and the thermal storage are used when the CHP cannot cover the thermal load on its own.

The time profile of the characteristic temperatures of the two thermal generators employed for the heating production (the CHP and the EHP) reached in the three iterations of process are reported in the two graphs of Figure 4.8. Notice that when a component is not operating, the characteristic temperature is null, otherwise it assumes its real value. In both cases, the values found in the first iteration tend to be flatter, showing smaller variations during the time period analysed. This result is reasonable and can be explained considering that the MILP executed in the first iteration is the only one that does not undergo any influence from the operation of the thermal network. Consequently, the T_{cmp} reached in this step are the ones more favourable for the objective function, without taking into account the constraints that must be respected to allow the exchange of the thermal powers across the network. On the overall, the difference between the characteristic temperatures found by the MILP and the ones obtained with the QCP is minimized up to zero whenever as possible, which is favoured by the flexibility of connections in the layout of the thermal network. In addition, it can be observed that, beside the input power, the model uses the T_{cmp} as an additional parameter to regulate the operation of the component, according to the performance surface that describes its operation. However, it must be recognised that this behaviour of the characteristic temperatures is strictly related to the performance curves of the components provided as input data and cannot be taken as a universal feature.

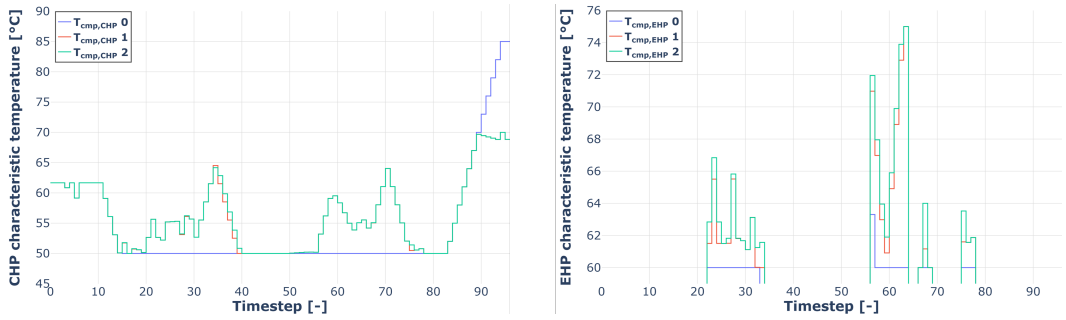

Fig. 4.8 Characteristic temperatures of CHP and EHP during the iterative process

Other interesting considerations can be made looking at the variation of the fluxes of the two main energy vectors for the most important components, reported in Figure 4.9. The curves represent the difference of the electrical (on the left) or thermal (on the right) powers between the values reached in the first and last iteration of the optimization process. In most of the timesteps the difference is small or null; however, in some cases the variations reach the order of magnitude of few tens of kW, which is not negligible. These adjustments are due to the variations of the characteristic temperatures, imposed in order to avoid the violations of the constraints of the thermal network. Imposing a different value of the characteristic temperature changes the performance of the component, whose operation can be modified if it results to be no more optimal in economic terms. As can be observed, in most of the cases these variations compensate each other. In fact, since the requirement of the loads is constants input parameter, the reduction in the power production of a component is balanced with the increase of the generation of another technology. The cases in which these variations are not compensated are due to the fact that are modified peculiar elements of the MES, such as the connection with the external power grid for selling/buying electricity.

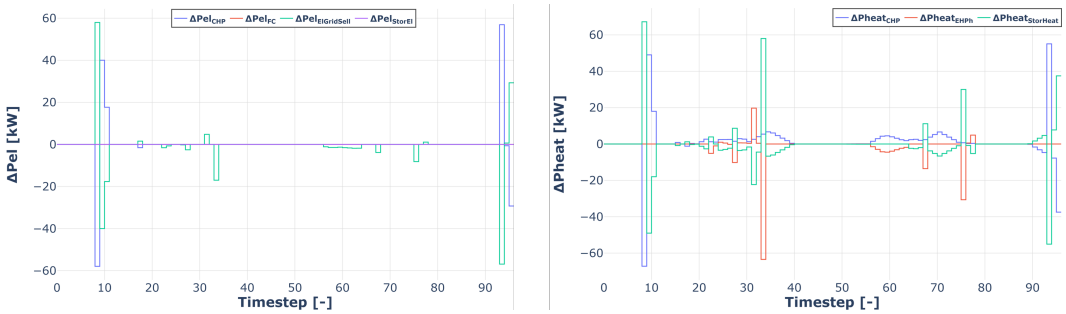

Fig. 4.9 Difference between first and last iteration of electrical (left) and thermal (right) fluxes

The temperatures and masses of the hot and cold water in the thermal storage are reported in Figure 4.10. The model manages to integrate the storage operation (in terms of flowrates and temperatures) in the thermal network. At the first timestep, the storage is assumed to be empty (i.e. full of cold water). Then, it is charged up to its maximum for two times and at the end of the period it returns empty (as imposed by input data). The mass of hot water keeps a temperature in a range between 75°C and 85°C, while the cold water remains between 55°C and 65°C. On the overall, the storage increase the flexibility of the system and allows to achieve

lower operation costs, but, at the same time, increases the link among the timesteps and, as a consequence, the complexity of the management of the thermal network.

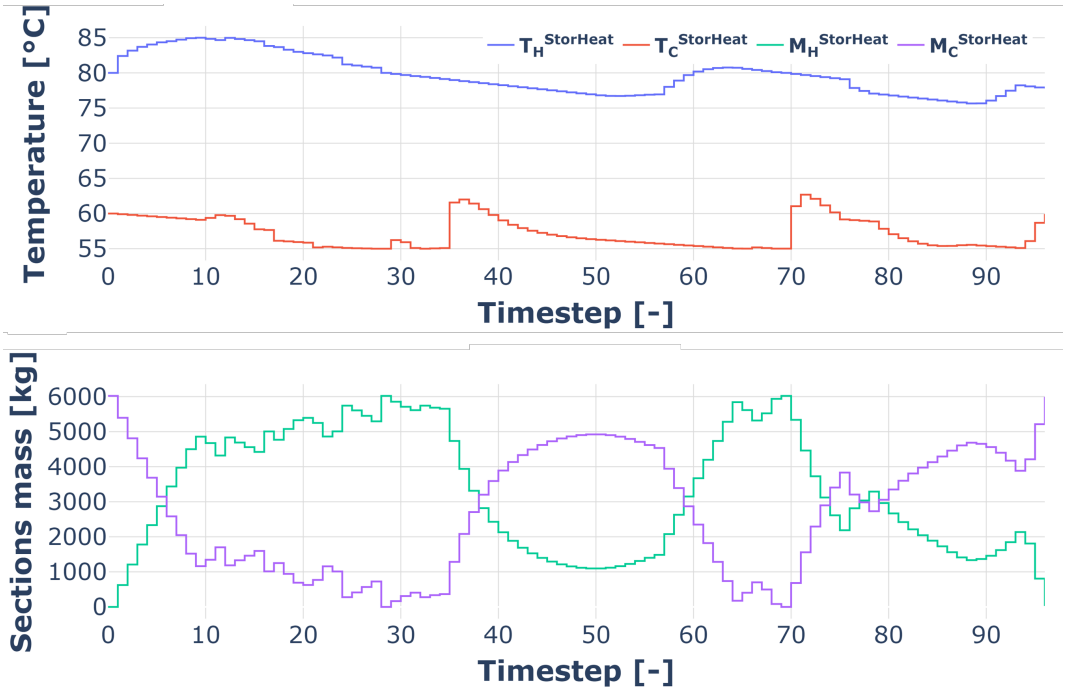

Fig. 4.10 Operating temperatures (up) and water masses (down) of the thermal storage

In light of the results obtained from the optimization, it is possible to make a final consideration. Performing an operation optimization of the MES without including the simulation of the TN would be equivalent to the very first step of the process presented. As already mentioned, in this case the economic cost obtained is very similar to the one reached executing the methodology developed in the present research, which integrate the TN simulation. The fundamental difference is that, in the former case, it would not be possible to adopt the configuration achieved with the optimization, since it would lead to the violation of physical/technical constraints of the thermal network. Therefore, the strength of the methodology presented relies on the fact that it is able to solve a wider operation problem in relatively short computational times, providing a good solution (in terms of objective function) that can be exploited in real applications.

Chapter 5

Operation optimization of a MES with a DHN

Given the encouraging results of the study presented in the previous chapter, the coupling between the MES optimization and the thermal network operation is deepened. Here, the model developed to include the simulation of a District Heating Network (operating with the VFVT strategy) in the operation optimization of a MES is presented. The differences with the previous study rely on the fact that, in this new case study, the thermal network included in the optimization is a small District Heating Network, while in the case analyzed before it was the internal network of the MES. This is a very important aspect since the model for the simulation of the network shares some variations according to the kind of network under consideration, and these differences lead to two distinct optimization processes.
The case study is presented in section 5.1, and the following one (5.2) is devoted to discuss the methodology developed. Finally, the results and conclusions are reported in section 5.4, while the limitations and future developments are discussed in 5.5.

5.1 Case study

The Multi Energy System considered as case study is represented with a conceptual scheme in Figure 5.1. It is composed by two CHPs, two HOBs, a thermal storage, an electric storage, a connection with the electric grid, a DHN, and the electric and thermal loads. The district heating network allows the heat transport among the

producers, the storage and the users. These lasts are synthetically represented in the figure by a single element.
A relatively basic system is chosen in order to allow to focus more on the development of the methodology than on the specific set of technologies selected and the quantitative aspects of the analysis.

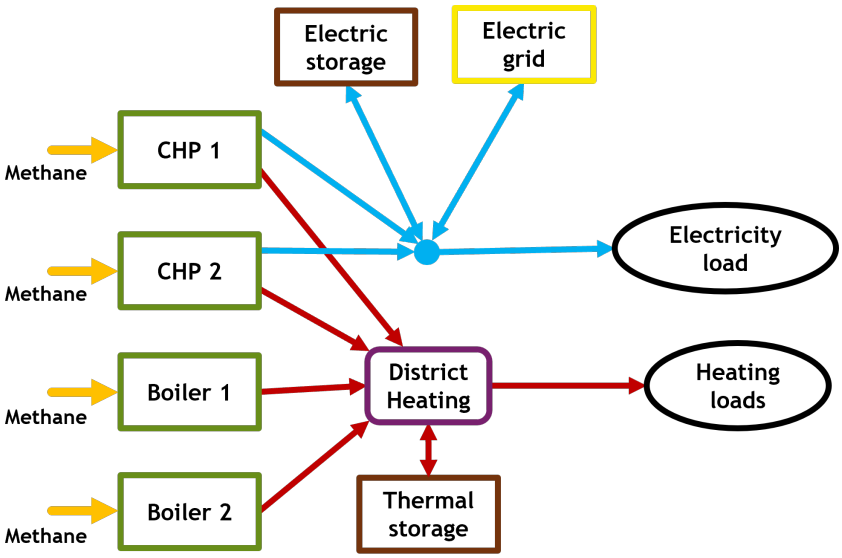

Fig. 5.1 Conceptual scheme of the MES assumed as case study

The layout of the DHN was arbitrarily created. Since this kind of integration is a first attempt, the network is tree-shaped, in order to face a simpler configuration. However, as will be further demonstrated, the developed methodology is able to manage loop-shaped networks as well. The layout of the network is showed in Figure 5.2, where, for simplification purposes, the network is represented with a single line despite being composed by two pipes. The supply and return lines of the network are assumed to have the same structure and dimensions, laying parallel between them.

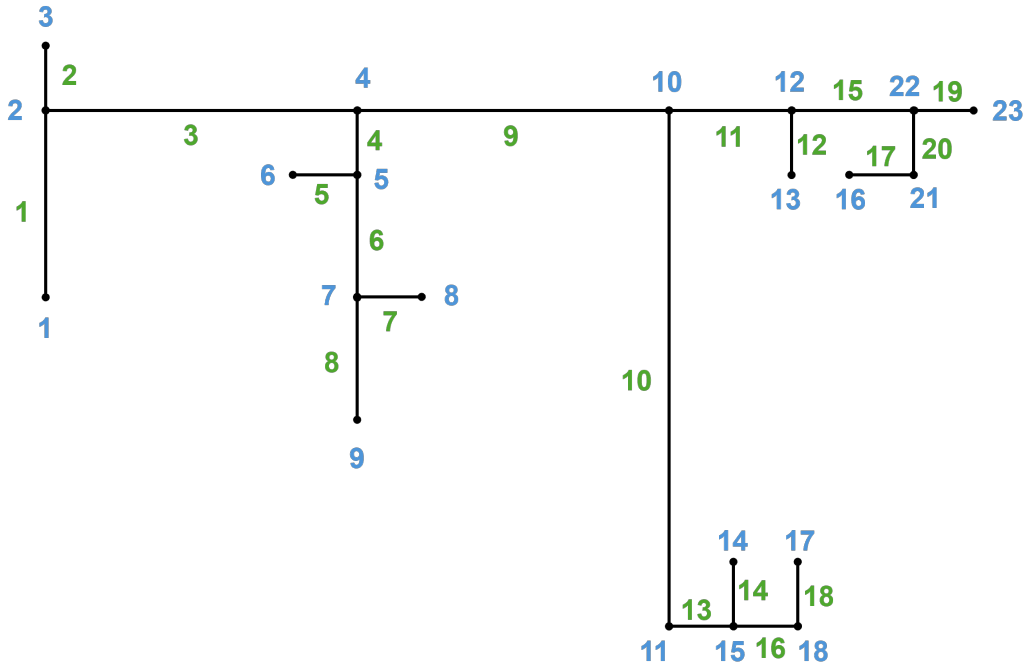

Fig. 5.2 Layout of the district heating network

As already mentioned, a small sized DHN is analyzed, with a total length of the branches equal to $12km$. Concerning the other assumptions related to the network, pipe diameters are in the range of $5cm$ - $10cm$ and a global thermal transmittance of $1\frac{W}{m^2K}$ is considered.
The elements exchanging mass flowrates with the DHN are reported in Figure 5.3 in correspondence of their location. Notice that, because of the position of the thermal generators and users, the flowrate can have different directions. The fact that the orientation of the flows is not known a priori will influence the optimization model and will determine an increase in the calculations required to simulate the network.

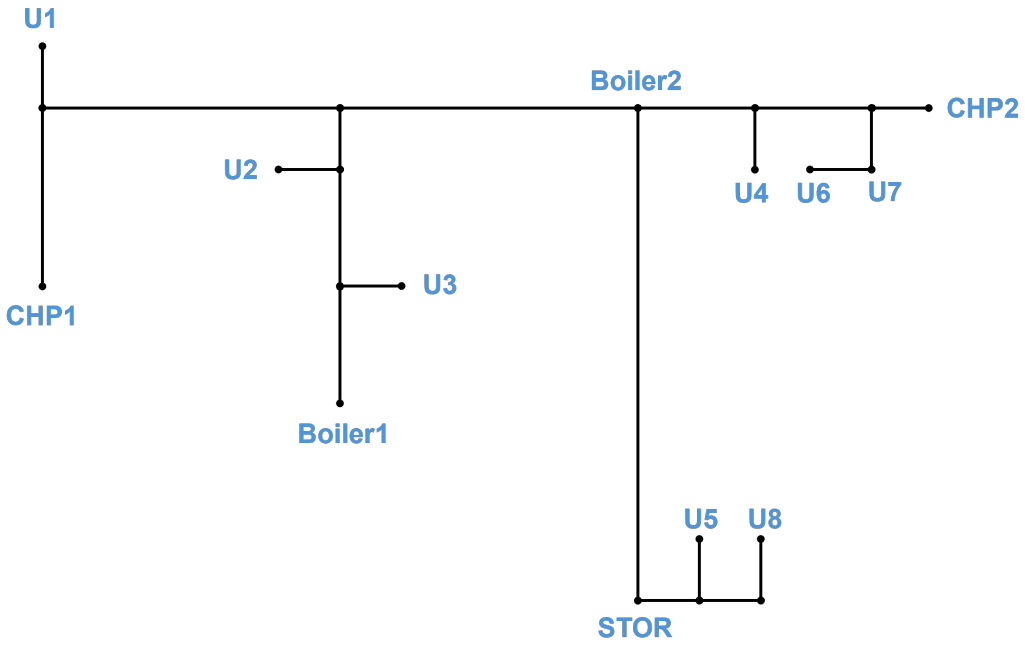

Fig. 5.3 Disposition of the thermal elements in the district heating network

Despite the network can be considered as small sized, all the physical phenomena occurring in bigger DHNs are assumed to take place in this case study. This means that the simplifying assumptions adopted in the optimization presented in the previous section are now removed. As a consequence, the thermal inertia and the heat losses are included during the system modelling.

The aim of the present analysis is to perform the operation optimization of a MES coupled with a DHN, paying a particular attention to the simulation of the district heating network and the inclusion of the most important flexibility sources. The extension of the optimization is proportional to the amount of parameters addressed as independent variables, such that a high number of degrees of freedom is reached. For this reason the model was developed trying to avoid to impose a specific operation whenever as possible.

The parameters that are intended to be optimized are reported in Table 5.1, in correspondence of the section of the system in which they have an impact. As will be further discussed in the Methodology paragraph, the fact that these parameters undergo an optimization process does not necessarily mean that they are addressed as independent variables.

Table 5.1 Operating parameters to be optimized

Section	Element	Parameter
MES	Generators	Operating power
	Storage	Operating power
	Thermal users	Operating power
DHN	Generators	Mass flow and temperatures
	Storage	Mass flow and temperatures
	Thermal users	Mass flow and temperatures

The period of time considered for the operation optimization is equal to 24 hours, as usually assumed in similar studies that can be found in the literature.

5.2 Methodology

The issues presented in the previous analysis (Chapter 4) are still present in this case study, with the addition of the ones determined by the thermal inertia and heat dispersion occurring in the DHN (further details are provided in the following paragraphs). The latter phenomenon can be (easily) included in the model by adding a thermal flux in the energy balance equations, while the former one brings much more complexities in the formulation of the model.

On the overall, the problem is a high-dimensional MINLP and it cannot be solved by simply providing the simulation model to an optimizer because of the limitations of commercial solvers in dealing with mixed integer non-convex problems with more than few hundreds variables. It results to be necessary to take advantage of the techniques presented in sections 3.2.2 and 3.2.6 to reshape the mathematical formulation and find a trade off between accuracy and computational time.
In light of the characteristics of this case study, the following considerations were made:

- the timesteps are linked among them by both the presence of a thermal storage and the physical effect of the thermal inertia. Consequently, the subdivision of the problem into a series of smaller and independent optimizations cannot be exploited;

- the non-convex sources are two: the non-linear performances of the generators and the energy balances of the DHN. In the first case, the polynomials describing the efficiencies can be piecewise linearized, such that the non-linearities are removed by accepting an approximation of the performances and an increase of the number of variables. In the second case, the bilinear terms constituted by the product between mass flowrates and temperatures are more difficult to be handled. Piecewise linearization is not useful since it would introduce an excessive number of variables and relaxation techniques would require a robust strategy for ensuring the global convergence;

- according to the aspect under consideration, different time discretizations can be adopted. For example, it is reasonable to assume small intervals (order of minutes) for the simulation of the DHN, while coarser steps (1 hour) can be used for the operation of the generators;

- it can be worth to attempt to reduce the problem size by introducing some assumptions tailored on the case study, taking advantage of its nature and features.

Reformulating the problem from MINLP to MILP would be the best way to solve the optimization, but it is not completely possible because of the bilinear terms in the operation simulation of the DHN. The main idea behind the methodology developed in this study relies on the fact that in case one of the two variables constituting the bilinear terms (temperature or flowrate) would be known, the entire problem could be written and solved as a MILP.
The structure of the optimization is presented in Figure 5.4 in form of flow chart. The process was decomposed on two levels, following a master-slave problem structure. On the upper level, the flowrates injected/extracted by the thermal generators, users and storage (G) are addressed as variables to be optimized and the fluid dynamic problem of the DHN is computed. On the lower level, the MES operation and the thermal problem of the DHN are jointly optimized. Here, the operating powers of the producers (P_{el}/Φ) and the temperatures of the water flows (T) exiting the generators are addressed as independent variables. Notice that, since this lower-level problem is nested into the upper-level optimization, it will be executed at each iteration of the master problem.

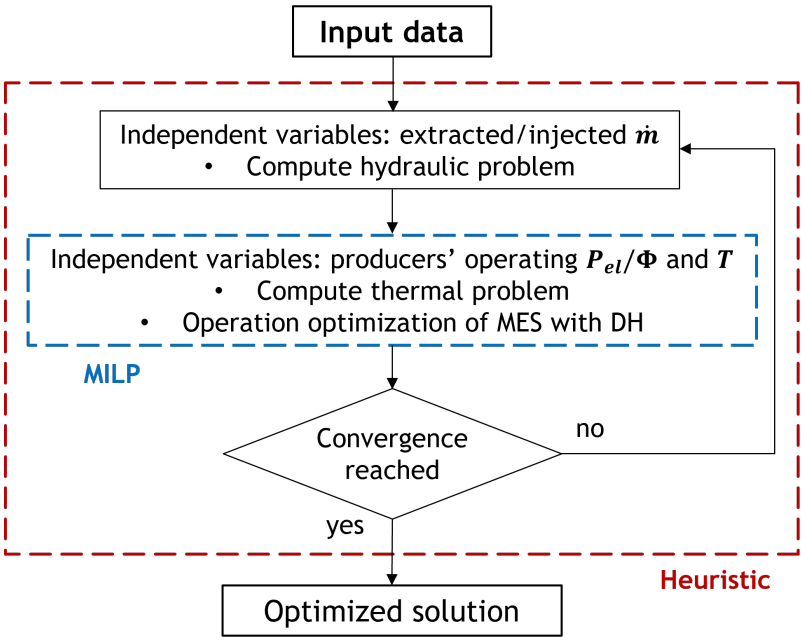

Fig. 5.4 Flow chart of the process for the operation optimization

The main differences with respect to the methodology presented in the previous section are:

1. heat losses and thermal inertia phenomena are included in the DHN;
2. the decomposition strategy is structured with a nested approach, solving the problem with a single execution;
3. the operation of the MES and DHN are contemporary simulated;
4. both deterministic and metaheuristic solvers are employed to perform the optimization;
5. the demand of thermal users is not fixed, it is considered as a parameter to optimize;
6. the dependence of thermal generators' performance on the operating temperatures is not anymore considered.

Before further discussing the optimization process, it is useful to present the approach used to model the elements constituting the system. These are distinguished

into: producers, users, storage, DHN. Note that the information missing from the following subsections are provided in the Appendix.

5.2.1 Producers

The operation of the producers is simulated by addressing a performance curve. This curve is linearized with the aim of obtaining a mathematical formulation in which the non-linearities are not explicitly addressed and MILP solvers can be exploited. The efficiency is assumed to be dependent on a single parameter, i.e. the power of the energy vector entering the component. The influence of the operating temperatures of the thermal generators on their performance is not considered in order to reduce the complexity of the problem analysed, which is already challenging because of the inclusion of the thermal losses and inertia of the DHN. The curve can be piecewise linearized, but a single interval is chosen in order to keep a low size of the problem. The formulation used for this purpose is the same presented in Equations 4.2 and 4.3. The approximation of the real performance will be relatively poor because of its linearization in a single interval, but this does not prevent to address the most important technical constraints, since the operation is defined by two continuous variables and a binary variable.
The boundaries for the operating range are addressed with Equation 3.11, the constraints on the minimum operating times are defined with Equations 3.12 - 3.14, while ramping constraints are omitted for simplicity purposes, despite their inclusion is possible and straightforward (see Equation 3.15).
A different strategy is developed to simulate the producers that interact with the DHN, which are the thermal generators. In fact, since their operation is jointed between the MES and the DHN, it is appropriate to model these components with a tailored approach. As will be later discussed, the mass flowrate and the inlet and outlet temperatures of the thermal generators are defined as variables to be optimized. Therefore, the heating power generated by the thermal producers can be computed as a function of these parameters, as reported in Equation 5.1, where $T_{s/r}$ is the supply/return temperature and n is the node where the component c is located. With this power output, the input power can be obtained by reversing the performance curve, such that the component's operation is calculated (Equation 5.2). Some auxiliary constraints must be addressed to ensure the satisfaction of the technical constraints: Equation 5.3 limits the thermal production in the component's operating

range; Equation 5.4 is defined to bounds the mass flowrate of the generators; and Equations 5.5 and 5.6 are for the compliance of the operating temperatures admitted by the heat producers.

$$\Phi_c^t = G_c^t \cdot c_{p,w}(T_{s,n}^t - T_{r,n}^t) \qquad \forall c \in C^{GEN},\ \forall t \in \{1,..,t^{end}\} \quad (5.1)$$

$$P_{in,c}^t = K \cdot \Phi_c^t + q \qquad \forall c \in C^{GEN},\ \forall t \in \{1,..,t^{end}\} \quad (5.2)$$

$$\Phi_{min,c} \cdot s_c^t \leq \Phi_c^t \leq \Phi_{max,c} \cdot s_c^t \qquad \forall c \in C^{GEN},\ \forall t \in \{1,..,t^{end}\} \quad (5.3)$$

$$G_{min,c} \cdot s_c^t \leq G_c^t \leq G_{max,c} \cdot s_c^t \qquad \forall c \in C^{GEN},\ \forall t \in \{1,..,t^{end}\} \quad (5.4)$$

$$T_{s,min,c} \leq T_{s,c}^t \leq T_{s,max,c} \qquad \forall c \in C^{GEN},\ \forall t \in \{1,..,t^{end}\} \quad (5.5)$$

$$T_{r,min,c} \leq T_{r,c}^t \leq T_{r,max,c} \qquad \forall c \in C^{GEN},\ \forall t \in \{1,..,t^{end}\} \quad (5.6)$$

The on/off state of the thermal generators is not defined with a binary variable, as for the other producers, but it is derived from the mass flowrate. In other words, the state is on (i.e. 1) if the water flow determined in the upper level optimization is different from 0, otherwise it is set to off (i.e. 0).
Finally, to improve the convergence of the process and reduce the computational time, an attempt was made to decrease the number of independent variables addressed in the upper-level optimization. This was made by observing that it is not mandatory to use the same time discretization chosen for simulating the thermal problem of the DHN for defining the mass flowrates of the heat producers. A different time discretization is used, with coarser and not uniform intervals. In particular, steps of 1 hour are used when the DHN is expected to sustain low or stable flow extractions,

while 20 minutes are set for the morning and evening hours, when usually the highest variations take place. This choice does not influence the formulation of the equations of the problem, but it reduces the size of the problem in terms of independent variables and constraints addressed.

5.2.2 Users

Since the electric load is assumed as known, the thermal users are the only consumers that require to be modelled. Two kinds of users are considered: residential and commercial. This distinction does not affect their modelling, but it is only related to the hours of the day in which they can be active.
In case of operation optimization of a MES, the users are typically simulated through the thermal power that they absorb [187], while the flowrate extracted defines the users when the DHN operation must be optimized [178]. One of the aims of this analysis is to optimize the operation with an approach as wide as possible. For this reason, the heat flux, the flowrate and the temperatures characterizing the users operation are treated as variables to be optimized. Despite these terms are not assumed as known inputs and will be free to vary during the optimization process, they will be asked to fulfill some requirements, which act as upper and lower limits. In particular, a variation range is established for the thermal energy extracted from the network in order to satisfy the heat demand of the users. In other words, the choice of not defining the thermal users with a fixed requirement of heating power or hot water flowrate is analogous to the inclusion of a demand response program in the process for the operation optimization.
In addition, it is important to remember that the thermal extraction performed by the users is executed by a heat exchanger, whose operation is constrained by the physical laws that rule the thermal transfer itself. Instead of addressing the entire simulation of the heat transfer, a simplified approach is exploited, based on a correlation that links the heating power with the product between the mass flowrate and the temperature at which the hot water is available. This correlation has been observed from the real data of the DHN of Turin and an example of this phenomenon is presented in Figure 5.5, where many stationary operating conditions belonging to different years are reported in scatter form.

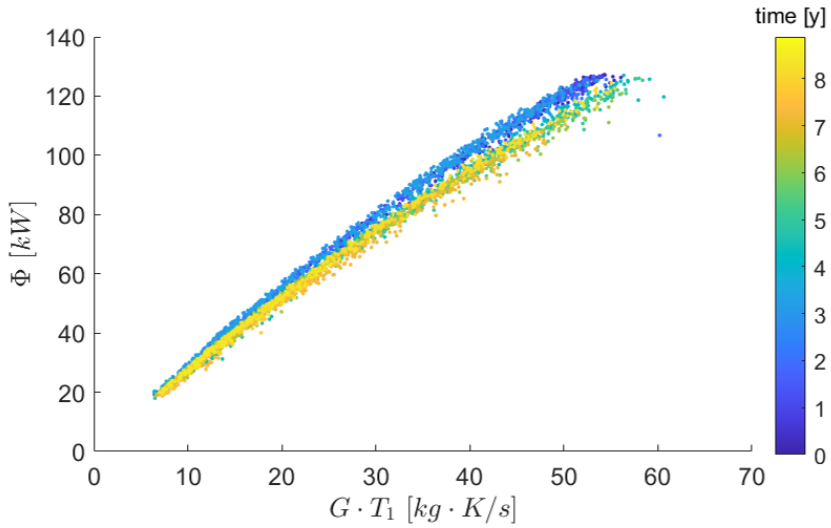

Fig. 5.5 Visualization of the correlation between thermal users' operating parameters

The mathematical formulation used to describe this correlation is reported in Equation 5.7, where K and q are coefficients.

$$\Phi_c^t = KG_c^t T_{s,n}^t + q \qquad \forall c \in C^{USERS},\ \forall t \in \{1,..,t^{end}\} \quad (5.7)$$

Performing the calculation for the hydraulic and thermal problem of the supply network, the flowrate and temperature on the supply side of the DHN are computed. At this point, the thermal power can be obtained with Equation 5.7.
By reversing the energy balance on the user (Equation 5.8) and merging it with Equation 5.7, the temperature of the water flow injected into the return network ($T_{r,n}$) is calculated as a function of the supply temperature and the mass flow itself.

$$\Phi_c^t = G_c^t \cdot c_{p,w}(T_{r,n}^t - T_{s,n}^t) \qquad \forall c \in C^{USERS},\ \forall t \in \{1,..,t^{end}\} \quad (5.8)$$

At this point, it is important to discuss how the parameters defining the operation of the users are handled. As already mentioned, the flowrates processed by the users are intended to be considered as variables to be optimized, and, in particular, as independent variables. However, considering that the number of thermal users is usually much higher than the number of thermal generators, and that an adequately

refined time discretization should be assumed in order to perform a realistic analysis, it results that the problem would reach a challenging size, both in terms of computational time and feasibility. As an attempt to reduce the problem dimension and, in particular, the number of variables addressed for the users' mass flowrates, the following strategies have been adopted:

- an operation interval (or multiple intervals) is defined for each thermal user. This means that no mass flow is extracted from the supply network outside of the time periods defined as input data. In fact, in real case studies, the operation time of residential and industrial users is known, and defining the mass flowrates only in correspondence of the timesteps belonging to these periods does not limits the extent of the optimization;
- instead of defining the mass flow with an independent variable for each of the timesteps of the operating period, a polynomial curve is defined to describe the user's flowrate along the time. The flowrates are obtained by computing the curve in the selected timesteps. In this way, the coefficients of the polynomial curve are the only parameters addressed as variables, and the time discretization does not have an influence on the problem's size, at least for what concerns the thermal users. The mathematical formulation used for this purpose is reported in Equation 5.9, where a, b, c, and d are the coefficients whose values must be optimized and t is the time expressed in hours since the beginning of the period under consideration.

$$G_c(t) = a \cdot t^3 + b \cdot t^2 + c \cdot t + d \tag{5.9}$$

The resulting effect of this approach is showed in graphical form in Figure 5.6. Here, the polynomial curve is reported with a red dotted line, the values assumed in the timesteps are marked with dots and the blue stepped line is the discretized G, obtained by keeping constant the value of the flow in the corresponding time period. Notice that the regions in gray are excluded a priori because they rely on the time intervals in which it is already known that the user will not require heat.

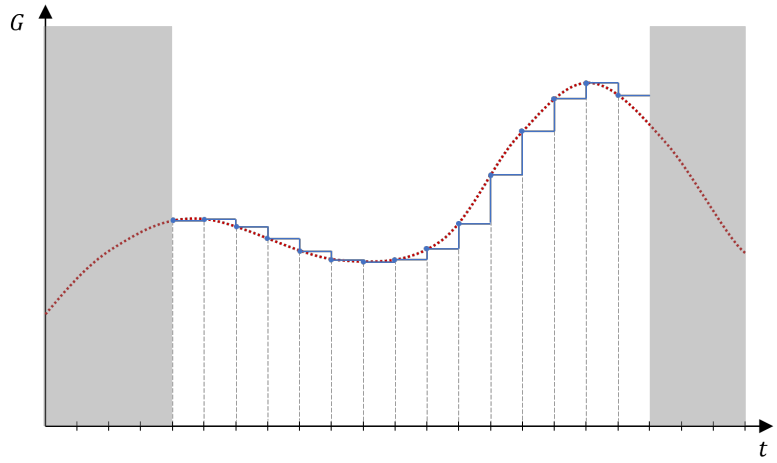

Fig. 5.6 Representation of the approach used to address the users' extracted flowrates

This strategy presents interesting advantages but, at the same time, it has a drawback, which consists in the fact that the flowrates of the users cannot vary completely freely, but can only assume the values that can be represented by a third degree polynomial curve. This curve can reach a very high number of shapes, but it must be recognized that there will exist shapes that cannot be created by the combinations of the terms constituting the polynomial, such as discontinuous and non-smooth profiles. However, the limitations introduced by the adoption of this approach have a relatively limited impact on the operation. In fact, in the real applications, the variation of the flowrates is continuous and it can be approximated with an interpolation curve, whose quality can be eventually improved by increasing the degree of the polynomial or by introducing other mathematical forms to perform the interpolation.

When the discretization is performed for all the users' flowrates, a first check is executed to correct their value in case necessary. This may happen in two cases: a) when the flowrate is computed outside of the operation period of the user; b) when the flowrate assumes incompatible values (i.e. positive values for extracted streams). In both the cases, the correction consists in setting to zero the value of the flowrate, which means that the user will not be active. Once that the corrected flowrates are computed, the boundaries for the minimum and maximum values that the flowrates of the users can assume are addressed with the constraint reported in Equation 5.10.

$$G_{min,c} \leq G_c^t \leq G_{max,c}$$
$$\forall c \in C^{USERS},\ \forall t \in \{1,..,t^{end}\} \quad (5.10)$$

Finally, since the thermal demand of the users is not provided as an input data, it is necessary to address some limitations to the heat absorbed by the consumers. For the present analysis, the constraints reported in Equation 5.11 are defined, which set a lower and upper bound to the thermal energy extracted by the users in different moments of their operation. Here, E is the energy absorbed by user u (computed with Equation 5.12), which is part of the set U, while the timesteps t for which the constraints are defined belongs to the set T^u. In this way it will be guaranteed that a minimum amount of heating will be provided to the users to satisfy their minimum requirement, and the same happens for the maximum quantity of heat that can be absorbed by the consumers.

$$E_{u,min}^t \leq E_u^t \leq E_{u,max}^t$$
$$\forall u \in U,\ \forall t \in T^u \quad (5.11)$$

$$E_u^t = \sum_{k=t_0}^{t} \left[G_n^k \cdot c_{p,w} \cdot (T_{s,n}^k - T_{r,n}^k) \cdot \Delta t^k \right] \quad (5.12)$$

5.2.3 Storage

The case study under consideration includes an electric storage and a thermal storage.

The electric storage is simulated with the approach based on two continuous variables and one binary variable, as already done in the analysis previously presented (chapter 4). Make reference to Equations 3.4 - 3.8 for the mathematical formulation.

The model for the thermal storage is completely different since it must account the different physics of the device. It is based on the simplified approach presented in Section 4.3, with the mass of water in the tank ideally separated in two parts, each of them at an uniform temperature, as was schematically represented in Figure 4.5. Both the hot and cold water masses have two connections with the DHN to perform the injection or extraction of water from the corresponding line of the network. Therefore, once that the initial condition is defined (i.e. water masses and temperatures) and the entering/exiting flowrates and temperatures are defined, the storage

can be simulated by applying the energy balances on the two water masses. The details for the mathematical formulation are presented and discussed in Equations 4.13 - 4.19.
In addition, the approach developed to address the parameters describing the storage operation in the optimization process is reported below. The flowrates are obtained in the upper-level optimization with a mass balance on the flows injected/extracted by the generators/consumers, as reported in Equation 5.13. Here, c is used as index for both the consumers and producers, grouped in C^{USERS} and C^{PROD} respectively.

$$G^t_{stor} = \sum_{c \in C^{USERS}} \left[G^t_c\right] - \sum_{c \in C^{PROD}} \left[G^t_c\right] \qquad \forall t \in T \quad (5.13)$$

The temperatures of the flowrates entering the storage are obtained from the computation of the thermal problem of the DHN and can be imposed in the energy balance of the storage.
Finally, the temperatures of the flowrates exiting the storage are set to be equal to the corresponding water masses in the vessel, which are obtained simulating the storage operation itself.

To sum up the inclusion of the thermal storage simulation in the optimization process, the flowrate of the storage is computed as the difference between the flows injected by the heat producers and the flows extracted by the users (such that the mass balance is met), and the temperatures of the stored water are calculated as a function of the temperatures of the network in correspondence of the location of the storage itself. As a result, no independent variables were addressed to include the thermal storage in the optimization model and the equation for the mass balance was not provided as a constraint, since it is automatically respected.

5.2.4 DHN

Taking into consideration the aims of the study and the importance of performing a realistic treatment of the DHN to obtain meaningful results, the simulation of both the supply and return lines of the network is included in the optimization process. The space discretization is performed with a $25m$ step, while the time period of $24h$

is divided in 5*min* intervals.
The DHN is simulated and optimized in both the two levels of the process:

- **Upper level optimization**
  As already mentioned, the fluid dynamic problem is computed in the upper-level optimization. The injected and extracted flowrates are assumed as independent variables for all the units, except for the thermal storage.
  The mass balance in differential form is reported in Equation 5.14, where **v** is the velocity vector. After having discretized the DHN in nodes and branches and having executed the spatial integration of the differential equation assuming the case as one-dimensional, the mathematical form presented in Equation 5.15 is obtained. Here, CV is the control volume on which the integration is performed, v is the velocity of the fluid crossing the section S, and B_n is the set containing the branches b crossing the control surface.

$$\frac{\partial \rho}{\partial t} + \nabla \cdot \rho \mathbf{v} = 0 \tag{5.14}$$

$$\left.\frac{dM}{dt}\right|_{CV} + \sum_{b \in B_n} [\rho v_b S_b] = 0 \tag{5.15}$$

  Assuming the water as an incompressible fluid, the time derivative of the mass in the control volume becomes equal to zero, since the water mass cannot vary if both its density and volume are constant. In addition, the term $\rho v_b S_b$ can be recognized as the mass flow circulating in branch b. As a result, Equation 5.16 is obtained, where the injected/extracted flowrate at node n (i.e. $G_{ext,n}$) is reported separately from the other flows. Notice that this equation is referred to a generic timestep t.

$$\sum_{b \in B_n} [G_b] + G_{ext,n} = 0 \tag{5.16}$$

  Addressing this balance for all the nodes of the network and rewriting them in matrix form, the formulation presented in Equation 5.17 is obtained for each timestep, where A is the incidence matrix and G_{ext} is the vector of the extracted and injected flows. More in detail, the dimensions of the incidence matrix are [NNxNB] (i.e. Number of Nodes x Number of Branches) and its values

are $-1/+1$ for inlet/outlet branches (0 otherwise), while G_{ext} has dimensions [NNx1].

$$A \cdot G + G_{ext} = 0 \tag{5.17}$$

Since the injected/extracted flowrates are addressed in the upper-level problem, which will be optimized with a heuristic solver, Equation 5.17 can be reversed and solved with Equation 5.18, where the $\backslash$ is a multi algorithm operator that solves the linear system by applying the most suitable strategy for the matrices provided.

$$G = -A \backslash G_{ext} \tag{5.18}$$

At this point, the thermal problem can be computed in the lower-level optimization.

- **Lower level optimization**
  This step is entirely nested into the upper level optimization and it has the aim of optimizing the operation of the components of the MES and the temperatures of the DHN. Since the combination of these two problems can be written with a MILP formulation, a deterministic solver is used to execute this task. Assuming that: a) the DHN can be simulated with a one-dimensional formulation; b) the heat transfer is only convective; c) the properties of the materials are homogeneous; d) perfect mixing in case of merging flows, it is possible to write the energy balance in differential form, as reported in Equation 5.19. Here, v is the flow velocity on the x direction, and φ_{source} is the volumetric heat flux, which is actually constituted by a single term, the heat loss due to the thermal dispersion (φ_{loss}).

$$\frac{\partial(\rho c_p T)}{\partial t} + \frac{\partial(\rho c_p v T)}{\partial x} = \varphi_{source} \tag{5.19}$$

By integrating the differential form over the control volume of a generic node n (i.e. V_n), Equation 5.20 is obtained. Here, T_n and $\Phi_{loss,n}$ are respectively the temperature and thermal loss of the node, while T_b is the temperature of the flow G_b entering/exiting the volume. Make reference to Equation 5.21 for the

calculation of the thermal dispersion (A is the surface area of the b-branch, while T_g is the ground temperature).

$$V_n \frac{\partial(\rho c_p T_n)}{\partial t} + \sum_{b \in B_n} [G_b c_p T_b] = -\Phi_{loss,n} \tag{5.20}$$

$$\Phi_{loss,n} = \sum_{b \in B_n} [A_b U_b] (T_n - T_g) \tag{5.21}$$

In addition, it is important to specify the criterion used for the choice of the T_b temperature in Equation 5.20, which is the temperature of the flow circulating in the b-branch entering/exiting the control volume of node n. The upwind scheme is chosen for this purpose because it allows to obtain a formulation that leads to acceptable computational times for solving the thermal problem. Therefore, in case the flow enters the control volume, T_b will assume the value of the upstream node, while it will be assumed equal to the temperature of node n in case the flow exits the volume. This concept is reported in Equation 5.22 by exploiting the sign convention for the flowrate.

$$T_b = \begin{cases} T_{up\ node} & if\ G_b < 0 \\ T_n & if\ G_b \geq 0 \end{cases} \tag{5.22}$$

The time integration is executed with a discretization approach, the backward Euler method, allowing to obtain the formulation reported in Equation 5.23, written for the generic n-node.

$$V_n \frac{\rho c_p T_n^t - \rho c_p T_n^{t-\Delta t}}{\Delta t} + \sum_{b \in B_n} \left[G_b^t c_p T_b^t \right] = -\sum_{b \in B_n} \left[\frac{l_b}{2} D_b U_b \right] (T_n^t - T_g) \tag{5.23}$$

As already done for the hydraulic problem, Equation 5.23 can be written in matrix form in order to obtain a compact and clear formulation the entire network. The resulting version of the energy balance is reported in Equation 5.24, where the terms multiplying the temperatures are grouped in two different matrices.

$$(M + K) T^t = M T^{t-\Delta t} + f \tag{5.24}$$

Matrix M is called mass matrix, it is diagonal with dimensions [Number of Nodes x Number of Nodes] and its elements are composed as reported in Equation 5.25 including the terms related to the thermal inertia of the network.

$$M_{n,n} = \frac{V_n \rho c_p}{\Delta t} \qquad \forall n \in \{1,..,NN\} \quad (5.25)$$

The K matrix is called stiffness matrix and has dimensions [Number of Nodes x Number of Nodes]. Make reference to Equation 5.26 for its construction.

$$K_{n,m} = \begin{cases} c_p G_{in} & if\ m\ is\ upstream\ node\ of\ n \\ -\sum_{i \in outflows} [c_p G_{out,i}] + \sum_{b \in B_n} \left[\frac{l_b}{2} D_b U_b\right] & if\ m\ =\ n \\ 0 & otherwise \end{cases} \qquad \forall n \in \{1,..,NN\},\ \forall m \in \{1,..,MM\} \quad (5.26)$$

Finally, f is a column vector (dimensions [Number of Nodes x 1]) composed by constant terms, as reported in Equation 5.27.

$$f_n = \sum_{b \in B_n} [A_b]\, T_g \qquad \forall n \in \{1,..,NN\} \quad (5.27)$$

Notice that, since both the supply and return lines are considered in the present work, the matrices mentioned above must be defined for each of them. Once that M, K and f are created, it is necessary to insert the boundary conditions. The temperatures of the injected flowrates are specified and a correction for the extracted flows is introduced to prevent errors in the calculation.
Going more into the detail of the optimization process developed for this study, the steps are the following:

1. matrices M, K and f are defined for the supply line and the temperatures of the injected flows are imposed as boundary conditions. These temperatures are mostly the temperatures at which the hot water is produced by the generators, which are addressed as independent variables and can be

imposed in the boundary conditions. The only exception is represented by the discharge temperature of the thermal storage, which is computed ;

2. the temperatures of the supply line are computed through Equation 5.24;
3. matrices M, K and f are defined for the return line and the temperatures of the injected flows are imposed as boundary conditions. These are the temperatures of the flowrates exiting the thermal users after the heat transfer, and, as already explained, they are computed with Equation 5.7. In case the injected flow comes from the thermal storage, the same consideration done for the supply line is is made for the return line;
4. the temperatures of the return line are computed through Equation 5.24.

Finally, it is worth to mention two practical issues that must be faced to perform the lower-level optimization.

The first one consists in the fact that it is not possible to compute T^t by solving Equation 5.24 with the $\backslash$ operator, since many elements of the $T^{t-\Delta t}$ vector are made of independent variables or their combinations, which are not handled by the backslash operator. To bypass this inconvenience, the T^t temperatures are computed by implementing the strategy based on the LU decomposition by hand. The resulting process is now explained for the generic linear system $Ax = b$. The LU factorization of A provides many outcomes: the upper triangular matrix U, the lower triangular matrix L, the right permutation vector p, the left permutation vector q, and the vector of scaling factors Rs. The relation among these terms is reported in Equation 5.28, where the symbol $\odot$ represents the Hadamard product, which performs a term-by-term multiplication of two matrices.

$$LU = (Rs \odot A)[p,q] \tag{5.28}$$

Then, the right-hand side vector b is permuted with Equation 5.29, and the linear system in Equation 5.30 is solved for z with the forward substitution method.

$$b_{prm} = (Rs \odot b)[P] \tag{5.29}$$

$$Lz = b_{prm} \tag{5.30}$$

Successively, the linear system in Equation 5.31 is solved for y with the backward substitution method, such that x can be obtained with a simple permutation, as showed in Equation 5.32.

$$Uy = z \tag{5.31}$$

$$x = y[q] \tag{5.32}$$

The second issue to face is related to the fact that, according to the methodology used for the DHN simulation and optimization, the temperatures in the T^t vector are computed as a function of $T^{t-\Delta t}$, which is the vector of the temperatures of the previous timestep. In a physical perspective, the temperature of one node is the result of the temperatures of many upstream nodes in many previous timesteps. This means that the elements of the T^t vector are composed as the sum of numerical coefficients and/or a series of independent variables (i.e. the temperatures of the flowrates injected in the supply line). Regarding this series of variables, there are two aspects that can increase its length: one is the dimension of the network, and the other is the amount of timesteps already computed. As a consequence, according to the values reached by these two elements, the temperature of a single node in a single timestep can be defined as the sum of tents or hundreds of independent variables. This constitutes a problem when relatively fine space and/or time discretizations are intended to be used, since the definition and computation of the vectors for the temperatures of the supply and return lines require a non-negligible amount of computational time and computer memory, up to compromising the convergence of the optimization process.
To overcome this issue, a simple but effective strategy was adopted. As already discussed, the temperature vector T^t is computed from vector $T^{t-\Delta t}$, whose elements are composed by a series of independent variables (in particular, the injection temperatures of the supply line) multiplied by numerical coefficients. To reduce the computation related to the handling of these elements, the terms of the series providing a negligible contribution to the total value are identified and discarded before performing the calculations for solving the thermal problem. In this way, the amount of terms constituting the elements of the temperature vectors is kept at an adequate level and the the computations involving these elements (and, in general, the temperature vector $T^{t-\Delta t}$) do

not represents a problem for the optimization process. The criterion used for removing the negligible terms consists in excluding the elements constituted by an independent variable multiplied by a low coefficient.
After having performed some trials and having observed the effects of this truncation on the accuracy of the DHN simulation, a threshold of 10^{-5} is set for identifying the coefficients with a small value.

5.3 Optimization overview

Once that the modelling of the main elements constituting the MES is presented, the methodology developed for the operation optimization can now be discussed in greater detail than before. The best way to fully understand the optimization method is to follow the complete execution of single iteration of the recursive process. This procedure is reported in Figure 5.7 in form of flow chart.
Starting from the input data and the set of variables constituting a single element of the heuristic solver's population, the injected/extracted mass flowrates of the users and producers (G_{ext}) are computed. With these terms and the incidence matrix A, the flows circulating in all the branches of the supply and return line of the DHN are computed. Once that the fluid dynamic problem is solved, it is necessary to check the satisfaction of the constraints related to the flowrates. In case some of them are not fulfilled, a penalty value is assigned to the objective function associated to the current set of variables of the master problem, and the process is restarted by taking a new element. The reason why the process is terminated in case of infeasibility is to prevent the execution of the slave problem, which would be an useless effort since it would solve a problem related to a configuration that is already known to be incorrect.
Otherwise, if the MP constraints are respected, the independent variables of the slave problem can be defined and the remaining part of the problem can be addressed. Starting form the first step of the time discretization, the nodal temperatures of the supply line of the DHN are computed from the initial condition and the parameters corresponding to the timestep considered (i.e. the mass flowrates and the temperatures of the injected streams). Since the thermal power absorbed by the consumers depends on the extracted flowrate and the supply temperature, the heat consumption of the users and the temperatures of injection in the return line can be computed.

The temperatures of the return line are obtained as has already been carried out for the supply line, using the users' injection temperatures as boundary conditions. Once the thermal problem of the DHN is completely addressed, the electrical and thermal powers of the generators are computed. These steps are repeated until the last element of the time discretization is reached. Notice that the DHN nodal temperatures and the generators' powers obtained from these steps are functions of the SP independent variables and, despite it was used the term "computed", their value remains unknown. Once that the SP constraints are addressed, the optimization can be executed. If the SP results to be unfeasible, a new optimization run is performed, where the possibility to violate some constraints is admitted at the price of including a penalty on the objective function.

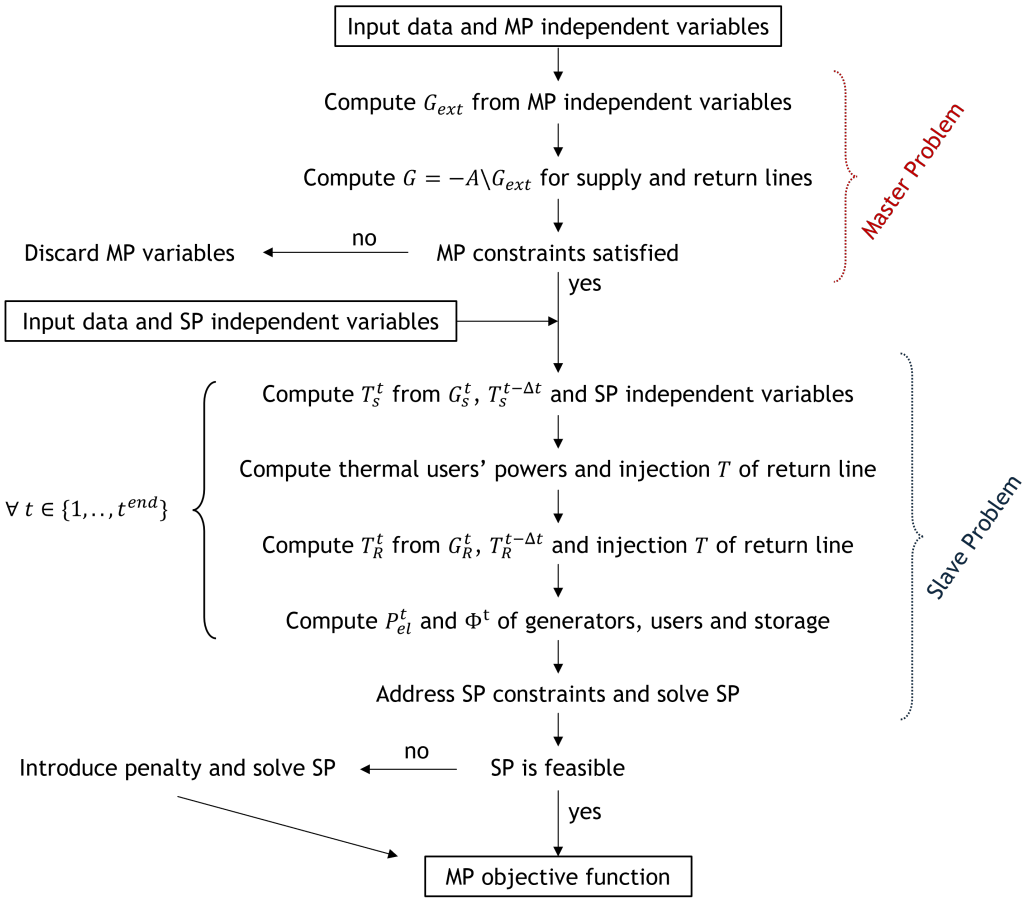

Fig. 5.7 Flow chart for computing the value of the objective function of the Master Problem

Concerning the more practical aspects of the optimization, the entire code for the execution of the process is written in the Julia language. The Particle Swarm

Optimization is the heuristic method used to optimize the master problem. For this purpose, the PSO of the Julia package Metaheristics.jl [362] is used. It has been necessary to make a non-trivial structural addition to this package for allowing to execute the optimization in parallel processes, which was not supported by default. On the other hand, the MILP addressed in the SP is solved by Gurobi [363].
The number of variables and constraints addressed on the two optimization levels are reported in Table 5.2. As already mentioned, the process for addressing the SP optimization is computationally intensive. However, the size of this problem is not challenging for MILP solvers like Gurobi. On the other hand, the MP dimensions are quite demanding for most of the heuristic solvers. Consequently, it is important to facilitate as much as possible the PSO convergence, for example, by trying to provide a "good" initial population.

Table 5.2 Data on problem dimensions

	Variables	Constraints	Population
MP	197	3636	104
SP	1028	8984	-

5.4 Results and discussion

The present section is devoted to report and discuss the results obtained from the optimization of the case study.

The most effective and synthetic way to analyse the convergence of the process is to observe the evolution of the objective function across the PSO iterations, which is showed in Figure 5.8. A maximum number of iterations (500) was set as stopping criterion and it was reached in slightly less than 4 hours (3 hours and 52 minutes). However, a stable solution was actually found after 250 iterations, which corresponds to a computational time of 1 hour and 40 minutes. These times can be recognized to be higher compared to the average computational efforts presented in the studies in the scientific literature, which tends to reach few tens of minutes. However, two very important aspects must be considered: first, the works in the literature do not include the DHN simulation and optimization or, if they do, the DHN is typically included with less detail and a lower capability to address technical constraints in

the operation; second, most of the already developed methodologies rely completely on deterministic methods, which are faster in solving big problems but do not allow to address some kind of complexities.

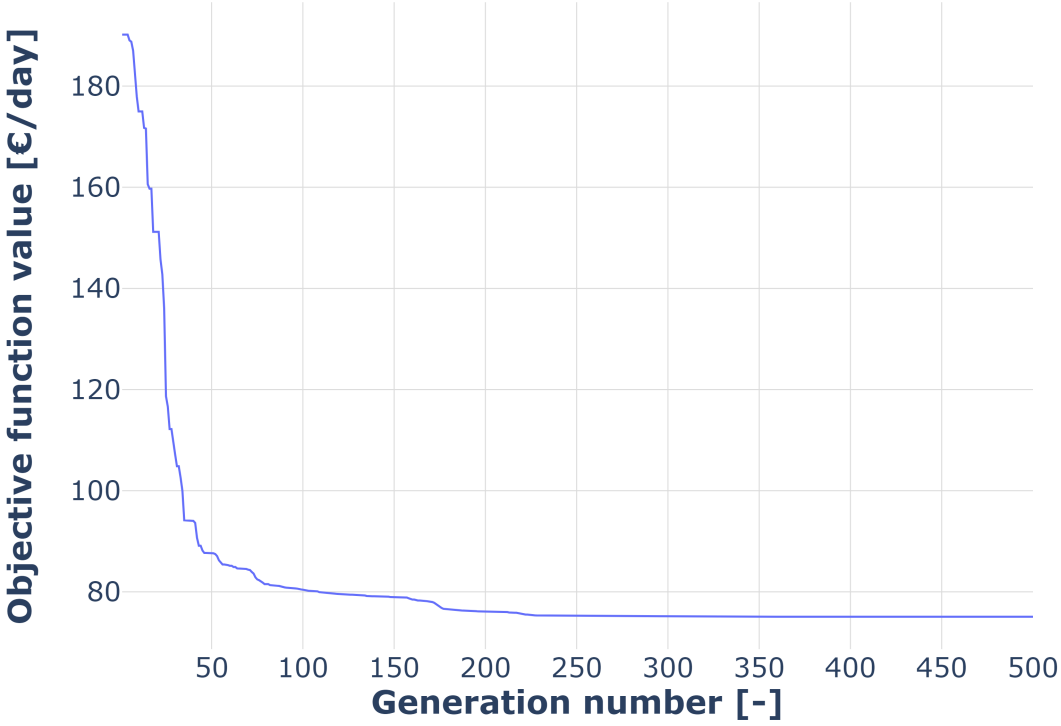

Fig. 5.8 Convergence chart of the optimization process

The operation of the electrical components is reported in Figure 5.9 in form of stacked area chart, where the powers produced have positive sign and vice versa for the powers absorbed. As can be noticed, in the first hours of the day the electrical load is covered by buying the electricity from the external grid. Successively, the two cogenerators are activated, providing much more electricity than the one requested by the load, which will be sold to the grid. In particular, $CHP2$ presents a more continuous operation, while $CHP1$ is switched on and off for three times. To comment comprehensively the operation of the CHPs it is necessary to observe the thermal production profiles, since their functioning is driven by the heating power provided to the DHN. The operation of the electrical storage is not particularly interesting since the MP converges to a configuration in which the storage is charged and discharged in two adjacent timesteps. This behaviour has the aim of minimizing the losses occurring during the storage time and taking advantage of the differences

in the price of electricity being sold. Notice that, since the electrical balance is addressed as stationary, the profile built by the stacked areas of the producers is symmetrical to the one of the consumers.

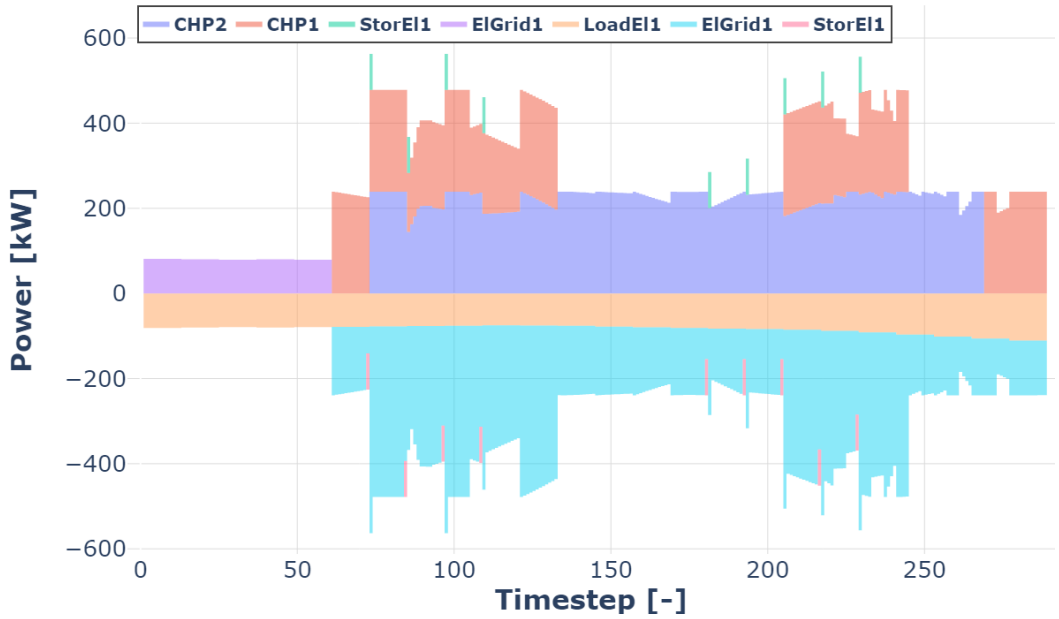

Fig. 5.9 Electrical powers of generators, load and storage

On the other hand, the thermal power exchanged among the producers, users, and storage are presented in Figure 5.10. Since the early hours of the day do not have any thermal demand, all the thermal generators are off. Then, the storage vessel is filled with hot water by $CHP1$ until $CHP2$ is turned on, which happens when the users start to extract water from the supply line. At this point, the storage is partially discharged and $Boiler2$ is activated for a short period to compensate the high thermal demand and mass flow extraction.

A single CHP is not able to provide the heating power required by the consumers, especially when the residential and commercial users are simultaneously extracting water from the DHN. As a consequence, when the two CHPs are operating, the storage is charged such that it can provide an additional thermal power when only one cogenerator is operating.

It is interesting to notice that, despite no user is extracting water in the last hours of the time period analysed, $CHP1$ is still operating and it charges the storage. This behaviour appears as counter intuitive since there are no needs to fill the tank with an amount of thermal energy that will not be exploited, and it could seem reasonable to

leave it empty. However, since for the case of CHPs the electricity production is joint to the heating production, the final filling of the thermal storage allows to produce an amount of electricity that can be sell to the grid, providing an economic advantage. As concern the thermal demand, differently from what observed for the electrical powers, the profile created by the sum of the thermal powers produced is not perfectly symmetrical compared to the one obtained from the sum of the absorbed ones. This is due to the fact that the energy balance is compensated by the thermal inertia of the DHN, which can act as a storage that absorbs and provides heat according to the operating conditions.

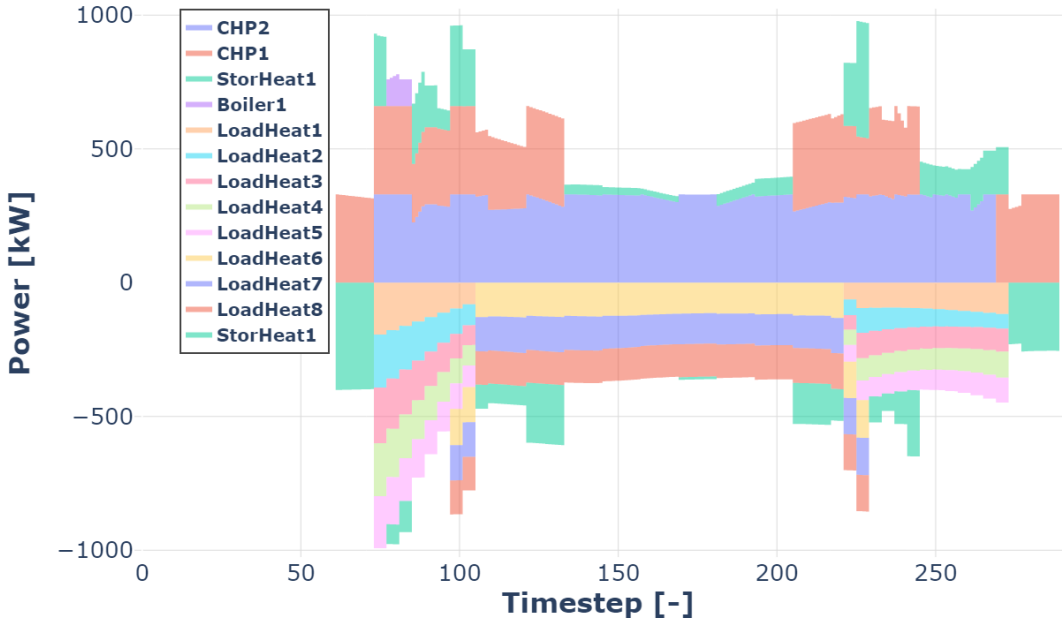

Fig. 5.10 Thermal powers of generators, load and storage

One of the most important parameters defining the thermal users is the mass flow extracted from the supply line of the DHN. The water streams required by the eight consumers are reported in Figure 5.11. These flows are obtained from the operation optimization process and their shape is a discretization of the polynomial presented in Equation 5.9. The extraction is the highest at the beginning of the day, when the range imposed for the thermal requirement of the residential users is the highest, simulating the need for heating the houses that were not heated during the night. A similar behaviour is observed in the final part of the day, when the same users start newly to extract water from the DHN.

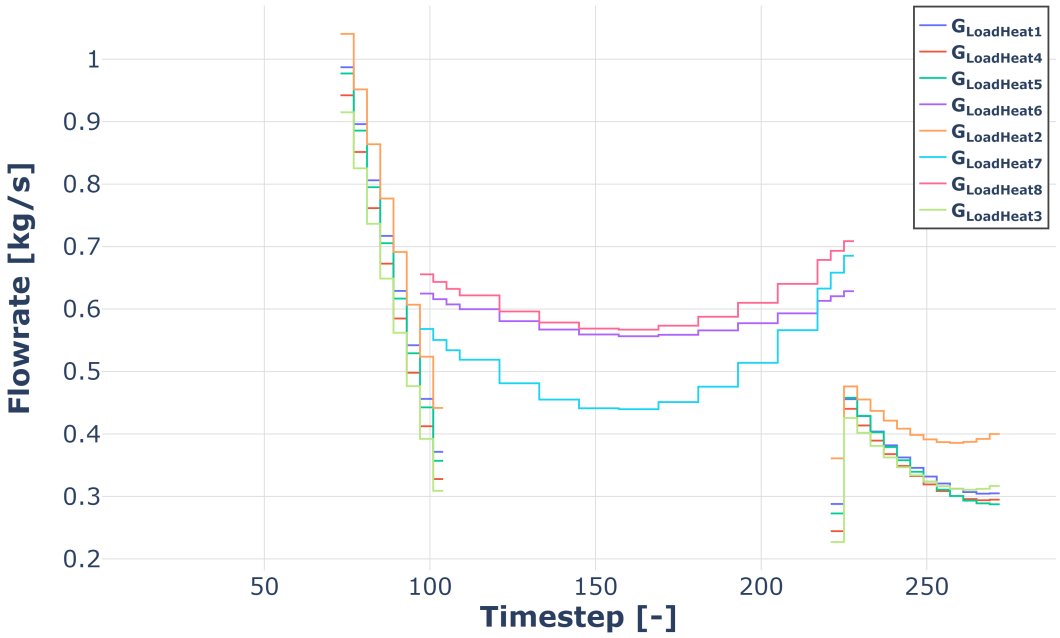

Fig. 5.11 Mass flowrates extracted by the thermal users

Another result that is worth to be observed is the thermal storage operation found by the optimization, which is showed in Figure 5.12. The termeratures and the masses of the two portions of water are reported for the day under consideration. The vessel is assumed to be full of "cold" water (i.e. at $50°C$) in the first timestep, it is fully charged four times and two times only partially, while two full discharges and two partial discharges are performed. The temperature of the hot water mass is in the range $100°C$ - $110°C$, while the cold water is in the interval between $50°C$ and $60°C$.

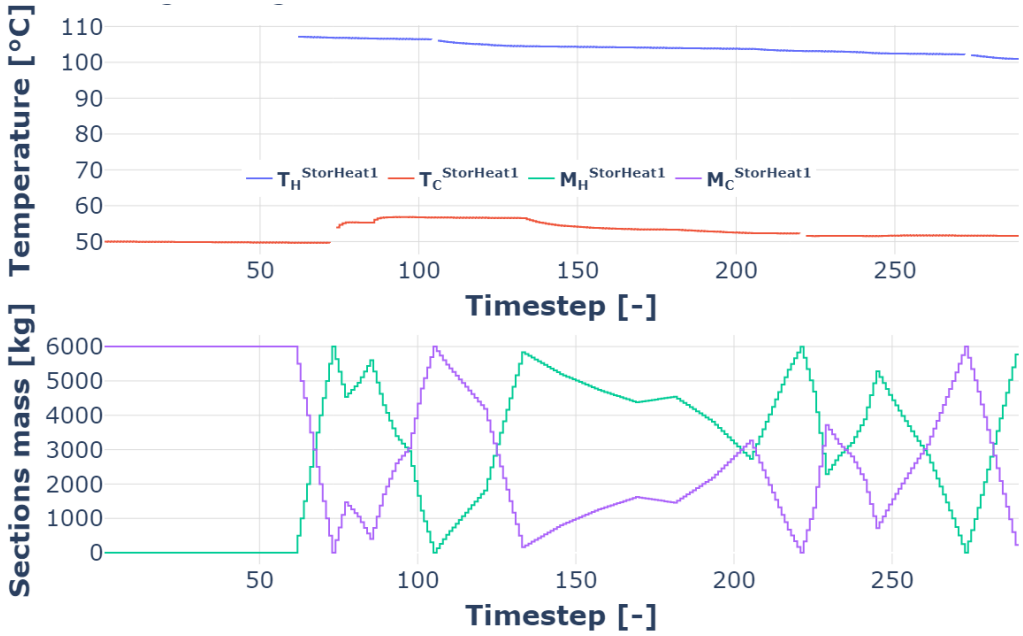

Fig. 5.12 Thermal storage operation: temperature profiles (up) and water masses stored (down)

Another aspect that is important to be discussed regards the result obtained in terms of objective function. The process converges to a solution with an OF value equal to $75.06\frac{€}{day}$, which is computed as the sum between the real operation cost and the penalty for not meeting all the constraints addressed in the slave problem. By executing the simulation of the solution obtained, the operation cost results to be $72\frac{€}{day}$, which means that the penalty value is not null. However, the constraints that are not met are verified to be only slightly violated, and these are the ones for the minimum and maximum thermal requirement of the users. This means that the solution is completely feasible in a physical perspective, but its implementation in a real case study would not meet the users' expectations, even if the variation is negligible. The constraints' violation is observed for $User6$, $User7$ and $User8$ and it affects only the first timesteps in which the users start to extract the water from the supply line. The thermal profile of $User6$ and its corresponding boundaries are reported in Figure 5.13 to provide an example of this mismatch and to demonstrate their small size.

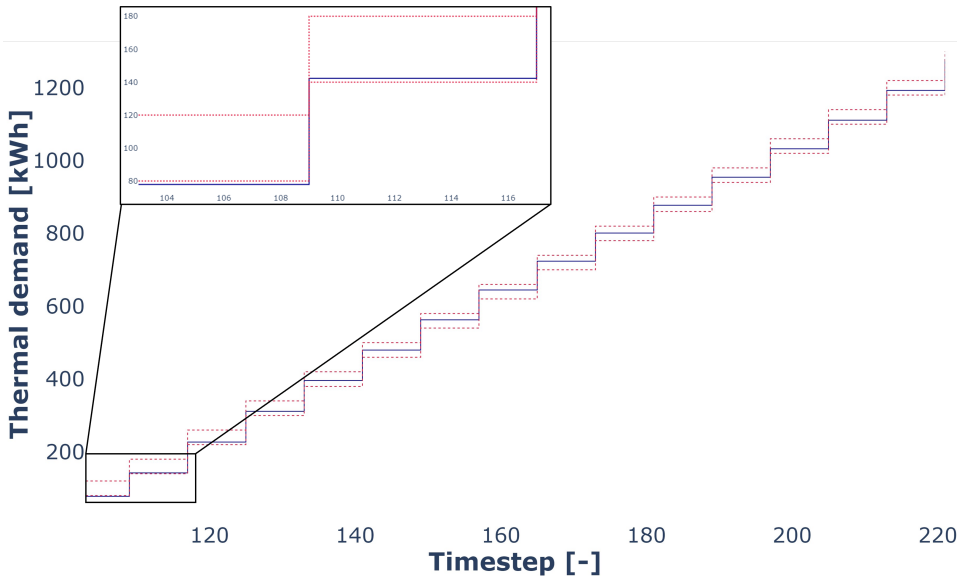

Fig. 5.13 Profile of the thermal demand of User 6

The flawed satisfaction of the constraints is due to three reasons: first, the slave problem is actually infeasible; second, the solution obtained is not the global optimum for the master problem; third, the solution is the MP's global optimum despite not being the SP's global optimum. In the first case, a penalty value equal to zero cannot be reached since the SP's constraints cannot be fully met. In the second case, the process does not converge to the global optimum (which would have a null penalty value) because it reaches the stopping criterion, which could be modified to prevent this unwanted behaviour. In the last case, the solution results to be the global optimum even if the penalty value is not null, which may happen when the full satisfaction of the constraints determines a worsening of the operation cost that is higher than the penalty occurring in case of constraints not met. This issue can be simply overcome by increasing the weight of the penalty on the MP's objective function.

5.5 Limitations and future improvements

The behaviour described in the previous paragraph could constitute an issue for the convergence quality but it must be recognised that it is caused by the particular choice of including a penalty factor in the objective function. This means that it

could be avoided by improving or changing the approach for the inclusion of the possible non-satisfactions of the SP constraints.
A different type of limitation is intrinsically represented by the capability of the heuristic algorithm to reach the convergence, which cannot be guaranteed for each optimization run. In fact, considering the size of the problem, the possibility of reaching a local minimum of poor quality and the need to repeat the optimisation run several times must be taken into account. Otherwise, some strategies to prevent or mitigate this phenomenon can be considered. Among them, the more effective aim to reduce the size of the problem or to relax some constraints of the master problem.

Chapter 6

Conclusions

This last chapter is devoted to discuss the conclusions that can be made in light of the research work presented in this thesis. The main findings and contributions are highlighted in section 6.1, while some suggestions for possible developments of the analysis performed are reported in section 6.2.

6.1 Research contributions

The objective of the research presented in the preceding chapters is to identify and develop methodologies for the optimisation of energy-related problems.

The discussion started from the energy technologies and/or plants, where a single process is involved for the transformation of energy sources into energy products. A central tower CSP plant with an innovative thermochemical storage based on Calcium-Looping was considered as case study. This allowed to develop an optimization model that included all the most important features that can characterize these problems: non-convexities; implicit objective functions; presence of heat transfer processes; synthesis, design and operation scope. The methodology developed for this purpose is based on a meta-heuristic solver, within which a bisection method and the pinch analysis are nested. The CSP-CaL plant was investigated with different kinds of configurations and integration, and the results obtained are compared among them.
The direct integration and the indirect integration of a He Brayton cycle resulted to be the most interesting options in terms of energy efficiency, economic cost and

layout complexity. These aspects were simultaneously investigated by performing a multi-objective optimization, which can be implemented without making any change to model for the single-objective optimization, which is another advantage of the strategy developed.
Although being developed for a well-defined case study, the strategy presented in the first part of this thesis is not tied to the CSP-CaL plant. In fact, this methodology is able to deal with the presence of many sources of complexity, such that most of the technologies in the energy field can be simulated and optimized. For example, the proposed model is able to deal with problems whose simulation includes nonlinear and non-convex terms. This is possible thanks to the use of the Genetic Algorithm, which can manage implicit mathematical formulations as well since it belongs to the category of black-box solvers. At the same time, the extent of the analysis that can be performed is very wide, being able to simultaneously optimize the synthesis, design and operation problems. Finally, the model is structured such that almost any kind of energy process can be addressed (e.g. thermal cycles, industrial processes, energy infrastructures), since it can handle the combination of thermodynamic transformations, heat transfer processes and power generation.

The research continued with the investigation of a methodology capable of optimising an entire Multi Energy System, which can be composed of different energy plants and use multiple energy sources to produce multiple energy vectors. As first step, a detailed literature review was performed in order to have an overview as wide as possible of the existing strategies for the optimization of MESs. This research brought to the publication of a review paper on an international journal. In this area of research, it has been recognised that the simulation of individual plants is carried out with a simplified approach, compared to the strategy developed in the previous analysis. This is a necessary simplification, as the complexity of MES is considerable and a detailed simulation of all the processes that take place in all the energy installations that make up the system is not possible. Considerable efforts are made to linearize the non-linear terms characterizing the physical phenomena ruling the MES operation and the functions for the costs computation. In this way, the high dimensions problems can be solved with efficient MILP solvers. Many research gaps were identified: a) lack of validation studies; b) development of suitable control systems; c) integration of energy transport infrastructures and flexibility sources in MESs operation optimization. In light of the state of the art identified from the literature review, a first attempt to include a heat transport network in the MES

operation optimization was made.
At first, the internal thermal network of a MES was considered (no thermal losses and inertia are assumed) in which the temperatures and flowrates of the network are included in the operation optimization. A thermal storage was included in the case study and simulated with an essential approach. The most important source of complexity is represented by the equations for the energy balance on the nodes of the network, which present bilinear terms (i.e. multiplications between mass flowrates and temperatures). An iterative approach was developed, based on the decomposition of the original problem into two optimizations in series (one MILP and one QCP). The resulting process allows to obtain high-quality near-optimal solutions in relatively short computational times.
With the experience gained from this first research, another strategy was developed for the operation optimization of a case study with a wider scope. In this case a small size DHN was assumed for the heat transportation and the previous simplifying hypotheses were removed. A heating storage was included among the components of the MES and the thermal users' demand was defined by broad boundaries, allowing to include a demand response program to increase the system flexibility. The mathematical formulation for the simulation of this system resulted to be particularly complex (high dimensional non-convex MIQCP). It was decomposed with a master-slave approach, resulting in a MILP nested into a PSO. The level of detail reached in the simulation of the components' operation is noticeable, as the operating states, the load levels, the mass flowrates and the temperatures are only some of the parameters whose value is optimized. The price for the higher optimization quality reached with this second work is a worsening of the computational times and the convergence.
In conclusion, these methodologies, based on similar but different case studies, were developed as an attempt to provide a strategy for solving the MES operation problem in a comprehensive perspective, i.e. including the heat transport network. The finite volume method is the most commonly used method to simulate the thermal network (or DHN) and was adopted in the joint optimization of the MES and the network. In this case, it was necessary to develop suitable expedients to deal with the size of the problems and the nature of its mathematical formulation. At the same time, it was avoided to introduce excessive simplifications in order to follow as much as possible the initial intention of performing a detailed and realistic analysis. As a result, the complexity of the problems does not allow to address the entire optimizations with deterministic methods, which would have been more advantageous in terms of

convergence and computational times. However, the drawbacks due to the use of a non-purely deterministic methodology are compensated by the capability to include a noticeable variety of features and constraints on the MES operation.

6.2 Suggestions for future developments

The strategies developed to optimize energy plants and multi energy systems were presented in the preceding sections, along with their pros and cons. To further increase the quality and effectiveness of the models presented, some developements or changes can be considered to be implemented in the future. The proposed enhancements are tailored to ensure global optimality, computational efficiency, scalability to large-scale systems, validation through pilot plants or real systems, integration of control systems for operational implementation, and inclusion of prosumers.

Global optimality and computational times

To advance the optimization's robustness, exploring alternative algorithms could result to be very useful. Metaheuristic, deterministic and hybrid optimization methods are the three main families and each of them contains a considerable number of algorithms. It is not possible to identify a priori the most suitable solver to execute an optimization problem because of the complexity of the aspects that must be considered and the counter-intuitive effects that they can determine. Consequently, it is reasonable to assume that there may exist algorithms capable of solving the problems addressed in this thesis in a more efficient way, and the only way to identify them is to observe their performance when executing the optimisation problems.

Testing the models' scalability

The scalability of an optimization model is fundamental for its applicability in real-case studies, particularly in the context of large-scale systems characterized by demanding processes for their simulation. Rigorous testing on datasets representative of industrial-scale operations are indispensable to determine the model's efficacy across different sizes and contexts. The same purpose can be referred to ensure the suitability of the models to optimize case studies in which the high dimensions are not determined by the physical size but by the operation period considered and/or the level of refinement of the time discretization.

Validation of results

Validating the optimization results through pilot plants or real systems serves as a proof of the model's real-world applicability and fidelity. Developing prototypes, collaborating with industry partners to conduct field trials, and deploying the optimized strategies in operational settings are some options to achieve an empirical validation and fine-tuning of the model parameters. At the same time, facing to real contexts can be an opportunity to receive feedback from domain experts to further refine and enhance the optimization models.

Control systems integration

In real case studies, the operation of energy plants and multi energy system is managed by control systems, which are based on control strategies that are usually composed by logical propositions, setpoint values, cause-effect sequences, etc. Adopting a schedule based on the result of an optimization process would require to change (at least in part) the system used for setting the components' operation. Translating the optimized operational strategies into actionable directives necessitates to integrate the plant/MES control system within the manufacturing environment. Connecting the optimization model with supervisory controls, data acquisition systems, programmable logic controllers, and distributed control systems would enable real-time implementation of the optimized configurations, as well as feedback about the current state of the system to the model. This integration would facilitates dynamic adjustment of operational parameters based on fluctuating demand patterns, resource availability, and external environmental factors, thereby enhancing operational flexibility and responsiveness.

Prosumers inclusion in MES optimization

Considering the evolving landscape of energy consumption and production, including prosumers (i.e. entities that both consume and produce energy) into the MES optimization framework represents an addition that is worth to be made. In this case, suitable strategies to differentiate the production and consumption phases should be developed and addressed in the optimization, which could increase the problem's complexity. This addition could bring noticeable benefits in terms of energy savings, costs reduction and mitigation of environmental impact, as well as increasing the flexibility and robustness of the system.

References

[1] United Nations. *World population prospects 2022: Summary of results*. UN, 2022.

[2] IEA, IRENA, UNSD, World Bank, and WHO. Tracking sdg 7: The energy progress report. Technical report, World Bank, 2023.

[3] British Petroleum (BP). Statistical review of world energy 2021, 2021.

[4] Valérie Masson-Delmotte, Panmao Zhai, Anna Pirani, Sarah L Connors, Clotilde Péan, Sophie Berger, Nada Caud, Y Chen, L Goldfarb, MI Gomis, et al. Climate change 2021: the physical science basis. *Contribution of working group I to the sixth assessment report of the intergovernmental panel on climate change*, 2, 2021.

[5] John Barrett, Steve Pye, Sam Betts-Davies, Oliver Broad, James Price, Nick Eyre, Jillian Anable, Christian Brand, George Bennett, Rachel Carr-Whitworth, et al. Energy demand reduction options for meeting national zero-emission targets in the united kingdom. *Nature Energy*, 7(8):726–735, 2022.

[6] COP28, IRENA, and GRA. Tripling renewable power and doubling energy efficiency by 2030: Crucial steps towards 1.5°c. Technical report, International Renewable Energy Agency, 2023.

[7] IEA. Energy technology perspectives 2023. Technical report, IEA, 2023.

[8] IRENA. World energy transitions outlook 2023: 1.5° c pathway, 2023.

[9] IEA. Government energy spending tracker, 2023. https://www.iea.org/reports/government-energy-spending-tracker-2 [Accessed: November 2023].

[10] J.R.R.A. Martins and A. Ning. *Engineering Design Optimization*. Cambridge University Press, 2021.

[11] B.G. Liptak. *Optimization of Unit Operations*. CRC Press, 2021.

[12] Kalyanmoy Deb. *Optimization for engineering design: Algorithms and examples*. PHI Learning Pvt. Ltd., 2012.

[13] Marco Astolfi, Emanuele Martelli, and L Pierobon. Thermodynamic and technoeconomic optimization of organic rankine cycle systems. In *Organic Rankine cycle (ORC) power systems*, pages 173–249. Elsevier, 2017.

[14] Hang Zhao, Qinghua Deng, Wenting Huang, Dian Wang, and Zhenping Feng. Thermodynamic and economic analysis and multi-objective optimization of supercritical co2 brayton cycles. *Journal of Engineering for Gas Turbines and Power*, 138(8):081602, 2016.

[15] Shichang Yun, Dalin Zhang, Xinyu Li, Xingguang Zhou, Dianqiang Jiang, Xindi Lv, Wenqiang Wu, Zhenyu Feng, Xin Min, Wenxi Tian, et al. Design, optimization and thermodynamic analysis of sco2 brayton cycle system for fhr. *Progress in Nuclear Energy*, 157:104593, 2023.

[16] Jinxing Zhao, Min Xu, Mian Li, Bin Wang, and Shuangzhai Liu. Design and optimization of an atkinson cycle engine with the artificial neural network method. *Applied energy*, 92:492–502, 2012.

[17] Gürcan Çetin and Ali Keçebaş. Optimization of thermodynamic performance with simulated annealing algorithm: A geothermal power plant. *Renewable Energy*, 172:968–982, 2021.

[18] Hamid Saffari, Sadegh Sadeghi, Mohsen Khoshzat, and Pooyan Mehregan. Thermodynamic analysis and optimization of a geothermal kalina cycle system using artificial bee colony algorithm. *Renewable Energy*, 89:154–167, 2016.

[19] Omar A Al-Shahri, Firas B Ismail, MA Hannan, MS Hossain Lipu, Ali Q Al-Shetwi, RA Begum, Nizar FO Al-Muhsen, and Ebrahim Soujeri. Solar photovoltaic energy optimization methods, challenges and issues: A comprehensive review. *Journal of Cleaner Production*, 284:125465, 2021.

[20] Christopher N Elkinton, James F Manwell, and Jon G McGowan. Algorithms for offshore wind farm layout optimization. *Wind Engineering*, 32(1):67–84, 2008.

[21] Abdus Samad Azad, Md Shokor A Rahaman, Junzo Watada, Pandian Vasant, and Jose Antonio Gamez Vintaned. Optimization of the hydropower energy generation using meta-heuristic approaches: A review. *Energy Reports*, 6:2230–2248, 2020.

[22] Aala Kalananda Vamsi Krishna Reddy and Komanapalli Venkata Lakshmi Narayana. Meta-heuristics optimization in electric vehicles-an extensive review. *Renewable and Sustainable Energy Reviews*, 160:112285, 2022.

[23] S Donovan. Wind farm optimization. In *Proceedings of the 40th annual ORSNZ conference*, pages 196–205. Citeseer, 2005.

[24] Ian C Kemp. *Pinch analysis and process integration: a user guide on process integration for the efficient use of energy*. Elsevier, 2011.

[25] Lorin L Vant-Hull. Central tower concentrating solar power (csp) systems. In *Concentrating solar power technology*, pages 240–283. Elsevier, 2012.

[26] Marc T. Dunham and Brian D. Iverson. High-efficiency thermodynamic power cycles for concentrated solar power systems. *Renewable and Sustainable Energy Reviews*, 30:758–770, 2014.

[27] Paul Gauché, Stefan Pfenninger, Adriaan J Meyer, Theodor W von Backström, and Alan C Brent. Modeling dispatchability potential of csp in south africa. In *Southern African Solar Energy Conference (SASEC)*, volume 1, pages 1–11, 2012.

[28] Ugo Pelay, Lingai Luo, Yilin Fan, Driss Stitou, and Mark Rood. Thermal energy storage systems for concentrated solar power plants. *Renewable and Sustainable Energy Reviews*, 79(March 2016):82–100, 2017.

[29] Ihsan Barin and Gregor Platzki. *Thermochemical data of pure substances*, volume 304. Wiley Online Library, 1989.

[30] J Blamey, EJ Anthony, Jinsheng Wang, and PS Fennell. The calcium looping cycle for large-scale co2 capture. *Progress in Energy and Combustion Science*, 36(2):260–279, 2010.

[31] C Ortiz, JM Valverde, Ricardo Chacartegui, Luis A Perez-Maqueda, and P Giménez. The calcium-looping (caco3/cao) process for thermochemical energy storage in concentrating solar power plants. *Renewable and Sustainable Energy Reviews*, 113:109252, 2019.

[32] Xiaoyi Chen, Xiaogang Jin, Xiang Ling, and Yan Wang. Exergy analysis of concentrated solar power plants with thermochemical energy storage based on calcium looping. *ACS Sustainable Chemistry & Engineering*, 8(21):7928–7941, 2020.

[33] WH Stein and Reiner Buck. Advanced power cycles for concentrated solar power. *Solar Energy*, 152:91–105, 2017.

[34] Xiaoyi Chen, Dong Zhang, Yan Wang, Xiang Ling, and Xiaogang Jin. The role of sensible heat in a concentrated solar power plant with thermochemical energy storage. *Energy Conversion and Management*, 190:42–53, 2019.

[35] Antonio Perejón, Luis M Romeo, Yolanda Lara, Pilar Lisbona, Ana Martínez, and Jose Manuel Valverde. The calcium-looping technology for co2 capture: On the important roles of energy integration and sorbent behavior. *Applied Energy*, 162:787–807, 2016.

[36] Jose Manuel Valverde. A model on the cao multicyclic conversion in the ca-looping process. *Chemical Engineering Journal*, 228:1195–1206, 2013.

[37] Jonatan D Durán-Martín, Pedro E Sánchez Jimenez, José M Valverde, Antonio Perejón, Juan Arcenegui-Troya, Pablo García Triñanes, and Luis A Pérez Maqueda. Role of particle size on the multicycle calcium looping activity of limestone for thermochemical energy storage. *Journal of Advanced Research*, 22:67–76, 2020.

[38] Nuria Rodríguez, Mónica Alonso, and JC Abanades. Average activity of cao particles in a calcium looping system. *Chemical Engineering Journal*, 156(2):388–394, 2010.

[39] Monica Benitez-Guerrero, Beatriz Sarrion, Antonio Perejon, Pedro E Sanchez-Jimenez, Luis A Perez-Maqueda, and Jose Manuel Valverde. Large-scale high-temperature solar energy storage using natural minerals. *Solar Energy Materials and Solar Cells*, 168:14–21, 2017.

[40] Jose Manuel Valverde and Santiago Medina. Crystallographic transformation of limestone during calcination under co 2. *Physical Chemistry Chemical Physics*, 17(34):21912–21926, 2015.

[41] EE Berger. Effect of steam on the decomposition of limestone1, 1. *Industrial & Engineering Chemistry*, 19(5):594–596, 1927.

[42] Jose Manuel Valverde and Santiago Medina. Reduction of calcination temperature in the calcium looping process for co2 capture by using helium: in situ xrd analysis. *ACS Sustainable Chemistry & Engineering*, 4(12):7090–7097, 2016.

[43] C Ortiz, JM Valverde, R Chacartegui, and Luis A Perez-Maqueda. Carbonation of limestone derived cao for thermochemical energy storage: from kinetics to process integration in concentrating solar plants. *ACS Sustainable Chemistry & Engineering*, 6(5):6404–6417, 2018.

[44] C Ortiz, R Chacartegui, JM Valverde, A Alovisio, and JA Becerra. Power cycles integration in concentrated solar power plants with energy storage based on calcium looping. *Energy Conversion and Management*, 149:815–829, 2017.

[45] Ming Zhao, Andrew I Minett, and Andrew T Harris. A review of techno-economic models for the retrofitting of conventional pulverised-coal power plants for post-combustion capture (pcc) of co 2. *Energy & Environmental Science*, 6(1):25–40, 2013.

[46] Ricardo Chacartegui, A Alovisio, C Ortiz, JM Valverde, V Verda, and JA Becerra. Thermochemical energy storage of concentrated solar power by integration of the calcium looping process and a co2 power cycle. *Applied energy*, 173:589–605, 2016.

[47] A Alovisio, Ricardo Chacartegui, C Ortiz, JM Valverde, and V Verda. Optimizing the csp-calcium looping integration for thermochemical energy storage. *Energy Conversion and Management*, 136:85–98, 2017.

[48] C Ortiz, MC Romano, JM Valverde, M Binotti, and R Chacartegui. Process integration of calcium-looping thermochemical energy storage system in concentrating solar power plants. *Energy*, 155:535–551, 2018.

[49] Reyes Fernández, C Ortiz, Ricardo Chacartegui, JM Valverde, and JA Becerra. Dispatchability of solar photovoltaics from thermochemical energy storage. *Energy Conversion and Management*, 191:237–246, 2019.

[50] Susan EB Edwards and Vlatko Materić. Calcium looping in solar power generation plants. *Solar Energy*, 86(9):2494–2503, 2012.

[51] Evgenios Karasavvas, Kyriakos D Panopoulos, Simira Papadopoulou, and Spyros Voutetakis. Design of an integrated csp-calcium looping for uninterrupted power production through energy storage. *Chemical Engineering Transactions*, 70:2131–2136, 2018.

[52] Ian H. Bell, Jorrit Wronski, Sylvain Quoilin, and Vincent Lemort. Pure and pseudo-pure fluid thermophysical property evaluation and the open-source thermophysical property library coolprop. *Industrial & Engineering Chemistry Research*, 53(6):2498–2508, 2014.

[53] Malcolm W Chase and National Information Standards Organization (US). *NIST-JANAF thermochemical tables*, volume 9. American Chemical Society Washington, DC, 1998.

[54] Kenwalt. Syscad: Plant simulation software, 2023. https://www.syscad.net/ [Accessed: 2019].

[55] Banca d'Italia. Tassi di cambio medi, 2023. https://tassidicambio.bancaditalia.it/terzevalute-wf-ui-web/averageRates [Accessed: 2023].

[56] Sebastian Michalski, Dawid P Hanak, and Vasilije Manovic. Techno-economic feasibility assessment of calcium looping combustion using commercial technology appraisal tools. *Journal of Cleaner Production*, 219:540–551, 2019.

[57] Edoardo De Lena, Maurizio Spinelli, Manuele Gatti, Roberto Scaccabarozzi, Stefano Campanari, Stefano Consonni, Giovanni Cinti, and Matteo C Romano. Techno-economic analysis of calcium looping processes for low co2 emission cement plants. *International Journal of Greenhouse Gas Control*, 82:244–260, 2019.

[58] Kevin J Albrecht and Clifford K Ho. Design and operating considerations for a shell-and-plate, moving packed-bed, particle-to-sco2 heat exchanger. *Solar Energy*, 178:331–340, 2019.

[59] M Le. *Tackling challenges in solar: 2014 portfolio*. U.S. Department of Energy, 2014.

[60] Pouria Ahmadi. *Modeling, analysis and optimization of integrated energy systems for multigeneration purposes*. PhD thesis, Ontario Tech University, 2013.

[61] Navid Nazari, Parisa Heidarnejad, and Soheil Porkhial. Multi-objective optimization of a combined steam-organic rankine cycle based on exergy and exergo-economic analysis for waste heat recovery application. *Energy conversion and management*, 127:366–379, 2016.

[62] Alicia Bayon, Roman Bader, Mehdi Jafarian, Larissa Fedunik-Hofman, Yanping Sun, Jim Hinkley, Sarah Miller, and Wojciech Lipiński. Techno-economic assessment of solid–gas thermochemical energy storage systems for solar thermal power applications. *Energy*, 149:473–484, 2018.

[63] M Jonemann. Advanced thermal storage system with novel molten salt, national renewable energy laboratory (nrel) report, 2012.

[64] Gkiokchan Moumin, Maximilian Ryssel, Li Zhao, Peter Markewitz, Christian Sattler, Martin Robinius, and Detlef Stolten. Co2 emission reduction in the cement industry by using a solar calciner. *Renewable energy*, 145:1578–1596, 2020.

[65] Clifford K Ho. A new generation of solid particle and other high-performance receiver designs for concentrating solar thermal (cst) central tower systems. *Advances in Concentrating Solar Thermal Research and Technology*, pages 107–128, 2017.

[66] Karani Kurtulus, Ahmet Coskun, Shadan Ameen, Ceyhun Yilmaz, and Ali Bolatturk. Thermoeconomic analysis of a co2 compression system using waste heat into the regenerative organic rankine cycle. *Energy Conversion and Management*, 168:588–598, 2018.

[67] Giandomenico Ferrara, Andrea Lanzini, Pierluigi Leone, MT Ho, and DE Wiley. Exergetic and exergoeconomic analysis of post-combustion co2 capture using mea-solvent chemical absorption. *Energy*, 130:113–128, 2017.

[68] Gabriel Zsembinszki, Aran Solé, Camila Barreneche, Cristina Prieto, A Inés Fernández, and Luisa F Cabeza. Review of reactors with potential use in thermochemical energy storage in concentrated solar power plants. *Energies*, 11(9):2358, 2018.

[69] Anton Meier, Enrico Bonaldi, Gian Mario Cella, Wojciech Lipinski, and Daniel Wuillemin. Solar chemical reactor technology for industrial production of lime. *Solar Energy*, 80(10):1355–1362, 2006.

[70] Gkiokchan Moumin, Stefania Tescari, Pradeepkumar Sundarraj, Lamark de Oliveira, Martin Roeb, and Christian Sattler. Solar treatment of cohesive particles in a directly irradiated rotary kiln. *Solar Energy*, 182:480–490, 2019.

[71] Yu Qiu, Ya-Ling He, Peiwen Li, and Bao-Cun Du. A comprehensive model for analysis of real-time optical performance of a solar power tower with a multi-tube cavity receiver. *Applied energy*, 185:589–603, 2017.

[72] Kirk W Battleson. Solar power tower design guide: Solar thermal central receiver power systems. a source of electricity and/or process heat. Technical report, Sandia National Lab.(SNL-CA), Livermore, CA (United States), 1981.

[73] Anton Meier, Nicolas Gremaud, and Aldo Steinfeld. Economic evaluation of the industrial solar production of lime. *Energy conversion and management*, 46(6):905–926, 2005.

[74] Andrea Lazzaretto and Andrea Toffolo. A method to separate the problem of heat transfer interactions in the synthesis of thermal systems. *Energy*, 33(2):163–170, 2008.

[75] Andrea Toffolo, Andrea Lazzaretto, and Matteo Morandin. The heatsep method for the synthesis of thermal systems: An application to the s-graz cycle. *Energy*, 35(2):976–981, 2010.

[76] Andrea Toffolo. A synthesis/design optimization algorithm for rankine cycle based energy systems. *Energy*, 66:115–127, 2014.

[77] Giovanni Manente and Andrea Lazzaretto. Improved layouts and performance of single-and double-flash steam geothermal plants generated by the heatsep method. *Journal of Energy Resources Technology*, 142(9):090902, 2020.

[78] T Tanuma. Introduction to steam turbines for power plants. In *Advances in Steam Turbines for Modern Power Plants*, pages 3–10. Elsevier, 2022.

[79] Matteo C Romano, Maurizio Spinelli, Stefano Campanari, Stefano Consonni, Giovanni Cinti, Maurizio Marchi, and Enrico Borgarello. The calcium looping process for low co2 emission cement and power. *Energy Procedia*, 37:7091–7099, 2013.

[80] Bhabesh K Thakur. *A new correlation for heat transfer during flow boiling*. PhD thesis, Rochester Institute of Technology, 1981.

[81] HE Emara-Shabaik, MA Habib, and I Al-Zaharna. Prediction of risers' tubes temperature in water tube boilers. *Applied Mathematical Modelling*, 33(3):1323–1336, 2009.

[82] Maurizio Spinelli, Isabel Martínez, and Matteo C Romano. One-dimensional model of entrained-flow carbonator for co2 capture in cement kilns by calcium looping process. *Chemical engineering science*, 191:100–114, 2018.

[83] Dipak K. Sarkar. Chapter 2 - steam generators. In Dipak K. Sarkar, editor, *Thermal Power Plant*, pages 39–89. Elsevier, 2015.

[84] Marco Binotti, Marco Astolfi, Stefano Campanari, Giampaolo Manzolini, and Paolo Silva. Preliminary assessment of sco2 power cycles for application to csp solar tower plants. *Energy Procedia*, 105:1116–1122, 2017.

[85] Han-Hui Zhu, Kun Wang, and Ya-Ling He. Thermodynamic analysis and comparison for different direct-heated supercritical co2 brayton cycles integrated into a solar thermal power tower system. *Energy*, 140:144–157, 2017.

[86] Alireza Javanshir, Nenad Sarunac, and Zahra Razzaghpanah. Thermodynamic analysis of simple and regenerative brayton cycles for the concentrated solar power applications. *Energy conversion and management*, 163:428–443, 2018.

[87] Mohamed Noaman, George Saade, Tatiana Morosuk, and George Tsatsaronis. Exergoeconomic analysis applied to supercritical co2 power systems. *Energy*, 183:756–765, 2019.

[88] Mathias Penkuhn and George Tsatsaronis. Exergoeconomic analyses of different sco2 cycle configurations. In *Proceedings of the 6th International Symposium—Supercritical CO2 Power Cycles, Pittsburgh, PA, USA*, pages 27–29, 2018.

[89] MA Reyes-Belmonte, A Sebastián, M Romero, and J González-Aguilar. Optimization of a recompression supercritical carbon dioxide cycle for an innovative central receiver solar power plant. *Energy*, 112:17–27, 2016.

[90] Kevin J Albrecht, Matthew D Carlson, and Clifford K Ho. Integration, control, and testing of a high-temperature particle-to-sco2 heat exchanger. In *AIP Conference Proceedings*, volume 2126. AIP Publishing, 2019.

[91] Jeffrey Moore, St Cich, M Day, T Allison, J Wade, and D Hofer. Commissioning of a 1 mwe supercritical co2 test loop. In *The 6th International Supercritical CO2 Power Cycles Symposium*, 2018.

[92] Matthew D Carlson, Bobby M Middleton, and Clifford K Ho. Techno-economic comparison of solar-driven sco2 brayton cycles using component cost models baselined with vendor data and estimates. In *Energy Sustainability*, volume 57595, page V001T05A009. American Society of Mechanical Engineers, 2017.

[93] Abdullah E Alali and Khaled F Al-Shboul. Performance analysis of the closed brayton power cycle in a small-scale pebble bed gas cooled reactor using different working fluids. *Annals of Nuclear Energy*, 121:316–323, 2018.

[94] Hee-Cheon No, Ji-Hwan Kim, and Hyeun-Min Kim. A review of helium gas turbine technology for high-temperature gas-cooled reactors. *Nuclear Engineering and Technology*, 39(1):21–30, 2007.

[95] Colin F McDonald. Helium turbomachinery operating experience from gas turbine power plants and test facilities. *Applied Thermal Engineering*, 44:108–142, 2012.

[96] Karsten Kusterer, René Braun, Norbert Moritz, Takao Sugimoto, Kazuhiko Tanimura, and Dieter Bohn. Comparative study of solar thermal brayton cycles operated with helium or argon. In *Turbo Expo: Power for Land, Sea, and*

Air, volume 55188, page V004T05A007. American Society of Mechanical Engineers, 2013.

[97] V Zare and MJEC Hasanzadeh. Energy and exergy analysis of a closed brayton cycle-based combined cycle for solar power tower plants. *Energy conversion and management*, 128:227–237, 2016.

[98] Olumide Olumayegun, Meihong Wang, and Greg Kelsall. Closed-cycle gas turbine for power generation: A state-of-the-art review. *Fuel*, 180:694–717, 2016.

[99] Vaclav Dostal, Pavel Hejzlar, and Michael J Driscoll. The supercritical carbon dioxide power cycle: comparison to other advanced power cycles. *Nuclear technology*, 154(3):283–301, 2006.

[100] Haihua Zhao and Per F Peterson. Multiple reheat helium brayton cycles for sodium cooled fast reactors. *Nuclear Engineering and Design*, 238(7):1535–1546, 2008.

[101] C Wang, RG Ballinger, PW Stahle, E Demetri, and M Koronowski. Design of a power conversion system for an indirect cycle, helium cooled pebble bed reactor system. *HTR-2002: Conference on high temperature reactors*, 2002.

[102] Colin F McDonald. *Helium and combustion gas turbine power conversion systems comparison*, volume 78804. American Society of Mechanical Engineers, 1995.

[103] Sally E Mink, Stephanie E Gedal, Dillon M Weber, and Abhinav Dantuluri. *High-Temperature Nuclear Power Cycle Using Either Helium or s-CO2*. PhD thesis, University of Pennsylvania, Department of Chemical and Biomolecular Engineering, 2016.

[104] Manuel Romero and José González-Aguilar. Solar thermal csp technology. *Wiley Interdisciplinary Reviews: Energy and Environment*, 3(1):42–59, 2014.

[105] Latifa Sabri and Mohammed Benzirar. Determination of the maximum efficiency of concentrated solar power (parabolic trough and central tower) using a genetic algorithm. *Asian Journal of Applied Sciences*, 3(2), 2015.

[106] Michal Dvořák and Petr Havel. Combined heat and power production planning under liberalized market conditions. *Applied Thermal Engineering*, 43:163–173, 2012.

[107] Sumit Mitra, Lige Sun, and Ignacio E Grossmann. Optimal scheduling of industrial combined heat and power plants under time-sensitive electricity prices. *Energy*, 54:194–211, 2013.

[108] Longxi Li, Hailin Mu, Weijun Gao, and Miao Li. Optimization and analysis of cchp system based on energy loads coupling of residential and office buildings. *Applied Energy*, 136:206–216, 2014.

[109] Hongbo Ren, Weijun Gao, and Yingjun Ruan. Optimal sizing for residential chp system. *Applied Thermal Engineering*, 28(5-6):514–523, 2008.

[110] Paolo Arcuri, Gaetano Florio, and Petronilla Fragiacomo. A mixed integer programming model for optimal design of trigeneration in a hospital complex. *Energy*, 32(8):1430–1447, 2007.

[111] Davood Rakipour and Hassan Barati. Probabilistic optimization in operation of energy hub with participation of renewable energy resources and demand response. *Energy*, 173:384–399, 2019.

[112] Julien F Marquant, Ralph Evins, L Andrew Bollinger, and Jan Carmeliet. A holarchic approach for multi-scale distributed energy system optimisation. *Applied energy*, 208:935–953, 2017.

[113] Yun Yang, Shijie Zhang, and Yunhan Xiao. Optimal design of distributed energy resource systems coupled with energy distribution networks. *Energy*, 85:433–448, 2015.

[114] VS Agababov and PN Borisova. Comparison of separate and combined generation of energy carriers at a condensing power plant. In *Journal of Physics: Conference Series*, volume 1111, page 012075. IOP Publishing, 2018.

[115] Michel Noussan, Matteo Jarre, Roberta Roberto, and Daniele Russolillo. Combined vs separate heat and power production–primary energy comparison in high renewable share contexts. *Applied energy*, 213:1–10, 2018.

[116] Yong Zeng, Yanpeng Cai, Guohe Huang, and Jing Dai. A review on optimization modeling of energy systems planning and ghg emission mitigation under uncertainty. *Energies*, 4(10):1624–1656, 2011.

[117] Reza Hemmati, Hedayat Saboori, and Mehdi Ahmadi Jirdehi. Stochastic planning and scheduling of energy storage systems for congestion management in electric power systems including renewable energy resources. *Energy*, 133:380–387, 2017.

[118] DaWei Wu and RuZhu Wang. Combined cooling, heating and power: A review. *progress in energy and combustion science*, 32(5-6):459–495, 2006.

[119] Mukund K Deshmukh and Sandip S Deshmukh. Modeling of hybrid renewable energy systems. *Renewable and sustainable energy reviews*, 12(1):235–249, 2008.

[120] Gianfranco Chicco and Pierluigi Mancarella. Distributed multi-generation: A comprehensive view. *Renewable and sustainable energy reviews*, 13(3):535–551, 2009.

[121] Pierluigi Mancarella. Mes (multi-energy systems): An overview of concepts and evaluation models. *Energy*, 65:1–17, 2014.

[122] Houssein Al Moussawi, Farouk Fardoun, and Hasna Louahlia-Gualous. Review of tri-generation technologies: Design evaluation, optimization, decision-making, and selection approach. *Energy Conversion and Management*, 120:157–196, 2016.

[123] Yizhe Xu, Chengchu Yan, Huifang Liu, Jin Wang, Zhang Yang, and Yanlong Jiang. Smart energy systems: A critical review on design and operation optimization. *Sustainable Cities and Society*, 62:102369, 2020.

[124] Mingxi Liu, Yang Shi, and Fang Fang. Combined cooling, heating and power systems: A survey. *Renewable and Sustainable Energy Reviews*, 35:1–22, 2014.

[125] Wei Gu, Zhi Wu, Rui Bo, Wei Liu, Gan Zhou, Wu Chen, and Zaijun Wu. Modeling, planning and optimal energy management of combined cooling, heating and power microgrid: A review. *International Journal of Electrical Power & Energy Systems*, 54:26–37, 2014.

[126] M Jradi and S Riffat. Tri-generation systems: Energy policies, prime movers, cooling technologies, configurations and operation strategies. *Renewable and sustainable energy reviews*, 32:396–415, 2014.

[127] Hans-Kristian Ringkjøb, Peter M Haugan, and Ida Marie Solbrekke. A review of modelling tools for energy and electricity systems with large shares of variable renewables. *Renewable and Sustainable Energy Reviews*, 96:440–459, 2018.

[128] Wai Lip Theo, Jeng Shiun Lim, Wai Shin Ho, Haslenda Hashim, and Chew Tin Lee. Review of distributed generation (dg) system planning and optimisation techniques: Comparison of numerical and mathematical modelling methods. *Renewable and Sustainable Energy Reviews*, 67:531–573, 2017.

[129] Ahmad Abdallah Mohammad Aljabery, Hasan Mehrjerdi, Sajad Mahdavi, and Reza Hemmati. Multi carrier energy systems and energy hubs: Comprehensive review, survey and recommendations. *International Journal of Hydrogen Energy*, 46(46):23795–23814, 2021.

[130] Jiajia Li, Jinfu Liu, Peigang Yan, Xingshuo Li, Guowen Zhou, and Daren Yu. Operation optimization of integrated energy system under a renewable energy dominated future scene considering both independence and benefit: A review. *Energies*, 14(4):1103, 2021.

[131] Lei Gao, Yunho Hwang, and Tao Cao. An overview of optimization technologies applied in combined cooling, heating and power systems. *Renewable and Sustainable Energy Reviews*, 114:109344, 2019.

[132] Zeineb Abdmouleh, Adel Gastli, Lazhar Ben-Brahim, Mohamed Haouari, and Nasser Ahmed Al-Emadi. Review of optimization techniques applied for the integration of distributed generation from renewable energy sources. *Renewable Energy*, 113:266–280, 2017.

[133] Heejin Cho, Amanda D Smith, and Pedro Mago. Combined cooling, heating and power: A review of performance improvement and optimization. *Applied Energy*, 136:168–185, 2014.

[134] Risto Lahdelma and Henri Hakonen. An efficient linear programming algorithm for combined heat and power production. *European Journal of Operational Research*, 148(1):141–151, 2003.

[135] Marco Cavazzuti and Marco Cavazzuti. Deterministic optimization. *Optimization methods: From theory to design scientific and technological aspects in mechanics*, pages 77–102, 2013.

[136] Yang Liu, Jitian Han, and Huailiang You. Exergoeconomic analysis and multi-objective optimization of a cchp system based on sofc/gt and transcritical co2 power/refrigeration cycles. *Applied Thermal Engineering*, 230:120686, 2023.

[137] Lintong Liu, Rongrong Zhai, Yu Xu, Yangdi Hu, Siyuan Liu, and Lizhong Yang. Comprehensive sustainability assessment and multi-objective optimization of a novel renewable energy driven multi-energy supply system. *Applied Thermal Engineering*, 236:121461, 2024.

[138] Hamed Bagheri-Esfeh and Mohammad Reza Dehghan. Techno-economic design of a solar combisystem in a residential building. *Journal of Building Engineering*, 71:106591, 2023.

[139] Yan Cao, Hima Nikafshan Rad, Danial Hamedi Jamali, Nasim Hashemian, and Amir Ghasemi. A novel multi-objective spiral optimization algorithm for an innovative solar/biomass-based multi-generation energy system: 3e analyses, and optimization algorithms comparison. *Energy Conversion and Management*, 219:112961, 2020.

[140] Seung-Hoon Park, Yong-Sung Jang, and Eui-Jong Kim. Multi-objective optimization for sizing multi-source renewable energy systems in the community center of a residential apartment complex. *Energy Conversion and Management*, 244:114446, 2021.

[141] Cristina Baglivo, Paolo Maria Congedo, Andrea Fazio, and Domenico Laforgia. Multi-objective optimization analysis for high efficiency external walls of zero energy buildings (zeb) in the mediterranean climate. *Energy and Buildings*, 84:483–492, 2014.

[142] Amir Hassan Keshavarzzadeh and Pouria Ahmadi. Multi-objective techno-economic optimization of a solar based integrated energy system using various optimization methods. *Energy conversion and management*, 196:196–210, 2019.

[143] G Human, G Van Schoor, and KR Uren. Power management and sizing optimisation of renewable energy hydrogen production systems. *Sustainable Energy Technologies and Assessments*, 31:155–166, 2019.

[144] Fatemeh Teymoori Hamzehkolaei, Nima Amjady, Mohammad Ghamsari-Yazdel, and Mostafa Jazaeri. A new multi-objective profit-driven micro-chp planning model under participation in thermal and electrical markets. *Applied Thermal Engineering*, 218:119237, 2023.

[145] Qiwei Qin and Louis Gosselin. Multiobjective optimization and analysis of low-temperature district heating systems coupled with distributed heat pumps. *Applied Thermal Engineering*, 230:120818, 2023.

[146] Hanif Auwal Ibrahim and Michael Kweneojo Ayomoh. Optimum predictive modelling for a sustainable power supply mix: A case of the nigerian power system. *Energy Strategy Reviews*, 44:100962, 2022.

[147] Bhamidi Lokeshgupta and S Sivasubramani. Multi-objective home energy management with battery energy storage systems. *Sustainable Cities and Society*, 47:101458, 2019.

[148] Marialaura Di Somma, Bing Yan, Nicola Bianco, Peter B Luh, Giorgio Graditi, Luigi Mongibello, and Vincenzo Naso. Multi-objective operation optimization of a distributed energy system for a large-scale utility customer. *Applied Thermal Engineering*, 101:752–761, 2016.

[149] George Mavrotas. Effective implementation of the ε-constraint method in multi-objective mathematical programming problems. *Applied mathematics and computation*, 213(2):455–465, 2009.

[150] Honglei Yuan, Kun Feng, Wei Li, and Xianke Sun. Multi-objective optimization of virtual energy hub plant integrated with data center and plug-in electric vehicles under a mixed robust-stochastic model. *Journal of Cleaner Production*, 363:132365, 2022.

[151] Antoine Dubois, Jonathan Dumas, Paolo Thiran, Gauthier Limpens, and Damien Ernst. Multi-objective near-optimal necessary conditions for multi-sectoral planning. *arXiv preprint arXiv:2302.12654*, 2023.

[152] Jonas Finke and Valentin Bertsch. Implementing a highly adaptable method for the multi-objective optimisation of energy systems. *Applied Energy*, 332:120521, 2023.

[153] David Steen, Michael Stadler, Gonçalo Cardoso, Markus Groissböck, Nicholas DeForest, and Chris Marnay. Modeling of thermal storage systems in milp distributed energy resource models. *Applied Energy*, 137:782–792, 2015.

[154] Mohammad Shaterabadi, Mehdi Ahmadi Jirdehi, Nima Amiri, and Sina Omidi. Enhancement the economical and environmental aspects of plus-zero energy buildings integrated with invelox turbines. *Renewable Energy*, 153:1355–1367, 2020.

[155] Luca Moretti, Giampaolo Manzolini, and Emanuele Martelli. Milp and minlp models for the optimal scheduling of multi-energy systems accounting for delivery temperature of units, topology and non-isothermal mixing. *Applied Thermal Engineering*, 184:116161, 2021.

[156] Yibo Jiang, Jian Xu, Yuanzhang Sun, Congying Wei, Jing Wang, Siyang Liao, Deping Ke, Xiong Li, Jun Yang, and Xiaotao Peng. Coordinated operation of gas-electricity integrated distribution system with multi-cchp and distributed renewable energy sources. *Applied energy*, 211:237–248, 2018.

[157] Marialaura Di Somma, Giorgio Graditi, Ehsan Heydarian-Forushani, Miadreza Shafie-khah, and Pierluigi Siano. Stochastic optimal scheduling of distributed energy resources with renewables considering economic and environmental aspects. *Renewable energy*, 116:272–287, 2018.

[158] Paolo Gabrielli, Matteo Gazzani, Emanuele Martelli, and Marco Mazzotti. Optimal design of multi-energy systems with seasonal storage. *Applied Energy*, 219:408–424, 2018.

[159] Xiaohong Guan, Zhanbo Xu, and Qing-Shan Jia. Energy-efficient buildings facilitated by microgrid. *IEEE Transactions on smart grid*, 1(3):243–252, 2010.

[160] L Bartolucci, S Cordiner, V Mulone, S Pasquale, and A Sbarra. Design and management strategies for low emission building-scale multi energy systems. *Energy*, 239:122160, 2022.

[161] S Polimeni, L Moretti, G Manzolini, S Leva, L Meraldi, and P Raboni. Numerical and experimental testing of predictive ems algorithms for pv-bess residential microgrid. In *2019 IEEE Milan PowerTech*, pages 1–6. IEEE, 2019.

[162] Mousa Marzband, Majid Ghadimi, Andreas Sumper, and José Luis Domínguez-García. Experimental validation of a real-time energy management system using multi-period gravitational search algorithm for microgrids in islanded mode. *Applied energy*, 128:164–174, 2014.

[163] Gregory Von Wald, Kaarthik Sundar, Evan Sherwin, Anatoly Zlotnik, and Adam Brandt. Optimal gas-electric energy system decarbonization planning. *Advances in Applied Energy*, 6:100086, 2022.

[164] Hugo Morais, Péter Kádár, Pedro Faria, Zita A Vale, and HM Khodr. Optimal scheduling of a renewable micro-grid in an isolated load area using mixed-integer linear programming. *Renewable Energy*, 35(1):151–156, 2010.

[165] Faeze Brahman, Masoud Honarmand, and Shahram Jadid. Optimal electrical and thermal energy management of a residential energy hub, integrating demand response and energy storage system. *Energy and Buildings*, 90:65–75, 2015.

[166] Reza Hemmati. Technical and economic analysis of home energy management system incorporating small-scale wind turbine and battery energy storage system. *Journal of Cleaner Production*, 159:106–118, 2017.

[167] Iman Gerami Moghaddam, Mohsen Saniei, and Elaheh Mashhour. A comprehensive model for self-scheduling an energy hub to supply cooling, heating and electrical demands of a building. *Energy*, 94:157–170, 2016.

[168] A Nottrott, Jan Kleissl, and Byron Washom. Energy dispatch schedule optimization and cost benefit analysis for grid-connected, photovoltaic-battery storage systems. *Renewable Energy*, 55:230–240, 2013.

[169] Haichao Wang, Wusong Yin, Elnaz Abdollahi, Risto Lahdelma, and Wenling Jiao. Modelling and optimization of chp based district heating system with renewable energy production and energy storage. *Applied Energy*, 159:401–421, 2015.

[170] Hongbo Ren, Weisheng Zhou, Ken'ichi Nakagami, Weijun Gao, and Qiong Wu. Multi-objective optimization for the operation of distributed energy systems considering economic and environmental aspects. *Applied Energy*, 87(12):3642–3651, 2010.

[171] Zhou Wu, Henerica Tazvinga, and Xiaohua Xia. Demand side management of photovoltaic-battery hybrid system. *Applied Energy*, 148:294–304, 2015.

[172] Heejin Cho, Pedro J Mago, Rogelio Luck, and Louay M Chamra. Evaluation of cchp systems performance based on operational cost, primary energy consumption, and carbon dioxide emission by utilizing an optimal operation scheme. *Applied Energy*, 86(12):2540–2549, 2009.

[173] David Torres, Jorge Crichigno, Gregg Padilla, and Ruben Rivera. Scheduling coupled photovoltaic, battery and conventional energy sources to maximize profit using linear programming. *Renewable energy*, 72:284–290, 2014.

[174] Giorgos S. Georgiou, Paul Christodoulides, and Soteris A. Kalogirou. Optimizing the energy storage schedule of a battery in a pv grid-connected nzeb using linear programming. *Energy*, 208:118177, 2020.

[175] Zhaoguang Pan, Qinglai Guo, and Hongbin Sun. Feasible region method based integrated heat and electricity dispatch considering building thermal inertia. *Applied Energy*, 192:395–407, 2017.

[176] D. Lauinger, P. Caliandro, J. Van herle, and D. Kuhn. A linear programming approach to the optimization of residential energy systems. *Journal of Energy Storage*, 7:24–37, 2016.

[177] G. Cardoso, M. Stadler, A. Siddiqui, C. Marnay, N. Deforest, A. Barbosa-Póvoa, and P. Ferrão. Microgrid reliability modeling and battery scheduling using stochastic linear programming. *Electric Power Systems Research*, 103:61–69, 2013.

[178] Martina Capone, Elisa Guelpa, Giulia Mancò, and Vittorio Verda. Integration of storage and thermal demand response to unlock flexibility in district multi-energy systems. *Energy*, 237, 2021.

[179] Yuxuan Li, Junli Zhang, Xiao Wu, Jiong Shen, and Kwang Y. Lee. Optimal design of combined cooling, heating and power multi-energy system based on load tracking performance evaluation of adjustable equipment. *Applied Thermal Engineering*, 211, 2022.

[180] E. Carpaneto, P. Lazzeroni, and M. Repetto. Optimal integration of solar energy in a district heating network. *Renewable Energy*, 75:714–721, mar 2015.

[181] F. Freschi, L. Giaccone, P. Lazzeroni, and M. Repetto. Economic and environmental analysis of a trigeneration system for food-industry: A case study. *Applied Energy*, 107:157–172, 2013.

[182] Iman Gerami Moghaddam, Mohsen Saniei, and Elaheh Mashhour. A comprehensive model for self-scheduling an energy hub to supply cooling, heating and electrical demands of a building. *Energy*, 94:157–170, 2016.

[183] Yuehong Lu, Shengwei Wang, Yongjun Sun, and Chengchu Yan. Optimal scheduling of buildings with energy generation and thermal energy storage under dynamic electricity pricing using mixed-integer nonlinear programming. *Applied Energy*, 147:49–58, jun 2015.

[184] Mohsen Nemati, Martin Braun, and Stefan Tenbohlen. Optimization of unit commitment and economic dispatch in microgrids based on genetic algorithm and mixed integer linear programming. *Applied Energy*, 210:944–963, 2018.

[185] Yibo Jiang, Jian Xu, Yuanzhang Sun, Congying Wei, Jing Wang, Siyang Liao, Deping Ke, Xiong Li, Jun Yang, and Xiaotao Peng. Coordinated operation of gas-electricity integrated distribution system with multi-CCHP and distributed renewable energy sources. *Applied Energy*, 211(November 2017):237–248, 2018.

[186] Boran Morvaj, Ralph Evins, and Jan Carmeliet. Optimising urban energy systems: Simultaneous system sizing, operation and district heating network layout. *Energy*, 116:619–636, dec 2016.

[187] Aldo Bischi, Leonardo Taccari, Emanuele Martelli, Edoardo Amaldi, Giampaolo Manzolini, Paolo Silva, Stefano Campanari, and Ennio Macchi. A detailed MILP optimization model for combined cooling, heat and power system operation planning. *Energy*, 74(C):12–26, 2014.

[188] Michal Dvořák and Petr Havel. Combined heat and power production planning under liberalized market conditions. *Applied Thermal Engineering*, 43:163–173, 2012.

[189] Hadis Moradi, Mahdi Esfahanian, Amir Abtahi, and Ali Zilouchian. Optimization and energy management of a standalone hybrid microgrid in the presence of battery storage system. *Energy*, 147:226–238, mar 2018.

[190] Luca Moretti, Giampaolo Manzolini, and Emanuele Martelli. MILP and MINLP models for the optimal scheduling of multi-energy systems accounting for delivery temperature of units, topology and non-isothermal mixing. *Applied Thermal Engineering*, 184(October 2020):116161, 2021.

[191] Francesco F. Nicolosi, Jacopo C. Alberizzi, Carlo Caligiuri, and Massimiliano Renzi. Unit commitment optimization of a micro-grid with a MILP algorithm: Role of the emissions, bio-fuels and power generation technology. *Energy Reports*, may 2021.

[192] Paolo Gabrielli, Matteo Gazzani, Emanuele Martelli, and Marco Mazzotti. Optimal design of multi-energy systems with seasonal storage. *Applied Energy*, 219(July 2017):408–424, 2018.

[193] Paolo Marocco, Domenico Ferrero, Emanuele Martelli, Massimo Santarelli, and Andrea Lanzini. An milp approach for the optimal design of renewable battery-hydrogen energy systems for off-grid insular communities. *Energy Conversion and Management*, 245:114564, 2021.

[194] P. Arcuri, P. Beraldi, G. Florio, and P. Fragiacomo. Optimal design of a small size trigeneration plant in civil users: A MINLP (Mixed Integer Non Linear Programming Model). *Energy*, 80:628–641, 2015.

[195] Boris N. Pshenichnyj. *The Linearization Method for Constrained Optimization*, volume 22. Springer Berlin Heidelberg, Berlin, Heidelberg, 1994.

[196] Claudia D'Ambrosio, Andrea Lodi, and Silvano Martello. Piecewise linear approximation of functions of two variables in MILP models. *Operations Research Letters*, 38(1), jan 2010.

[197] Sumit Mitra, Lige Sun, and Ignacio E. Grossmann. Optimal scheduling of industrial combined heat and power plants under time-sensitive electricity prices. *Energy*, 54:194–211, 2013.

[198] Marialaura Di Somma, Bing Yan, Nicola Bianco, Peter B. Luh, Giorgio Graditi, Luigi Mongibello, and Vincenzo Naso. Multi-objective operation optimization of a Distributed Energy System for a large-scale utility customer. *Applied Thermal Engineering*, 101:752–761, may 2016.

[199] Gabriele Comodi, Andrea Giantomassi, Marco Severini, Stefano Squartini, Francesco Ferracuti, Alessandro Fonti, Davide Nardi Cesarini, Matteo Morodo, and Fabio Polonara. Multi-apartment residential microgrid with electrical and thermal storage devices: Experimental analysis and simulation of energy management strategies. *Applied Energy*, 137:854–866, 2015.

[200] Mohammad Shaterabadi, Mehdi Ahmadi Jirdehi, Nima Amiri, and Sina Omidi. Enhancement the economical and environmental aspects of plus-zero energy buildings integrated with INVELOX turbines. *Renewable Energy*, 153:1355–1367, jun 2020.

[201] Zhe Zhou, Pei Liu, Zheng Li, Efstratios N. Pistikopoulos, and Michael C. Georgiadis. Impacts of equipment off-design characteristics on the optimal design and operation of combined cooling, heating and power systems. *Computers and Chemical Engineering*, 48:40–47, 2013.

[202] Simo Makkonen and Risto Lahdelma. Non-convex power plant modelling in energy optimisation. *European Journal of Operational Research*, 171(3):1113–1126, 2006.

[203] M. Di Somma, B. Yan, N. Bianco, G. Graditi, P. B. Luh, L. Mongibello, and V. Naso. Operation optimization of a distributed energy system considering energy costs and exergy efficiency. *Energy Conversion and Management*, 103:739–751, 2015.

[204] M. A. Lozano, M. Carvalho, and L. M. Serra. Operational strategy and marginal costs in simple trigeneration systems. *Energy*, 34(11):2001–2008, 2009.

[205] Mohammad Chehreghani Bozchalui, Syed Ahsan Hashmi, Hussin Hassen, Claudio A. Cañizares, and Kankar Bhattacharya. Optimal operation of residential energy hubs in smart grids. *IEEE Transactions on Smart Grid*, 3(4):1755–1766, 2012.

[206] Faeze Brahman, Masoud Honarmand, and Shahram Jadid. Optimal electrical and thermal energy management of a residential energy hub, integrating demand response and energy storage system. *Energy and Buildings*, 90:65–75, 2015.

[207] Hugo Morais, Péter Kádár, Pedro Faria, Zita A. Vale, and H. M. Khodr. Optimal scheduling of a renewable micro-grid in an isolated load area using mixed-integer linear programming. *Renewable Energy*, 35(1):151–156, jan 2010.

[208] Mahsa Daraei, Anders Avelin, and Eva Thorin. Optimization of a regional energy system including CHP plants and local PV system and hydropower: Scenarios for the County of Västmanland in Sweden. *Journal of Cleaner Production*, 230:1111–1127, sep 2019.

[209] Marco Wirtz, Maria Hahn, Thomas Schreiber, and Dirk Müller. Design optimization of multi-energy systems using mixed-integer linear programming: Which model complexity and level of detail is sufficient? *Energy Conversion and Management*, 240:114249, 2021.

[210] Yang Zhao, Yuehong Lu, Chengchu Yan, and Shengwei Wang. MPC-based optimal scheduling of grid-connected low energy buildings with thermal energy storages. *Energy and Buildings*, 86:415–426, 2015.

[211] Xuyue Zheng, Guoce Wu, Yuwei Qiu, Xiangyan Zhan, Nilay Shah, Ning Li, and Yingru Zhao. A MINLP multi-objective optimization model for operational planning of a case study CCHP system in urban China. *Applied Energy*, 210:1126–1140, 2018.

[212] Pei Liu, Efstratios N. Pistikopoulos, and Zheng Li. A mixed-integer optimization approach for polygeneration energy systems design. *Computers and Chemical Engineering*, 33(3):759–768, 2009.

[213] Xiaolin Chu, Dong Yang, Xiaohong Li, and Rui Zhou. Evaluation of CCHP system performance based on operational cost considering carbon tax. *Energy Procedia*, 142:2930–2935, 2017.

[214] Mingxi Liu, Yang Shi, and Fang Fang. Optimal power flow and PGU capacity of CCHP systems using a matrix modeling approach. *Applied Energy*, 102:794–802, 2013.

[215] Ni Linna, Feng Changsen, Fushuan Wen, and Abdus Salam. Optimal power flow of multiple energy carriers with multiple kinds of energy storage. *IEEE Power and Energy Society General Meeting*, 2016-Novem(2015), 2016.

[216] Athil S. Al-Ezzi and Mohamed Nainar M. Ansari. Photovoltaic Solar Cells: A Review, 2022.

[217] Na Deng, Rongchang Cai, Yuan Gao, Zhihua Zhou, Guansong He, Dongyi Liu, and Awen Zhang. A MINLP model of optimal scheduling for a district heating and cooling system: A case study of an energy station in Tianjin. *Energy*, 141:1750–1763, 2017.

[218] Mads R. Almassalkhi and Anna Towle. Enabling city-scale multi-energy optimal dispatch with energy hubs. *19th Power Systems Computation Conference, PSCC 2016*, 2016.

[219] P. Arcuri, G. Florio, and P. Fragiacomo. A mixed integer programming model for optimal design of trigeneration in a hospital complex. *Energy*, 32(8):1430–1447, 2007.

[220] Torben Ommen, Wiebke Brix Markussen, and Brian Elmegaard. Comparison of linear, mixed integer and non-linear programming methods in energy system dispatch modelling. *Energy*, 74(1):109–118, 2014.

[221] Gaurav Singh and Ranjan Das. Experimental study of a combined biomass and solar energy-based fully grid-independent air-conditioning system. *Clean Technologies and Environmental Policy*, 23(6), 2021.

[222] Christos A. Frangopoulos, Michael R. Von Spakovsky, and Enrico Sciubba. A brief review of methods for the design and synthesis optimization of energy systems. *International Journal of Applied Thermodynamics*, 5(4):151–160, 2002.

[223] Zeineb Abdmouleh, Adel Gastli, Lazhar Ben-Brahim, Mohamed Haouari, and Nasser Ahmed Al-Emadi. Review of optimization techniques applied for the integration of distributed generation from renewable energy sources. *Renewable Energy*, 113:266–280, 2017.

[224] Salvador Acha, Arthur Mariaud, Nilay Shah, and Christos N. Markides. Optimal design and operation of distributed low-carbon energy technologies in commercial buildings. *Energy*, 142:578–591, 2018.

[225] Xingyi Zhu, Xiangyan Zhan, Hao Liang, Xuyue Zheng, Yuwei Qiu, Jian Lin, Jincan Chen, Chao Meng, and Yingru Zhao. The optimal design and operation strategy of renewable energy-CCHP coupled system applied in five building objects. *Renewable Energy*, 146:2700–2715, 2020.

[226] Mirko M. Stojiljković, Mladen M. Stojiljković, and Bratislav D. Blagojević. Multi-objective combinatorial optimization of trigeneration plants based on metaheuristics. *Energies*, 7(12):8554–8581, 2014.

[227] Yi Wang, Ning Zhang, Zhenyu Zhuo, Chongqing Kang, and Daniel Kirschen. Mixed-integer linear programming-based optimal configuration planning for energy hub: Starting from scratch. *Applied Energy*, 210(July 2017):1141–1150, 2018.

[228] Samira Fazlollahi, Gwenaelle Becker, and François Maréchal. Multi-objectives, multi-period optimization of district energy systems: III. Distribution networks. *Computers and Chemical Engineering*, 66:82–97, 2014.

[229] Si Doek Oh, Ho Jun Lee, Jung Yeul Jung, and Ho Young Kwak. Optimal planning and economic evaluation of cogeneration system. *Energy*, 32(5):760–771, 2007.

[230] Carlos Rubio-Maya, Javier Uche, and Amaya Martínez. Sequential optimization of a polygeneration plant. *Energy Conversion and Management*, 52(8-9):2861–2869, 2011.

[231] Monica Carvalho, Miguel A. Lozano, and Luis M. Serra. Multicriteria synthesis of trigeneration systems considering economic and environmental aspects. *Applied Energy*, 91(1):245–254, 2012.

[232] Tor Martin Tveit, Tuula Savola, Alemayehu Gebremedhin, and Carl Johan Fogelholm. Multi-period MINLP model for optimising operation and structural changes to CHP plants in district heating networks with long-term thermal storage. *Energy Conversion and Management*, 50(3):639–647, 2009.

[233] Rui Jing, Xingyi Zhu, Zhiyi Zhu, Wei Wang, Chao Meng, Nilay Shah, Ning Li, and Yingru Zhao. A multi-objective optimization and multi-criteria evaluation integrated framework for distributed energy system optimal planning. *Energy Conversion and Management*, 166(November 2017):445–462, 2018.

[234] Azadeh Maroufmashat, Sourena Sattari, Ramin Roshandel, Michael Fowler, and Ali Elkamel. Multi-objective Optimization for Design and Operation of Distributed Energy Systems through the Multi-energy Hub Network Approach. *Industrial and Engineering Chemistry Research*, 55(33):8950–8966, 2016.

[235] Yun Yang, Shijie Zhang, and Yunhan Xiao. Optimal design of distributed energy resource systems coupled with energy distribution networks. *Energy*, 85:433–448, 2015.

[236] Mohammad Ameri and Zahed Besharati. Optimal design and operation of district heating and cooling networks with CCHP systems in a residential complex. *Energy and Buildings*, 110:135–148, 2016.

[237] Guangsheng Pan, Wei Gu, Zhi Wu, Yuping Lu, and Shuai Lu. Optimal design and operation of multi-energy system with load aggregator considering nodal energy prices. *Applied Energy*, 239(February):280–295, 2019.

[238] Tetsuya Wakui and Ryohei Yokoyama. Optimal structural design of residential cogeneration systems in consideration of their operating restrictions. *Energy*, 64:719–733, 2014.

[239] Dario Buoro, Melchiorre Casisi, Piero Pinamonti, and Mauro Reini. Optimal synthesis and operation of advanced energy supply systems for standard and domotic home. *Energy Conversion and Management*, 60:96–105, 2012.

[240] Monica Carvalho, Luis Maria Serra, and Miguel Angel Lozano. Optimal synthesis of trigeneration systems subject to environmental constraints. *Energy*, 36(6):3779–3790, 2011.

[241] Nan Yu, Jin Su Kang, Chung Chuan Chang, Tai Yong Lee, and Dong Yup Lee. Robust economic optimization and environmental policy analysis for microgrid planning: An application to Taichung Industrial Park, Taiwan. *Energy*, 113:671–682, 2016.

[242] Jarmo Söderman and Frank Pettersson. Structural and operational optimisation of distributed energy systems. *Applied Thermal Engineering*, 26(13):1400–1408, 2006.

[243] Miguel A. Lozano, José C. Ramos, Monica Carvalho, and Luis M. Serra. Structure optimization of energy supply systems in tertiary sector buildings. *Energy and Buildings*, 41(10):1063–1075, 2009.

[244] Wei Wei, Jingwen Wu, Yunfei Mu, Jianzhong Wu, Hongjie Jia, Kai Yuan, Yi Song, and Chongbo Sun. Assessment of the solar energy accommodation

capability of the district integrated energy systems considering the transmission delay of the heating network. *International Journal of Electrical Power and Energy Systems*, 130(March):106821, 2021.

[245] Eugenia D. Mehleri, Haralambos Sarimveis, Nikolaos C. Markatos, and Lazaros G. Papageorgiou. A mathematical programming approach for optimal design of distributed energy systems at the neighbourhood level. *Energy*, 44(1):96–104, 2012.

[246] Akomeno Omu, Ruchi Choudhary, and Adam Boies. Distributed energy resource system optimisation using mixed integer linear programming. *Energy Policy*, 61:249–266, 2013.

[247] Benoit Olsommer, Daniel Favrat, and Michael von Spakovsky. An Approach for the Time-Dependent Thermoeconomic Modeling and Optimization of Energy System Synthesis, Design and Operation Part I: Methodology and Results. *International Journal of Thermodynamics*, 2(3):97–114–114, 1999.

[248] Li Guo, Wenjian Liu, Jiejin Cai, Bowen Hong, and Chengshan Wang. A two-stage optimal planning and design method for combined cooling, heat and power microgrid system. *Energy Conversion and Management*, 74:433–445, 2013.

[249] Changbin Zhu, Baoping Xu, and Ya Zhou Nie. An integrated design and operation optimal method for CCHP system. *Energy Procedia*, 158:1360–1365, 2019.

[250] Saliya Jayasekara, Saman K. Halgamuge, Rahula A. Attalage, and Rohitha Rajarathne. Optimum sizing and tracking of combined cooling heating and power systems for bulk energy consumers. *Applied Energy*, 118:124–134, 2014.

[251] Cristina Elsido, Aldo Bischi, Paolo Silva, and Emanuele Martelli. Two-stage MINLP algorithm for the optimal synthesis and design of networks of CHP units. *Energy*, 121:403–426, 2017.

[252] Ligang Wang, Matthias Lampe, Philip Voll, Yongping Yang, and André Bardow. Multi-objective superstructure-free synthesis and optimization of thermal power plants. *Energy*, 116:1104–1116, 2016.

[253] Ligang Wang, Philip Voll, Matthias Lampe, Yongping Yang, and André Bardow. Superstructure-free synthesis and optimization of thermal power plants. *Energy*, 91:700–711, 2015.

[254] Philip Voll, Matthias Lampe, Gregor Wrobel, and André Bardow. Superstructure-free synthesis and optimization of distributed industrial energy supply systems. *Energy*, 45(1):424–435, 2012.

[255] Longxi Li, Hailin Mu, Weijun Gao, and Miao Li. Optimization and analysis of CCHP system based on energy loads coupling of residential and office buildings. *Applied Energy*, 136:206–216, 2014.

[256] Haosheng Lin, Changzhi Yang, and Xiaoqin Xu. A new optimization model of CCHP system based on genetic algorithm. *Sustainable Cities and Society*, 52(August 2019):101811, 2020.

[257] Rong Zeng, Hongqiang Li, Lifang Liu, Xiaofeng Zhang, and Guoqiang Zhang. A novel method based on multi-population genetic algorithm for CCHP-GSHP coupling system optimization. *Energy Conversion and Management*, 105:1138–1148, 2015.

[258] Zhengyi Luo, Sheng Yang, Nan Xie, Weiwei Xie, Jiaxing Liu, Yawovi Souley Agbodjan, and Zhiqiang Liu. Multi-objective capacity optimization of a distributed energy system considering economy, environment and energy. *Energy Conversion and Management*, 200(September):112081, 2019.

[259] Jiangjiang Wang, Yi Liu, Fukang Ren, and Shuaikang Lu. Multi-objective optimization and selection of hybrid combined cooling, heating and power systems considering operational flexibility. *Energy*, 197:117313, 2020.

[260] K. C. Kavvadias and Z. B. Maroulis. Multi-objective optimization of a trigeneration plant. *Energy Policy*, 38(2):945–954, 2010.

[261] Longxi Li, Shiwei Yu, Hailin Mu, and Huanan Li. Optimization and evaluation of CCHP systems considering incentive policies under different operation strategies. *Energy*, 162:825–840, 2018.

[262] Rong Zeng, Xiaofeng Zhang, Yan Deng, Hongqiang Li, and Guoqiang Zhang. Optimization and performance comparison of combined cooling, heating and power/ground source heat pump/photovoltaic/solar thermal system under different load ratio for two operation strategies. *Energy Conversion and Management*, 208:112579, mar 2020.

[263] Bolun Li, Pingfang Hu, Na Zhu, Fei Lei, and Lu Xing. Performance analysis and optimization of a CCHP-GSHP coupling system based on quantum genetic algorithm. *Sustainable Cities and Society*, 46(December 2018):101408, 2019.

[264] Haifeng Wu, Qibin Liu, Gengxin Xie, Shaopeng Guo, Jie Zheng, and Bosheng Su. Performance investigation of a novel hybrid combined cooling, heating and power system with solar thermochemistry in different climate zones. *Energy*, 190:116281, 2020.

[265] Hamed Ershadi and Arash Karimipour. Present a multi-criteria modeling and optimization (energy, economic and environmental) approach of industrial combined cooling heating and power (CCHP) generation systems using the genetic algorithm, case study: A tile factory. *Energy*, 149:286–295, 2018.

[266] Jiangjiang Wang, Zhiqiang John Zhai, Youyin Jing, Xutao Zhang, and Chunfa Zhang. Sensitivity analysis of optimal model on building cooling heating and power system. *Applied Energy*, 88(12):5143–5152, 2011.

[267] Hongwei Li, Razi Nalim, and P. A. Haldi. Thermal-economic optimization of a distributed multi-generation energy system - A case study of Beijing. *Applied Thermal Engineering*, 26(7):709–719, 2006.

[268] Jiangjiang Wang, Yanchao Lu, Ying Yang, and Tianzhi Mao. Thermodynamic performance analysis and optimization of a solar-assisted combined cooling, heating and power system. *Energy*, 115:49–59, 2016.

[269] Yan Cao, Qiangfeng Wang, Zhijie Wang, Kittisak Jermsittiparsert, and Mohammadreza Shafiee. A new optimized configuration for capacity and operation improvement of CCHP system based on developed owl search algorithm. *Energy Reports*, 6:315–324, 2020.

[270] Mehran Jamshidi and Alireza Askarzadeh. Techno-economic analysis and size optimization of an off-grid hybrid photovoltaic, fuel cell and diesel generator system. *Sustainable Cities and Society*, 44:310–320, 2019.

[271] Saman Soheyli, Mohamad Hossein Shafiei Mayam, and Mehri Mehrjoo. Modeling a novel CCHP system including solar and wind renewable energy resources and sizing by a CC-MOPSO algorithm. *Applied Energy*, 184:375–395, 2016.

[272] Gan Yang and Xiaoqiang Zhai. Optimization and performance analysis of solar hybrid CCHP systems under different operation strategies. *Applied Thermal Engineering*, 133(December 2017):327–340, 2018.

[273] Zhihui Song, Tao Liu, Yanju Liu, Xuedan Jiang, and Qizhao Lin. Study on the optimization and sensitivity analysis of CCHP systems for industrial park facilities. *International Journal of Electrical Power and Energy Systems*, 120(March):105984, 2020.

[274] Georgios Mavromatidis, Kristina Orehounig, and Jan Carmeliet. A review of uncertainty characterisation approaches for the optimal design of distributed energy systems. *Renewable and Sustainable Energy Reviews*, 88(February):258–277, 2018.

[275] Pierluigi Mancarella. MES (multi-energy systems): An overview of concepts and evaluation models. *Energy*, 65:1–17, 2014.

[276] Wai Lip Theo, Jeng Shiun Lim, Wai Shin Ho, Haslenda Hashim, and Chew Tin Lee. Review of distributed generation (DG) system planning and optimisation techniques: Comparison of numerical and mathematical modelling methods. *Renewable and Sustainable Energy Reviews*, 67:531–573, 2017.

[277] Morteza Aien, Ali Hajebrahimi, and Mahmud Fotuhi-Firuzabad. A comprehensive review on uncertainty modeling techniques in power system studies. *Renewable and Sustainable Energy Reviews*, 57:1077–1089, 2016.

[278] Yong Zeng, Yanpeng Cai, Guohe Huang, and Jing Dai. A review on optimization modeling of energy systems planning and GHG emission mitigation under uncertainty. *Energies*, 4(10):1624–1656, 2011.

[279] Xiufeng Yue, Steve Pye, Joseph DeCarolis, Francis G.N. Li, Fionn Rogan, and Brian Gallachóir. A review of approaches to uncertainty assessment in energy system optimization models. *Energy Strategy Reviews*, 21(June):204–217, 2018.

[280] Alessandra Parisio, Carmen Del Vecchio, and Alfredo Vaccaro. A robust optimization approach to energy hub management. *International Journal of Electrical Power and Energy Systems*, 42(1):98–104, 2012.

[281] Hyeunguk Ahn, Donghyun Rim, Gregory S. Pavlak, and James D. Freihaut. Uncertainty analysis of energy and economic performances of hybrid solar photovoltaic and combined cooling, heating, and power (CCHP+PV) systems using a Monte-Carlo method, 2019.

[282] Atefeh Alirezazadeh, Masoud Rashidinejad, Amir Abdollahi, Peyman Afzali, and Alireza Bakhshai. A new flexible model for generation scheduling in a smart grid. *Energy*, 191:116438, 2020.

[283] Carsten Croonenbroeck and Georg Stadtmann. Renewable generation forecast studies – Review and good practice guidance. *Renewable and Sustainable Energy Reviews*, 108(April):312–322, 2019.

[284] Sanjeev Kumar Aggarwal, Lalit Mohan Saini, and Ashwani Kumar. Electricity price forecasting in deregulated markets: A review and evaluation. *International Journal of Electrical Power and Energy Systems*, 31(1):13–22, 2009.

[285] Tao Hong and Shu Fan. Probabilistic electric load forecasting: A tutorial review. *International Journal of Forecasting*, 32(3):914–938, 2016.

[286] Rafał Weron. Electricity price forecasting: A review of the state-of-the-art with a look into the future. *International Journal of Forecasting*, 30(4):1030–1081, 2014.

[287] Muhammad Qamar Raza and Abbas Khosravi. A review on artificial intelligence based load demand forecasting techniques for smart grid and buildings. *Renewable and Sustainable Energy Reviews*, 50:1352–1372, 2015.

[288] Stefano Mazzoni, Sean Ooi, Benedetto Nastasi, and Alessandro Romagnoli. Energy storage technologies as techno-economic parameters for master-planning and optimal dispatch in smart multi energy systems. *Applied Energy*, 254, 2019.

[289] A.T.D. Perera, R.A. Attalage, K.K.C.K. Perera, and V.P.C. Dassanayake. Designing standalone hybrid energy systems minimizing initial investment, life cycle cost and pollutant emission. *Energy*, 54:220–230, 2013.

[290] Davood Rakipour and Hassan Barati. Probabilistic optimization in operation of energy hub with participation of renewable energy resources and demand response. *Energy*, 173:384–399, 2019.

[291] M. J. Vahid-Pakdel, Sayyad Nojavan, B. Mohammadi-ivatloo, and Kazem Zare. Stochastic optimization of energy hub operation with consideration of thermal energy market and demand response. *Energy Conversion and Management*, 145:117–128, 2017.

[292] Mohammad Amin Mirzaei, Ahmad Sadeghi Yazdankhah, Behnam Mohammadi-Ivatloo, Mousa Marzband, Miadreza Shafie-khah, and João P.S. Catalão. Stochastic network-constrained co-optimization of energy and reserve products in renewable energy integrated power and gas networks with energy storage system. *Journal of Cleaner Production*, 223:747–758, 2019.

[293] Xu Wang, Zhaohong Bie, Fan Liu, and Yu Kou. Co-optimization planning of integrated electricity and district heating systems based on improved quadratic convex relaxation. *Applied Energy*, 285(July 2020):116439, 2021.

[294] Samaneh Pazouki, Mahmoud Reza Haghifam, and Albert Moser. Uncertainty modeling in optimal operation of energy hub in presence of wind, storage and demand response. *International Journal of Electrical Power and Energy Systems*, 61:335–345, 2014.

[295] S. A. Mansouri, A. Ahmarinejad, M. Ansarian, M. S. Javadi, and J. P.S. Catalao. Stochastic planning and operation of energy hubs considering demand response programs using Benders decomposition approach. *International Journal of Electrical Power and Energy Systems*, 120(March):106030, 2020.

[296] Leonard Kaufman and Peter J Rousseeuw. *Finding groups in data: an introduction to cluster analysis*. John Wiley & Sons, 2009.

[297] Holger Heitsch and Werner Römisch. Scenario reduction algorithms in stochastic programming. *Computational Optimization and Applications*, 24(2-3), 2003.

[298] Yuwei Wang, Liu Tang, Yuanjuan Yang, Wei Sun, and Huiru Zhao. A stochastic-robust coordinated optimization model for CCHP micro-grid considering multi-energy operation and power trading with electricity markets under uncertainties. *Energy*, 198:117273, 2020.

[299] Mohsen Kia, Mehrdad Setayesh Nazar, Mohammad Sadegh Sepasian, Alireza Heidari, and Pierluigi Siano. Optimal day ahead scheduling of combined heat and power units with electrical and thermal storage considering security constraint of power system. *Energy*, 120:241–252, 2017.

[300] Wenjie Gang, Shengwei Wang, Godfried Augenbroe, and Fu Xiao. Robust optimal design of district cooling systems and the impacts of uncertainty and reliability. *Energy and Buildings*, 122:11–22, 2016.

[301] Jiajia Li, Jinfu Liu, Peigang Yan, Xingshuo Li, Guowen Zhou, and Daren Yu. Operation optimization of integrated energy system under a renewable energy dominated future scene considering both independence and benefit: A review. *Energies*, 14(4), 2021.

[302] Nikolaos E. Koltsaklis, Pei Liu, and Michael C. Georgiadis. An integrated stochastic multi-regional long-term energy planning model incorporating autonomous power systems and demand response. *Energy*, 82:865–888, 2015.

[303] Rong Li and Yong Yang. Multi-objective capacity optimization of a hybrid energy system in two-stage stochastic programming framework. *Energy Reports*, 7:1837–1846, 2021.

[304] Zhe Zhou, Jianyun Zhang, Pei Liu, Zheng Li, Michael C. Georgiadis, and Efstratios N. Pistikopoulos. A two-stage stochastic programming model for the optimal design of distributed energy systems. *Applied Energy*, 103:135–144, 2013.

[305] Georgios Mavromatidis, Kristina Orehounig, and Jan Carmeliet. Design of distributed energy systems under uncertainty: A two-stage stochastic programming approach. *Applied Energy*, 222:932–950, 2018.

[306] Annelies Vandermeulen, Bram van der Heijde, and Lieve Helsen. Controlling district heating and cooling networks to unlock flexibility: A review. *Energy*, 151:103–115, 2018.

[307] Jide Niu, Zhe Tian, Jie Zhu, and Lu Yue. Implementation of a price-driven demand response in a distributed energy system with multi-energy flexibility measures. *Energy Conversion and Management*, 208(September 2019):112575, 2020.

[308] Andreas Rieder, Andreas Christidis, and George Tsatsaronis. Multi criteria dynamic design optimization of a small scale distributed energy system. *Energy*, 74(C):230–239, 2014.

[309] Philip Voll, Mark Jennings, Maike Hennen, Nilay Shah, and André Bardow. *The Good, the Bad, and Your Real Choices - Decision Support for Energy Systems Synthesis through Near-Optimal Solutions Analysis*, volume 33. Elsevier, 2014.

[310] Stefano Bracco, Gabriele Dentici, and Silvia Siri. Economic and environmental optimization model for the design andthe operation of a combined heat and power distributed generation system in an urban area. *Energy*, 55:1014–1024, 2013.

[311] Carl Haikarainen, Frank Pettersson, and Henrik Saxén. A model for structural and operational optimization of distributed energy systems. *Applied Thermal Engineering*, 70(1):211–218, 2014.

[312] Zhaoguang Pan, Qinglai Guo, and Hongbin Sun. Feasible region method based integrated heat and electricity dispatch considering building thermal inertia. *Applied Energy*, 192:395–407, 2017.

[313] Yongli Wang, Yudong Wang, Yujing Huang, Jiale Yang, Yuze Ma, Haiyang Yu, Ming Zeng, Fuwei Zhang, and Yanfu Zhang. Operation optimization of regional integrated energy system based on the modeling of electricity-thermal-natural gas network. *Applied Energy*, 251(January):113410, 2019.

[314] Honglin Chen, Mingbo Liu, Yingqi Liu, Shunjiang Lin, and Zhibin Yang. Partial surrogate cuts method for network-constrained optimal scheduling of multi-carrier energy systems with demand response. *Energy*, 196:117119, 2020.

[315] Rui Li, Wei Wei, Shengwei Mei, Qinran Hu, and Qiuwei Wu. Participation of an Energy Hub in Electricity and Heat Distribution Markets: An MPEC Approach. *IEEE Transactions on Smart Grid*, 10(4):3641–3653, 2019.

[316] Rufeng Zhang, Tao Jiang, Wenming Li, Guoqing Li, Houhe Chen, and Xue Li. Day-ahead scheduling of integrated electricity and district heating system with an aggregated model of buildings for wind power accommodation. *IET Renewable Power Generation*, 13(6):982–989, 2019.

[317] Xuezhi Liu, Jianzhong Wu, Nick Jenkins, and Audrius Bagdanavicius. Combined analysis of electricity and heat networks. *Applied Energy*, 162:1238–1250, 2016.

[318] Elisa Guelpa. Impact of network modelling in the analysis of district heating systems. *Energy*, 213, 2020.

[319] Elisa Guelpa. Impact of thermal masses on the peak load in district heating systems. *Energy*, 214, 2021.

[320] Dan Wang, Yun qiang Zhi, Hong jie Jia, Kai Hou, Shen xi Zhang, Wei Du, Xu dong Wang, and Meng hua Fan. Optimal scheduling strategy of district integrated heat and power system with wind power and multiple energy stations considering thermal inertia of buildings under different heating regulation modes, 2019.

[321] Zhigang Li, Wenchuan Wu, Jianhui Wang, Boming Zhang, and Taiyi Zheng. Transmission-Constrained Unit Commitment Considering Combined Electricity and District Heating Networks. *IEEE Transactions on Sustainable Energy*, 7(2):480–492, 2016.

[322] Shuai Lu, Wei Gu, Ke Meng, Shuai Yao, Bin Liu, and Zhao Yang Dong. Thermal Inertial Aggregation Model for Integrated Energy Systems. *IEEE Transactions on Power Systems*, 35(3):2374–2387, may 2020.

[323] Chenhui Lin, Wenchuan Wu, Boming Zhang, and Yong Sun. Decentralized Solution for Combined Heat and Power Dispatch Through Benders Decomposition. *IEEE Transactions on Sustainable Energy*, 8(4):1361–1372, 2017.

[324] Wei Gu, Jun Wang, Shuai Lu, Zhao Luo, and Chenyu Wu. Optimal operation for integrated energy system considering thermal inertia of district heating network and buildings. *Applied Energy*, 199:234–246, 2017.

[325] Ping Li, Haixia Wang, Quan Lv, and Weidong Li. Combined heat and power dispatch considering heat storage of both buildings and pipelines in district heating system for wind power integration. *Energies*, 10(7), 2017.

[326] Atli Benonysson, Benny Bøhm, and Hans F. Ravn. Operational optimization in a district heating system. *Energy Conversion and Management*, 36(5):297–314, may 1995.

[327] Xin Qin, Xinwei Shen, Hongbin Sun, and Qinglai Guo. A quasi-dynamic model and corresponding calculation method for integrated energy system with electricity and heat. *Energy Procedia*, 158:6413–6418, 2019.

[328] Yuanhang Dai, Lei Chen, Yong Min, Qun Chen, Junhong Hao, Kang Hu, and Fei Xu. Dispatch Model for CHP With Pipeline and Building Thermal Energy Storage Considering Heat Transfer Process. *IEEE Transactions on Sustainable Energy*, 10(1):192–203, 2019.

[329] Jianxiao Wang, Haiwang Zhong, Ziming Ma, Qing Xia, and Chongqing Kang. Review and prospect of integrated demand response in the multi-energy system, 2017.

[330] Wujing Huang, Ning Zhang, Chongqing Kang, Mingxuan Li, and Molin Huo. From demand response to integrated demand response: review and prospect of research and application, 2019.

[331] Yongbao Chen, Peng Xu, Jiefan Gu, Ferdinand Schmidt, and Weilin Li. Measures to improve energy demand flexibility in buildings for demand response (DR): A review, 2018.

[332] Niamh Oconnell, Pierre Pinson, Henrik Madsen, and Mark Omalley. Benefits and challenges of electrical demand response: A critical review. *Renewable and Sustainable Energy Reviews*, 39:686–699, 2014.

[333] Martina Capone, Elisa Guelpa, and Vittorio Verda. Multi-objective optimization of district energy systems with demand response. *Energy*, 227, 2021.

[334] Martina Capone and Elisa Guelpa. Implementing Optimal Operation of Multi-Energy Districts with Thermal Demand Response. *Designs*, 7(1), 2023.

[335] Shenbo Yang, Zhongfu Tan, Hongyu Lin, Peng Li, Gejirifu De, Feng'ao Zhou, and Liwei Ju. A two-stage optimization model for Park Integrated Energy System operation and benefit allocation considering the effect of Time-Of-Use energy price. *Energy*, 195:117013, 2020.

[336] Xinhui Lu, Zhaoxi Liu, Li Ma, Lingfeng Wang, Kaile Zhou, and Shanlin Yang. A robust optimization approach for coordinated operation of multiple energy hubs. *Energy*, 197, 2020.

[337] Phillip Oliver Kriett and Matteo Salani. Optimal control of a residential microgrid. *Energy*, 42(1):321–330, 2012.

[338] Hongming Yang, Tonglin Xiong, Jing Qiu, Duo Qiu, and Zhao Yang Dong. Optimal operation of DES/CCHP based regional multi-energy prosumer with demand response. *Applied Energy*, 167:353–365, 2016.

[339] Aras Sheikhi, Mohammad Rayati, and Ali Mohammad Ranjbar. Demand side management for a residential customer in multi-energy systems. *Sustainable Cities and Society*, 22:63–77, 2016.

[340] Arne Olson, Ryan A. Jones, Elaine Hart, and Jeremy Hargreaves. Renewable Curtailment as a Power System Flexibility Resource. *Electricity Journal*, 27(9):49–61, 2014.

[341] Zongxiang Lu, Haibo Li, and Ying Qiao. Probabilistic Flexibility Evaluation for Power System Planning Considering Its Association With Renewable Power Curtailment. *IEEE Transactions on Power Systems*, 33(3):3285–3295, 2018.

[342] Peter D. Lund, Juuso Lindgren, Jani Mikkola, and Jyri Salpakari. Review of energy system flexibility measures to enable high levels of variable renewable electricity, 2015.

[343] S. Martin Martinez, E. Gomez Lazaro, A. Honrubia Escribano, M. Canas Carreton, and A. Molina-Garcia. Wind Power Curtailment Analysis under generation flexibility requirements: The Spanish case study. In *IEEE Power and Energy Society General Meeting*, volume 2015-Septe, 2015.

[344] P. Denholm. Energy storage to reduce renewable energy curtailment. In *IEEE Power and Energy Society General Meeting*, 2012.

[345] Ning Zhang, Xi Lu, Michael B. McElroy, Chris P. Nielsen, Xinyu Chen, Yu Deng, and Chongqing Kang. Reducing curtailment of wind electricity in China by employing electric boilers for heat and pumped hydro for energy storage. *Applied Energy*, 184, 2016.

[346] Marc Brunner, Krzysztof Rudion, and Stefan Tenbohlen. PV curtailment reduction with smart homes and heat pumps. In *2016 IEEE International Energy Conference, ENERGYCON 2016*, 2016.

[347] H. Holttinen, M. Milligan, E. Ela, N. Menemenlis, J. Dobschinski, B. Rawn, R. J. Bessa, D. Flynn, E. Gómez-Lázaro, and N. K. Detlefsen. Methodologies to determine operating reserves due to increased wind power, 2012.

[348] X. Guan, P. B. Luh, H. Yan, and J. A. Amalfi. An optimization-based method for unit commitment. *International Journal of Electrical Power and Energy Systems*, 14(1):9–17, 1992.

[349] Zhigang Li, Wenchuan Wu, Mohammad Shahidehpour, Jianhui Wang, and Boming Zhang. Combined heat and power dispatch considering pipeline energy storage of district heating network. *IEEE Transactions on Sustainable Energy*, 7(1):12–22, 2016.

[350] Abdelfattah A. Eladl and Azza A. ElDesouky. Optimal economic dispatch for multi heat-electric energy source power system. *International Journal of Electrical Power and Energy Systems*, 110(February):21–35, 2019.

[351] Xinyu Chen, Michael B. McElroy, and Chongqing Kang. Integrated Energy Systems for Higher Wind Penetration in China: Formulation, Implementation, and Impacts. *IEEE Transactions on Power Systems*, 33(2):1309–1319, 2018.

[352] Yuwei Chen, Qinglai Guo, Hongbin Sun, Zhengshuo Li, Zhaoguang Pan, and Wenchuan Wu. A water mass method and its application to integrated heat and electricity dispatch considering thermal inertias. *Energy*, 181:840–852, 2019.

[353] Qin Wang and Bri Mathias Hodge. Enhancing power system operational flexibility with flexible ramping products: A review. *IEEE Transactions on Industrial Informatics*, 13(4):1652–1664, 2017.

[354] Mohammad Khoshjahan, Mahmud Fotuhi-Firuzabad, and Moein Moeini-Aghtaie. Effects of flexible ramping product on improving power system real-time operation. In *2017 Iranian Conference on Electrical Engineering (ICEE)*, pages 1187–1192. IEEE, 2017.

[355] Emmanuel Karlo Nyarko, Robert Cupec, and Damir Filko. A Comparison of several heuristic algorithms for solving high dimensional optimization Problems. *International journal of electrical and computer engineering systems.*, 5(1), 2014.

[356] Bernhard Meindl and Matthias Templ. Analysis of commercial and free and open source solvers for the cell suppression problem. *Transactions on Data Privacy*, 6(2), 2013.

[357] Josef Jablonský. Benchmarks for current linear and mixed integer optimization solvers. *Acta Universitatis Agriculturae et Silviculturae Mendelianae Brunensis*, 63(6), 2015.

[358] Emmanuel Fragnière, Jacek Gondzio, and J-P Vial. A planning model with one million scenarios solved on an affordable parallel machine. Technical report, Ecole des Hautes Etudes Commerciales, Universite de Geneve, 1998.

[359] Hans Mittelmann. Decision tree for optimization software, 2021. http://plato.asu.edu/bench.html [Accessed: January 2021].

[360] Andreas Lundell. minlpbenchmarks, 2021. https://andreaslundell.github.io/minlpbenchmarks/ [Accessed: January 2021].

[361] Luca Urbanucci. Limits and potentials of Mixed Integer Linear Programming methods for optimization of polygeneration energy systems. *Energy Procedia*, 148:1199–1205, 2018.

[362] Jesús-Adolfo Mejía de Dios and Efrén Mezura-Montes. Metaheuristics: A julia package for single- and multi-objective optimization. *Journal of Open Source Software*, 7(78):4723, 2022.

[363] Gurobi Optimization, LLC. Gurobi Optimizer Reference Manual, 2023.

Chapter 7

Appendix

Data for the operation optimization of a MES with an internal thermal network

In this appendix are reported the data assumed for the research presented in Chapter 4, the operation optimization of a MES with an internal thermal network.

The time profiles of the electrical and thermal loads are arbitrary assumed and are reported in Figure 7.1.

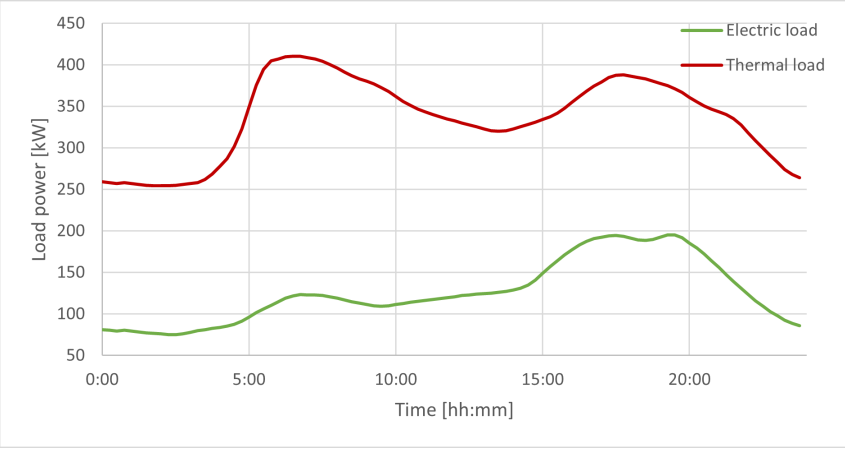

Fig. 7.1 Electric and thermal load profiles

The coefficients for the performance curve (Equation 4.1) of the different technologies involved in the MES operation are arbitrary taken and reported in Table

7.1. In addition, the input/output powers and the size are presented. Concerning the two technologies exploiting renewable powers (PV and wind turbine), their power production is considered as an input data since it cannot be regulated. The profile of a typical winter day with a generation peak of 43.6 kW is assumed for the PV, while a constant production of 25 kW is considered for the wind turbine.

Table 7.1 Coefficients for the performance curves of the MES's components

Unit	a	b	c	d	e	P_{in}	P_{out}	P_{in}^{min} $[kW]$	P_{in}^{max} $[kW]$
CHP	$-4.9 \cdot 10^{-7}$	$7.8 \cdot 10^{-4}$	0.09	0.0	0.0	P_{NG}	P_{el}	358	625
CHP	$-9.2 \cdot 10^{-8}$	$1.3 \cdot 10^{-4}$	0.48	−0.47	23.6	P_{NG}	P_{th}	358	625
Boiler	$-6.3 \cdot 10^{-7}$	$4.1 \cdot 10^{-4}$	0.87	−0.57	28.6	P_{NG}	P_{th}	110	430
EHP	$4.6 \cdot 10^{-4}$	$-1.2 \cdot 10^{-2}$	3.63	−0.34	24.0	P_{el}	P_{th}	17	55
GHP	$5.6 \cdot 10^{-5}$	$-8.0 \cdot 10^{-3}$	1.37	−0.27	19.0	P_{NG}	P_{th}	45	140
FC	$-3.3 \cdot 10^{-7}$	$6.7 \cdot 10^{-5}$	0.40	0.0	0.0	P_{H_2}	P_{el}	48	350

The prices of the fuels and energy vectors considered in the analysis are synthetically presented in Table 7.2. Only the electricity price is considered as variable during the period analysed and its range is reported.

Table 7.2 Prices of fuels and energy vectors

	NG	LPG	H_2	El_{bougth}	El_{sold}
Price	0.195 $€/Sm^3$	0.034 $€/kWh$	0.03 $€/kWh$	$0.136-0.19$ $€/kWh$	$0.036-0.09$ $€/kWh$

Data for the operation optimization of a MES with a District Heating Network

In this appendix are reported the data assumed for the research presented in Chapter 5, the operation optimization of a MES with a District Heating Network.

The minimum and maximum operating powers of the different technologies involved in the MES operation are arbitrary taken and reported in Table 7.3.

Table 7.3 Coefficients for the performance curves of the MES's components

Unit	P_{in}	P_{out}	P_{in}^{min} $[kW]$	P_{in}^{max} $[kW]$	P_{out}^{min} $[kW]$	P_{out}^{max} $[kW]$
CHP	P_{NG}	P_{el}	385	625	200	330
CHP	P_{NG}	P_{th}	385	625	120	240
Boiler	P_{NG}	P_{th}	110	430	100	400

The prices of the fuels and energy vectors are the same used in Chapter 4 and presented Table 7.2. The size of the thermal storage is set to 6 m^3 and .
The values of the coefficients used in the correlation (see Equation 5.7) between the $G \cdot T_s$ product and the thermal power absorbed by the users are reported in Table 7.4.

Table 7.4 Coefficients of users' correlation

Unit	K	q
User1	1.9	3.3
User2	1.8	3
User3	2.1	2.5
User4	2	4
User5	1.9	3.5
User6	1.8	3
User7	2.1	3.3
User8	2	3.5

Finally, the boundaries of the coefficients of the polynomial (see Equation 5.9) used to define the mass flowrate of the thermal users are reported in Table 7.5.

Table 7.5 Boundaries of the coefficients of the polynomial curve of the heat loads

	a	b	c	d
Minimum	-4.5	-0.3	$-4 \cdot 10^{-3}$	$-2 \cdot 10^{-4}$
Maximum	4.5	0.3	$4 \cdot 10^{-3}$	$2 \cdot 10^{-4}$